

**Optimising solvent production in
Clostridium
saccharoperbutylaceticum
N1-4(HMT)**

Thesis for the degree of PhD in Microbiology

School of Biosciences
Faculty of Sciences
University of Kent

Taylor Ian Monaghan
2019

Declaration

I confirm that no part of this thesis has been submitted in support of an application for any degree or qualification at either the University of Kent, any other university or higher education learning institution.

Taylor Monaghan

2019

Abstract

The ever-increasing population and resource demand are putting a stress upon the planet's resources. This increased demand places an even greater need today for the exploration of alternative, greener fuels that can aid in the alleviation of the traditionally used fossil fuels. One such method is in the production of acetone, butanol and ethanol (ABE) by the bacteria genus *Clostridium spp.* These gram-positive anaerobic bacteria were first characterised in the late 19th century and have been used throughout the 20th and 21st centuries for their solvent producing capability, most notably in the supply of weapons grade acetone during the first world war. After falling out of favour in the last half of the 20th century due to competition with cheaper and more readily available petrochemicals; interest in ABE production via *Clostridium spp.* has been on the rise in recent years as the ABE fermentation is investigated for its potential as a greener more renewable source of fuel production. As interest in ABE fermentation has been on the rise in recent years, so too has our understanding of the genus as a whole. Traditionally *C. Acetobutylicum* first described by Chaim Weizmann in the early 20th century has been the industrial strain of choice. However, as the overall understanding of the strains has improved other strains have been explored for their industrial relevance. These are largely split into two characterisations, autotrophs who are able to fix CO₂ and CO, converting them acetyl-CoA for solvent production and heterotrophs who are able to metabolise hexose sugars in solvent production. The strain used in this study is *Clostridium saccharoperbutylacetonicum* N1-4(HMT). *Clostridium saccharoperbutylacetonicum* N1-4(HMT) is a heterotrophic *Clostridium* species first described by (Hongo and Ogata, 1969) .

Herein we have utilised CLEAVE™, this is a CRISPR/Cas system developed by Green biologics ltd. CLEAVE™ was used for the deletion of the gene *gapN* from the genome of *Clostridium saccharoperbutylacetonicum* N1-4(HMT). GapN is a cytosolic non-phosphorylating NADP-dependant GAPDH that catalyses the irreversible oxidation of glyceraldehyde-3-phosphate (G3P) to 3-phosphoglycerate. Deletion of *gapN* causes a reduction in acid production, an increased rate of solvent production to pre-toxic concentrations, as well as an increase in ATP and ratio of NADH:NAD⁺. Additionally, the deletion of *gapN* results in an increase in formic and lactic acid production that is believed to be as a result of pyruvate accumulation in response to the earlier shift into solventogenesis in *gapN* deletion strain

Acknowledgements

First and foremost, I would like to thank my supervisor Mark Shepherd for giving me the opportunity to do this PhD and for his encouragement and expertise throughout this process. To my PhD supervisory chair Gary Robinson, thank you for your insight and help throughout the project. To both Mark and Gary, I am extremely grateful.

To everyone at Green Biologics past and present I am forever indebted to you for all the help, time and expertise you have provided to me throughout the years. To Preben Krabben, Amanda Harding, Chris Hills, Holly Smith and Liz Jenkinson thank you so much for all of your expertise and advice throughout. To Josh, Yatin, Devang, Roary, Tamsin, Sasha and everyone else at GBL thank you for making me feel welcomed during my visit. This work would not have been possible without the kindness of our collaborators. Again, thank you to Green Biologics for allowing me to use your CLEAVE™ technology as well as all of your faculties throughout my placements. To Dr. Ian Goodhead, a massive thank you for letting me visit the University of Salford (Manchester) and for letting me use your Illumina sequencing platform, as well as for your patience, help, and advice throughout the analysis of the sequencing data. I am thankful to the University of Kent, to the BBSRC and GBL for funding my PhD; as well as the Biochemical Society for travel funding to help fund my conference trip to Freising Germany to attend Clostridium XV, and to the Microbiology Society for the grant that helped me attend the Fuel to waste workshop in Naples Italy. Finally, thank you to everyone related to the J.A.M talk sessions, thank you for the opportunity to come to Birmingham and share my research with you.

During my time at the University of Kent I have been fortunate enough to be part of a student community that is inviting and friendly. To everyone, past and present from the Sheblomson Lab, Cláudia, Sarah, Büke, Louis, Joe, James Yorke, Charlie, Ying and Calum thank you for your encouragement, advice and help in keeping each other sane throughout the process. To everyone in office 10GB thank you, to Edith and Nathan in particular.

To Lucy, thank you for making me stronger throughout this whole process.

To my parents, Melodie and Philip thank you for all your support and encouragement throughout my life and letting me live with you to the ripe young age of 26. To my siblings Connor and Declan thank you for always keeping me grounded and reminding me that I am still only at school. Finally, well done me! This PhD was hard, challenging in ways I never assumed it could be and I have managed to come out the other side and I am a much better person because of the challenges I have overcome throughout.

Presentations and Publications

2017 - *New worlds of synthetic biology* - SynEARC:

- Poster presented
- Talk given during postgraduate session

March 9th 2018 - *J.A.M Talks Sessions*:

- Talk given at University of Birmingham IMI centre for a JAM talk session.

July 9th - 2018 - *Waste2Fuels - Naples - Italy*:

- Talk given at Towards bio-butanol as fuel: biorefinery, processes and technologies Workshop

September 20th 2018 - *Clostridium XV*

- Talk given on Engineering
C. saccharoperbutylacetonicum N1-4(HMT) for enhanced butanol, acetone production using CLEAVE™

List of abbreviations

Fatty acid methyl esters (FAMES)

Carbon catabolite repression (CCR)

Formate dehydrogenase (FDH)

Bifunctional CO Dehydrogenase/Acetyl-CoA Synthase complex (CODH/ACS)

Pentose Phosphate Pathway (PPP)

Phosphoketolase pathway (PKP).

Phosphate acetyltrans-ferase (Pta)

Acetate kinase (Ack),

Butyryltransferase (Ptb)

Butyrate kinase (Buk1)

CoA-transferase (CoA-T)

Reverse encoding transcriptases (RT)

Ribonuclease complex (RNP)

Retrotransposition-activated selection markers (RAM)

Homologous recombination (HR)

Allelic coupled exchange (ACE)

Clustered Regulatory Interspaced Palindromic Repeats (CRISPR)

Target DNA assisted by crRNA with an additional RNA (tracrRNA)

Protospacer adjacent motif (PAM)

Anti-sense RNA (asRNA)

Single nucleotide polymorphisms (SNPs)

Reinforced clostridium media (RCM)

Lysogeny Broth (LB)

Yeast extract tryptone media (YETM)

Electroporation buffer with salt (EPB_S)

Electroporation buffer with no salt (EPB_NS)

2-(N-Morpholino) ethanesulfonic Acid (MES)

Clostridia growth media (CGM)

Colony PCR reactions (CPCR)

Gas Chromatography Mass Spectrometry (GCMS)

Nuclear magnetic resonance (NMR)

Whole genome sequencing (WGS)

Leader sequence (LDR)

Integrated genome viewer (IGV)

CRISPR interference (CRISPRi)

Non-homologous end-joining (NHEJ)

Catabolite control protein A (CcPA)

Table of Contents

Declaration	2
Abstract	3
Acknowledgements.....	4
Presentations and Publications.....	5
List of abbreviations.....	6
Table of Contents.....	8
List of Figures	12
Supplementary material	15
Chapter 1 Introduction.....	16
1.1 Introduction	17
1.2 Fossil Fuels.....	17
1.3 Biofuels.....	18
1.3.1 First generation biofuels	18
1.3.2 Second generation and third generation biofuels	19
1.3.3 Biofuel applications for <i>n</i> -butanol	20
1.4 History of biobutanol production	21
1.5 ABE Fermentation	24
1.5.1 Solventogenic clostridial species	24
1.5.2 Feedstock Metabolism	24
1.5.3 Acidogenesis.....	27
1.5.4 Solventogenesis.....	30
1.6 Limitation of ABE fermentation and possible strategies for improvement of ABE fermentation.....	31
1.7 Metabolic engineering in Clostridium.....	33
1.7.2 Double crossover recombination events.....	34
1.7.3 CRISPR	36
1.8 Well-characterised examples of metabolic engineering in Clostridium spp.....	39
1.8.1 Engineered strains	39
1.8.2 Engineered <i>C. saccharoperbutylacetonicum</i> N1-4(HMT) strains.....	41
1.8.3 Alternative butanol producing strains.....	44
1.9 Aims of thesis	42
Chapter 2 Materials and Methods	44
2.1 Bacteriology Methods	45
2.1.1 Bacterial strains and plasmids	45
2.1.2 Oligonucleotides	46
2.1.3 Chemicals and water	46
2.2 Media	46
2.2.1 Luria-Bertani medium	46
2.2.2 Reinforced Clostridium Medium.....	47
2.2.3 Yeast extract tryptone media:	47
2.2.4 X2 CGM Media:.....	47
2.2.5 10% Sugar Stocks:	47
2.2.6 X1 CGM Media:.....	48
2.2.7 Electroporation buffer with salt:.....	48
2.2.8 Electroporation buffer without salt:	48
2.2.9 SOB Media:	48

2.2.10 SOC Media	49
2.3 Media Supplementation.....	49
2.3.1 Antibiotics.....	49
2.3.2 -(N-Morpholino) ethanesulfonic acid.....	49
2.3.3 Calcium Carbonate.....	49
2.4 Culture conditions	50
2.4.1 E. coli.....	50
2.4.2 Preparation of glycerol stocks	50
2.4.3 Culture optical density	50
2.4.4 Butanol Toxicity	50
2.4.5 Seeding of <i>Clostridium</i>	50
2.5 Fermentations.....	51
2.5.1 Batch Fermentation – University of Kent Set up.....	51
2.5.2 Batch Fermentation – GBL.....	52
2.5.3 Fed Batch Fermentation – GBL	52
2.5.4 Gas Stripping – GBL.....	52
2.6 Genetic Methods.....	53
2.6.1 Isolation of plasmid DNA.....	53
2.6.2 Polymerase chain reaction (PCR)	53
2.6.3 DNA electrophoresis on agarose gels.....	55
2.6.5.1 Sticky end ligations.....	55
2.6.5.2 Blunt end Ligations.....	56
2.6.5 Gibson assembly	56
2.6.6 Transformation of E coli competent cells.....	56
2.6.7 <i>Clostridium</i> transformations.....	57
2.6.8 CLEAVE™	58
2.6.9 Sequencing of DNA	58
2.8 Biochemical Methods.....	59
2.8.1 NADPH: NADH Assay	59
2.8.2 ATP Luminescence assay	60
2.8.3 GCMS quantification of acids and solvents	62
2.8.4 HPLC quantification of sugars.....	61
2.8.5 HPLC quantification of sugars and solvents – GBL	62
2.8.6 Glucometer Sugar measurements	62
2.9 Genomic sequencing and analysis methods	63
2.9.1 <i>Clostridium</i> Genomic DNA isolation.....	63
2.9.2 Whole Genome sequencing.....	63
2.9.3 Assembly and annotation.....	63
2.9.4 Variant identification.....	63
Chapter 3 Design and construction of fermentation platform and establishment of analytical tools for ABE fermentation analysis	64
3.1 Summary	65
3.2 Introduction	66
3.3 Results.....	67
3.3.1 Fermenter design and construction.....	70
3.3.2 Growth optimisation of <i>C. saccharoperbutylacetonicum</i> N1-4(HMT).....	71
3.3.3 Assessment of analytical techniques for measurement of acids, solvents and sugars.	73
3.3.3.1 Solvent and acid quantitation	73
3.3.3.2 Optimisation of sugar quantification.....	76
3.3.4 Implementation of new fermentation approaches for integrated analysis of ABE fermentation	77
3.7 Discussion	79
3.7.1 General Discussion.....	79
3.7.2 Dissolved oxygen control and control	79
3.7.3 pH control and acid crash.....	80

3.7.4 Concluding remarks	81
Chapter 4 Deletion of the <i>gapN</i> gene from <i>C. saccharoperbutylacetonicum</i> N1-4(HMT) with the use of CLEAVE, subsequent evaluation of the CLEAVE technology using whole genome sequencing and insight into the effect of the <i>gapN</i> deletion on nucleotide ratio and ATP concentration within the cell	82
4.1 Summary	83
4.2 Introduction	84
4.3 Results.....	87
4.3.1 Deletion of <i>gapN</i> in <i>C. Saccharoperbutylacetonicum</i> N1-4(HMT) using CLEAVE™	88
4.3.1.1 Creation of the Homologous recombination vector and sub-cloning	90
4.3.1.2 Design and construction of Killing Vector.....	90
4.3.1.3 Confirmation of <i>gapN</i> deletion from the genome of <i>C. saccharoperbutylacetonicum</i> N1-4(HMT).....	92
4.4 Whole genome sequencing and comparison of $\Delta gapN$ and wild type <i>C. saccharoperbutylacetonicum</i> N1-4(HMT).	93
4.4.1 Genomic read mapping of Illumina reads	94
4.4.2 Sequence variant analysis and SNP identification.....	95
4.4.3 Whole genome alignment of Wild type and $\Delta gapN$ illumina reads	96
4.6 Discussion	97
4.6.1 CLEAVE™ results in successful deletion of $\Delta gapN$ and analysis reveals that it is accurate.....	97
4.6.2 NGS results of $\Delta gapN$ <i>C. saccharoperbutylacetonicum</i> N1-4(HMT)	98
Chapter 5 Characterisation of $\Delta gapN$ and its potential for improved ABE production ...	99
5.1 Summary	100
5.1 Introduction	101
5.2 Results.....	102
5.2.1 Characterisation of $\Delta gapN$ strain during a batch fermentation on glucose YETM.....	103
5.3 Characterisation of $\Delta gapN$ strain on a synthetic C5/C6 hydrolysate mixture	106
5.4 Fed batch fermentation to assess glucose uptake and sugar utilisation in relation to solvent production.....	109
5.5 Discussion	112
5.5.1 Observed increase in ATP production as a result of <i>gapN</i> deletion, leads to decreased acid production, earlier shift into solventogenesis as well as increased solvent production until pre-toxic concentrations	112
5.5.2 Increased production of lactic and formic acid in the $\Delta gapN$ strain	113
5.5.3 The $\Delta gapN$ strain has same plight of CCR common amongst <i>Clostridium</i>	114
Chapter 6 Final Discussion	115
6.0 General Discussion	115
6.1 Establishment of growth conditions	116
6.2 The overall impact of the deletion of <i>gapN</i> in <i>C. saccharoperbutylacetonicum</i> N1-4(HMT).....	116
6.4 Future Studies.....	118
References	120
Appendix.....	133

List of Figures

Figure 1.1 Timeline of notable events and advances in butanol fermentation from 1916 to 2019	25
Figure 1.2 Overview of metabolism of autotrophs and heterotrophs leading to Acetyl -CoA in Clostridia..	28
Figure 1.3 ABE Fermentation pathway	30
Figure 1.4 Type I and Type II Sol operon.....	32
Figure 1.5 Counter selection markers used in Clostridium spp.....	38
Figure 1.6 Model of crRNA processing and interference.....	41
Figure 2.1 Seed train for Clostridium fermentation.	54
Figure 2.2 NADH and NADPH Standard curve	59
Figure 2.3 ATP Standard curve	59
Figure 3.1 Schematic overview of the shepherd lab fermentation units.	70
Figure 3.2 Buffering agents used in ABE fermentation.....	71
Figure 3.3 Fermentation analysis using CaCO ₃ and MES as pH buffering systems..	72
Figure 3.4. GCMS Chromatographs from <i>C. saccharoperbutylacetonicum</i> N1-4(HMT) YETM 40 g L ⁻¹ batch fermentation for the identification of the acids (acetic acid and butanoic acid) and solvents (acetone and butanol.....	74
Figure 3.5 GCMS standard curves.....	75
Figure 3.6 Glucose concentrations during fed batch fermentation comparing the ability of the Glucometer vs HPLC analysis..	76
Figure 3.7 Overview of growth, acids and solvents of a <i>C. saccharoperbutylacetonicum</i> N1-4(HMT) batch fermentation in the shepherd fermentation system.....	78
Figure 4.1 The pathways involved in conversion of glyceraldehyde 3-phosphate to 3-phosphoglyceric in <i>C. saccharoperbutylacetonicum</i> N1-4(HMT).....	86
Figure 4.2 Diagrammatic representation of the PCR reaction used to create the deletion cassette insert for the Homologous Recombination vector	88
Figure 4.3 Cloning of the homologous recombination vector for deletion of gapN.	89
Figure 4.4 Overview of the killing vector targeting cassette for endogenous CRISPR-Cas for genome editing.	90
Figure 4.5 PCR screening for successful ligation of DR_gapN_DR spacer sequence into the pMTL83125 vector.....	91
Figure 4.6 Colony PCR screening of <i>C. saccharoperbutylacetonicum</i> N1-4(HMT) Δ gapN mutants.....	92
Figure 4.7 Diagram detailing the process of genome evaluation following illumina Miseq of the wild type and Δ gapN <i>C. saccharoperbutylacetonicum</i> N1-4(HMT).	93
Figure 4.8 Whole genome comparison of the reference <i>C. saccharoperbutylacetonicum</i> N1-4(HMT) to genome assembly of the Δ gapN and wild type strains illumina sequenced strains	96

Figure 5.1 Fermentation measurements for $\Delta gapN$) and wild type <i>C. saccharoperbutylacetonicum</i> N1-4(HMT) grown on 40 g L ⁻¹ glucose in YETM media....	102
Figure 5.2 Acid and solvent profiles for $\Delta gapN$ and wild type <i>C. saccharoperbutylacetonicum</i> N1-4(HMT) grown on 40 g L ⁻¹ glucose in YETM media....	103
Figure 5.3 Butanol toxicity test of wild type (black bars) and $\Delta gapN$ (grey bars) strains of <i>C. saccharoperbutylacetonicum</i> N1-4(HMT).....	104
Figure 5.4 ATP measurements for $\Delta gapN$	105
Figure 5.5 Concentration of nucleotide cofactors in both the wild type and the $\Delta gapN$ during acidogenesis (4h) and Solventogenesis (24 h).....	106
Figure 5.6 Sugar profiles for $\Delta gapN$ and wild type <i>C. saccharoperbutylacetonicum</i> N1-4(HMT) grown on C5 hydrolysate mixture.	108
Figure 5.7 Acid and solvent profiles for $\Delta gapN$ and wild type <i>C. saccharoperbutylacetonicum</i> N1-4(HMT) grown on C5 hydrolysate mixture.	109
Figure 5.8 Growth parameters and glucose profiles for $\Delta gapN$ and wild type <i>C. saccharoperbutylacetonicum</i> N1-4(HMT) grown in fed batch fermentations.	110
Figure 5.9 Acid and solvent profiles for $\Delta gapN$ and wild type <i>C. saccharoperbutylacetonicum</i> N1-4(HMT) grown in fed batch fermentations.	111
Figure 6.1 Overview of impact of <i>gapN</i> knockout on <i>C. saccharoperbutylacetonicum</i> N1-4(HMT)	118

List of Tables

Table 1.1 Properties and applications of n-butanol.....	21
Table 2.1 Bacterial Strains and Plasmids used in Thesis	45
Table 2.2 Plasmids used in the thesis.....	46
Table 2.3 Oligonucleotides used in this study.....	49
Table 2.4 Lysis PCR reaction for Clostridium PCR.....	53
Table 2.5 2x Q5 Master Mix PCR reaction mixture	53
Table 2.6 2x Q5 PCR reaction.....	54
Table 2.7 Phusion PCR reaction mixture	54
Table 2.8 Phusion PCR reaction	54
Table 2.9 HPLC Conditions for Solvents, acids and common sugars.....	62
Table 3.1 Comparison of main functionality of commercially available fermentation systems compared to the Shepherd lab designed system	69
Table 4.1 Qualimap results of <i>C. saccharoperbutylacetonicum</i> N1-4(HMT) Δ gapN and Wild type following read mapping via bwa to the reference <i>C. saccharoperbutylacetonicum</i> N1-4(HMT) obtained from Gene bank (CP004121.1)	94
Table 4.2 Breakdown of the total number of mutations identified in the wild type and Δ gapN strains compared to reference <i>C. saccharoperbutylacetonicum</i> N1-4(HMT) genome obtained from Gene bank (CP004121.1) by Snippy	95

Supplementary material

<i>Appendix A-1 – Jacketed water system for fermentation system</i>	135
<i>Appendix A-2 – List of components used in designed fermentation system</i>	137
<i>Appendix A3 – Custom built gas out and sample port:</i>	139
<i>Appendix B – Final set up of fermentation units based upon schematics from Figure 3.1</i>	141
<i>Appendix C – Calculations for correct pmol of DNA for Clostridium transformation</i>	143
<i>Appendix D – Sanger sequences of newly created ΔgapN strains:</i>	144
<i>Appendix E – Qualimap results.</i>	145
<i>Appendix F – List of SNP's identified in NGS sequences of wild type and ΔgapN C. sacc</i>	182
<i>Appendix G – IGV Manually investigated SNP's in both WT and ΔgapN strain</i>	183
<i>Appendix H – Gene presence and absence Via Roary analysis</i>	190
<i>Appendix I – Initial screening of ΔgapN deletion</i>	191

Chapter 1

Introduction

1.1 Introduction

The work in this thesis focuses on improving processes of renewable *n*-butanol and acetone production from the solvent-producing bacterium *C. saccharoperbutylacetonicum* N1-4 (HMT). In addition to the establishment of fermentation and growth techniques, new molecular biology methodology has been explored to further understand the metabolism *C. saccharoperbutylacetonicum* N1-4(HMT) and improve the capacity for solvent production. This chapter will first provide the background knowledge on the current state of fossil fuel utilisation and renewable energy alternatives. The focus will then shift to introducing the unique metabolism of solventogenic *Clostridia* strains, and provide an in-depth analysis of the available tools for genetic manipulation across *Clostridia*. Finally examples of how these tools have been used in each strain alongside introducing alternative hosts for ABE production

1.2 Fossil Fuels

1.2.1 Global supply and demand for fossil fuels

Currently, the global appetite for energy is ever increasing as more and more countries become wealthier and more industrialised. This insatiable appetite for energy is being met mainly by traditional fossil fuels, coal, gas and oil. Currently 91.6% of power generation globally is met by fossil fuels, with the remaining 8.4% being met by renewables (British Petroleum, 2018). Overall the global energy demand for the year 2017 rose by 2.2%, substantially higher than the average per year from the last 10 years of 1.7%. This sharp growth has been mainly due to global increases in GDP driven by the expanding markets in China and India accounting for 40% of the overall observed increase (British Petroleum, 2018).

Up to this point there has been little change in the mixture of sources used for power generation compared to that in 1998. This is large part due to the decrease in nuclear power, alongside the massive economic growth China has seen in the past 20 years. The knowledge that little has changed on a global scale in terms of energy production is daunting, especially as renewables have seen the largest growth rates in recent years (16.2 % between 2006 – 2016) over traditional fossil fuels. Renewables however, still only account for 8.4% of power generation globally. In addition to this, 2017 saw CO₂ rise by 1.6% (British Petroleum, 2018; "Global Energy & CO 2 Status Report," 2018), the first time a rise was witnessed in the 3 years prior.

Currently the best models predict that if the world continues to use fuel at a rate similar to that of 2006 then oil, coal and gas will be diminished in around 40,200 and 70 years respectively (Shafiee and Topal, 2009). However as has been shown in years from 2006-2016, overall consumption of oil, coal and particularly natural gas has been on the rise by 1.1%, 1.3% and 2.3% respectively. This paints a dreary picture for energy consumption globally as the demand is increasing year on year.

The increase in demand for fossil fuels in particular oil as it is the main source of energy for global transport, raises the additional question of energy security. Currently, the majority of the oil produced globally comes from regions of political, social and economic uncertainty, such as Iraq, Venezuela and Nigeria (Bang, 2010; Lilliestam, 2012). It is because of the ever-increasing demand on fossil fuels that regions such as the USA and Europe have become dependent on these unstable regions for their energy demands. However, because of these factors of instability, the USA and Europe have recognised that their dependency on imported energy must be reduced, and they have identified a need to explore alternative sources to meet their energy demands.

1.3 Biofuels

Biofuels are energy carriers whose energy has been stored by means of carbon fixation in biological material over a relatively short period, i.e. decades as opposed to millennia such as in the form of petroleum-based fossil fuels. Biofuel production is diverse ranging from gasses such as hydrogen and methane, liquids in the form of ethanol, butanol, fatty acid methyl esters (FAMES) and to solids such as wood. In recent years a number of regulatory requirements in the face of depletion of fossil fuels has created a market place for biofuels as a commodity. The EU adopted legislation in 2009 stating that 10% of all transport fuel should be renewable by the year 2020 (EASAC, 2012). In addition, the USA in 2007 passed legislation that would require an aggregate of 36 billion gallons of ethanol (or equivalents) from renewables to be used in transport by 2020 (United States Congress, 2007).

1.3.1 First generation biofuels

First generation biofuels are those that are derived from biomass that could be more often than not considered edible, such as crop plants in the form of starch from corn and wheat, sucrose from sugar cane / sugar beets and oils in the form of palm oil and canola oil. Currently, bioethanol and bio-diesel are the two main first generation biofuels produced using these feedstocks. The production of bio ethanol largely relies upon the fermentation of starch and sugar biomass. The USA leads global production of bio ethanol at 33.7×10^9

L / year produced, followed by Brazil at 24.3×10^9 L / year produced (Lee and Lavoie, 2013)(Aro, 2016). Unlike bioethanol production which typically involves fermentation straight from a sucrose source or following a simple hydrolysis of starch material such as corn or wheat, biodiesel production is considered a chemical process. The production of biodiesel requires filtering and transesterification of fatty acids to allow it to be used. Germany is the largest producer of biodiesel at 9.2×10^9 L / year (Sorda et al., 2010)

Despite good intentions, first generation biofuels are largely now banned, in the EU due to the fact that they not only compete with land for food production, in the EASAC 2012 study revealed that once the processing of first generations biofuels was taken into consideration from the biomass cultivation, to fuel production they provide no or little benefit to the greenhouse gas effect and have a detrimental effect on food agriculture as well as natural ecosystems (EASAC, 2012). In addition to this, the fluctuation and cost associated with first generation biofuel feedstocks can often result in abandonment of biofuel production. This was seen in Brazil in 2012, where the production of around 1 L of bioethanol from sugar cane was around \$ 0.30/0.35 / L whereas the price of raw sugar cane was around \$ 0.20 / lb and due to these low margins, the market favoured the production of the raw sugar instead of bioethanol (Sorda et al., 2010).

1.3.2 Second generation and third generation biofuels


Second generation biofuels are produced using biomass that is considered not suitable for consumption. Most commonly this takes the form of waste lignocellulosic biomass from wheat stover, corn stover and rice stover (i.e. the plant material left over from harvest). The use of waste lignocellulose helps create synergy in the agricultural cycle, enabling the productive use of an otherwise wasted by product. In addition to waste lignocellulose second generation biofuels are also produced from plants that have been specifically grown as bioenergy crops. Bioenergy crops such as perennial grasses, *Miscanthus giganteus* (Boehmel et al., 2008) and *Panicum virgatum* (switchgrass) (David and Ragauskas, 2010) are grown in marginal lands that are not able to sustain agricultural crops but can be used in the production of second-generation biofuels. The unfortunate drawback of second-generation biofuels is that they require extensive pre-treatment from mechanical, chemical or enzymatic methods (Braguglia et al., 2017; Hijosa-Valsero et al., 2017). Third generation biofuels are often described as those produced from algal biomass, although these are more poorly categorised and are not applicable to this study.

1.3.3 Biofuel applications for *n*-butanol

Currently, bioethanol is the largest produced biofuel globally. This, however is down to its ease of production rather than its ability as a biofuel. Butanol is a far superior biofuel in comparison to ethanol and a number of other fuel types, and a breakdown of the properties of butanol in comparison to a number of other fuel types can be seen in Table 1.1. The advantages of Butanol over bioethanol include: (i) Higher energy density over ethanol (25 %), allowing for increased range in Km/ h per mass of fuel. (ii) lower volatility due to the increased length of carbon chain. This is advantageous as gasoline / butanol fuel blends will have less of a tendency towards cavitation or vapour lock problems; (iii) Heat vaporisation, and autoignition of butanol is lower than both ethanol and methanol; (iv) increased viscosity of butanol results in decreased wear for rubber tubing, pumps and general infrastructure, this will increase longevity of infrastructure and reduce frequency of maintenance of perishables; (v) Lower water solubility; meaning reduced hygroscopicity and better miscibility with fuel, meaning that cars would not require modifications even with a 10% butanol gasoline blend (Bharathiraja et al., 2017; Dürre, 2008; Green, 2011; Lee et al., 2008). It has also been demonstrated that butanol can be used on its own as a pure motor fuel. This was accomplished by David Ramey (*Autoblogcom*. 2019) in the USA in 2005 and 2007 when he travelled across America fuelled only by butanol in a car with no modifications. This has also been demonstrated in the form of biobutanol by Celtic renewables (Bbccouk. 2019. BBC News) demonstrating the ability of butanol as a drop-in fuel replacement to gasoline.

Butanol is not only useful in fuel blends or as a drop-in replacement for conventional gasoline, it is also used in a number of industrial applications. Butanol is used for the production of butyl acrylic, which is subsequently used in the manufacturing of polymer coatings, adhesives, plastics, resins and as an additive in the leather and paper industry. Additional products produced from butanol are butyl glycol in industrial solvents, butyl acetate used in prints and as a flavouring agent in the food and drink industry (Dürre, 2008). As of 2008 the global market for *n*-butanol was around 2.8 million tons at a valuation of roughly \$ 5 billion USD, with projected valuation of \$ 247 billion dollars by 2020, due to the advantageous properties of butanol over ethanol and biodiesel (Bharathiraja et al., 2017). As long as the process economics are kept competitive with those of petrochemical-derived butanol, the production of biobased *n*-butanol will continue to be an economically viable biofuel and bulk chemical.

Table 1.1 Properties and applications of n-butanol

Properties		Butanol
Melting point	-89.3 °C	Molecular formula: C ₄ H ₉ OH
Boiling point	117.7 °C	Molecular weight: 74.121 g/mol
Ignition temperature	35 °C	Structure: 

	Properties of fuels		
	n-Butanol	Gasoline	Ethanol
Energy density (MJ/L)	29.2	32	19.6
Air-fuel ratio	11.2	14.6	9
Heat of vaporization (MJ/kg)	0.43	0.36	0.92
Octane number	96	80-99	108

1.4 History of biobutanol production

The industrial application of solvent-producing *Clostridium* was first exploited at the turn of the 20th century. Strange and Graham Ltd. were the first manufacturer to incorporate fermentative alcohol in the production of their synthetic rubbers in 1910. During this period the company hired a Jewish Russian Chemist Chiam Weizmann, who had arrived in Manchester from Berlin in 1904. At Manchester Chiam Weizmann assisted on the investigation into the production of butadiene and isoprene via microbial fermentative. Not a microbiologist by trade Weizmann set about becoming one between the years of 1912 and 1914. Following his termination of contract with Strange and Graham in 1912 he continued his investigation into fermentative microbiology for the production of synthetic rubber, concluding that production of butanol by fermentative microbiology was key for the success of synthetic rubber production. From 1912 to 1914 period, Weizmann isolated a number of bacterial strains, one of which he had called “BY” that later became known as *Clostridium acetobutylicum* and further known as the Weizmann strain, this strain was able to metabolise a number of starch substrates as well as produce higher concentrations of acetone and butanol than the original Fernbach strain (Bengelsdorf and Dürre, 2017; Gi Moon et al., 2015; Jones and Woods, 1986).

The outbreak of the first world war shifted Weizmann’s focus away from rubber production to the production of acetone as a component of nitro cellulose, to form cordite. Cordite is a smokeless gunpowder that was used in naval munitions during the first world war. Having spent time developing his fermentation methodology for the production of acetone via

microbial fermentation, he was awarded a patent for this method in March of 1915. The following year Weizmann was summoned by Winston Churchill, who at the time was acting Lord of the Admiralty, who tasked Weizmann with undertaking the pilot plant production of acetone for cordite. These pilot plants were so successful that the Royal Naval Cordite factory was established in Dorset, where 6 distilleries were adapted for the production of acetone for cordite using the patented Weizmann methodology.

Commercial production of acetone and butanol continued globally using licenced version of the Weizmann patent until the late 1950's / early 1960's. Unfortunately, production was unable to keep up with unprecedented growth of the petrochemical industry. Due to this alongside the increase in the cost of substrates (starch and molasses) production had all but stopped in most of Europe and the USA during the 1960's (Jones and Woods, 1986). However, increased oil prices and the global drive for discovery of green energy countries such as China (Jiang et al., 2015) and Brazil (Green, 2011) have been quick to re-adopt ABE fermentation. More recently companies such as Green Biologics (Lane and Digest, 2014) and Celtic Renewables (2019. BBC News) have initiated industrial solvent production via ABE fermentation in the USA and Scotland, respectively. An overview of key milestones in the history of ABE fermentation can be seen in Figure 1.1.

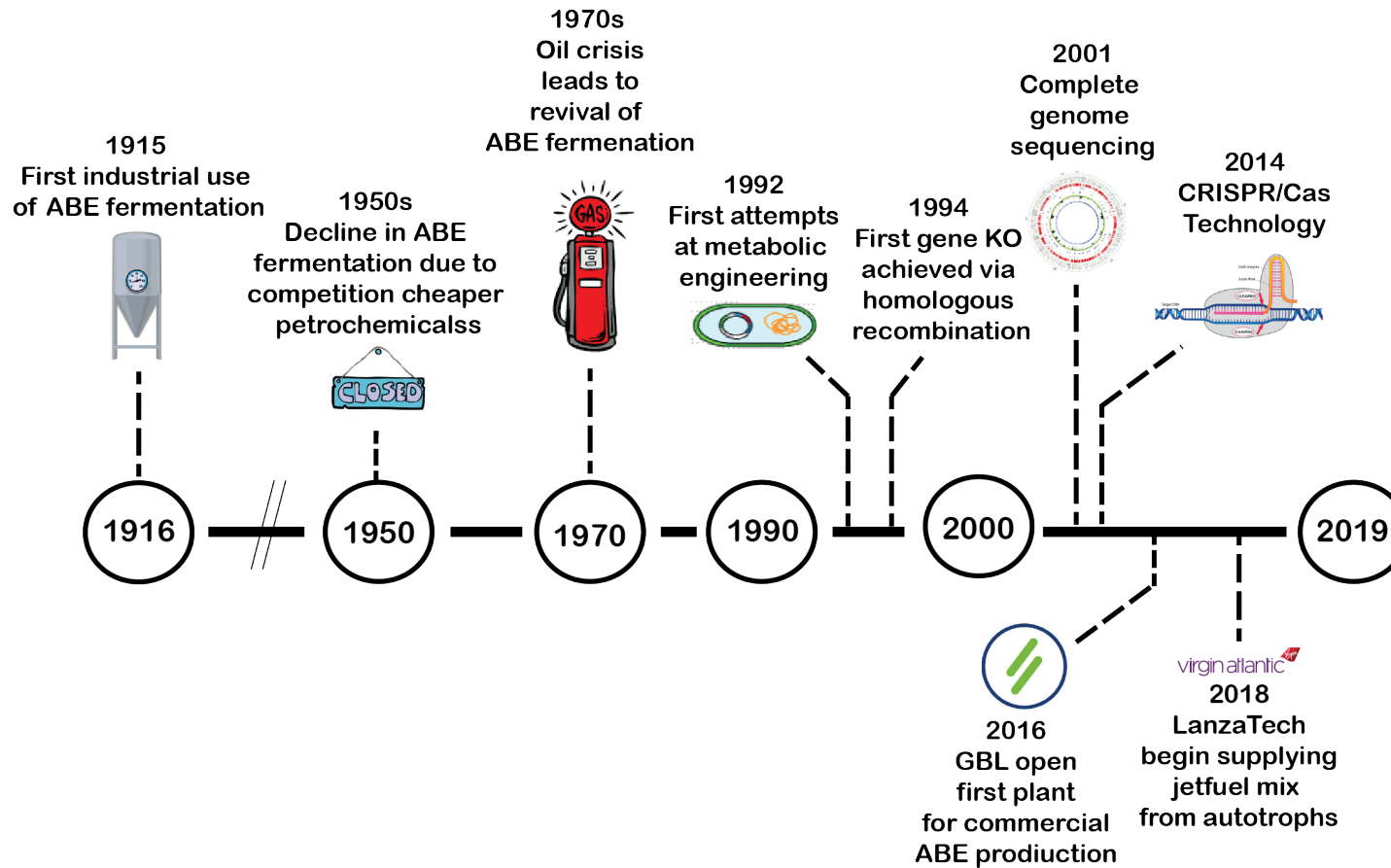


Figure 1.1 Timeline of notable events and advances in butanol fermentation from 1916 to 2019

1.5 ABE Fermentation

1.5.1 Solventogenic clostridial species

Clostridia are a class of Gram-positive, anaerobic, rod shaped endospore forming bacteria with a low GC content. Clostridia play key roles in both human health and disease with *Clostridium perfringens*, *C. difficile*, *C. tetani* and *C. botulinum* known opportunistic pathogenic bacteria (Kenneth Todar, n.d.). However, solventogenic clostridia have a safe history of use in the production of acetone and butanol. The best known and most studied of the industrial solventogenic clostridial species is *C. acetobutylicum* (Aristilde et al., 2015; Cho et al., 2012; Clare M. Cooksley et al., 2012; Heap et al., 2007; Jones and Keis, 1995; Kaminski et al., 2011; Poehlein et al., 2017; Ryan S. Senger, 2009) also known as the Weizmann strain; it is second only to yeast in terms of global ethanol production (Bao et al., 2011) and since its original discovery has been used as a model organism for endospore formation (Nölling et al., 2001). In the century that has passed since the discovery of the original Weizmann strain, strains such as *Clostridium beijerinckii* (Jones and Keis, 1995) and *Clostridium saccharoperbutylacetonicum* (Hongo and Ogata, 1969) have surpassed the original Weizmann strain as the preferred choice for ABE fermentation when grown on carbohydrate material. Acetogens such as *Clostridium ljungdahlii* (Köpke et al., 2010) and *Clostridium autoethanogenum* (Marcellin et al., 2016; Minton et al., 2016) have shown that these versatile bugs are able to fix simple C1 carbons for the production of biofuels (Jiang et al., 2015; Köpke et al., 2010; Marcellin et al., 2016).

1.5.2 Feedstock Metabolism

Clostridia are able to utilize a large variety of carbohydrate sources, from simple mono- and disaccharides, through to complex polysaccharides such as cellulose and hemicellulose, making them ideal candidates to metabolise a large variety of waste material (Al-Shorgani et al., 2012b; Lynd et al., 2002; Shaheen et al., 2000; Takors et al., 2018). A recent genomic study found that throughout commonly used industrial strains such as *C. beijerinckii*, *C. saccharobutylicum*, *C. acetobutylicum* and *C. saccharoperbutylacetonicum* genes for sucrose-specific phosphotransferase systems and sucrose degradation were present, as well as for starch degradation (Poehlein et al., 2017). In addition to heterotrophic growth, some clostridia can also grow autotrophically by fixing CO₂ and CO chemolithotrophically (Drake et al., 2008) converting them to acetyl-CoA for solvent production.

Industrial feedstocks such as brewers' grain can often contain a mixture of C5 and C6 sugars including glucose, xylose, arabinose and mannose (Tracy et al., 2012). This C5/C6 mixture has a high propensity to cause carbon catabolite repression (CCR), whereby

utilisation of one sugar (usually a C6 sugar) will predominate and metabolism of any other sugars present in the media will not take place (Bruder et al., 2015). CCR is a problem for ABE fermentation as the C5 sugar xylose is an abundant component in lignocellulosic feedstocks, and in the presence of glucose this xylose is not metabolised until glucose and other C6 sugars have been used up (Ren et al., 2010).

Autotrophic and heterotrophic growth both lead to the production of acetyl-CoA. In the case of autotrophic metabolism, the production of acetyl-CoA involves the use of the Wood–Ljungdahl pathway in which two moles of CO₂ are reduced to one mole of acetyl-CoA using H₂ and CO to produce reducing equivalents. The Wood–Ljungdahl pathway itself is split into two parts, an Eastern and a Western branch. In the Eastern branch formate dehydrogenase (FDH) is used to reduce CO₂ to formate, and formate is then attached to a tetrahydrofolate and further reduced to a methyl-group. In the Western branch one molecule of CO₂ is reduced directly to CO by part of the bifunctional CO Dehydrogenase/Acetyl-CoA Synthase complex (CODH/ACS). Carbonyl- and methyl- groups from both branches are combined in the Acetyl-CoA Synthase complex with a molecule of coenzyme-A to form acetyl-CoA (Ragsdale, 2008) (Figure 1.2)

During heterotrophic growth, hexose and cellulose sugars are metabolised through glycolysis, resulting in 2 moles of pyruvate per 1 mole of hexose with a net production of 2 moles of ATP and 2 moles of NADH, or in the production of NADPH at a loss of 1 ATP at the conversion stage of Glyceraldehyde 3-phosphate to 3 – Phosphoglyceric acid (Ren et al., 2016). Pentose sugars flow into glycolysis via the Pentose Phosphate Pathway (PPP) or via the Phosphoketalse pathway (PKP). Recently it has been shown that in a hexose pentose mixture, flux from the PPP into glycolysis is minimal with a large accumulation of PPP intermediates (Aristilde et al., 2015). The pyruvate resulting from the process of glycolysis is cleaved by pyruvate ferredoxin oxidoreductase in the presence of coenzyme A to produce acetyl-CoA and reduced ferredoxin. (Figure 1.2).

Now that an overview of feedstock metabolism has been given, the following sections will focus on the unique growth physiology of solventogenic *Clostridia*. This growth physiology is unique in that can often be broken up into two distinct phases, acidogenesis, in which there is the production of acetic and butyric acid; and solventogenesis in which the acids produced in acidogenesis are re-assimilated to form acetone, butanol and ethanol.

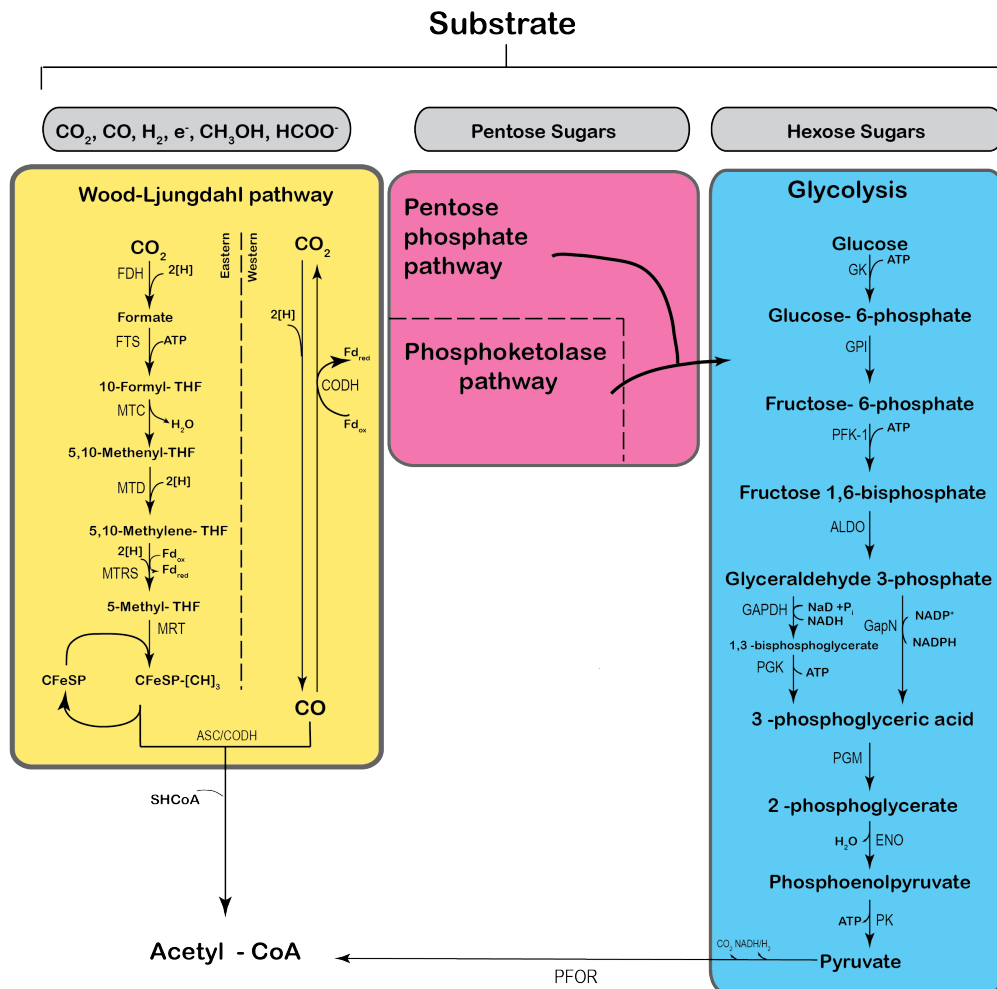


Figure 1.2 Overview of metabolism of autotrophs and heterotrophs leading to Acetyl - CoA in Clostridia. Glycolysis is shown in blue, the pentose phosphate and phosphoketolase pathway are shown in pink. The Wood-Ljungdahl pathway is shown in yellow. Enzyme abbreviations are as follows; FDH, formate dehydrogenase; FTS, formyl-THF synthase; MTC, methenyl-THF cyclohydrolase; MTD, methylene-THF dehydrogenase; MTR, methyl transferase; MTRS, methylene-THF reductase; PFK-1, ACS/ CODH, acetyl-CoA synthase/CO dehydrogenase; GPI, phosphoglucose isomerase; PFK-1, phosphofructokinase;ALDO, fructose biphosphate aldolase; GAPDH, glyceraldehyde phosphate dehydrogenase; GapN, glyceraldehyde -3 phosphate dehydrogenase; PGM, phosphoglycerate mutase; ENO, enolase; PK, pyruvate kinase; PFOR, pyruvate:ferredoxin oxidoreductase; PGK, phosphoglycerate kinase.

1.5.3 Acidogenesis

During acidogenesis, sugars consumed during growth are typically metabolised to form acetic acid and butyric acid, H_2 and CO_2 . The production of acetic acid and butyric acid involves the enzymes phosphate acetyltransferase (Pta), acetate kinase (Ack), butyryltransferase (Ptb), and butyrate kinase (Buk1) (Figure 1.2). In both pathways of acidogenesis, additional ATP is generated in the final phosphorylation reaction. Acidogenesis typically occurs during the log phase of growth when the cells are at their most vegetative in conditions where the pH is typically greater than 5 and there is a depletion of iron. The significant production of the acids leads to acid accumulation externally in the media and a significant drop in the surrounding pH. If left unchecked, the undissociated acids would diffuse back into the cell, destroying the proton gradient and inhibiting cell growth. To overcome this, the cells trigger what is commonly known as “solventogenic switch” whereby the genes involved in solvent production become expressed, producing the traditionally seen ABE solvents to overcome rising acid concentrations (Jones and Woods, 1986; Lee et al., 2008).

If unchecked by the solventogenesis switch acid accumulation in concentrations of between 57-60 mmol L⁻¹ can result in acid crash, whereby the cells will fail to shift into solventogenesis. This results in decreased solvent production and cessation of glucose uptake. In addition to this, at acid concentrations of between 240-350 mmol L⁻¹ solventogenesis can be inhibited completely, resulting in cell death (Chen and Blaschek, 1999; Maddox et al., 2000). Acid crash is typically seen in unregulated batch fermentations where acids are neither buffered or removed from the fermentation media

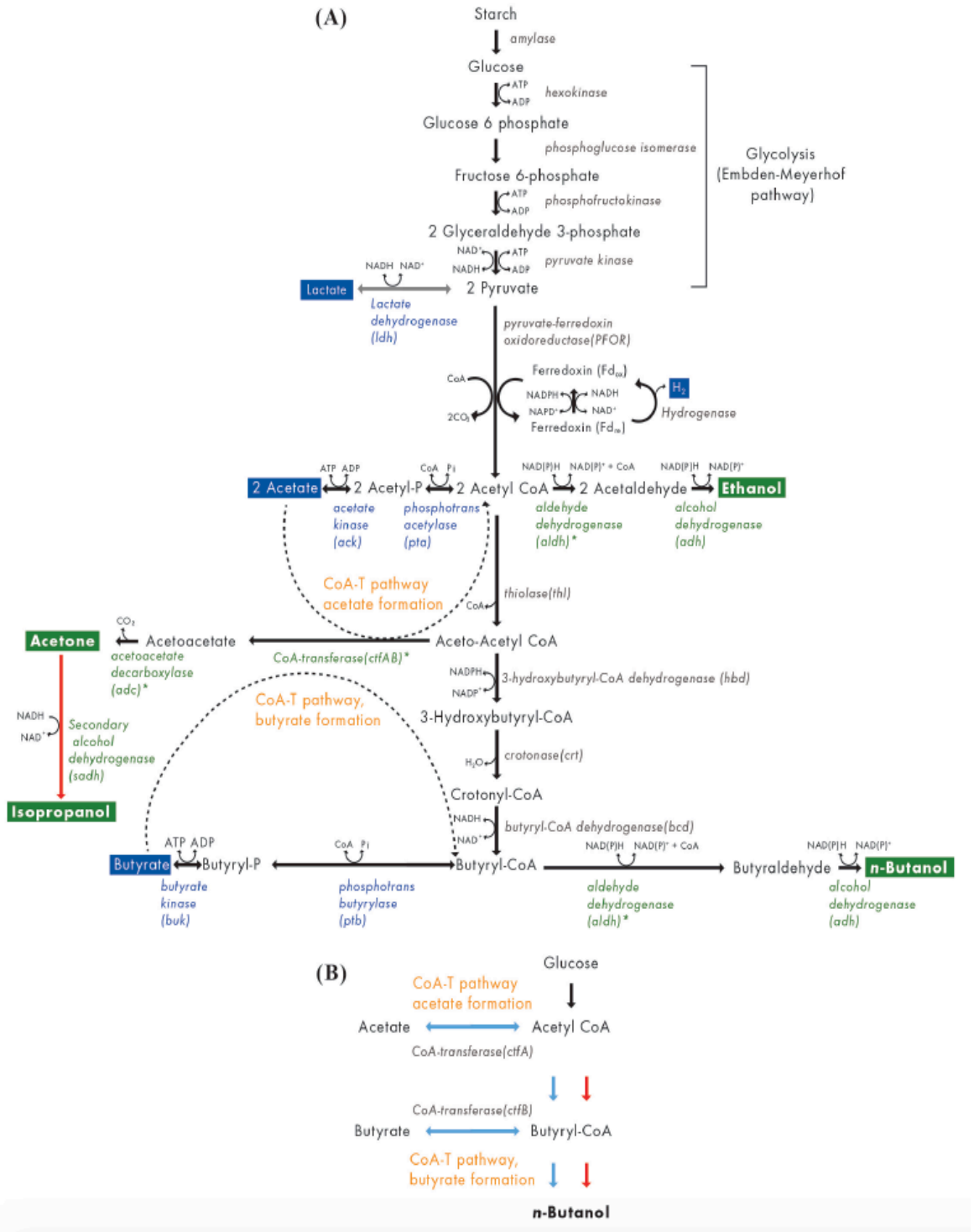


Figure 1.3 ABE Fermentation pathway A). The major products during acidogenesis are shown in the blue boxes, while those mainly produced during solventogenesis are shown in the green boxes. The dashed lines show the CoA-T pathway, where organic acids are re-assimilated during solventogenic growth. Enzymes are shown in italics. Asterisk (*) indicates genes and enzymes encoded by the sol operon. Pathway in red arrow indicates isopropanol production naturally occurs *C. beijerinckii*; Pathway in grey arrow indicates lactate production under unfavourable condition B). Butanol formation routes via “hot and cold channel(s)” in *Clostridium*. Blue arrows indicate the cold channel, which is the organic acid assimilation route. Red arrows indicate the hot channel, which is the direct route. Taken from (Ying., 2018)

1.5.4 Solventogenesis

The shift from acidogenesis into solventogenesis is closely linked to that of sporulation, as solvent production allows the cells to survive in a metabolically active form for a longer period of time under acid stress. Solventogenesis does come at a cost as the solvents produced (mainly butanol) are by in large toxic to the cells. The initiation of solventogenesis initiates the process of long-term survival through the formation of endospores. The master regulator for the solventogenic shift is the transcription factor Spo0A (Ravagnani et al., 2000). Spo0A is activated when it is phosphorylated by the phosphorelay two-component signal transduction system (Sandoval et al., 2015) in response to the drop in pH and accumulation of ATP, H₂ and CO₂ during acidogenesis. Upon phosphorylation Spo0A acts as the master regulator of both solventogenesis as well as sporulation, and deletion of Spo0A in *Clostridium saccharoperbutylacetonicum* N1-4(HMT) resulted in abolished solvent production on top of a detrimental effect on vegetative cells (Atmadjaja et al., 2019). Expression of Spo0A is a balancing act, and previous work shows that Spo0A overexpression favours a shift towards sporulation over solvent production (Harris et al., 2002).

Regulation for the shift from acidogenesis to solventogenesis is not only dependent upon the drop in pH due to acid production, the reducing environment created in the production of acetyl-CoA also play a key role. Electron flow within *Clostridium* is governed by ferredoxin. The cleavage of pyruvate to acetyl-CoA results in the transfer of an electron from a reduced ferredoxin to the hydrogenase, which uses the proton as its final electron acceptor and results in a rapid drop in the redox potential due to the increased H₂ produced at this step. Additionally, fermentation of carbohydrates increases the NAD(P)H:NAD(P)⁺ ratio within the cell, this ratio shift has been shown to result in the dissociation of the Rex complex from genes involved in butanol production aiding in the shift into solventogenesis (McLaughlin et al., 2010; Wietzke and Bahl, 2012). Overall the shift from acidogenesis to solventogenesis is regulated a complex network of phosphorylation, redox and pH drop due to acid production.

Upon shifting into solventogenesis, expression of genes involved in the solvent production takes place. The operon responsible for this is the *sol* operon. and the placement and arrangement of the *sol* operon can vary depending upon the *Clostridium* species. The Type I operon found in strains such as *C. acetobutylicum* is comprised of an *adhE-ctfA-ctfB* cluster (encoding a bifunctional butyraldehyde/butanol dehydrogenase and the two subunits of CoA transferase), and an adjacent, convergently transcribed, monocistronic *adc* operon (encoding acetoacetate decarboxylase). The Type II operon consisting of *ald-ctfA-ctfB-adc* (encoding NADH-dependent aldehyde dehydrogenase, CoA transferase, and acetoacetate decarboxylase) found in the genome in strains such as *C.*

saccharoperbutylacetonicum N1-4(HMT) and *C. beijerinckii* (Poehlein et al., 2017)(KOSAKA et al., 2007). Both operons are shown in Figure 1.4

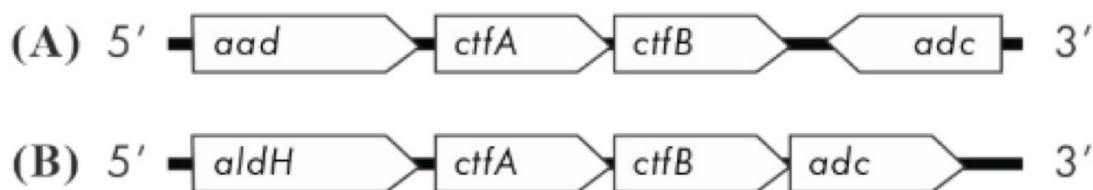


Figure 1.4 Type I and Type II Sol operon. A). Type I operon found in *C. acetobutylicum*. The sol operon structure of *C. acetobutylicum* is different from *beijerinckii*, and *C. saccharoperbutylacetonicum*, where the *aad* replaces *aldH*, and *adc* is part of a separate operon; B). Type II *C. beijerinckii*, and *C. saccharoperbutylacetonicum*. The sol operon structure of *C. beijerinckii*, and *C. saccharoperbutylacetonicum* are the same (Ying., 2018)

There are two pathways for butanol production, these are known as the “hot” and “cold” channels. The “cold channel” generates butanol via the re-assimilation of acetate and butyrate into acetyl-CoA and butyryl-CoA via the CoA- transferase (CoA-T) pathway. From here, acetyl-CoA is either converted to butyryl-CoA or reduced to ethanol. If converted to butyryl-CoA, butyryl-CoA will be reduced to form butanol. In the “Hot Channel” organic acid assimilation is prevented and is responsible for the direct conversion of acetyl-CoA to butyryl-CoA followed by reduction to butanol (Jang et al., 2012). The hot channel for butanol production prevents yield losses to CO₂ and acetone, as 1 mole of acetoacetate is generated from each mol of assimilated organic acid. acetoacetate is then decarboxylated into CO₂ and acetone (Jang et al., 2012; Ou et al., 2015). In their study Jang *et. Al.*, (2012) show that a reduction in the “cold channel” does indeed lead to a reduction in organic acid production however it also results in reduced butanol yields, hence decreasing the “cold channel” does not increase butanol yield unless organic acid production is stopped at the same time (Jang et al., 2012) (Figure 1.3).

1.6 Limitation of ABE fermentation and possible strategies for improvement of ABE fermentation

The industrial interest in the ABE fermentation process has continued to grow in recent years as butanol's potential as a chemical or fuel is ever-increasing. Companies such as Green Biologics Ltd who specialise in traditional lignocellulose ABE fermentation, and Lanzatech who specialise in C1 waste utilisation using acetogens and autotrophs have been paving the way for the industrial usage of *Clostridium*. As desirable as the idea of butanol production from ABE fermentation may be, the process itself needs to be economically viable. To achieve this economic viability improvements to current systems must be made. These improvements include (i) Acquisition of cheap readily available substrate that does not compete with land or human survivability; (ii) improvements of overall solvent yields and improvements to solvent recovery; (iii) improvements in strain capability to withstand toxicity of solvents, produce higher concentrations of solvents and diversification of compounds created using butanol as a precursor.

The cost of substrate in a conventional ABE corn starch process accounts for up to 79% of the total cost of production (Green, 2011). Due to this cost, it is imperative that cheap alternative feedstocks are sourced. As suggested previously in Section 1.3.2, lignocellulosic material has excellent potential as a feedstock. Lignocellulose is the most abundant renewable resource on earth, with India alone producing in excess of 370 million tonnes of this biomass every year from plant, rice husk and saw from saw mills (Kumar and Gayen, 2011). Due to the saccharolytic ability of *Clostridium*, lignocellulose has the potential to be an ideal substrate for ABE fermentation. However, to be efficiently metabolised during fermentation the lignocellulose must first be pre-treated. Pre-treatment enables (1) breakdown of lignin shell of lignocellulosic material; (2) breakdown of a large proportion of crystalline cellulose, this is key as it aids the *Clostridium* cellulosomes to further metabolise cellulose (Ezeji et al., 2007; Mitchell et al., 1995); (3) Increasing porousness, enabling access for enzymes. Pre-treatment methodologies have been reviewed extensively by Bharathiraja et al., (2017) who revealed that most methodologies for lignocellulose pre-treatment are highly efficient and can recover approximately 90 % of the fermentable sugar material. As discussed in Section 1.4.2 certain strains of solventogenic *Clostridium* are able to metabolise simple C1 carbons for the production of ethanol and acetate primarily (Köpke et al., 2010; Marcellin et al., 2016). In addition to lignocellulose the C1 waste gases from power plants and steel mills, syngas from agricultural waste, or reformed methane from bio gas offer additional renewable feedstock avenues (Takors et al., 2018).

One of the key issues that faces the industrialisation of the ABE fermentation process is the overall low yields of butanol that are obtainable. Typically, in fermentation broths there is a low percentage of butanol present usually around 1-2 % ($<20 \text{ g L}^{-1}$). This low yield is largely due to the toxic effect of butanol on the cells. Low butanol yields of $< 0.36 \text{ g / g}$ of sugar may be due to the heterofermentation of sugars and low butanol productivity due to low cell counts, which will also increase the cost of product recovery (Green, 2011; Ni and Sun, 2009; Tashiro et al., 2013). Fermentation conditions and optimisation have been extensively studied for various strains (Braguglia et al., 2017; Ezeji et al., 2003; Green, 2011; Latif et al., 2014; Liao et al., 2017; Procentese et al., 2018; Wang et al., 2012; Zhang et al., 2018) and batch fermentation is widely adopted for industrial ABE fermentation due to ease of use. Fed batch and continual fermentation are other alternative fermentation techniques used, although extended production times come with the trade-off of having lower concentrations of solvents per litre compared to batch processes. For successful fed batch or continuous fermentation, solvent recovery must take place throughout not only in a bid to maximise overall yield but also to maintain butanol concentrations that are below toxic levels. A number of recovery methods have been trialled over the years including pervaporation, gas stripping, liquid-liquid extraction, and liquid-membrane extraction (Bharathiraja et al., 2017). Fed batch cultures using pervaporation have been shown to produce butanol concentrations of 105 gL^{-1} , whereas traditional batch fermentation achieved butanol concentrations of around 12.8 gL^{-1} (Qureshi and Blaschek, 2000).

Finally, a major inefficiency within in the ABE process is the bacteria themselves. The butanol that they produce is inherently toxic, and because of this butanol concentrations rarely exceed 1- 2 % (v/v) in the fermentation media. Butanol has membrane distorting properties, where the hydrophobic chain and polar group can elicit severe damage to the cell (Baer et al., 1987)(Bowles, 1985). Butanol toxicity affects the cells in a number of ways; (i) ion transport is disrupted; (ii) nutrient transportation; (iii) composition of the phospholipid membrane is destroyed; (iv) finally the cells metabolism breaks down (Ezeji et al., 2010). Several attempts at elevating butanol toxicity have been attempted with limited success (Dunlop et al., 2011; Liu et al., 2014). In addition to this, phage infections have occurred previously in an industrial setting, in the 1980's in South Africa, a phage infection resulted in loss of ABE production. This resulted in strain rotation and isolation to strains resistant to the infection to be able to restart production (Jones et al., 2000).

1.7 Metabolic engineering in *Clostridium*

Despite the significant understanding of the *Clostridium* genus and its genome, the genus is notoriously difficult to engineer. As a result, tools available for genetic engineering of *Clostridium* have lagged behind those for Gram-negative species such as *E. coli*. Moreover, development of tools for creation of robust strain development in *C. saccharoperbutylacetonicum* N1-4(HMT) has lagged behind that of other *Clostridium* strains such as *C. acetobutylicum* and *C. beijerinckii*. Herein, we investigate the current technologies used for genetic engineering and how these tools have been applied in the improvement of industrial strains. Finally, other possible butanol-producing strains are introduced.

1.7.1 ClosTron

The ClosTron system was developed by Heap et al., (2007) as a *Clostridium* specific system that takes advantage of the TargetTron system developed by Sigma Aldrich, with the initial ClosTron vector (pMTL007) a tailored version of the plasmid pACD4k-C. Bacterial group II intron technology allows for site directed mutagenesis by retrohoming of the Mobile group II introns. Mobile group type II introns are retroelements responsible for reverse encoding transcriptases (RT), inserting into specific DNA target sites at a high frequency. The process of retrohoming involves the self-splicing of group II introns that are then reverse transcribed by their own reverse transcriptases. The process of retrohoming is mediated by a ribonuclease (RNP) complex consisting of an RNA lariat and an intron encoded protein. The RNP inserts bound RNA into one strand of the double stranded genomic target site, the RNA is then reverse transcribed resulting in its removal and replacement of it by DNA by the host repair machinery. This results in a stable integrated intron (Zhong et al., 2003) **(Figure 1.5)**.

The ClosTron system was developed to include a set of standardized parts such as promoters, origins of replication and retrotransposition-activated selection markers (RAM) suitable in *Clostridium*. The ClosTron introns were designed *in silico* using software that identifies sequences based for a 35 bp region that is recognised by the intron-encoded protein, allowing for targeting of the intron into the desired gene (Heap et al., 2010). ClosTron has been used for a number of targeted gene disruptions within a number of *Clostridium* spp. (Antunes et al., 2011; Cartman et al., 2010; Clare M Cooksley et al., 2012; Cooksley et al., 2010; Underwood et al., 2009; Wietzke and Bahl, 2012; Xu et al., 2014).

1.7.2 Double crossover recombination events

Double crossover recombination events allow for targeted gene disruption. The first crossover event incorporates a vector containing a pair of homology arms flanking a cargo sequence into the target locus via homologous recombination (HR). The second crossover event deletes the specific region between the homologous sequence, replacing it with the cargo DNA Figure 1.5. Double crossover events rely on the use of counter selection markers, these being elements that when present result in cell death. Counter selection markers are useful for selecting chromosomal insertions that do not contain any undesirable parts, i.e. vector backbone from the incomplete cross over event. Counter selection markers specific to *Clostridium spp.* were first developed by (Awad et al., 1995; Bannam et al., 1995).

One such system developed by Soucaille and colleagues (Soucaille et al., 2008) uses a negative selection marker for the second cross over event similar to that developed in *B. subtilis* (Fabret et al., 2002). In order to work correctly, this method requires a *C. acetobutylicum* strain that lacks the gene *upp*. The *upp* gene encodes the uracil phosphoribosyl-transferase and the *upp* deficient strain will be resistant to 5-fluorouracil. A knockout plasmid is required for this to work correctly. The knockout plasmid will contain DNA sequences that flank the region that is going to be deleted from the genome. An erythromycin cassette flanked on both sides by FRT sites is inserted into the plasmid that already contains a functional copy of the *upp* gene previously removed from the genome. Following transformation of the knockout plasmid, colonies were selected based upon their resistance to 5-fluorouracil and erythromycin. Introduction of a plasmid containing a Flp recombinase will allow for the removal of the erythromycin cassette and allow for additional genes to be cloned in as part of the process.

Allelic coupled exchange (ACE) is another form of coupling a counter selection marker gene to a desired double crossover event Figure 1.5. ACE methodology has been demonstrated in two ways. The first method involves exploitation of resistance to 5-fluorouracil by disruption of the *pyrE* or *pyrF* gene. ACE does not rely on the cells being auxotrophic for uracil prior to recombination, it also does not require a heterologous version of the gene to be used as counter selection marker. The process of ACE involves the use of asymmetric homology arms that direct the order in which the recombination occurs. The longer of the two arms ~1200 bp is immediately downstream of the *pyrE* or *pyrF* and directs first crossover event that incorporates the entire plasmid into the genome. The second crossover event is led by the shorter of the arms ~ 300 bp, which is homologous to a 300 bp internal region *pyrE* or *pyrF* and results in removal of the plasmid backbone. Following the second recombination event the wild type *pyrE* gene is replaced by a truncated form that will then allow for screening via 5-fluorouracil resistance (Heap et al., 2012).

Alternatively, a promoter-less heterologous *pyrE* gene or antibiotic marker can be inserted in the integration vector with the regions of homology. This is done in such a way that a successful double crossover event would place the silent gene directly downstream of a constitutive promoter (Heap et al., 2012). The use of ACE technology allows for the circumvention of prerequisite mutant strains created using the pMTL Clostron plasmids because of the use of antibiotic markers.

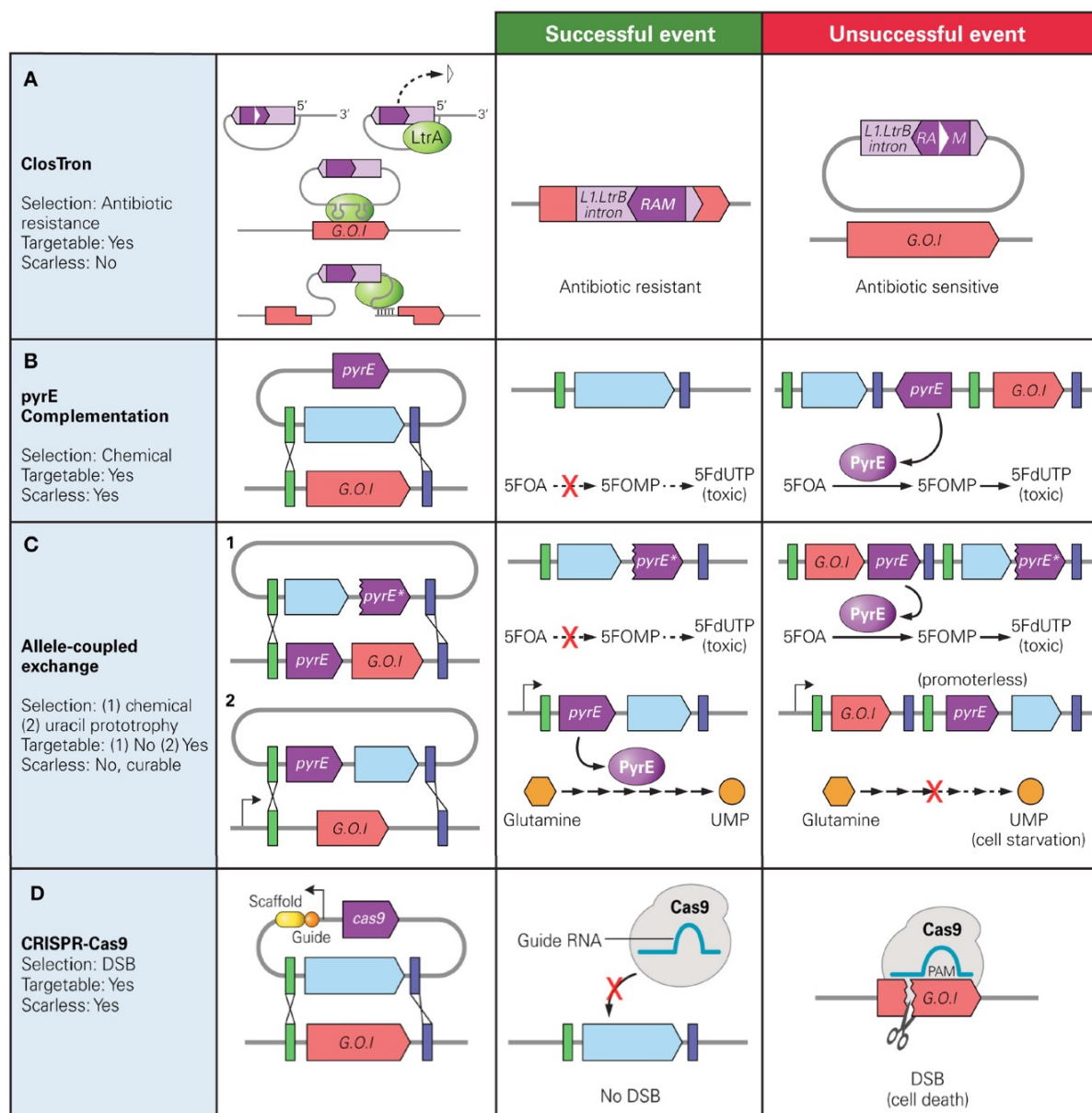


Figure 1.5 Counter selection markers used in *Clostridium* spp. and their mechanisms of action. The gene of interest (G.O.I) is represented in red with the intended insert in blue and the counter selection marker in dark purple. Green and Blue bars represent regions of homology between the insert and the genome. A). Clostron: RAM disrupted by a Group I intron (white triangle) is only active after the L1.LtrB intron is inserted into the chromosom; ; B). *pyrE* complementation: PyrE catalyzes conversion of 5-fluoroorotic acid (5FOA) to 5-fluororotidine monophosphate (5FOMP) producing toxic fluorodeoxyuridine monophosphate (FdUTP); C). Allele-Coupled Exchange: (1) double-crossover event at the *pyrE* locus results in truncated version of *pyrE* for counter selection with same mechanism as (B), (2) successful homologous recombination inserts a promoter-less copy of the *pyrE* gene directly downstream a native constitutive promoter, allowing production of uracil 5' monophosphate (UMP). Note: must be performed on *pyrE* deficient strain; (D) Cas9: successful homologous recombination gRNA-targeted double stranded break resulting in cell death. Diagram adapted from (Joseph et al., 2018)

1.7.3 CRISPR

Clustered Regulatory Interspaced Palindromic Repeats (CRISPR) alongside their associated Cas proteins are part of the adaptive immune system found in bacteria. This CRISPR/Cas defence process is best described in three main stages; (i) adaption of new genetic material, results in spacer sequence acquisition and insertion into the CRISPR locus within the cell; (ii) once acquired, *cas* genes are expressed and the CRISPR locus is transcribed into long CRISPR-RNA (pre-crRNA). The pre-crRNA is processed into mature crRNA by the Cas proteins and accessory factors; (iii) interfering DNA matching the crRNA and Cas proteins is destroyed (Boyaval et al., 2007).

Sequence repeats and spacer length used in the CRISPR locus are typically conserved within organisms but can vary between species. Repeat regions in the CRISPR cassette have been shown to be between 21-48 bp in length and spacers 26 -72 bp in length. Not all Cas proteins are found adjacent to the CRISPR loci, and sometimes these CRISPR loci rely upon trans-encoded factors. In addition to the spacer and repeat regions, there is a leader sequence that is conserved within the CRISPR locus relating to the direction of transcription of the crRNA (Rath et al., 2015). There is high diversity within the Cas proteins, with Cas1 and Cas 2 involved in the adaption stage of the adaptive immune mechanism and are thought to be universal in CRISPR/Cas systems (Makarova et al., 2002). Outside of that, Cas proteins are typically broken down into three main groups, Type I, Type II and Type III (Figure 1.6). Type I systems are defined by the presence of the protein Cas3, which has both helicase and DNase domains responsible for the degradation of target DNA. There are 6 subtypes of Type I systems A through F all with varying Cas genes present. Outside of *cas1*, *cas2* and *cas3* Type I systems all encode a Cascade complex. This complex binds to crRNA and locate the target. Cascade complexes have been shown to enhance the acquisition stage (Sinkunas et al., 2011). Type II systems are responsible for encoding Cas1, Cas2 and the Cas9 protein. Like the cascade complex Cas9 assists in the adaption stage, takes part in crRNA processing and cleaves target DNA assisted by crRNA with an additional RNA (*tracrRNA*). Like Type I systems, Type II systems are divided into sub types, A and B (Chylinski et al., 2013; Martin Jinek et al., 2012). Finally Type III, contain the signature protein Cas10 who's function is unclear at this point. Unlike Type I and Type II systems however, Type III systems have shown to target DNA as well as RNA (Staals et al., 2013).

The first use of CRISPR/Cas systems for genetic modifications was by the Type II Cas9 system known as *spyCas9* (Martin Jinek et al., 2012). This system originated from *Streptococcus pyogenes* and was formed of a single Cas9 protein that is able to bind and implement a double stranded break to targeted DNA sequences. To be able to target sequences the *spyCas9* system required a single guide RNA ~20 bp that was immediately adjacent to the protospacer adjacent to a motif (PAM). The PAM sight in this system was NGG and can be used to provide many possible target sites within a sequence.

Within *Clostridium* genetic engineering by CRISPR/Cas has mostly been used as a counter-selection method to screen against homologous recombination events Figure 1.5 (Bruder et al., 2016; Huang et al., 2016; Nagaraju et al., 2016; Wang et al., 2017a; Wasels et al., 2017). One major drawback of CRISPR/Cas systems in *Clostridium spp.* is their lack of non-homologous end-joining (NHEJ) systems meaning that Cas9-activated site directed breakage (DSB) can only be used to select against non-edited genes i.e. wild types (Xu et al., 2017). Despite recent advancements in genetic engineering tools and the advent of CRISPR/Cas toolkits within *Clostridium spp.*, the influence of low plasmid transformation efficiencies, lack of recombineering, and lack of NHEJ tools and other characterized genetic parts still act as a barrier that needs to be overcome to take full advantage the *Clostridium* metabolic chassis.

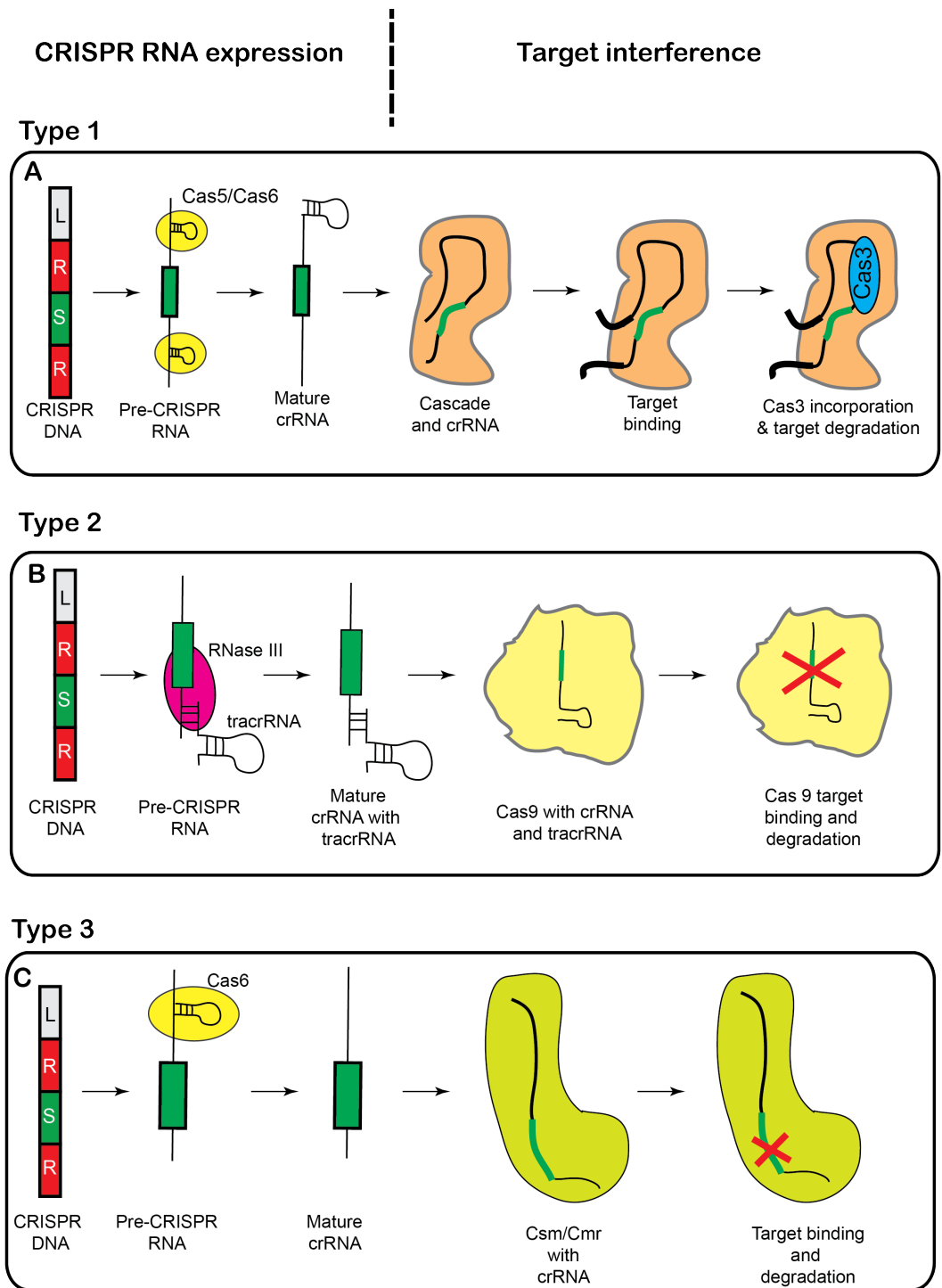


Figure 1.6 Model of crRNA processing and interference. A). In Type I systems, the pre-crRNA is processed by Cas5 or Cas6. DNA target interference requires Cas3 in addition to Cascade and crRNA. B). Type II systems use RNase III and tracrRNA for crRNA processing together with an unknown additional factor that perform 50 end trimming. Cas9 targets DNA in a crRNA-guided manner. C). The Type III systems also use Cas6 for crRNA processing, but in addition an unknown factor perform 30 end trimming. Here, the Type III Csm/Cmr complex is drawn as targeting DNA, but RNA may also be targeted

1.8 Well-characterised examples of metabolic engineering in *Clostridium* spp.

1.8.1 Engineered strains

Throughout the short history of genetic manipulation of *Clostridium* spp., a major focus has been on increasing solvent production by targeting the genes that are involved in acid and solvent production. The first successful example of such metabolic engineering reported a recombinant *C. acetobutylicum* with up-regulated *adc* (encoding acetoacetate decarboxylase) and *ctfAB* (encoding CoA transferase) genes (Mermelstein et al., 1993). Batch fermentation of this recombinant strain resulted in the earlier expression of acetone-forming enzymes leading to earlier acetone production. This recombinant strain produced elevated concentrations of acetone, butanol and ethanol of 95%, 37% and 90 % respectively. Another early study by Nair *et al.* (Nair and Papoutsakis, 1994) utilised the degenerated strain *C. acetobutylicum* M5 (Clark et al., 1989) that could no longer produce solvents or sporulate due to the loss of the pSOL1 mega plasmid encoding the alcohol dehydrogenase gene *adhE*. This strain could not be used for acetone production, but was able to produce butanol and ethanol. Despite its ability to produce butanol and ethanol, when butanol concentrations were around 10 g L⁻¹ the *adhE* M5 strain shifted to ethanol production over butanol. The M5 strain of *C. acetobutylicum* has been used as a background strain in a number of studies as a platform for the introduction of solvent production minus acetone production as demonstrated by (Nair and Papoutsakis, 1994). However, recent studies by (Sillers et al., 2008) showed that the M5 strain lacks the metabolic flexibility to be able to change its redox poise effectively enough achieve a desirable electron balance. In the study, when Silles *et al.* attempted to over express the *adhE* only strains with inactivated acetate kinases were able to produce transformants (Sillers et al., 2008), although these lead to increased acid production and decreased solvent production. This suggested that the strain was limited in its ability to balance redox potential and relied heavily on butyrate production as a means of balancing its production of reducing equivalents. Additional experiments have since been carried out to examine the effect of disruption of the butyrate forming pathway. In one study, the deletion of the *buk1* and *pta* genes encoding the butyrate kinase and phosphotransacetylase was carried out in an attempt to re-direct carbon flow through to solvent production and away from acid production (Green et al., 1996). The mutations were obtained by homologous, single cross-over events. Overall, the *pta* knockout had decreased acetate production and increased butyrate production, with the opposite being true for the *buk1* mutant. Solvent production was only affected in the *buk1* mutant, in fact the *buk1* deletion resulted in the strain being a butanol super producer. When tested under optimised conditions, this strain was able to

produce concentrations of 16.7 g L⁻¹ butanol, 4.4 g L⁻¹ acetone, and 2.6 g L⁻¹ ethanol (Harris et al., 2000).

In addition to over expression and gene knockouts, the use of technology for the disruption of genes without the need for full knockouts has been investigated. First of the technologies tested was anti-sense RNA (asRNA). The use of asRNA was first used to test its effectiveness in the reduction of the genes involved in butyrate formation (Desai and Papoutsakis, 1999). In this study two asRNA's were designed, one for the gene *buk* and the other for *ptb*. This work successfully reduced the butyrate kinase and phosphotransbutyrylase activities by 85% and 70%, respectively, with the concentrations of solvent and acid production from the asRNA comparable with the previous knockout strains (Green et al., 1996). The use of asRNA was also later used to demonstrate that CoA transferase was the rate limiting step in acetone production and not acetoacetate decarboxylase as previously believed (Tummala et al., 2003). A more recent and modern technique for the disruption of desired genes, is through the use of CRISPR interference (CRISPRi). This method was used by (Woolston et al., 2018) for the downregulation target genes in *Clostridium ljungdahlii*, an autotrophic *Clostridium*. CRISPRi was deployed in a strain engineered for 3-hydroxybutyrate (3HB) production. Downregulation of phosphotransacetylase (*pta*) with a single sgRNA led to a 97% decrease in enzyme activity and a 2.3-fold increase in titre. Unfortunately, acetone production still accounted for 40 % of carbon flux. In an attempt to overcome this acetone production, sgRNA downregulation of aldehyde:ferredoxin oxidoreductase (*aor2*) and an additional sgRNA targeted to *pta* reduced overall acetate production from 40 % of the carbon flux to 25 %, which lead to an increase in 3HB titre and yield.

Finally, due to the destabilising effects that butanol has on proteins and membrane fluidity, another prospective target for metabolic engineering is to engineer strains that have increased tolerance to butanol (Ezeji et al., 2010). The solvent tolerance mechanism of solventogenic clostridium involves the expression of molecular pumps, chaperone proteins such as *groES*, *dnaKJ*, *hsp18*, and *hsp90*, as well as genes involved in sporulation and fatty acid synthesis (Ezeji et al., 2010; Tomas et al., 2004). Tomas *et al.* were able to increase final solvent concentrations by the overexpression of GroES and GroEL heat shock proteins as part of the *groESL* operon (Tomas et al., 2003). When cells were exposed to stress conditions, GroES and GroEL assist in the refolding of misfolded proteins. During overexpression of the *groESL* operon, growth inhibition by butanol was reduced by 85 % in 2 g L⁻¹ butanol and 40 % in 4 g L⁻¹ butanol, compared to the control strain. This increase in butanol resistance enabled strains to tolerate solvent titres that were elevated by 33 %. Selective enrichment has also been used to try and increase resistance to solvents. Microarray analysis revealed that enrichment of a fragment containing the gene *ca_c1869*.

The strain that was responsible for the over expression of the gene *ca_c1869* (*ca_c1869* was annotated as a singleton transcriptional regulator) had an 80 % increase in its resistance towards butanol relative to the control (Borden and Papoutsakis, 2007).

1.8.2 Engineered *C. saccharoperbutylacetonicum* N1-4(HMT) strains

Unlike the more well characterised strain *C. acetobutylicum*, *C. saccharoperbutylacetonicum* N1-4(HMT) is a relative new comer to the world of industrial ABE production. First discovered in 1969 (Hongo and Ogata, 1969) the full genome sequence of the strain was not published until 2014 (Poehlein et al., 2014). Throughout the year's fermentation experiments using a wide variety of feedstocks have been carried out using this known butanol hyperproducing strain (Noguchi et al., 2013; Tashiro et al., 2007, 2004)(Al-Shorgani et al., 2012b). Early investigative work demonstrated that unlike *C. acetobutylicum* strains, cell degradation did not come from loss of the *sol* genes but more so from the breakdown of the regulation of the *sol* operon and upstream proteins in the system (Kosaka et al., 2007). Further to this, the mega plasmid found in *C. saccharoperbutylacetonicum* N1-4(HMT) has also been linked to ester production of butyl acetate and butyl butyrate (Gu et al., 2019) . Recently the development of CRISPR/Cas based tools for the genetic manipulation of *C. saccharoperbutylacetonicum* N1-4(HMT) has been established (Jenkinson et al., 2015; Wang et al., 2017a), with both systems published working by means of a counter-selection method to screen against homologous recombination events (Section 1.7.3). A large majority of the published strain engineering in this strain has been carried out by the Wang group from the University of Auburn. The group have carried out a number of strain metabolic engineering experiments in *C. saccharoperbutylacetonicum* N1-4(HMT). To better understand the butanol production mechanism of the strain, the key biosynthetic genes (either endogenous or exogenous) including the *sol* operon (*bld-ctfA-ctfB-adc*), *adhE1*, *adhE1^{D485G}*, *thl*, *thIA1^{V5A}*, *thIA^{V5A}* and the expression cassette EC (*thl-hbd-crt-bcd*) were over- expressed in the strain (Wang et al., 2017b). Overall over expression of the *sol* operon resulted in a 400% increase in the production of ethanol with the highest increase in butanol (13.7 %) seen in the strain with the over expression of the EC cassette. In an attempt to better understand and elevate the process of CCR, the group inactivated the sucrose metabolic pathway by inactivation of the gene *scrO*, doing this resulted in a decrease sucrose consumption by 28.9% and a decrease in ABE production by 44.1% using sucrose as the main carbon source. Additionally, deletion of the gene *scrR* alleviated CCR in the glucose/sucrose mixed fermentation; and over expression of the endogenous sucrose pathway resulted in increased ABE production (Zhang et al., 2018). (Atmadjaja et al., 2019) have demonstrated that it is possible to use the CRISPR/Cas technology for the creation of successful single nucleotide polymorphisms (SNPs), deletion and integrations within the genome of *C. saccharoperbutylacetonicum* N1-4(HMT).

1.8.3 Alternative butanol producing strains.

An alternative to metabolic engineering the *Clostridium spp.* directly is to bypass the species all together and produce *n*-butanol in other organisms circumventing many of pitfalls of the species. These circumvention tactics have typically involved the heterologous expression of the butanol production machinery from *Clostridium* into strains such as *E. coli* and *S. cerevisiae* (Fisher et al., 2014; Iddar et al., 2002; Kutty and Bennett, 2007; Morimoto et al., 2005) as they typically are more well-studied and more genetically accessible than *Clostridium*. However, these organisms typically are more sensitive to butanol concentrations in their media as well as a narrower substrate range amongst other issues (Luttke-Eversloh and Bahl, 2011). Despite these drawbacks, studies in *E. coli* from (Atsumi et al., 2008), (Inui et al., 2008) and (Nielsen et al., 2009) were able to successfully detect butanol production in concentrations of 550 mg L⁻¹, 1200 mg L⁻¹ and 520 mg L⁻¹ respectively. Finally, due to the powerhouse of reduction that solventogenic *Clostridium* are known for, similar to butanol production, introduction of genes from *Clostridium* have been introduced into *E. coli* in a bid to alter the reducing potential within *E. coli* (Iddar et al., 2002; Klein et al., 2010)

1.9 Aims of the Thesis

The research outlined in this thesis can be split into two major sections with the first section focusing on the design and construction of a cost effective, expandable, and easy to run fermentation system that enables like for like growth conditions that are found in industry leading fermentation systems. The second part focusing on improving the solvent producing capabilities of *C. saccharoperbutylacetonicum* N1-4(HMT) by the deletion of the gene *gapN*, deletion of *gapN* gene was achieved using proprietary CRISPR/Cas tooling known as CLEAVE developed by Green Biologics Ltd. Deletion of *gapN* was carried out as a means of recovering ATP that would otherwise be lost by transcription of the GAPN enzyme in *C. saccharoperbutylacetonicum* N1-4(HMT).

As part of the Shepherd lab fermentation testing, buffering compounds CaCO₃ and MES 'goods buffer' were tested with MES coming out as the pH buffering compound of choice due to its ability to effectively buffer the pH of the acids produced during fermentation, as well as its ability to dissolve easily into solution, something that CaCO₃ was unable to do. Successful culturing of *C. saccharoperbutylacetonicum* N1-4(HMT) was carried out using the shepherd lab fermenters and acids and solvents were successfully measured using GCMS.

The final section of this thesis focuses on the construction of the $\Delta gapN$ mutant *C. saccharoperbutylacetonicum* N1-4(HMT) strain and the characterisation of the phenotype differences of this strain compared to the wild type during fermentation. One of the main hypotheses in the deletion of the *gapN* gene was that there would be an increase in the internal concentrations of ATP which would result in increased concentrations of solvents acetone and butanol. Increased solvent production was hypothesised through the deletion of *gapN* as acid production in acidogenesis is responsible for generating a large concentration of the intracellular ATP, this in turn is then used for solvent production. Deletion of the gene *gapN* and the subsequent loss of GAPN in glycolysis would result in increased ATP concentrations which can then be used for solvent production, additionally, a decrease in acid production was expected to occur as the cell no longer needs to produce as much acid to generate the required ATP for solvent production and growth.

Chapter 2

Materials and Methods

2.1 Bacteriology Methods

2.1.1 Bacterial strains and plasmids

A list of all of the bacterial strains, plasmids this study can be found in Table 2.1 and Table 2.2 respectively. *Clostridium* strains were cultured in Reinforced clostridium media (RCM) (sigma 27546-500G-F) that was made anaerobic by autoclaving at 121 °C at 15 psi for 20 min in serum bottles sealed with butyl stoppers. Depending upon starter culture needed for an experiment either 30 mL or 100 mL of RCM was inoculated with 500 µL of 15% (v/v) glycerol stocks of *C. saccharoperbutylacetonicum* N1-4(HMT) and grown statically at 32 °C. *E. coli* strains were grown aerobically at 37 °C and shaken at 180 rpm in Luria-Bertani (LB) media. Starter cultures for *E. coli* growth were taken from single colonies plated out in LB agar plates.

Table 2.1 Bacterial Strains and Plasmids used in Thesis

Strain	Characterisation	Source or Reference
<i>C. saccharoperbutylacetonicum</i> N1-4(HMT)	DSM-14923 (=ATCC 27021)	DSM
	JM109 genotype: <i>endA1, recA1, gyrA96,</i> <i>thi, hsdR17 (r_k⁻, m_k⁺),</i> <i>relA1, supE44, Δ(lac-</i> <i>proAB), [F' traD36,</i> <i>proAB, laqI^qZΔM15].</i>	Promega
	Turbo Genotype: F' <i>proA⁺B⁺ lacI^q</i> <i>ΔlacZM15</i> <i>/ fhuA2 Δ(lac-</i> <i>proAB) glnV galK16</i> <i>galE15 R(zgb-</i> <i>210::Tn10)Tet^S endA1</i> <i>thi-1 Δ(hsdS-mcrB)5</i>	New England Biolabs
<i>E. coli</i>	DH5α genotype: <i>fhuA2</i> <i>Δ(argF-lacZ)U169</i> <i>phoA glnV44 Φ80</i> <i>Δ(lacZ)M15 gyrA96</i> <i>recA1 relA1 endA1 thi-</i> <i>1 hsdR17</i>	New England Biolabs

Name	Characteristic	Source or reference
PMTL Shuttle Vector System		
PMTL82154	Shuttle vector used in the construction of the homologous recombination vector. Contains Gram-positive origin (pBP1) element, antibiotic resistance marker (catP), gram negative replicon (ColE1 + tra) and a CatP reporter complex.	GBL, Clostron (<i>Heap et al. 2009</i>)
PMTL83251 +Ldr	Shuttle vector used in the construction of killing vector. Contains Gram-positive origin (pCB102), antibiotic resistance maker (emrB), gram negative replication (ColE1 + tra) and a MCS with the addition of the native leader sequence from the <i>C. saccharoperbutylacetonicum</i> N1-4(HMT) CRISPR/Cas system.	GBL, Clostron (<i>Heap et al. 2009</i>)
Gene Art – Spcr-dr-Spcr plasmid	Plasmid containing the spacer (Spcr), direct repeat (dr), spacer (Spcr) element that is blunt ligated into the killing vector. Vector additionally contains, gram negative replicon (ColE1), antibiotic resistance marker(Amp ^R).	Gene art

2.1.2 Oligonucleotides

All oligonucleotides used in this study are listed in Table 2.3. Oligonucleotides were designed using Benchling (<https://www.benchling.com/>). Each pair of primers were designed with less than 5°C difference in melting temperature (T_m) and less than a 5% difference in their GC content. Oligonucleotides were synthesised by Eurofins MWG.

2.1.3 Chemicals and water

All chemicals were purchased from sigma unless stated otherwise. Nutrient Agar, tryptone, yeast extract were all purchased from OXOID. Throughout distilled water was used for most experiments that did not require a high level of purity. For experiments that required a high level of purity, Milli-Q water was used. Solutions were sterilised by either autoclaving at 121 °C at 15 psi for 20 min or via filter sterilisation through a 0.2 µM filter.

2.2 Media/Buffer

2.2.1 Luria-Bertani medium

Luria-Bertani medium (LB) was prepared as described by Sambrook *et.al.*; (1987). The media consisted of 10 g sodium chloride (Fisher Scientific), 10 g peptone (Difco Laboratories), 5 g yeast extract and made up to 1 L with distilled water. Media was sterilised by autoclaving at 120 °C at 15 psi for 20 min.

LB agar was prepared by the addition of 1% (w/v) number 2 agar (Oxoid scientific) to LB medium and then autoclaved as before.

2.2.2 Reinforced Clostridium Medium

Reinforced Clostridium Medium (RCM) (Oxoid Scientific) consisted of 0.5g Agar, 0.5g L-Cysteine hydrochloride, 5 g D(+)-glucose, 10 g meat extract, 5 g peptone, 3 g sodium acetate, 5 g sodium chloride, 1 g starch, 3 g yeast extract and made up to 1 L with distilled water. RCM was sterilised by autoclaving at 120 °C at 15 psi for 20 min.

2.2.3 Yeast extract tryptone media

Yeast extract tryptone media (YETM) consists of 40 g L⁻¹ glucose, 2.5 g L⁻¹ yeast extract, 2.5 g L⁻¹ tryptone, 0.5 g L⁻¹ ammonium sulphate and 0.025 g L⁻¹ iron sulphate. YETM was sterilised by autoclaving at 120 °C at 15 psi for 20 mins.

2.2.4 X2 CGM Media

X2 stock GCM consists of 5.0g Yeast Extract, 0.75g Dipotassium Phosphate, 0.75g Monopotassium phosphate, 0.4g Magnesium sulphate, 0.01g Iron sulphate, 0.01g Manganese sulphate, 1 g sodium chloride, 2 g ammonium sulphate, 2 g Asparagine and made up to 500 mL with distilled water. Media was sterilised by autoclaving at 120 °C at 15 psi for 20 min.

LB x2 CGM is prepared as above but with the addition of 7.5 g agar (oxiod scientific) and made up to 500 mL. Media was sterilised by autoclaving at 120 °C at 15 psi for 20 min and then left at room temperature to set.

2.2.5 10% Sugar Stocks

10% Sugar stocks were made up in 500 mL and sterilised by autoclaving at 121 °C at 15 psi for 20 min.

2.2.6 X1 CGM Media

A bottle of 10% sugar is decanted into a bottle x2 CGM media. This now gives x1 CGM media with 5% sugar. X1 CGM agar is prepared in a similar way to x1 CGM minus agar, however prior to addition of 10% sugar the x2 CGM agar is melted in a microwave, and 10% is only added to solution when it is cool enough to be handled without thermal protection.

X1 CGM agar is prepared similar to x1 CGM minus agar, however prior to addition of 10% sugar the x2 CGM agar is melted in a microwave, 10% is only added to solution when it is cool enough to be handled without thermal protection.

2.2.7 Electroporation buffer with salt

Electroporation buffer with salt (EPB_S) consists of 300 mM sucrose, 0.6 mM sodium phosphate dibasic, 4.4 mM monosodium phosphate, 10mM magnesium chloride. Sucrose was sterilised by autoclaving at 121°C at 15 psi for 20 min. Sodium phosphate dibasic and monosodium phosphate were made into a phosphate stock. Phosphate stock buffer was then sterilised by 0.45 µM filter sterilisation. Magnesium chloride was sterilised by autoclaving at 121°C at 15 psi for 20 min. pH was adjusted to pH 6.0. Buffer components were assembled aseptically.

2.2.8 Electroporation buffer without salt

Electroporation buffer with salt (EPB_NS) consists of 300 mM sucrose, 0.6 mM sodium phosphate dibasic, 4.4 mM monosodium phosphate. Sucrose was sterilised by autoclaving at 121°C at 15 psi for 20 min. Sodium phosphate dibasic and Monosodium phosphate were made into a phosphate stock. Phosphate stock buffer was then sterilised by 0.45 µM filter sterilisation. pH was adjusted to pH 6.0. Buffer components were assembled aseptically.

2.2.9 SOB Media

SOB media contained the following: 20 g tryptone, 5 g yeast extract, 0.548 g sodium chloride and 0.186 g potassium chloride added to 990 mL of distilled water and autoclaved. Once cooled to room temperature 10 mL of 0.2 µM filter sterilised 2 M magnesium chloride was added.

2.2.10 SOC Media

To prepare SOC media, 20 mL of autoclaved 1 M glucose stock was added to 980 mL of SOB media.

2.3 Media Supplementation

2.3.1 Antibiotics

Media were supplemented, where indicated, with Thiamphenicol ($75 \mu\text{g mL}^{-1}$), Spectinomycin ($250 \mu\text{g mL}^{-1}$), Erythromycin ($100 \mu\text{g mL}^{-1}$ liquid and $40 \mu\text{g mL}^{-1}$ Solid) or chloramphenicol ($25 \mu\text{g mL}^{-1}$).

2.3.2 -(N-Morpholino) ethanesulfonic acid

2-(N-Morpholino) ethanesulfonic Acid (MES) (Millipore Corp. Cat: 475893-500GM) was used in fermentations at a concentration of 0.1 M as a buffering agent for pH control. MES was added to fermentation media and sterilised with the media by autoclaving at 121°C at 15 psi for 20 min.

2.3.3 Calcium Carbonate

Calcium carbonate (5 g L^{-1}) was used during fermentation as a buffering agent in the control of pH. Calcium carbonate was added to media and sterilised with the media by autoclaving at 121°C at 15psi for 20 min.

Table 2.3 Oligonucleotides used in this study

Name	Sequence	Description of Function
HR_F1	5' – ATAATGCTTGCTATTCTAGG – 3'	First forward primer used in the amplification of one of the HR 1kB fragments.
HR_R1	5' –ATCTTACTATTAATTTGTAAT AGTTGCTTTATTTTCACCTCTATCCATTG – 3'	Frist reverse primer used in the implication of one of the HR 1kB fragments
HR_F2	5' – AACAATGGATAGAGGTGAAAATAAAGCAACTATT ACAAATTAATAGTAAG -3'	Second forward primer used in the amplification of one of the HR 1kB fragments.
HR_R2	5' – AGCTACTTCCATATCAGAAAATTG -3'	Second reverse primer used in the amplification of one of the HR 1kB fragments.
M13F	5' - TGTA AACGACGGCCAGT – 3'	M13 Primers were used to amplify regions of interest in the pMTL80k plasmids that fell between M13F and M13R
M13R	5' – CAGGAAACAGCTATGAC – 3'	

2.4 Culture conditions

2.4.1 *E. coli*

10 mL starter cultures were inoculated from a single colony on an agar plate. Cells grown up aerobically overnight in LB (37 °C and 180 rpm). A 1% inoculum from the overnight was as starter culture when inoculating fresh media. Liquid *E. coli* cultures were grown in a New Brunswick™ Innova® 3100 water bath at 37°C and 180 rpm in 50 mL conical flasks containing 10 mL of LB medium, unless otherwise stated.

2.4.2 Preparation of glycerol stocks

Glycerol growth stocks of *Clostridium* were prepared by mixing 750 µL of 50% (v/v) glycerol with 750 µL of an overnight culture. Glycerol Stocks of *C. saccharoperbutylacetonicum* N1-4 were prepared by mixing 750 µL of 30% (v/v) glycerol with 750 µL of *C. saccharoperbutylacetonicum* N1-4 at an OD₆₀₀ of between 1.8 and 2.2. Stocks were stored at -80°C.

2.4.3 Culture optical density

The optical density of cultures was measured at 600 nm (OD₆₀₀) using a Shimadzu UV-1800 spectrophotometer in cuvettes with a 1 cm path length.

2.4.4 Butanol Toxicity

To test butanol toxicity the *Clostridium* cells were first inoculated from 15 % glycerol stocks into 30 mL of RCM in 30 mL serum bottles overnight. Following this, a 1 /10 dilution of the overnight cultures was used to inoculate YETM media containing 40 g L⁻¹ glucose. Cells were left to grown for 4 h to maintain a stable OD₆₀₀. Once cells had reached an OD₆₀₀ of ~ 2 they were challenged with various percentages v/v of butanol ranging from 0.5-5 %. Once challenged, growth of the cells was monitored to see the impact on butanol toxicity on growth rates.

2.4.5 Seeding of *Clostridium*

To be able to carry out fermentation experiments at the required volumes, the correct volume of inoculum was required in the correct media. This was achieved by growing *C. saccharoperbutylacetonicum* N1-4 firstly overnight between 18-24 h in 30 mL or 100 mL

RCM at 32 °C in serum bottles. From here, a 10% inoculum from the RCM overnights was used to inoculate 100 mL of the fermentation media in serum bottles. This was left overnight for 16-18 h at 32 °C. From here, the overnights in the correct media were used as a 10 -15 % inoculum into fermentation media at the required volume for the fermentation. Cells were monitored until the OD₆₀₀ reached a value of around 1.8-2.5. Once this was achieved the 3rd and final seed was used to inoculate the fermenters. The seed train can be seen in Figure 2.1

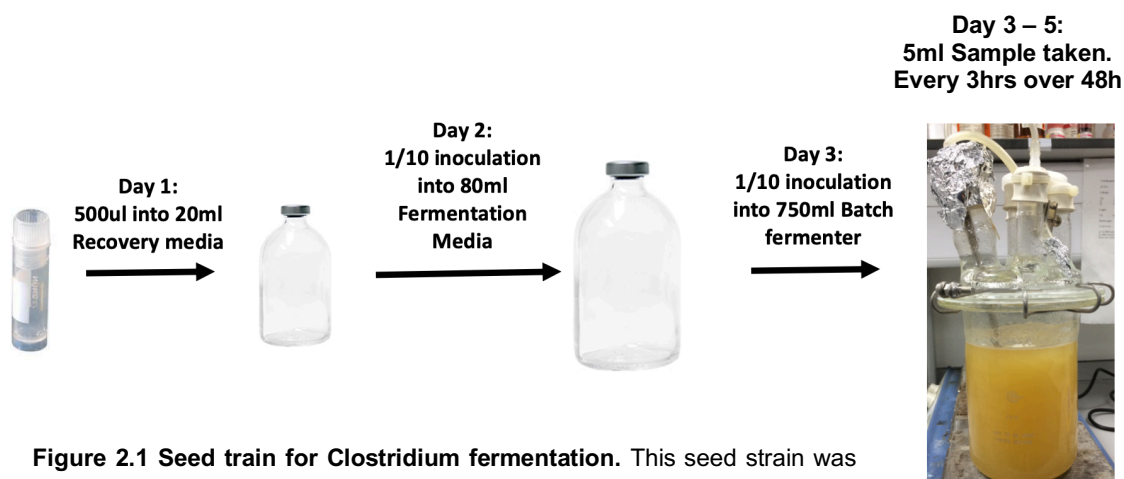


Figure 2.1 Seed train for Clostridium fermentation. This seed strain was used for fermentation experiments and allowed for establishment of a healthy starter culture for fermentation experiments.

2.5 Fermentations

2.5.1 Batch Fermentation – University of Kent Set up

Batch fermentation was carried out in 1 L culture vessels (SciLabware, Pyrex Quickfit) with a 500 mL culture volume at 32°C. Fermentation media consisted of a yeast extract tryptone media (YETM) (40 g L⁻¹ glucose, 2.5 g L⁻¹ yeast extract, 2.5 g L⁻¹ tryptone, 0.5 g L⁻¹ ammonium sulphate and 0.025 g L⁻¹ iron sulphate) at pH 6.2, supplemented with 0.1 M MES free acid (Merck, 475893) for pH control during fermentation. Anaerobic conditions in the fermentation were generated by sparging filtered (0.2 µm pore size) oxygen-free nitrogen through the fermentation media for 20 min pre-inoculation and then 5 min post-inoculation. Seed cultures were established by growing recovered RCM grown cells, in 80 mL YETM in serum bottles overnight to an OD₆₀₀ of ~4.0. The final fermentation inoculation was 10% (V/V). Fermentations were carried out in triplicate.

Throughout fermentation OD_{600} (Agilent technologies Cary 60 uv Vis), pH (Mettler Toledo, InLab pH) and redox potential (Mettler Toldeo, InLab Redox Micro) of the fermentation media was measured. Following measurement, supernatant and cells were separated by centrifugation at 8000 rpm for 10 min. Supernatant and cell pellet were separated and frozen at $-80\text{ }^{\circ}\text{C}$ for later use

2.5.2 Batch Fermentation – GBL

Batch fermentation was carried out in 2 L fermentation vessels (Electrolabs fermac 200) with a fermentation volume of 500 mL. Fermentation media consisted of a yeast extract tryptone media (YETM) (2.5 g L^{-1} yeast extract, 2.5 g L^{-1} tryptone, 0.5 g L^{-1} ammonium sulphate and 0.025 g L^{-1} iron sulphate), supplemented with 0.1 M MES free acid (Merck, 475893) for pH control during fermentation Anaerobic conditions in the fermentation were generated by sparging ($0.2\text{ }\mu\text{M}$ pore size) filtered oxygen free nitrogen through the fermentation media for 1 h pre-inoculation at a rate of 1 L min^{-1} . Fermentation sugars totalled 50 g L^{-1} consisting of 11 g L^{-1} glucose, 14 g L^{-1} xylose, 4.65 g L^{-1} galactose, 1.95 g L^{-1} and 18.4 g L^{-1} mannose.

2.5.3 Fed Batch Fermentation – GBL

Fed batch fermentation was carried out in 2 L fermentation vessels (Electrolabs fermac 200) with a fermentation volume of 1000 mL. Fermentation media consisted of a yeast extract tryptone media (YETM) (50 g L^{-1} glucose, 2.5 g L^{-1} yeast extract, 2.5 g L^{-1} tryptone, 0.5 g L^{-1} ammonium sulphate and 0.025 g L^{-1} iron sulphate), with a starting pH of 5.3. The pH was maintained via the addition of ammonium hydroxide (Fermac 260 pH controller) and fermentation media was agitated at 50 rpm throughout. The process of fed batch first involved an initial batch fermentation to allow sugars to drop to below 15 g L^{-1} and for cell culture to reach a high density. Following this initial batch fermentation, gas stripping (Section 2.5.4) was initiated to enable removal of solvents, preventing them reaching toxic concentrations. In addition to this, cell feeding was initiated. The media fermentation media was used as the media for feed. Feeding rate was altered throughout to maintain sugars below 15 g L^{-1} while still maintaining gas stripping.

2.5.4 Gas Stripping – GBL

To maintain non-toxic levels of solvents throughout the fed batch fermentation, $0.2\text{ }\mu\text{M}$ filtered N_2 was bubbled through the fermentation media at a rate of x3 the fermentation volume per minute which in our case was 3 L min^{-1} . Evaporated gases were not collected.

2.6 Genetic Methods

2.6.1 Isolation of plasmid DNA

Plasmid DNA was isolated using QIAprep Spin Miniprep Kit (QIAGEN) according to manufacturers' instructions. Overnight cultures were pelleted at 5000 x g for 10 min using a Sigma Laboratory Centrifuge 2k15. Following this first stage, all further centrifugation was carried out at 16000 x g in an Eppendorf 5415R micro centrifuge.

2.6.2 Polymerase chain reaction (PCR)

A number of different PCR reactions were carried out throughout the project. For *E. coli* colony PCR reactions (CPCR), a small fragment of a colony was taken with a sterile pipette tip and mixed directly into the pre-assembled reaction. For PCR reactions from isolated genomic material, firstly the genomic material was quantified using a nanodrop. Following quantification, <1000 ng of DNA was added to the pre-mixed PCR reaction mix. For *Clostridium* CPCR reactions, the colonies are first exposed to a lysis step. This lysis step involves a scrape of a colony being add to a lysis solution consisting of 0.25 µL of 20 mg ml⁻¹ proteinase K and 24.75 µl TE buffer pH 8.0. Following addition of colony and prior to CPCR, lysis PCR reaction was carried out, shown in Table 2.4 All PCR reactions carried out at the university of Kent used the 2x Q5 master mix (NEB) reaction mix shown in Table 2.5. 2x Q5 reactions are shown in Table 2.6 For all PCR reactions carried out at GBL Phusion polymerase mixture was used, reaction mixture Table 2.7 and experiment conditions Table 2.8 for Phusion are shown below.

Table 2.4 Lysis PCR reaction for *Clostridium* PCR

Temperature (°C)	Time (Min)
55	15
80	15
10	Final hold

Table 2.5 2x Q5 Master Mix PCR reaction mixture

Component	25 µl Reaction	50 µl Reaction	Final Concentration
Q5 High-Fidelity 2X Master Mix	12.5 µl	25 µl	1X
10 µM Forward Primer	1.25 µl	2.5 µl	0.5 µM
10 µM Reverse Primer	1.25 µl	2.5 µl	0.5 µM
Template DNA	variable	variable	< 1,000 ng
Nuclease-Free Water	to 25 µl	to 50 µl	

Table 2.6 2x Q5 PCR reaction

STEP	TEMP	TIME
Initial Denaturation	98°C	30 s
	98°C	5–10 s
25–35 Cycles	*50–72°C	10–30 s
	72°C	20–30 s/kb
Final Extension	72°C	2 min
Hold	4–10°C	

Table 2.7 – Phusion PCR reaction mixture

Component	20 µL Reaction	50 µL Reaction	Final Concentration
Nuclease-free water	to 20 µL	to 50 µL	
5X Phusion HF or GC Buffer	4 µL	10 µL	1X
10 mM dNTPs	0.4 µL	1 µL	200 µM
10 µM Forward Primer	1 µL	2.5 µL	0.5 µM
10 µM Reverse Primer	1 µL	2.5 µL	0.5 µM
Template DNA	variable	variable	< 250 ng
DMSO (optional)	(0.6 µL)	(1.5 µL)	3%
Phusion DNA Polymerase	0.2 µL	0.5 µL	1.0 units/50 µL PCR

Table 2.8 – Phusion PCR reaction

STEP	TEMP	TIME
Initial Denaturation	98°C	30 s
	98°C	5-10 s
25-35 Cycles	45-72°C	10-30 s
	72°C	15-30 s/kb
Final Extension	72°C	5-10 min
Hold	4-10°C	

2.6.3 DNA electrophoresis on agarose gels

1 % (w/v) agarose gels were prepared and ran in 1 x TEA buffer and electrophoresis was carried out using gel apparatus at 80 V 300 mA for 45 min to 1 h depending upon fragment size. Samples were mixed with a 6x blue/orange loading dye (Promega). A 1 kb DNA ladder (Promega) was used for Kent samples or 1 kb gene ruler (Thermo) for GBL samples. Following running of the gel, DNA samples in the gels were stained with 100 mL of 0.5 mg mL⁻¹ ethidium bromide (in water) and visualised on a UV box.

2.6.4 Preparation of *E. coli* competent cells

E. coli from overnight cultures were used as a 1% (V/V) inoculum into 100 ml of fresh LB. These fresh inoculations were left to aerobically grow at 37 °C shaking at 180 rpm until OD₆₀₀ reached 0.4 – 0.5. When optimum OD₆₀₀ was reached, cells were immediately put on ice for 30 minutes, once the 30 minutes was up, the cells were centrifuged at 2300 xg for 5 min to pellet the cells. The pelleted cells were then resuspended in 10 ml of pre-chilled ice cold 100 mM CaCl₂ and left for 2 h. Once the two hours had passed, the cells were pelleted again, and then resuspended in 2 ml ice cold 100 mM 30% glycerol and snap frozen in a dry ice ethanol bath and stored at -80 °C for future use. Cells were kept a maximum of 6 months as to not lose competency.

2.6.5 DNA ligations

Sticky end ligations

Following digestion of both the desired insert and plasmid with compatible sticky end enzymes, a reaction mixture of 50 ng total vector backbone was mixed with varying molar ratios of insert at 1:1, 1:3, 1:5. Following mixing, 2 x rapid ligation buffer (Promega) was added alongside 2 µL of T4 Ligase (Promega) and total volume made up to 20 µL. Following this, reactions were incubated at 22 °C for 2-3 h or overnight at 4 °C and then transformed into a variety of chemically competent *E. Coli* cells. A vector cut with a single sticky end enzyme was also ligated and transformed during these experiments as a positive control.

Blunt end Ligations

Following identification of a blunt end restriction sites in the plasmid of choice, successful PCR amplification of insert and clean-up of DNA was then used to calculate molar ratios of vector to insert similar to stick end ligation, ratios: 1:1, 1:3 and 1:5 were calculated. Once molar ratios were calculated 50 ng of Vector, the required volume of PCR insert for correct

molar ratio, 5 μL of x 2 rapid ligation buffer (Promega), 0.5 μL of blunt cloning enzyme of choice were added to a PCR tube and made up to 9 μL with nuclease free water. Once assembled, reaction was incubated in thermos cycler for 30 min to allow optimum digestion of plasmid. When digestion is complete, 1 μL of T4 Ligase was added to the reaction mixture, reaction was then returned to incubation in the thermo cycler for 3 h at 22 °C. Finally, after the 3 h incubation was finished 2 μL of x10 cutsmart buffer (NEB), 0.5 μL blunt enzyme of choice (NEB) and 7.5 μL of nuclease free water were added to the reaction and left to incubate for 1 h at 37 °C. Following this incubation, 5 μL of final blunt mixture was transformed into chemically competent *E.coli*.

Gibson assembly

Using the NEBioCalulator (<http://nebiocalculator.neb.com/#/ligation>) the correct pmol concentration of vector and insert were calculated to ensure maximum success. For the Gibson assembly concentrations of between 0.02 – 0.5 pmol are required for an optimal reaction. Following these calculations, the inserts and vectors were added to 10 μL 2 x Gibson assembly master mix and then incubated in a thermocycler at 50 °C for 1 h. Reactions after incubation were stored at -20 °C or 2 μL of assembled reaction was transformed into chemically competent *E. Coli*.

2.6.6 Transformation of *E.coli* competent cells

Plasmid DNA (2-5 μL) or reactions from Gibson assembly or ligations were mixed with 50 μL of competent *E. coli* cells and incubated on ice for 30 min. Cells were then heat shocked for 45 s at 42 °C and then immediately placed on ice for 2 min. 200 μL of SOC media was added and the cells were left to recover at 37 °C shaking at 200 rpm for 1 h. The cells were then spread onto LB agar plates (containing appropriate antibiotic), and left to grow for either 37 °C overnight or on the bench for 48 h.

2.6.7 Clostridium transformations

Day 1:

54 mL of 1 x GCM glucose media was aliquoted into a 250 mL flask along with 10 mL of the same media into a 50 mL sterile universal tube. The aliquoted 1 x CGM glucose media was transferred into the anaerobic chamber (Whitley A85TG Workstation) along with 1 mL aliquots of EPB_S and 50 mL of EPB_NS (Section 2.1.4.8) and left overnight to equilibrate with the anaerobic atmosphere. Alongside media, overnight cultures of *C. saccharoperbutylacetonicum* N1-4(HMT) were prepared from glycerol stocks (Section 2.4.2). Glycerol stocks were inoculated into either 30 mL or 100 mL RCM and then left to grow overnight at 32 °C.

Day 2:

The overnight cultures that were grown in either 30 mL or 100 mL RCM serum bottles (Section 2.2.2) were degassed prior to aliquoting. Degassing involves piercing of the rubber septum of the serum bottle using a needle and syringe that has had the plunger removed. Degassing decreases the internal pressure within the serum bottle for safe removal of the metal cap and rubber septum. The degassing of the overnight cultures was carried out outside of the chamber. Following degassing 10 mL of the overnight culture was transferred to a 50 mL universal tube (this was done outside of the chamber). The 50 mL universal tube containing 10 mL of overnight culture was transferred to the anaerobic chamber where 6 mL of the overnight culture was used to inoculate the 54 mL of 1 x GCM from left to equilibrate in the chamber overnight from day 1. This culture was grown at 32 °C in the anaerobic chamber until the OD₆₀₀ reached 1.2. 25 mL of this culture was then decanted into 2 x 50 mL falcon tubes, which were placed on ice to cool for 15 min. After 15 min, cells were centrifuged at 4000 xg and 4 °C for 10 min. The pelleted cells were transferred back into the anaerobic chamber, the supernatant was discarded, and 20 mL of EPB was used to resuspend one of the cell pellets. These resuspended cells were transferred into the second falcon tube and the second pellet was resuspended. Following resuspension, cells were centrifuged at 4000 xg and 4 °C for 10 min and the supernatant was discarded. The cell pellet was placed on ice immediately and then resuspended in 1 mL EPB_NS. After resuspension, 200 µL of EPB_NS suspended cells were transferred to electroporation cuvettes that were pre-chilled on ice containing the correct amount of DNA (**Appendix D**) for electroporation and left on ice to chill for 5 min. The electroporator delivered 1.5 kV to the cuvette, and immediately following electroporation 1 mL of 1 x GCM was added to the cuvette and cells were left to recover in the anaerobic chamber in the cuvette overnight.

Day 3 – 7:

After recovering overnight, 200 µL of cells were plated out onto GCM agar containing the correct selective antibiotic and left for between 48 – 72 h to allow for the appearance of *Clostridium* colonies. After colonies appeared, a single colony was taken and CPCR was carried out to check for the correct plasmid. Following identification of the correct plasmid, the colony was grown overnight in 10 mL RCM at 32°C overnight inside of the anaerobic chamber, the following day subsequent 15% glycerol stocks (Section 2.4.2) were made and stored at – 80 °C for future use.

2.6.8 CLEAVE™

Patent: WO2015159087A1

CLEAVE is CRISPR/ Cas technology developed by Green Biologics limited (Jenkinson et al., 2015). Overview of functionality is described in Chapter 4.

2.6.9 Sequencing of DNA

To confirm successful mutagenesis DNA samples were sequenced by Eurofins and the data was analysed using Benchling (<https://www.benchling.com/>). For whole genome sequencing libraries were prepped using Nextera® XT DNA Library Prep Kit from Illumina® following the manufacturer's instructions. Library preparations were then sequenced using an Illumina® MiSeq benchtop sequencer using a MiSeq reagent kit v3.

2.8 Biochemical Methods

2.8.1 NADPH: NADH Assay

Extraction Technique

The extraction technique from Beri et al., (2016) was used. 2 mL from exponentially growing and stationary phase culture was added to 1 mL of 1 M HCL for NAD(P)⁺ extraction and 1 mL of 1 M KCL for NAD(P)H extraction. Cells were incubated at 55°C for 10 minutes. Following incubation, the pH of the samples was neutralised to pH 6.5 for acid samples and pH 7.5 for base samples. This was achieved by adding 1 M HCL and 1 M KCL dropwise with continual vortexing. After neutralisation, samples were centrifuged for 15 min at 4400 x g, with the supernatant following centrifugation being saved for subsequent analysis. Two biological repeats and two technical repeats of each biological repeat were taken.

Quantitation of NADH and NADPH

Concentrations of NADH and NADPH were measured using previously described methods (Baker, 2016; Bernofsky and Swan, 1973; Nisselbaum and Green, 1969). In brief, the reaction mixture for the NADH assay consisted of 100 µL 1M tricine-NaOH (pH 8), 100 µL 40mM EDTA, 100 µL 0.1 M NaCl, 100 µL 4.2 mM MTT, 100 µL 16.6 mM PES, 100 µL 100 % EtOH . The reaction mixture for NADPH assay consisted of 100 µL 1M tricine-NaOH (pH 8), 100 µL 40mM EDTA, 100 µL 0.1 M NaCl, 100 µL 4.2 mM MTT, 100 µL 16.6 mM PES, 100 µL 10 mM Glucose-6-phosphaete. 500 µL of each of the assay mixture was added to 100 µL of extracted sample, topped up to 900 µL with 0.1 mM NaCl and incubated at 37 °C (change to °C throughout) for 5 min. To generate standard curves, similar reactions were set up where the extracted sample was replaced with nucleotide solutions of known concentration. 100 µL of Alcohol dehydrogenase and 100 µL Glucose-6-phosphate dehydrogenase were then added at 10 U of enzyme per reaction. The reaction was incubated at 37 °C for 1 h in the dark. 500 µL of 5 M NaCl was then added to stop the reaction and precipitate MTT. Samples were centrifuged at 4°C and x10,000 g for 5 min. Supernatants were decanted and the MTT pellets were resuspended in 1 mL of ethanol, and absorbance was measured at 570 nm

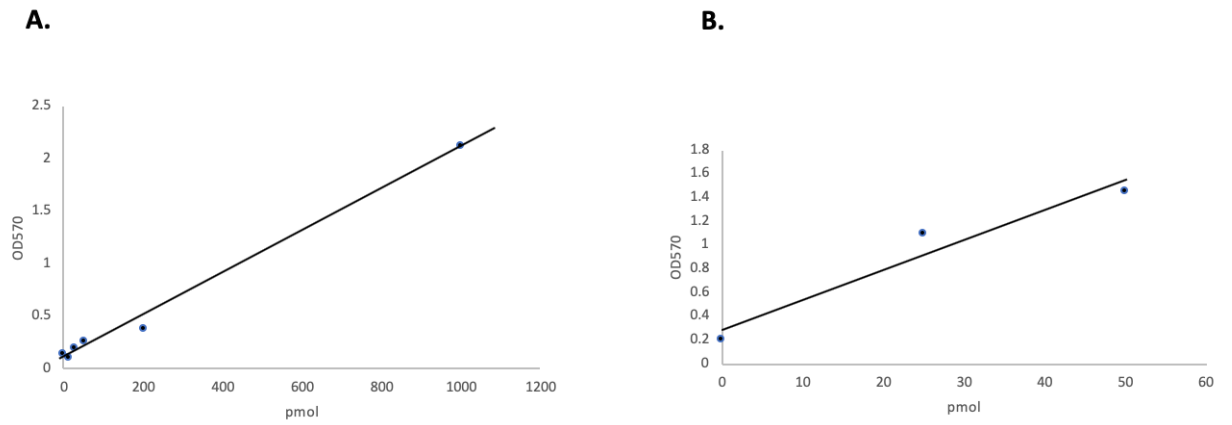


Figure 2.2 (A) NADH and (B) NADPH standard curves.

2.8.2 ATP Luminescence assay

ATP was quantified in cells grown anaerobically in P2 minimal media (Baer et al., 1987) using a luminescence assay according to the manufacturer's instructions (Abcam ab113849).

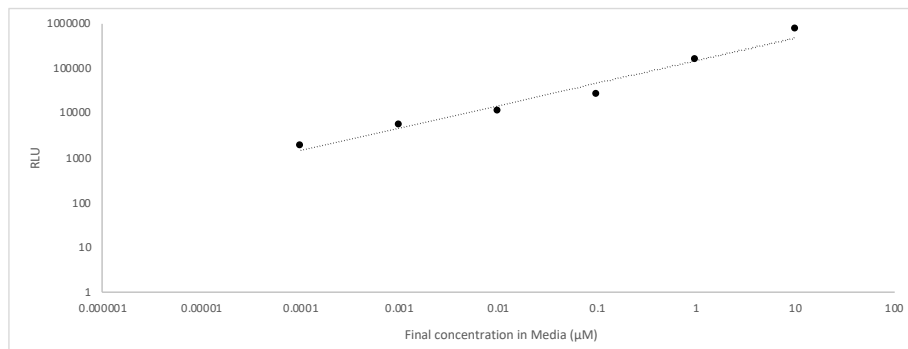


Figure 2.3 ATP standard curve diluted in YETM media. Relative light units were collected with 0.5 sec integration time

2.8.3 GCMS quantification of acids and solvents

Solvent analysis was carried out using Gas Chromatography Mass Spectrometry (GCMS) of the fermentation supernatant samples. Agilent 6890N at the University of Kent was used for this. The GC was equipped with 7HG-6013-11 Zebron. Helium (>99.999%) was used as the carrier gas, with a constant flow rate of 1 mL⁻¹ minute. A 0.2 µL water sample was injected with a 100:1 split. Injection temperature was set to 150°C, the GCMS transfer line temperature was set to 280 °C, ion source 230 °C, quadrapole 150 °C. After injection column temperature was held at 30 °C for 5 min, following this increased to 150°C at the 20 min mark. Compounds were identified by comparing retention times of each of the compounds with retention times of reference compounds.

2.8.4 HPLC quantification of sugars (Kent)

Fermentation supernatants were removed from the -20 °C and allowed to thaw to room temperature. Once samples had reached room temperature they were homogenised and centrifuged at 13400 xg for 5 min. 200 µL of the sample was then added to 600 µL of HPLC grade water, achieving a x4 dilution and a total volume of 800 µL. Glucose concentrations were measured using cation exchange chromatography. Column used was a phenomenex rezex ROA H+ 1 ml minute⁻¹ 5 mM sulphuric acid. Samples were run at 60°C and compared to known standard concentrations for glucose.

2.8.5 HPLC quantification of sugars and solvents – GBL

Fermentation supernatants were removed from the -20 °C and allowed to thaw to room temperature. Once samples had reached room temperature they were homogenised and centrifuged at 13400 xg for 5 min. 200 μL of the sample was then added to 600 μL of HPLC grade water, achieving a x4 dilution and a total volume of 800 μL . Prior to addition to HPLC tubes, samples were filtered through a 0.2 μm cellulose filter to remove any remaining bacteria, ensuring that they are unable to affect the results by still being metabolic active. Samples are analysed using Bio Rad Aminex HPX-87H column. Solvents, acids and common sugars run under the following conditions **Table 2.9**.

Condition	Setting
Elution type	Isocratic elution
Flow rate	0.9 mL/min
Oven temperature	85 °C
Run time	Maximum 30 min
Injection volume	10 μL
Detector type & detection temperature	Refractive index at 35 °C
Mobile phase	5 x 10 ⁻³ mol/L H ₂ SO ₄
Seal wash	10% methanol
Injector wash	HPLC grade water

2.8.7 Glucometer Sugar measurements

Glucose concentrations were measured during fermentation using a Sinocase Safe AQ Smart Blood glucose monitoring system. Samples were taken during fermentation and centrifuged at 13400 xg for 5 min. Following separation from the cell mass, a glucose test strip was submerged into the supernatant to gain a reading for glucose concentration in each sample.

2.9 Genomic sequencing and analysis methods

2.9.1 Clostridium Genomic DNA isolation

Genomic DNA was extracted using the GenElute™ bacterial genomic DNA kit (*Sigma NA2100-1KT*) following manufactures instructions.

2.9.2 Whole Genome sequencing

Whole genome sequencing was carried out using the illumina MiSeq system Genome library for both the wild type strain and the $\Delta gapN$ were prepared using the Nextera® XT DNA Library Prep Kit, which is optimized for small genomes. Once the libraries were prepared, they were sequenced using an Illumina MiSeq benchtop sequencer.

2.9.3 Assembly and annotation

Following Illumina® MiSeq, the read quality was assessed with FastQC (<http://www.bioinformatics.babraham.ac.uk/projects/fastqc>). To improve read quality reads were trimmed using Trimmomatic (Bolger et al., 2014). Trimmomatic improves read quality of the illumina reads by removing sequence adapters, trimming bases at the beginning and end of the reads if they fall below the stipulated threshold, finally it eliminates any of the reads that fall below the minimum read length, which by default is set to 36 bp. Following this, reads mapped using BWA (Li, 2013) to the reference genome for *C. saccharoperbutylacetonicum* N1-4(HMT) obtained from Genbank (CP004121.1). The quality of the genome maps were assessed using Qualimap (García-Alcalde et al., 2012). Functional annotation was performed using PROKKA (Seemann, 2014) and Roary (Page et al., 2015) was used for analysis of gene content and the pangenome.

2.9.4 Variant identification

To asses any variation between the Wild type and $\Delta gapN$ *C. saccharoperbutylacetonicum* N1-4(HMT) SNP analysis of the BWA assembled genomes to the reference genome *C. saccharoperbutylacetonicum* N1-4(HMT), Snippy was used (<https://github.com/tseemann/snippy>). In addition to SNP analysis, PROKKA (Seemann, 2014) was used to annotate the assembled illumina reads and identify properties such as tmRNA, CDS, rRNA and tRNA in each of the assemblies. Genome alignments were achieved using the online tool GVIEW (<https://server.gview.ca/>).

Chapter 3

Design and construction of fermentation platform and establishment of analytical tools for ABE fermentation analysis

3.1 Summary

Clostridium species are known to be difficult to handle due to their anaerobic nature and typically require specialist equipment for their culture such as anaerobic chambers, serum bottles and fermentation systems. As the overall goal of the project was to optimise solvent production in *Clostridium spp.* we required a three-vessel parallel fermentation system to provide consistent culture conditions. To achieve this, a bioreactor was designed and constructed that had the capabilities for batch and fed batch processes, and could even be set up for continuous fermentation experiments at a fraction of the cost of commercial systems. This system has a reduced cost per unit comparatively, and carries over many of the same functionality of those systems with a higher price point of entry, including in-line monitoring of temperature, pH, redox poise. In future, this system will be of interest to researchers in low to middle income counties that require high performance parallel fermentation platforms but commercial systems are financially out of reach.

Following instalment of the fermentation system, techniques to analyse the acids, solvents and sugars from the fermentation mixture were established allowing for small scale fermentation reactions to take place. This allowed for the characterisation of strains to take place in a scaled down industrial setting. CaCO_3 and MES were compared as buffering compounds for controlling the pH of the fermentation, MES provided more accurate measurements in comparison to CaCO_3 and was chosen preferentially going forward in batch experiments. GCMS was established as the preferential method for acid and solvent detection. HPLC was used to quantify sugar concentrations of fermentation supernatant samples. In addition to this, in keeping with the cost-effective theme of the project, glucometers that are typically used for the measurement of blood glucose concentrations in diabetics were tested alongside HPLC analysis of glucose. Overall the concentrations of glucose measured by the glucometer correlated with around 88% accuracy to the concentrations detected by HPLC.

3.2 Introduction

For the culture of solventogenic clostridial strains, three main types of fermentation have been studied in depth. These are, batch, fed batch and continuous fermentations. Of these techniques, batch culture is the quickest and simplest of the three methodologies. Batch fermentations start with an initial high concentration of feed. Throughout the process of batch fermentation, this feed is metabolised and the production of ABE solvents occurs. Batch fermentations have been carried out on a number of species using a number of differing feedstocks (Al-Shorgani et al., 2012a; Ellis et al., 2012; Mermelstein et al., 1993; Noguchi et al., 2013; Qureshi and Blaschek, 2000). The control of pH is crucial during batch fermentations as the drop of pH due to acid production allows for the solventogenic shift to occur. However, for optimum solvent production the pH cannot be allowed to drop and cause acid crash (Maddox et al., 2000), and the pH also cannot be maintained too high as this will lead to inefficient solvent production (Zheng et al., 2015). There are, however, a number of drawbacks from batch fermentations. These drawbacks include: (i) inhibition of solvent production and accumulation of vegetative cells as a result of butanol toxicity build up in the system; (ii) carbon catabolite repression during batch fermentation; (iii) lengthy downtime and start up time between fermentation cycles and treatment of fermentation media.

Fed-batch fermentations begin with high concentrations of feedstocks. Typically fed-batch systems are run initially as a batch fermentation alone, despite using a large majority of the feedstock this initial batch will allow for the establishment of a dense culture medium of cells. This high density of cells following the batch will be in the solventogenic phase of their growth. Once this phase is reached, the cells are fed with additional feedstock to take advantage of the cells solventogenic phase for an extended period of time that would not be possible in traditional batch fermentations. However, due to the toxicity of solvent accumulation, butanol in particular, fed-batch systems have traditionally been investigated in tandem with various solvent recovery methods to maximise the solvent production and yield during the fermentation process (Jang et al., 2012; Outram et al., 2017; Qureshi and Blaschek, 2001, 2000). Finally, continuous fermentation is a chemostat culture whereby the concentrations of cells, substrates and products are at a steady state following the gradual addition of multiple culture volumes of fresh fermentation broth. One of the main drawbacks of continuous fermentation with *Clostridium* is a low cell count. This has been overcome via the use of cell immobilisation in various carriers as well as cell recycling using membranes (Tashiro et al., 2013).

3.3 Results

3.3.1 Fermenter design and construction

Having the ability to run fermentation experiments is key to better understanding the process of the ABE fermentation, as it replicates a scaled down version of what is seen in an industrial setting. The fermentation facility will enable the following; (i) characterisation of a variety of growth conditions as well as feedstocks that could be used in an industrial setting; (ii) Characterisation of any genetic engineering that is achieved on *Clostridium* and how these changes affect the overall cell life cycle as well as the effects on ABE production during fermentation.

One of the main hurdles in establishing a fermentation protocol is the cost of entry per unit. Prices for these fermentation units can range from entry at 8000 GBP per unit, to upwards of 25,000 GBP per unit (Table 3.1). Knowing this, we set about to establish our own fermentation system that could retain as much of the functionality of the commercial units, but at a fraction of their cost. Overall, there were 3 main criteria for the fermenters:

1. Flexibility in fermentations style, i.e. batch, fed batch or continuous culture.
2. Affordable (Cheaper than current market products)
3. Upgradeable, i.e. new style head gaskets, culture volume change or additional probes/electrodes addition.

To ensure that these criteria could be met along with retaining all the required functionality, research of commercial fermentation units was carried out. This functionality included temperature control to accommodate varying preferential growth temperatures of different organisms. Most of the systems researched used either an electric heated jacket system, such as the fermac 200 and the F0-Baby, or a jacketed water system like that seen on the BioFlo 120 from Eppendorf (Table 3.1). In our system we opted for a water jacketed system in which the temperature was controlled via the use of an aquarium heater for tropical fish. Doing this enabled us to maintain temperatures between 18-37°C (Appendix A1).

Alongside temperature control, culture agitation was achieved via the use of a magnetic stirring bead with the fermenters placed on magnetic stirrers. Redox and pH measurements were achieved via the use of the Mettler Toledo InLab probe system, attached to a hand-held monitor.

Schematics for our fermentation system to be used in batch, fed batch as well as continuous were drawn up (Figure 3.1). From here a list of components was established (Appendix A2). Aside from all the purchased components, a custom gas escape/sample port had to be constructed, this was achieved by running metal piping at varying lengths through rubber bungs and sealing them to ensure airtight. These ports can be seen in Appendix A3. Pictures of the final system set ups can be found in (Appendix B), in addition to pictures there are a number of videos demonstrating the system functioning and set up as batch, fed batch and continuous without live cell culture.

Table 3.1 Comparison of main functionality of commercially available fermentation systems compared to the Shepherd lab designed system

Name	Electrolab FerMac 200	Eppendorf BioFlo® 120	BioNet F0-BABY	Shepherd Lab Set up
In Line Functionality				
Temperature control range (°C)	5 – 50 °C	0-70 °C	Temp Range not given	18-37 °C
pH control range	4-10	2-12	2-12	Controlled via buffering agent
Agitation (rpm)	50 -1100	25 – 1500	0-2000	0-1000
In line OD measurements	Yes - Optional Extra	No	No	No
Redox (mV)	Yes – Optional Probe	Yes – (-)2000 – (+) 2000	Yes - Optional probe	Yes
Dissolved O ₂	0-120%	0 200%	Yes – Optional Probe	No
Fermentation type				
Batch	Yes	Yes	Yes	Yes
Fed Batch	Yes – Optional extra pump	Yes – Built in	Yes – Optional extra pump	Yes – Optional extra pump
Continual	Yes – Optional extra pump	Yes – Built in	Yes – Optional extra pump	Y – Optional Extra
Volume Range (L)	2-1000	0.25 – 40	1-5	1
Price (GBP)	8000	20,000	19,995	2000

N

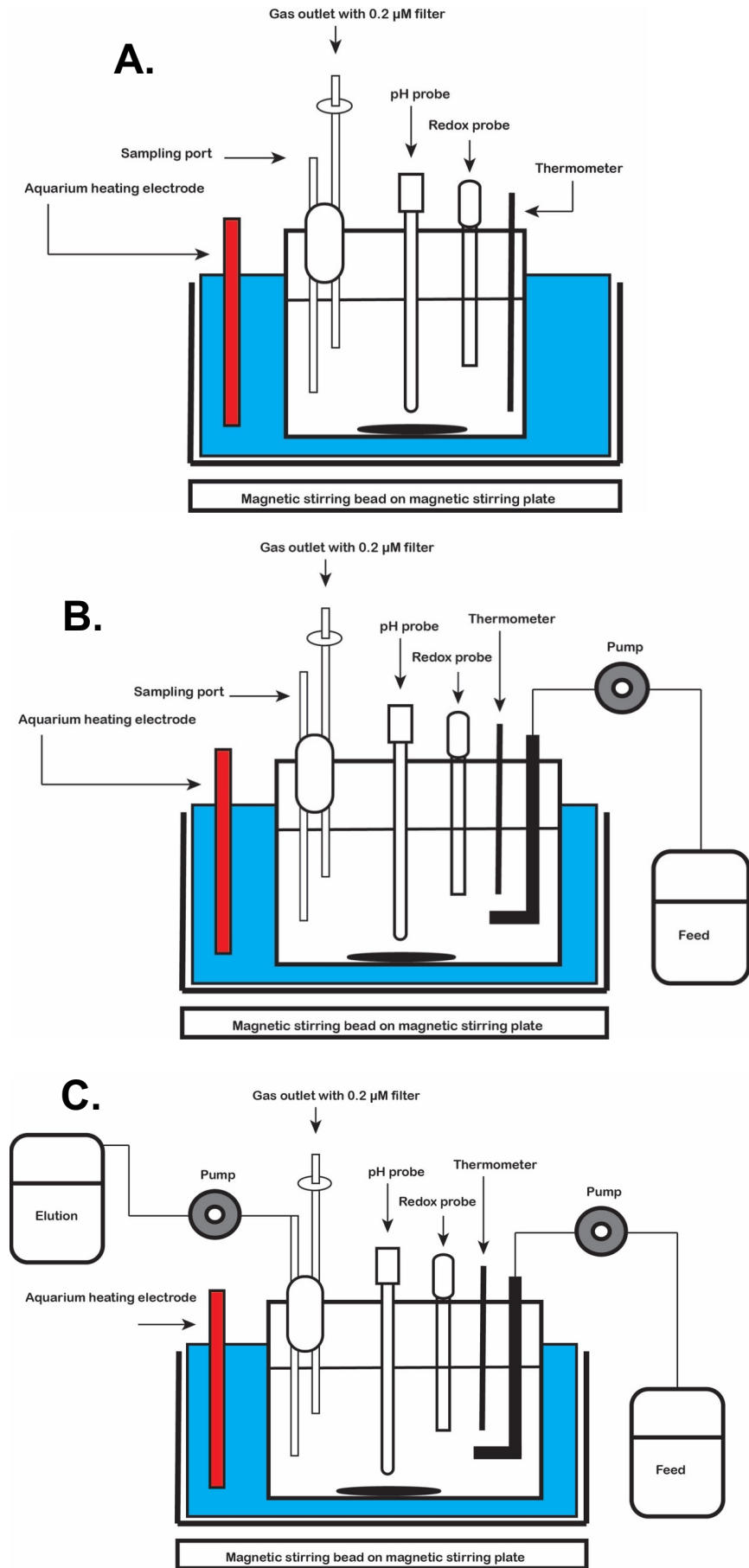


Figure 3.1 Schematic overview of the shepherd lab fermentation units. A). Schematic for batch fermentation system. B). Fed batch schematic. C). Continuous culture system.

3.3.2 Growth optimisation of *C. saccharoperbutylacetonicum* N1-4(HMT)

When establishing optimal fermentation conditions, a seeding system was developed Figure 2.1, this was used to ensure that a healthy, dense culture of *C. saccharoperbutylacetonicum* N1-4(HMT) was acclimatised in the fermentation media prior to fermentation. In total the seeding process took 3 days prior to inoculation into the fermenters. It was this seeding procedure that resulted in the highest rate of observed fermentation failing. This is an unfortunate result of the difficulties in working with anaerobic *Clostridium spp.* This problem was mitigated throughout by ensuring that over seeding took place, whereby a larger number of seeds cultures were started to ensure that enough of the starter and seeding cultures were made available come the time of fermentation.

The largest drawback of the current 'Shepherd Lab' fermenters is the lack of a pH control module that would allow for the addition of acids and alkali to control of pH within a tight window. The issue of pH control was largely overcome by the use of buffering agents during fermentation. Two buffers, calcium carbonate (CaCO_3) and 2-(N-morpholino) ethanesulfonic acid (MES Buffer) were tested and compared during batch fermentations.

The buffering action for both CaCO_3 and MES are shown in Figure 3.2. Previous studies have demonstrated the use of CaCO_3 as a buffer during ABE fermentations (Maddox et al., 2000; Sadie R. Bartholomew, 2006; Yang et al., 2013). The suitability for autoclaving and relative affordability makes CaCO_3 a strong buffer choice for ABE fermentations. MES buffer was first described as part of the Goods buffers (Frederic Monot, Jean-Marc Engasser, 1984) and has been shown to be the most effective between the pH ranges observed during ABE fermentation, with a pK_a value of 6 compared to 9 for CaCO_3 .

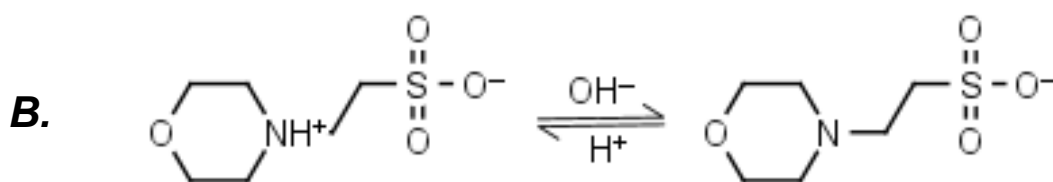
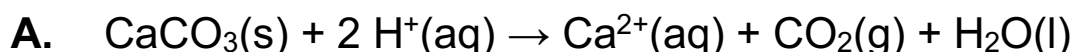


Figure 3.2 Buffering agents used in ABE fermentation A). Chemical reaction of CaCO_3 with acids and the formation of products from this reaction. B). Dissociation process of MES with acids and alkalis

To test both CaCO_3 and MES as buffering agents, batch fermentation experiments in YETM 40 g L^{-1} glucose were carried out, batch fermentation conditions were kept the same in both experiments with the only variable being MES and CaCO_3 in each. Both MES and CaCO_3 were able to adequately buffer the pH during a batch fermentation Figure 3.3B avoiding a drop in pH below 5 that would result in 'acid crash'. Despite both MES and CaCO_3 being adequate buffers, CaCO_3 appears to have inhibited cell growth with OD_{600} only reaching around 2.5 compared to around 6 in the MES buffered cultures Figure 3.3A. Despite the observed inhibition of growth in the CaCO_3 fermentations, the OD_{600} of the CaCO_3 fermentations is not representative of the actual culture turbidity or health. This is a result of CaCO_3 inability to fully dissolve into solution at the concentrations required for effective pH buffering. This causes large visible particles of CaCO_3 in solution, whereas MES is able to fully dissolve, is colourless and does not absorb visible light. Due to this, it becomes almost impossible to be able to accurately blank CaCO_3 buffered solutions at OD_{600} and results in it being less effective at accurately measuring the OD_{600} during fermentation. This inaccuracy is shown by the larger error bars and the flatter growth curve in Figure 3.3A compared to fermentations buffered with MES.

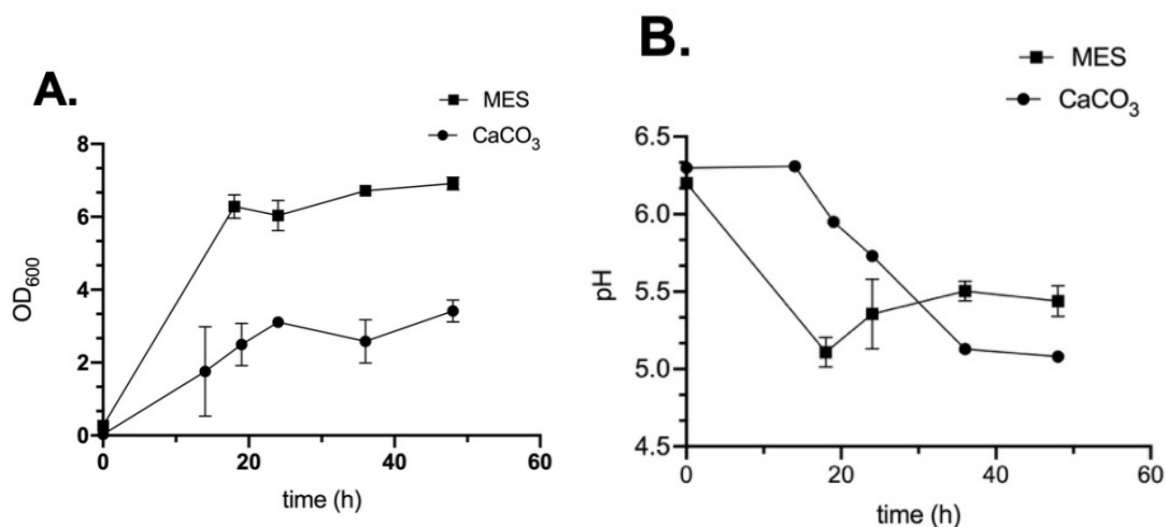


Figure 3.3 Fermentation analysis using CaCO_3 and MES pH buffering systems. A). OD_{600} and B). pH of *C. saccharoperbutylacetonicum* N1-4(HMT) grown in YETM with 40 g L^{-1} glucose with either MES (closed squares) or CaCO_3 (closed circles) as a buffering agent during fermentation.

3.3.3 Assessment of analytical techniques for measurement of acids, solvents and sugars.

Herein we assess the methodology used for the measurement of the end products of fermentation (i.e. acids and solvents) and establish methodology to measure the depletion in sugar concentrations. For the measurement of acids and solvents, Gas Chromatography Mass Spectrometry (GCMS) was used. To measure sugar concentrations in the fermentation mix, HPLC was used for sugar mixtures as well as single sugar fermentations. In addition to this, glucose concentrations were measured using HPLC (with refractometry detection) and were compared to measurements made with a hand-held glucometer similar to those used by diabetic patients.

3.3.3.1 Solvent and acid quantitation

As described above, GCMS was used as the methodology of choice for the detection and quantification of acids and solvents during fermentation. GCMS chromatographs in Figure 3.4 show the retention time of each of the compounds that are being measured during ABE fermentation, acetic acid (11.42 min), butanoic acid (12.9), acetone (2.8 min), butanol (8.5 min) and ethanol (5.4 min). Figure 3.4 also shows show the solventogenic shift that occurs during fermentation, with peak acetic acid and butanoic acid concentrations occurring between 6 -12 h, followed by their consumption as the cells switch to solventogenesis from 12 – 24 h. To enable quantification of ABE fermentation products, standard curves were established for the compounds of interest Figure 3.5.

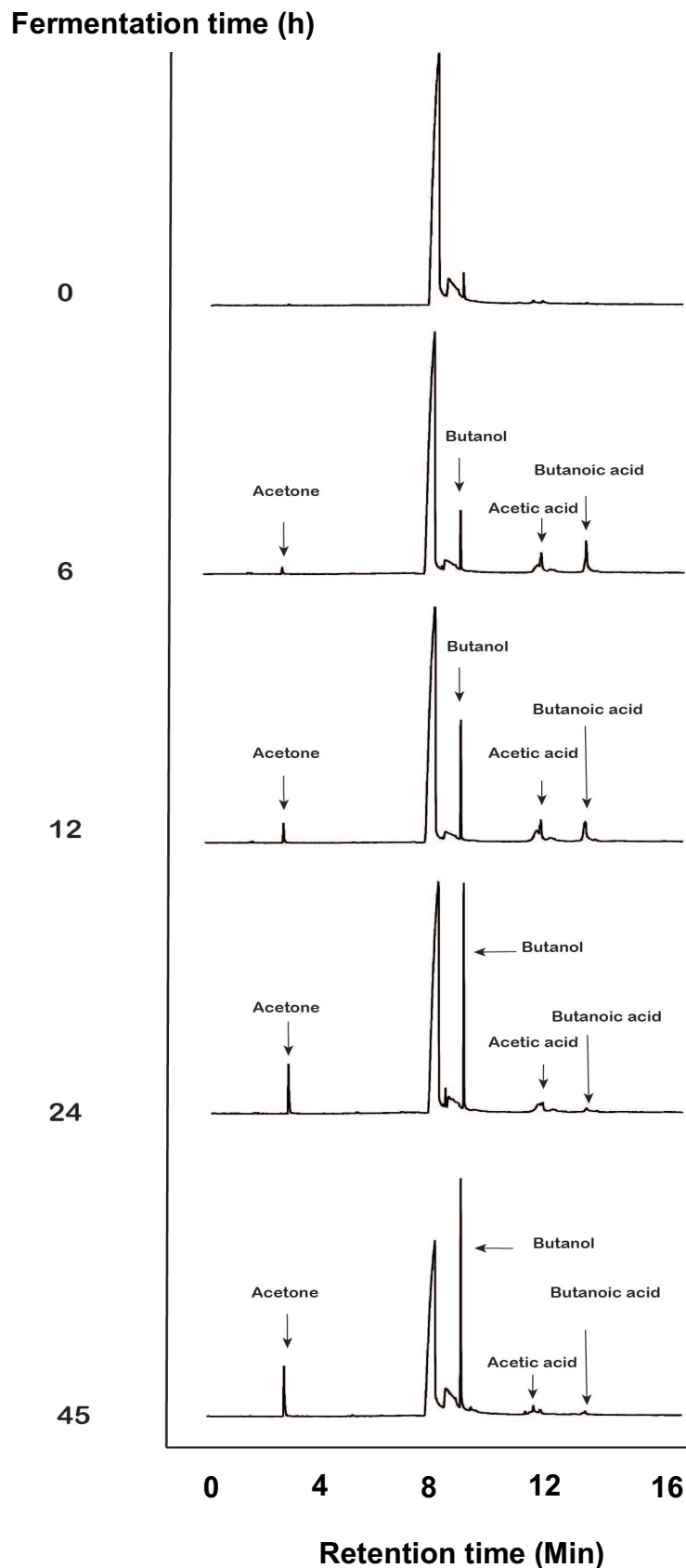
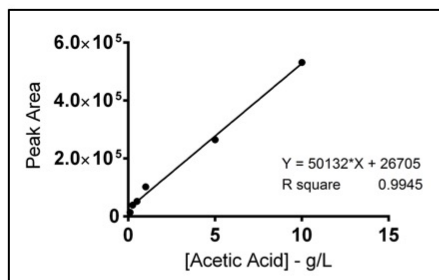
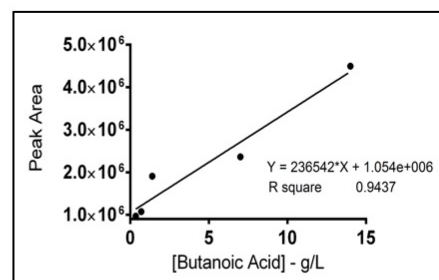


Figure 3.4. GCMS Chromatographs from *C. saccharoperbutylacetonicum* N1-4(HMT) YETM 40 g L⁻¹ batch fermentation for the identification of the acids (acetic acid and butanoic acid) and solvents (acetone and butanol). 2ml of cell culture taken from cells growing in a batch fermentation and separated by centrifugation. Sample supernatants were taken and run on the GCMS following protocol in section 2.8.4

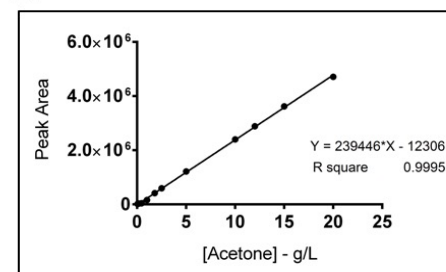
A.



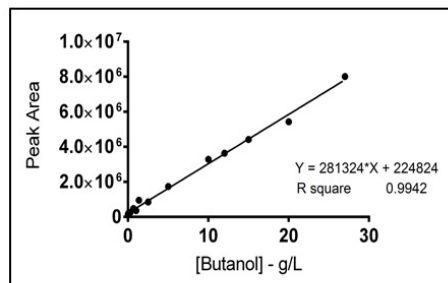
B.



C.



D.



E.

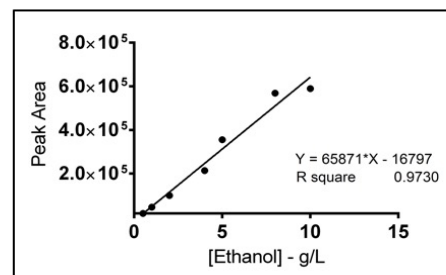


Figure 3.5 GCMS standard curves. Solvents were diluted in H₂O to corresponding g / L concentration and ran on the GCMS following the protocol in Section 2.8.4. A.) Acetic acid, B.)

3.3.3.2 Optimisation of sugar quantification

Alongside the ability to be quantify acids and solvents during fermentation, it is important to identify and quantify sugars due to the complex nature of different feedstocks and the changes in rates of feed and carbon utilisation that occurs. Sugars quantification was performed via High-pressure liquid chromatography (HPLC). While very sensitive, HPLC can be time consuming and expensive, especially for fed batch or continuous fermentation experiments where the concentrations of sugars are monitored regularly. To overcome this, the use of a glucometer, similar to those used by those by diabetics, was employed as a way of quickly and easily measuring glucose concentrations during fermentations. To test the accuracy of the glucometer, a fed batch fermentation was carried out. Following a 16 h batch overnight, the glucose concentrations were maintained below 20 g L⁻¹ for the remainder of the fermentation. During this time, the glucometer was used to measure glucose concentrations from each sample. This dictated the feed rate that maintained the glucose concentrations at the desired level. At the same time, samples were taken for subsequent analysis via HPLC to allow for comparison of the two methods. The data reveal that although the glucometer struggles at higher sugar concentrations (>25 gL⁻¹) it is a relatively accurate method for measuring glucose concentrations when compared to the HPLC approach (Figure 3.6) with a correlation of 88% with the data from the HPLC samples.

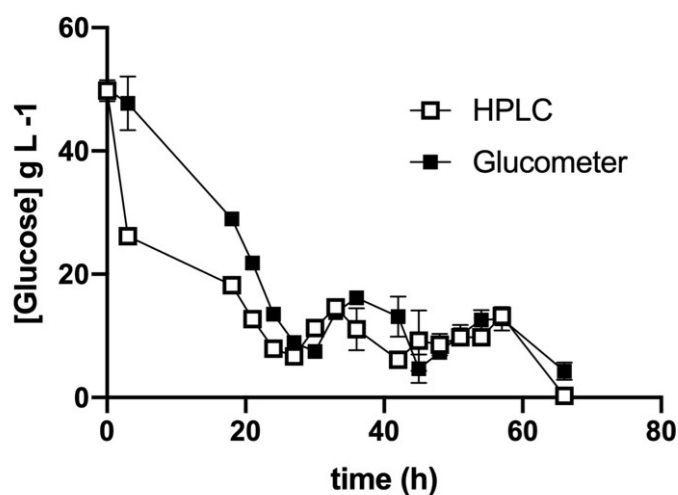


Figure 3.6 Glucose concentrations during fed batch fermentation comparing the ability of the Glucometer vs HPLC analysis. *C. saccharoperbutylacetonicum* N1-4(HMT) was grown in YETM 50g L⁻¹ glucose as a starting sugar concentration. Feed rate was kept the same at throughout. 300 g L⁻¹ glucose was consumed for the duration of the fermentation. 2 mL cell samples were taken during fermentation, separated via centrifugation and the supernatant separated and used to measure glucose concentrations using both the Glucometer and HPLC.

3.3.4 Implementation of new fermentation approaches for integrated analysis of ABE fermentation

To initially test the fermentation setup a batch fermentation was carried out. For this, wild type *C. saccharoperbutylacetonicum* N1-4(HMT) grown according to the seeding process described in section 2.4.4 into a final culture volume of 500 mL of YETM 40g L⁻¹ glucose with 0.1 M MES as a buffering agent. The batch fermentation was carried out at 32 °C for 48 h. Anaerobic conditions were established by purging with filtered (0.2 µm pore size) N₂ for 30 min per vessel prior to inoculation and then 10 min following inoculation. The batch fermentations were run in triplicate and set up as illustrated by the schematics in Figure 3.1A.

The final OD₆₀₀ measured was 7.2 ± 0.2, the lowest pH value reached was 5.09 ± 0.03, and the lowest redox value reached was -298 ± 9 mV vs. NHE (Figure 3.9A). Glucose consumption was measured using HPLC (Figure 3.9B). This showed that the glucose concentration diminished from the initial 40 g L⁻¹ to 1.3 ± 1.96 g L⁻¹.

Peak concentrations of acetic acid and butanoic acid at 12h (Figure 3.9C) were 0.203 ± 0.03 gL⁻¹ and 0.17 ± 0.005 gL⁻¹, respectively. Acid concentrations were fully depleted by 30 h and solvent production started at 12 h. Solvent concentrations were at maximum levels at 45 h, with a peak acetone concentration of 4.9 ± 0.48 g L⁻¹ and a peak butanol concentration of 13.4 ± 0.8 g L⁻¹.

To conclude, it has been demonstrated above that it is possible to design and construct a fermentation system that has similar functionality to commercial units at a fraction of the cost. In addition to this, a system for detection and quantification of acids, solvents and sugars was established.

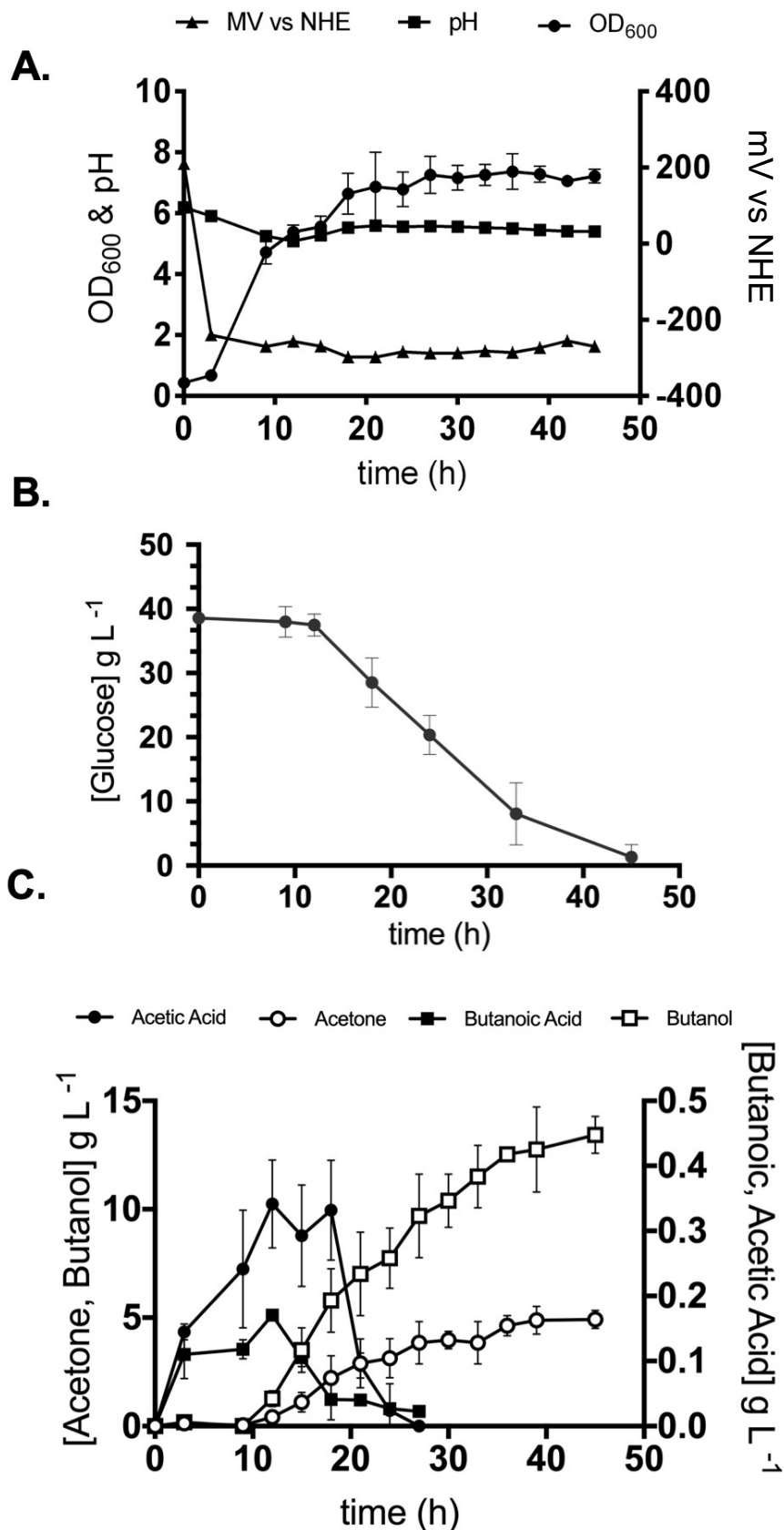


Figure 3.9 Overview of growth, acids and solvents of a *C. saccharoperbutylacetonicum* N1-4(HMT) batch fermentation in the shepherd fermentation system. A). Output obtained for OD₆₀₀, pH and Redox (mV vs NHE); B). Glucose consumption during fermentation measured using HPLC; C). Concentrations of Acetic acid (closed circles), Acetone (open circles), butanoic acid (Closed squares) and butanol (open squares) during the fermentation.

3.7 Discussion

3.7.1 General Discussion

As the revival of ABE fermentation in *Clostridium* continues to grow in the wake of renewable energy demands, reducing cost barriers at the point of access will be important to promote research in this area, especially in lower income countries. As the cost of specialist fermentation technology can be high (Table 3.1.), the current project aimed to create a cost-effective alternative that uses affordable parts in conjunction with equipment available in most labs (e.g. spectrophotometer for OD₆₀₀ readings).

The system designed here is versatile, easy to set up and run, and shares many of the same functionality as current commercial models such as, pH and redox measurements, along with the ability to be set up for batch/fed batch or continuous processes (Figure 3.1). In addition to this, the techniques for measuring compounds of interest such as acids, solvents and sugar consumption have been established (Figure 3.4 & Figure 3.5 & Figure 3.6).

3.7.2 Dissolved oxygen control and control

The functional repertoire of the current fermentation system could be expanded by introducing in-line dissolved oxygen (DO) measurements, similar to commercial systems from Electrolabs, Eppendorf or Bionet. While this is of limited value for anaerobic cultures other than to ensure that the media is indeed anaerobic, DO measurements may be useful for other fermentation applications such as the production of protein therapeutics in *E. coli*.

To measure DO in a system, a DO probe is required and typically, this is what commercial systems provide. Recently however (Sadie R. Bartholomew, 2006) have developed a cost-effective CHO K-1 cell bioreactor. The main goal set out by (Sadie R. Bartholomew, 2006) was to establish a method that could be used to introduce oxygen into the bioreactors, as well as measure the concentration of DO during growth. Oxygen was introduced into a bioreactor via the catalytic breakdown of hydrogen peroxide with manganese oxide. Alongside this, the Winkler dissolved oxygen assay (Winkler, 1888) was adapted to fit a microscale volume which when compared to DO reading from a DO probe gave a linear relationship of $r^2=0.9995$.

In the future, it would be possible to introduce the methods described by (Sadie R. Bartholomew, 2006) in the system designed in this chapter allowing for introduction of oxygen and measurement of dissolved oxygen in the system in a cost-effective manner.

3.7.3 pH control and acid crash

pH control of ABE fermentation is important for maximising solvent yields. Acid crash and the mechanisms involved have been investigated previously (Martin et al. 1983; Wang et al. 2011; Zverlov et al. 2006)(Yang et al., 2013). Acid crash, as the name suggests, is characterised by a dramatic decrease in pH leading to the cessation of glucose uptake and very little solvent production. Over-production of un-associating acids (i.e acetic and butyric acid) from acidogenesis at a concentration of 57-60 mmol/L are thought to be the main cause of acid crash (Maddox et al., 2000). Acid production, in particular butyric acid, is key in the shift from acidogenesis into solventogenesis. It has previously been reported that a minimum concentration of 1.5 g L⁻¹ butyric acid results in the shift into solventogenesis (Frederic Monot, Jean-Marc Engasser, 1984). However, it is not fully understood at which pH acid crash will occur and in addition to this George and Chen 1983 reported that acidic conditions are not required for the solventogenesis to occur.

The system designed in this chapter has the ability to control the pH via the addition of buffering compounds, although it is not able to buffer pH automatically via titration of acids or alkalis. In our system, bolus additions of CaCO₃ and MES were tested as pH buffering solutions. CaCO₃ as a buffer during fermentations has previously been extensively studied (Tsai et al., 2014)(Ai et al., 2014)(Yang et al., 2013)(Wang et al., 2019), and has been shown to extend cell growth time, alleviate inhibitory effects of acid production as well as toxicity of butanol (Kanouni et al., 1998), leading to higher overall yields of solvents. MES buffer was first described in Good et al. 1966 as part of an investigation into hydrogen ion buffers for biological research with various favourable properties.

As shown in Figure 3.3, CaCO₃ provided a good level of pH buffering acids, preventing the pH of the culture to drop below pH 5 similar results were achieved by MES. The accuracy of OD₆₀₀ measurements with CaCO₃ was much lower than with MES as shown by the larger error bars in Figure 3.3A. The higher error bars and the reduction in the actual measurable OD₆₀₀ of the samples buffered with CaCO₃, is not believed to be a result of the CaCO₃ itself. Unlike MES, the solubility of CaCO₃ is only 0.013 g L⁻¹ compared to MES, which has been documented at upwards of 0.5 M or 97 g L⁻¹ due to the lack of solubility of CaCO₃ when measurements of OD₆₀₀ the concentration of dissolved CaCO₃ in the sample is unknown making readings inaccurate and unrepresentative of the real cell density due to background absorption by undissolved CaCO₃.

Although CaCO₃ and MES have been chosen for use herein, ammonium acetate, sodium bicarbonate, acetate buffer, sodium acetate and citrate buffer (Yang et al., 2013) (Tsai et al., 2014) (Xue et al., 2016) have all been used to varying degrees of success. CaCO₃ was used here as it cheap, effective and buffering and has been extensively studied. A recent review of the functionality of the Goods buffers (Ferguson et al., 1980) has led to an understanding and selection of “better” buffers, providing schematics and insight into the best pH ranges for the non-complexing tertiary amine buffer compounds (Kandegedara and Rorabacher, 1999), this review reveals that MES has a more preferential *pka* values related to acidogenesis pH levels compared to other good buffers throughout temperature ranging from 15-45 °C, for this reason MES was used as the buffer of choice herein.

3.7.4 Concluding remarks

A cost-effective fermentation system was designed and constructed that incorporates many of the same functionalities as commercially available systems, and reliable approaches for pH modulation and metabolite analysis have also been established. This work will be important for researchers requiring reproducible and industrially relevant clostridial culture techniques, and indeed for researchers working on microbial biofuel formation with other organisms such as yeast and algae.

Chapter 4

Deletion of the *gapN* gene from *C. saccharoperbutylacetonicum* N1-4(HMT) using CLEAVE™ and subsequent evaluation $\Delta gapN$ *C. saccharoperbutylacetonicum* N1-4(HMT) using whole genome sequencing.

4.1 Summary

Despite the recent revival in research into *Clostridium spp.* and the growing interest into the industrial capabilities of solventogenic strains of *Clostridium*, the development of tools for genetic engineering of these strains has lagged behind those of Gram-negative species such as *E. coli*. In this chapter, we exploit the new CLEAVE™ methodology (Jenkinson et al., 2015) a CRISPR/Cas tool developed by Green biologics Ltd, to delete the *gapN* gene from the chromosome of *C. saccharoperbutylacetonicum* N1-4(HMT). Following successful deletion of *gapN*, whole genome sequencing (WGS) was carried out using illumina MiSeq technology on the wild type and *gapN* strains to screen for additional unwanted mutations that may be introduced by CLEAVE™. The WGS from the $\Delta gapN$ *C. saccharoperbutylacetonicum* N1-4(HMT) shows no undesired or unwanted mutations as a result of the CLEAVE™ process.

4.2 Introduction

Clustered Regulatory Interspaced Palindromic Repeats (CRISPR) alongside their associated Cas proteins are part of the adaptive immune system within prokaryotes (Figure 1.5). In recent years as the molecular biology toolkit available to *Clostridium* has grown, so has the adaption and use of CRISPR/Cas systems within a variety of *Clostridium spp.* (Bruder et al., 2016; Huang et al., 2016; Nagaraju et al., 2016; Wang et al., 2017a; Wasels et al., 2017). Typically, CRISPR/Cas systems used in *Clostridium spp.* involve screening against those strains that have successfully undergone a homologous recombination (HR) event. Those that have undergone a successful HR event are typically those that survive as the CRISPR/Cas machinery will be targeting wild type strains that have not undergone HR. The technology used herein was developed by Green Biologics Ltd. as their proprietary CRISPR/Cas system. CLEAVE™ makes use of the endogenous CRISPR-Cas systems of the bacteria and is not limited to *C. saccharoperbutylacetonicum* N1-4(HMT), it has previously been shown to successfully generate strains carrying desired SNPs as well as those with deletions and insertions (Atmadjaja et al., 2019), although detailed WGS analyses have not previously been performed on the engineered strains to screen for unwanted mutations. CLEAVE™ has been utilised herein for the deletion of the *gapN* gene that encodes the glyceraldehyde-3-phosphate dehydrogenase GapN from the genome of *C. saccharoperbutylacetonicum* N1-4(HMT), an industrially relevant butanol hyper-producing *Clostridium* strain.

The work carried out in this chapter focuses on GapN, a cytosolic non-phosphorylating NADP-dependant GAPDH that catalyses the irreversible oxidation of glyceraldehyde-3-phosphate (G3P) to 3-phosphoglycerate (Figure 4.1). However, three classes of glyceraldehyde-3-phosphate dehydrogenases (GAPDH) that are known to be involved in the central carbon metabolism pathway (Fothergill-Gilmore and Michels, 1993) With the other two being; (i) A NAD-dependant glycolytic enzyme found in the cytoplasm of all organisms, which plays a key role in the Embden-Meyerhoff pathway in glucose as well as gluconeogenesis; (ii) An NADPH-dependant GAPDH that is a key component of the reductive pentose-phosphate cycle (Iddar et al., 2002).

Originally discovered in photosynthetic eukaryotes (Mateos and Serrano, 1992), GapN has gone on to be confirmed in *Streptococcus mutans* and *S. salivarius* (Boyd et al., 1995). Recombinant GapN from *Streptococcus mutans* has been expressed in *Corynebacterium glutamicum* as a route for NADPH generation to facilitate L-Lysine production (Takeno et al., 2010). Additionally, recombinant GapN from *C. acetobutylicum* has been expressed in *E. coli* and has been shown to have an absolute specificity for NADPH (Iddar et al., 2002).

Despite developing complex metabolic networks for energy generation (Demmer et al., 2015), anaerobic bacteria lack the ability to generate ATP via oxidative respiration. In a sense this can be seen as a limiting factor in energy generation as generally having a larger pool of ATP is seen as a positive for the cells. As described above, GapN forms part of the glyceraldehyde-3-phosphate oxidation pathway (**Figure 4.1**). Previous flux analysis in *C. acetobutylicum* (Minyeong Yoo, Gwenaelle Bestel-Corre, Christian Croux, Antoine Riviere, Isabelle Meynial-Salles, 2015) has revealed that GapN is poorly expressed at 0.56 mRNA molecules per cell in comparison to 66 mRNA molecules per cell of GAPDH. This poor expression leads to only 3500 protein molecules per cell of GapN compared to 190000 protein molecules per cell of GAPDH. It was predicted that GapN would only be responsible for around 5% of flux through the glyceraldehyde-3-phosphate oxidation pathway. With the knowledge of predicted low flux and alongside the poor expression data, the *gapN* gene in *C. saccharoperbutylacetonicum* N1-4(HMT) was targeted for the creation of a $\Delta gapN$ *C. saccharoperbutylacetonicum* N1-4(HMT) as a way of recovering any ATP generation within the cell that may be as a result of the flux lost through GapN in the glyceraldehyde-3-phosphate oxidation pathway (Figure 4.1). In addition to this, recombinant GapN expression has been used a method of NADPH generation in other bacteria, deletion of GapN may alter the NADH/NADPH ratio within *C. saccharoperbutylacetonicum* N1-4(HMT) (Centeno-Leija et al., 2014).

Following deletion of the *gapN* gene from *C. saccharoperbutylacetonicum* N1-4(HMT) whole genome sequencing (WGS) was carried out to assess the precision of CLEAVE™ and these findings were compared to the current literature.

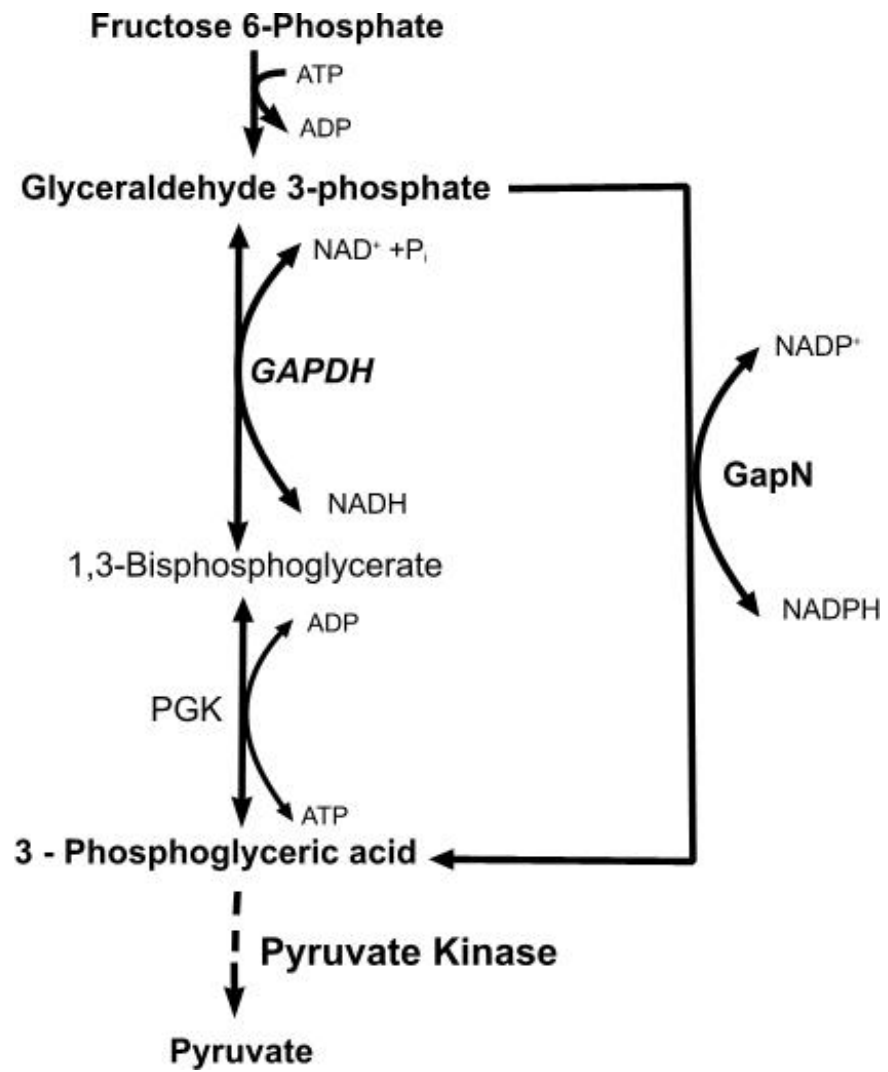


Figure 4.1 The pathways involved in conversion of glyceraldehyde 3-phosphate to 3-phosphoglyceric acid in *C. saccharoperbutylacetonicum* N1-4(HMT). Also known as the glyceraldehyde-3-phosphate oxidation pathway

4.3 Results

4.3.1 Deletion of *gapN* in *C. saccharoperbutylacetonicum* N1-4(HMT) using CLEAVE™

Deletion of *gapN* was carried out using the proprietary CRISPR/Cas technology CLEAVE™ developed by Green Biologics limited (Jenkinson et al., 2015). The CLEAVE™ process consistent of three main steps. (i) Homologous recombination vector generation and transformation. The homologous recombination vector consists of a substitution cassette, that contains homology arms that are able to replace all of or part of the intended site of mutation. The homologous recombination vector does not contain any CRISPR/PAM protospacer that is recognisable by the crRNA of the CRISPR/Cas system in the cells. (ii) Following transformation with the recombination vector, the bacteria population undergo several rounds of sub culturing. The sub culturing stage of CLEAVE™ is intended to encourage the bacterial population now transformed with the recombination vector to undergo a double recombination event at the intended site, replacing the wild type genome with that in the recombination vector; stopping the now replaced DNA from being recognised by the crRNA of CRISPR/Cas. (iii) Finally, following sub-culturing, the cells are finally transformed with the Killing vector. The killing vector is capable of producing crRNA which targets the PAM protospacer site within the intended region of mutation where the double recombination event has taken place. The crRNA within the killing vector will only be able to recognise the PAM/protospacer within cells that have been unable to undergo the double recombination event and still contain the wild type DNA, resulting in killing of those cells that have not undergone double recombination. Following transformation with the killing vector, cells are plated, colonies are selected and screened for desired mutations.

4.3.1.1 Creation of the Homologous recombination vector and sub-cloning

The first step in the CLEAVE™ process is the design and construction of the homologous recombination (HR) vector and the *gapN* deletion cassette. To construct the *gapN* deletion cassette, colony PCR of *C. saccharoperbutylacetonicum* N1-4(HMT) was carried out to amplify 2 x 1.5 kb regions upstream and downstream of *gapN*. The 1.5 kb fragments upstream of *gapN* was designed to contain a 25 bp 3' region that was complementary to the 5' end of the downstream fragment (Figure 4.2). In doing this, it was possible to generate a seamless in-frame deletion cassette fragment that lacked the *gapN* gene.

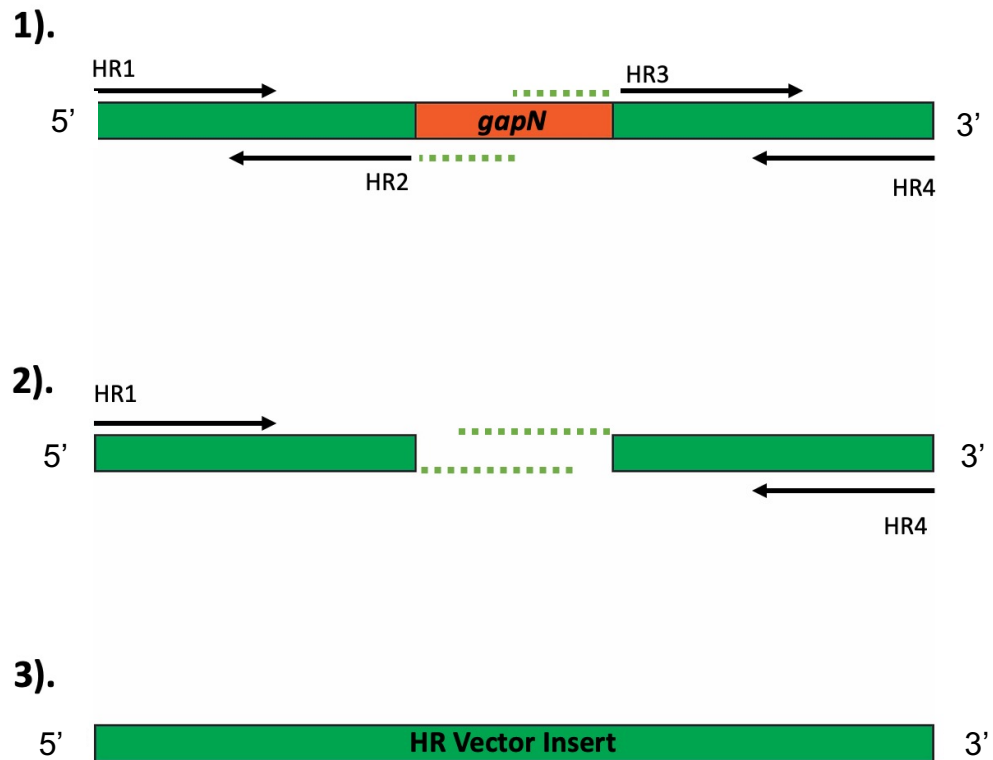


Figure 4.2 Diagrammatic representation of the PCR reaction used to create the deletion cassette insert for the Homologous Recombination vector. 1). Amplification of 1 kb fragment 3' of the *gapN* gene using primers HR1 and HR2 with HR2 containing complementary to the HR3 primer. 1 kb fragment 5' of *gapN* amplified using HR3 and HR4 with HR3 having complementary sequence to HR2. 2). HR1 and HR4 used with two newly PCR amplified 1 kb fragments with overhangs to fuse both fragments together. 3). Assembled fragment from two previous fragments with overhangs, ready to be blunt ligated into pMTL81254.

Following successful PCR reactions, fragment isolation and Sanger sequencing to confirm the correct sequence of the deletion cassette, it was successfully blunt cloned into the HR vector. This can be seen in Figure 4.3A whereby successful cloning would remove the *Stu*I restriction site within the plasmid, and when digested with *Nde*I + *Hind*III two fragments would be visible, one around 3kB and 250bp. The new HR *gapN* deletion vector was first transformed into *E. coli*. The HR vector pMTL82154 is a lineage of the pMTL80000 shuttle vector system first described by (Heap et al., 2007) The HR vector is formed of the following components a pBP1 Gram-positive replicon, *catP* antibiotic maker, *ColE1* +*tra* Gram-negative replicon and a *catP* reporter gene Figure 4.3B. After successful transformation into *E. coli* the HR_{gapN}_del vector isolated and was transformed into *C. saccharoperbutylacetonicum* N1-4(HMT).

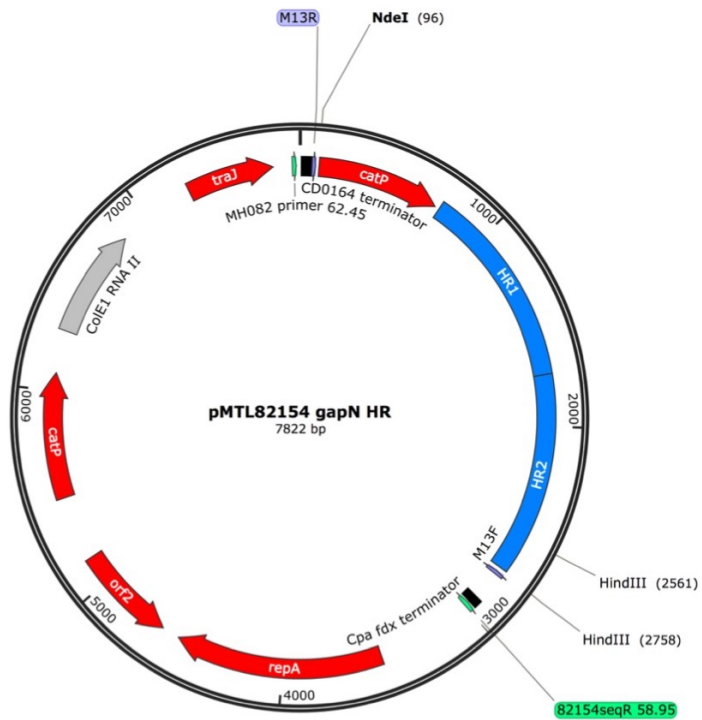
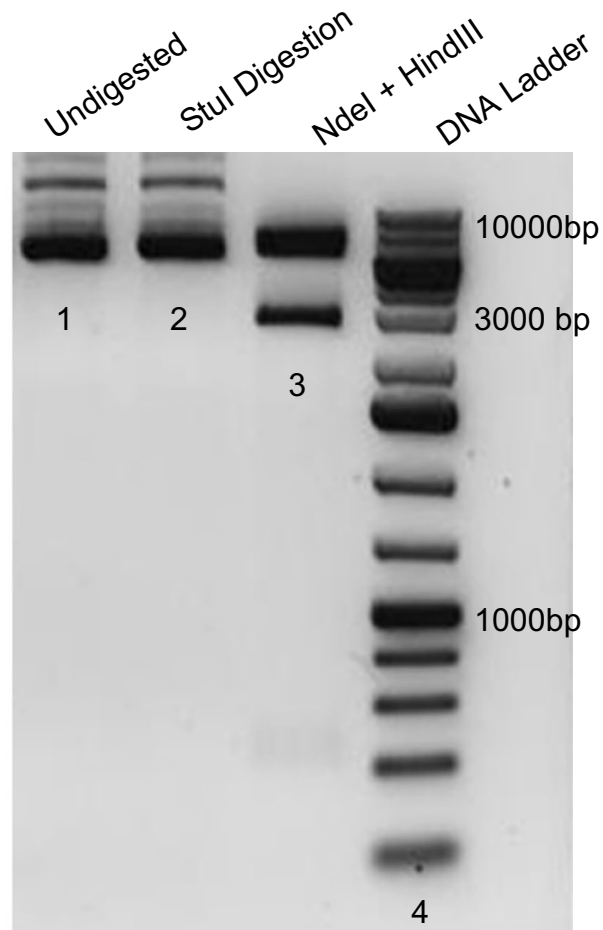


Figure 4.3 - Cloning of the homologous recombination vector for deletion of *gapN*. A). 1% agarose gel showing: lane 1 – Undigested miniprep pMTL82154 + homologous recombination (HR) fragment. Lane 2 – Miniprep pMTL82154 + HR fragment digested with *Stu*I. Lane 3 – Double digest with *Hind*III and *Nde*I of pMTL82154 + HR fragment. Lane 4 – 1kB Gene ladder. B). Vector map of the expected final construct.

1.3.1.2 Design and construction of Killing Vector

Like the HR vector, the killing vector (also known as the CRISPR/Cas targeting vector) is derived from the pMTL8000 shuttle vector system (Heap et al., 2007). The killing vector is a modified version of pMTL83251. Traditionally pMTL83251 consists of Gram-positive replicon pCB102, ermB antibiotic marker, ColE1 + tra Gram-negative replicon and a multiple cloning site (MCS). Pre-Engineered into the MCS of pMTL83251 is the native leader sequence (LDR), a 181 bp sequence that is found downstream of the Cas2 machinery in *C. saccharoperbutylacetonicum* N1-4(HMT). With the leader sequence pre-engineered into pMTL83251 it allows for the construction of CRISPR/Cas clusters on the plasmid that replicate how they are seen natively within the cells. The CRISPR/Cas targeting system seen in *C. saccharoperbutylacetonicum* N1-4(HMT) is formed of DR_Target-specific-spacer_DR clusters downstream of the Cas2. For the successful deletion of *gapN* a DR_*gapN*-spacer_DR cluster was created *insilico* (Figure 4.4), synthesised and successfully cloned into pMTL83125 (Figure 4.5). The ~50 bp *gapN* spacer sequence that was used in the DR_*gapN*_spacer_DR was found adjacent to a 5' – CCX sequence within the *gapN* gene itself.

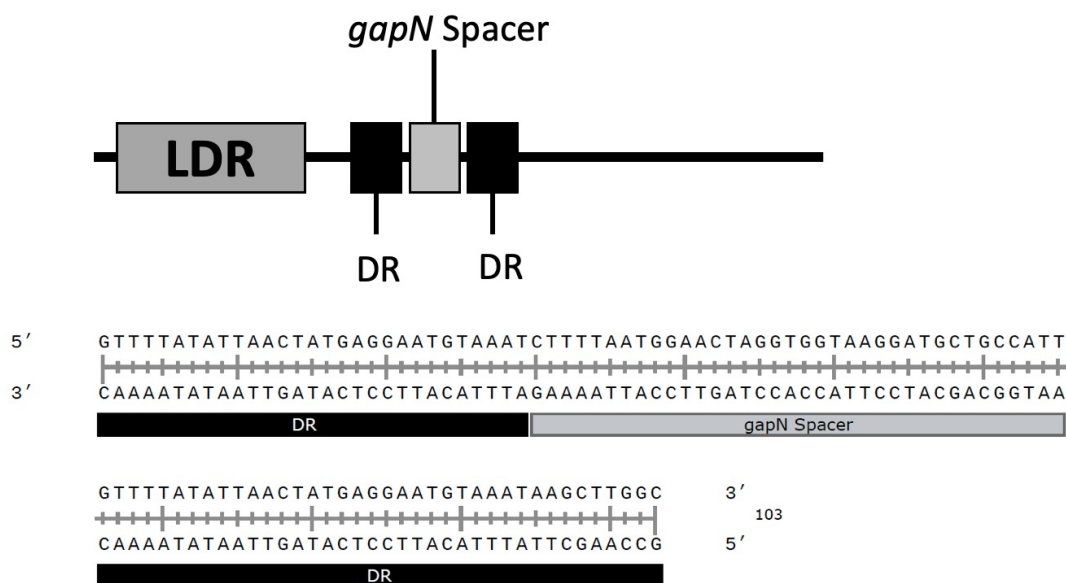


Figure 4.4 Overview of the killing vector targeting cassette for endogenous CRISPR-Cas for genome editing.

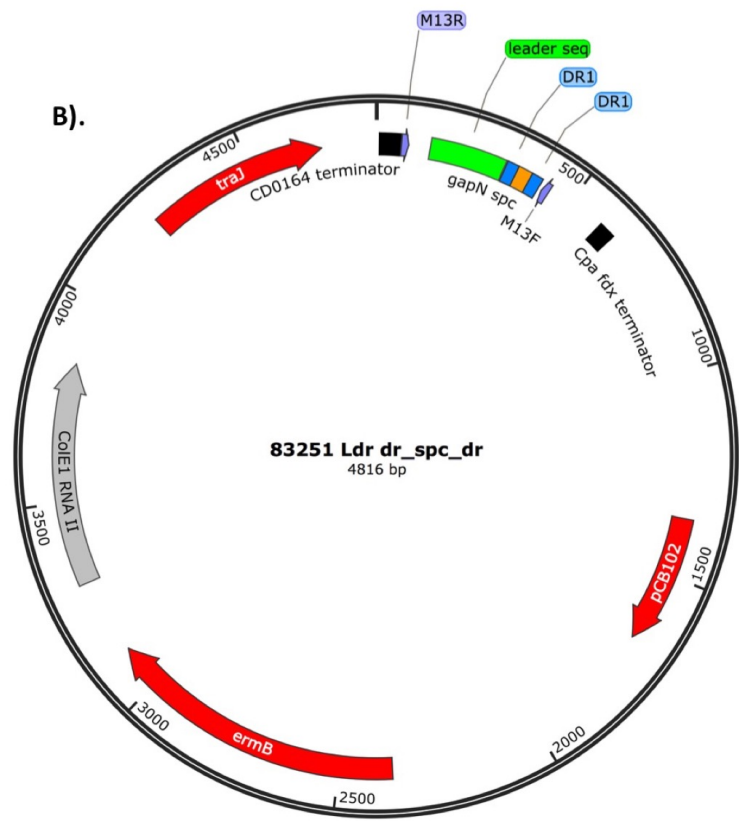
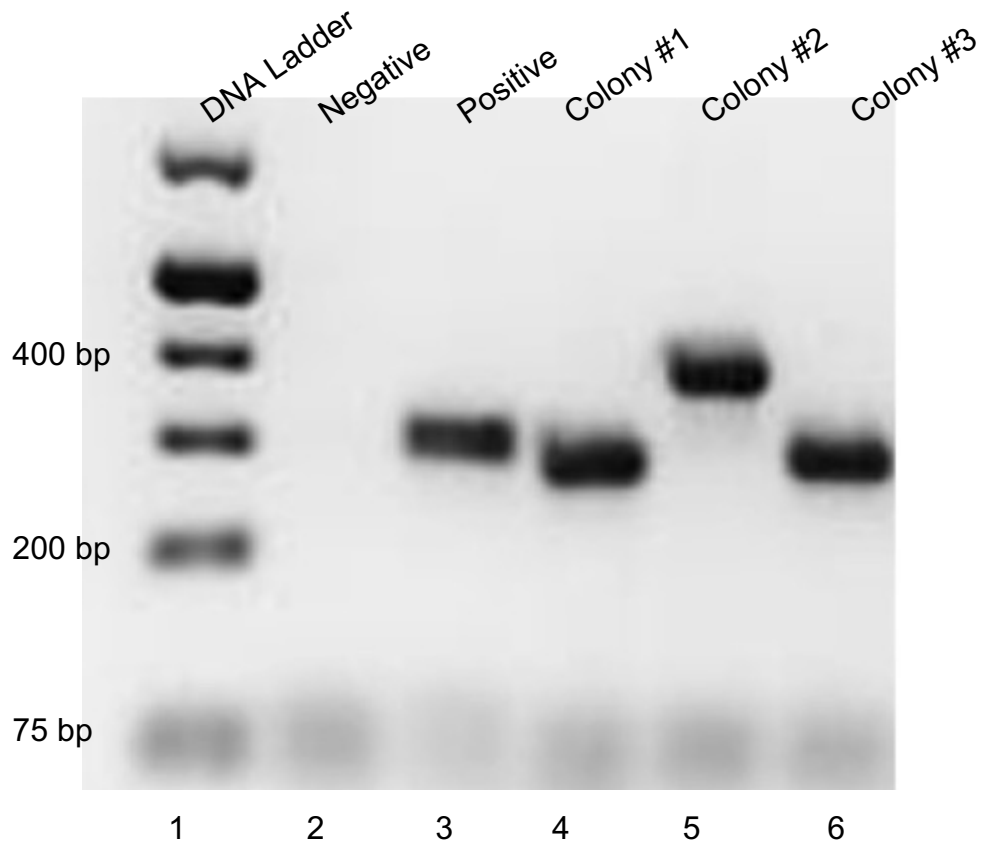


Figure 4.5 PCR screening for successful ligation of DR_gapN_DR spacer sequence into the pMTL83125 vector. (A) 2% agarose gel showing PCR products from *E. coli* colonies screened with M13 primers after ligation of killing vector fragment into pMTL83251 Lane 5 shows successful ligation. (B) Diagram of expected final killing vector construct after successful ligation into pMTL83251

4.3.1.3 Confirmation of *gapN* deletion from the genome of *C. saccharoperbutylacetonicum* N1-4(HMT)

Following successful transformation of the killing vector a total of 144 colonies post transformation from undiluted cultures and 10 colonies from 1/10 culture dilutions were obtained. 15 colonies were screened in total, from this initial screen, a large proportion of screened colonies appeared successful (Appendix I). From these initially screened colonies one colony was taken, re-screened and sent for sequencing (Figure 4.6). For the CPCPCR HR1 and HR4 primers were used. These primers anneal upstream and downstream of *gapN*, were used in the construction of the HR vector and following amplification resulted in a fragment that was 1256 bp in length compared to the wild type at around 3 kB containing the gene *gapN*. Successful colonies were sent for Sanger sequencing to confirm successful deletion of *gapN* (Appendix D).

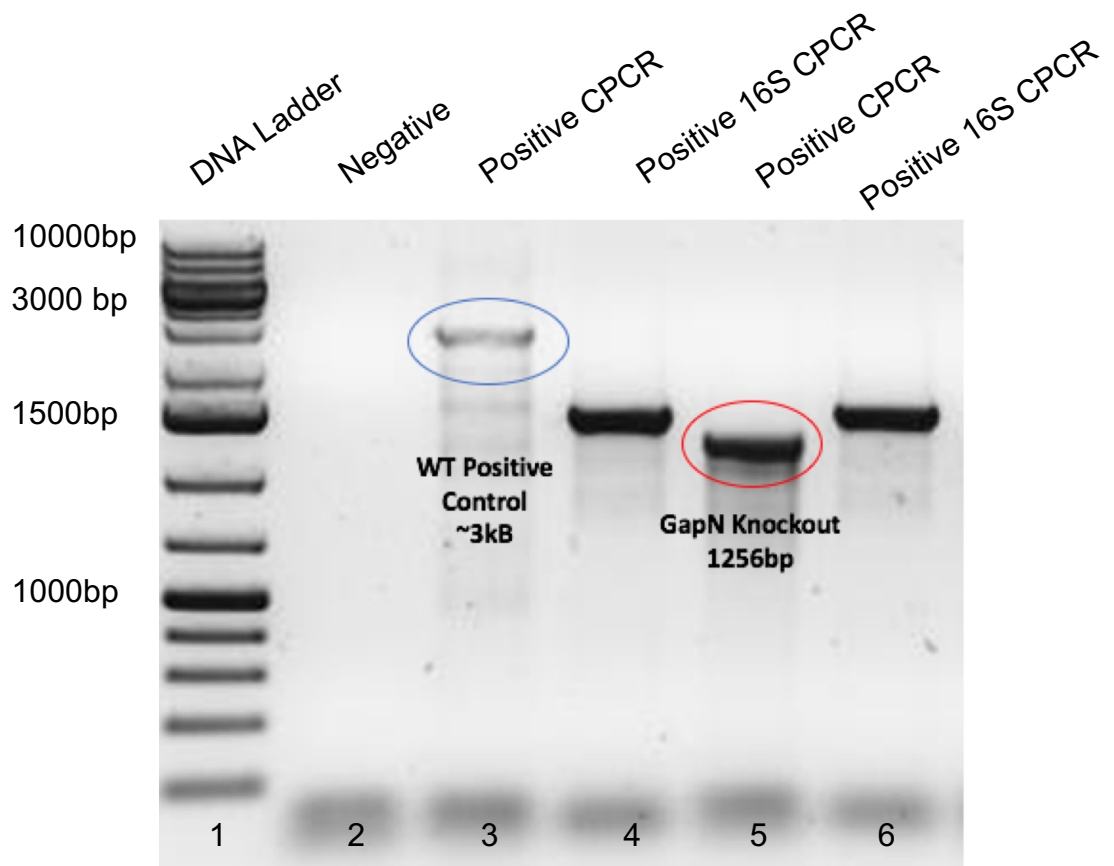


Figure 4.6 Colony PCR screening of *C. saccharoperbutylacetonicum* N1-4(HMT) Δ *gapN* mutants. 1% agarose gel was used to resolve PCR products. Lane 1: GeneRuler 1kB ladder (Thermo Fisher Scientific). Lane 2: Negative control of PCR without template DNA but still containing primers and Phusion. Lane 3: Positive control PCR of wild type strain. Lane 4: 16S PCR to ensure that cell lysis was successful for Lane 3 PCR. Lane 5: PCR confirming deletion of *gapN* in the genome. Fragment size with *gapN* deletion is expected to be around 1256bp. Lane 6: 16S PCR confirming cell lysis in Lane 5.

4.4 Whole genome sequencing and comparison of $\Delta gapN$ and wild type *C. saccharoperbutylacetonicum* N1-4(HMT).

To evaluate the effectiveness and specificity of CLEAVE™, whole genome sequencing via Illumina MiSeq was carried out on both wild type and $\Delta gapN$ *C. saccharoperbutylacetonicum* N1-4(HMT). It was deemed necessary to be directly involved in the sequencing process, rather than commercial outsourcing, to gain an in-depth understanding of the process to enable a thorough quality control analysis of the data generated. An overview of the pipeline and sequence evaluation techniques used are shown in Figure 4.7. A genome library for both the wild type strain and the $\Delta gapN$ were prepared using the Nextera® XT DNA Library Prep Kit, which is optimized for small genomes. This kit uses a transposome complex that simultaneously fragments genomic DNA and inserts adapter sequences. Following on fragmentation and adaptor insertion, a PCR step uses the adapter to amplify the DNA fragments and add specific index sequences to each genomic DNA sample, thus allowing sequencing of pooled libraries (this process is often termed 'barcoding'). Once the libraries for the wild type and $\Delta gapN$ strains were prepared, they were sequenced using an Illumina MiSeq benchtop sequencer.

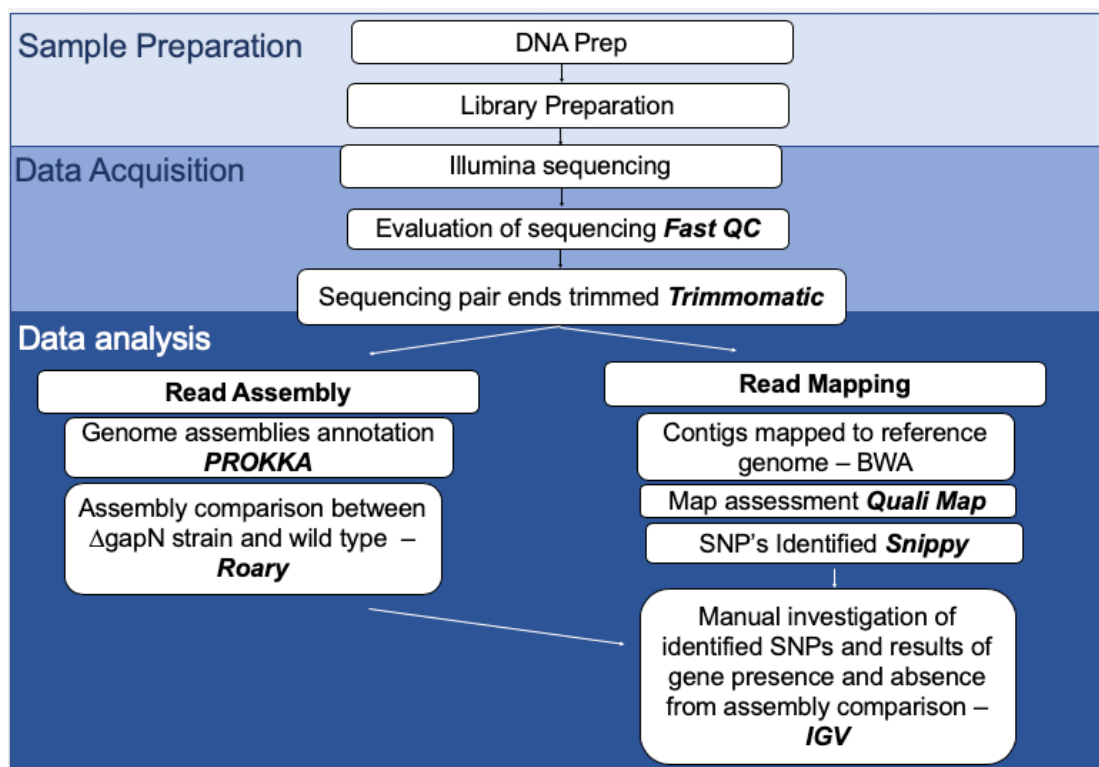


Figure 4.7 Diagram detailing the process of genome evaluation following illumina Miseq of the wild type and $\Delta gapN$ *C. saccharoperbutylacetonicum* N1-4(HMT).

4.4.1 Genomic read mapping of Illumina reads

The resulting short paired-end reads were assessed using FastQC before and after trimming of the reads using Trimmomatic (Bolger et al., 2014). Trimmomatic removes adaptor sequences inserted during library preparation, as well as low quality reads and bases from each dataset. The final trimmed reads from the wild type and the $\Delta gapN$ strain were mapped to the reference *C. saccharoperbutylacetonicum* N1-4(HMT) genome obtained from Genbank (CP004121.1). The mapping was carried out using BWA and Samtools (Li, 2013), and then Qualimap (García-Alcalde et al., 2012) was used to assess the quality of genome mapping of both strains (Table 4.1). Qualimap revealed that the main difference between the assemblies is that the coverage depth in the wild type strain is much lower than for the $\Delta gapN$ strain, meaning that during the process of sequencing the number of unique reads given to each nucleotide in the reconstruction process is much lower than in the wild type strain than in the $\Delta gapN$. A coverage depth of 68.59 ± 33.2 is seen in the $\Delta gapN$ strain and 18.8 ± 11.3 is seen the wild type *C. saccharoperbutylacetonicum* N1-4(HMT), this was thought to be a result of poorer quality starting material from the genomic DNA extraction process . Although coverage varied, 97.12 % of the total 596,655 reads for the wild type strain were mapped and 95.21% of the total 2,093,890 from the $\Delta gapN$ were successfully mapped to the reference genome obtained from Genebank (CP004121.1). The full Qualimap reports for wild type *C. saccharoperbutylacetonicum* N1-4(HMT) can be found in the Appendix E1 and appendix E2 for both the $\Delta gapN$ strain and wild type strain.

Table 4.1 Qualimap results of *C. saccharoperbutylacetonicum* N1-4(HMT) $\Delta gapN$ and Wild type following read mapping via bwa to the reference *C. saccharoperbutylacetonicum* N1-4(HMT) obtained from Gene bank (CP004121.1)

Characteristic	<i>C. saccharoperbutylacetonicum</i> N1-4(HMT) Strain	
	$\Delta gapN$	Wild Type
Reference size (bp)	6,530,257	6,530,257
Number of reads	2,093,890	596,655
Mapped reads	1,993,694 / 95.21%	579,484 / 97.12%
Supplementary alignments	1,509 / 0.07%	247 / 0.04%
Unmapped reads	100,196 / 4.79%	17,171 / 2.88%
Read min/max/mean length (bp)	30 / 251 / 224.9	30 / 251 / 212.68
Clipped reads	21,456 / 1.02%	4,726 / 0.79%
Mapping Quality	59.11	59.30
Mean Coverage	68.59 ± 33.2	18.8 ± 11.3

4.4.2 Sequence variant analysis and SNP identification

Once mapped, the illumina reads for the wild type and $\Delta gapN$ strain were analysed for variations between both sets of reads and the reference genome. Snippy (<https://github.com/tseemann/snippy>). is a software that finds SNPs between a reference and query next generation sequences (NGS). An overview of the variations found in the wild type and $\Delta gapN$ strain when compared to the reference genome for *C. saccharoperbutylacetonicum* N1-4(HMT) Genbank (CP004121.1) can be found in **Table 4.2**. Snippy reveals a total of 165 SNPs in the wild type NGS and 17 in the $\Delta gapN$ NGS, the complete list of all identified SNPs in both strains can be found in Appendix G.

Table 4.2 Breakdown of the total number of mutations identified in the wild type and $\Delta gapN$ strains compared to reference *C. saccharoperbutylacetonicum* N1-4(HMT) genome obtained from Gene bank (CP004121.1) by Snippy

	<i>C. saccharoperbutylacetonicum</i> N1-4(HMT) Strain	
	Wild Type	$\Delta gapN$
Mutation type:		
Complex	9	1
Deletion	9	4
Insertion	3	2
SNP	142	10
Total Variants	165	17

The SNP's identified by Snippy in the $\Delta gapN$ WGS were manually investigated using the Integrated genome viewer (IGV) (Robinson et al., 2011) alongside the wild type WGS mapping to further investigate whether or not the identified SNP's are a result of sequencing error. The SNP's predicted SNPs in the $\Delta gapN$ WGS occur within the following genes; *ybdI* (a predicted methionine transferase), *rocR_1* (predicted arginine utilization regulatory protein), *rsgI_2* (a predicted anti-sigma-I factor), *fdtB_2* (a predicted dTDP-3-amino-3,6-dideoxy-alpha-D-galactopyranose transaminase) and a hypothetical coding region.

Manual inspection of the SNP's identified in the $\Delta gapN$ WGS with the Wild type WGS in IGV (**Appendix G1-7**) show that all of the SNP's identified by Snippy (**Appendix H**) are also present in the WGS for the Wild type strain. This suggests that the Snippy predicted SNPs may not be genuine SNPs in the $\Delta gapN$ strain and they may be due to an error in sequencing or processing of the sequencing data and when compared to the published genome sequence Genbank (CP004121.1).

4.4.3 Whole genome annotation of Wild type and $\Delta gapN$ illumina reads

Once each of the genomes had been assembled both were annotated using Prokka (Seemann, 2014), a prokaryotic annotation software. Following annotation of the wild type *C. saccharoperbutylacetonicum* N1-4(HMT) and the $\Delta gapN$ NGS using Prokka, both annotations were compared to each other to gain a list of genes that are present or absent between the two assemblies. This analysis was carried out by Roary (Page et al., 2015). Typically used for the identification of large pan genomes in bacteria, Roary is able to compare two assembled and output a list of genes that are present and absent between both the wild type and $\Delta gapN$ assemblies. Roary identified a total of 5827 genes with a similarity of 97% (5659 genes) between the wild type and $\Delta gapN$. Of the total 5827 genes 130 (2.2%) were uniquely identified in the $\Delta gapN$ strain and only 38 genes (0.65%) were unique to the wild type annotation and not $\Delta gapN$. Complete Gene presence and absence can be found in **Appendix I**. Visualisation of the annotated genomes post Prokka was carried out using the BLAST atlas setting of the Gview server. (<https://server.gview.ca/>) (**Figure 4.8**).

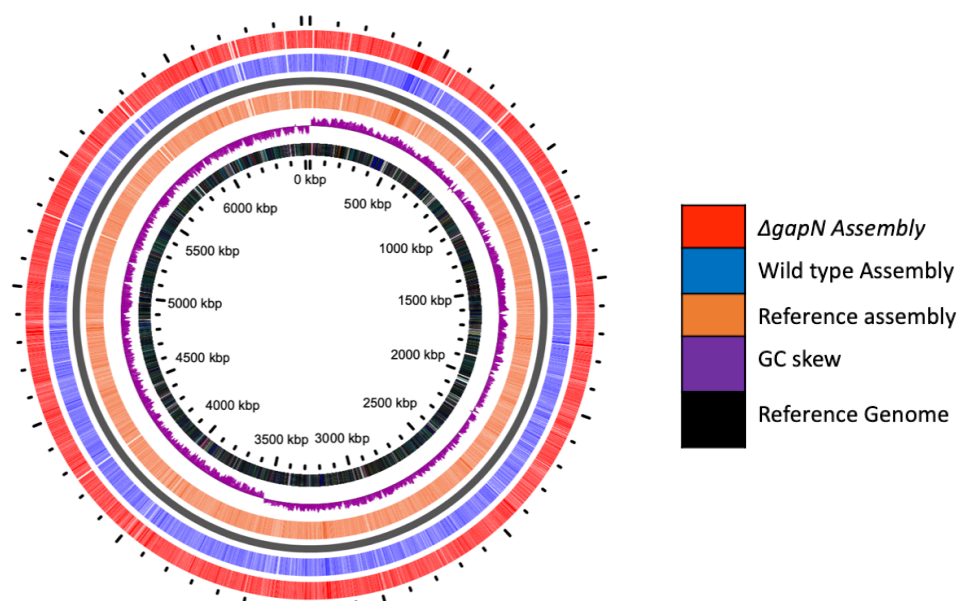


Figure 4.8 Whole genome comparison of the reference *C. saccharoperbutylacetonicum* N1-4(HMT) to genome assembly of the $\Delta gapN$ and wild type strains illumina sequenced strains. Inner ring (black) relates to the complete genome sequence of *C. saccharoperbutylacetonicum* N1-4(HMT), Fasta file for whole genome obtained from gene bank (CP004121.1). Purple ring related to the GC skew in the reference genome. Orange ring, genome annotation assembly from reference *saccharoperbutylacetonicum* N1-4(HMT), GBK for annotation obtained from gene bank (CP004121.1). Blue ring – Prokka assembly of illumina sequenced and Prokka annotated wild type *C. saccharoperbutylacetonicum* N1-4(HMT). Red ring – Prokka assembly of illumina sequenced and Prokka annotated $\Delta gapN$ *C. saccharoperbutylacetonicum* N1-4(HMT).

4.6 Discussion

4.6.1 CLEAVE™ results in successful deletion of $\Delta gapN$ and analysis reveals that it is accurate

Genetic manipulation of *Clostridium spp.* has lagged behind that of other well established industrially relevant organisms such as *E. coli* and *S. cerevisiae*. Prior to 2007 only a handful of targeted mutant strains had been established in *Clostridium spp.* (Clark et al., 1989; Harris et al., 2000; Mermelstein et al., 1993) with almost all of them being constructed by the process of either single or double recombination which themselves brought their own issues. In single recombination events a plasmid serves as an insertional mutagen, this is typically very unstable (Heap et al., 2012). In double recombination events the wild type allele is exchanged with the desired mutant allele. Double cross over events however were typically hard to screen for as the negative selection markers used in other more established strains were not yet developed in *Clostridium spp.*, until the advent of Group II mutagenesis system ClosTron (Heap et al., 2007) (**Figure 1.4A**). Post 2007 with the advent of available CRISPR/Cas and CRISPR interference (CRISPRi) technology the scope and flexibility of genetic tools in *Clostridium* has been quickly catching up to that of other industrial strains (Atmadjaja et al., 2019; Jenkinson et al., 2015; Joseph et al., 2018; Nagaraju et al., 2016; Wang et al., 2016; Woolston et al., 2018)

CLEAVE is a newly developed technology for CRISPR/Cas genome editing within *Clostridium spp.* because of this the literature around this technology is limited. Atmadjaja et al., (2019) have published work that details the discovery and design of the CLEAVE™ including the discovery of the CRISPR/Cas features within *C. saccharoperbutylacetonicum N1-4(HMT)*, including the identification of *C. saccharoperbutylacetonicum N1-4(HMT)* PAM sites. In addition to documenting the development of the CLEAVE™ the work also demonstrates the flexibility of CLEAVE for the creation of new strains containing SNPs, Deletions and Integrations. In the work, integration of varying sized lambda phage DNA (1,3,5 kb). into a site 4.8 kb downstream of the *pyrE* gene was tested. For the integration of 1 kb fragments a success rate of 60% was achieved, for 3 kb fragments a success rate of 53 % was achieved and for 5 kb fragments a success rate of 35% was achieved. It was noted that the decrease in integration of larger fragments might be due to the instability of larger plasmids generated when integrating larger Lambda DNA sequences.

Both deletion and SNP generation were attempted in the gene *spo0A*. For the SNP, a single nucleotide in the 782 position was modified in an attempted to cause the change I261T in *spo0A*, in addition a silent mutation was incorporated 180 bp upstream of the SNP to knock out the PAM site. Validation of the targeting spc vector as positive control resulting in a >99.5% efficiency in killing of wild type strains. However, when transformed with targeting

vector for the SNP, only 5 colonies were obtained with subsequently only 1 colony of the 5 being positive for the desired mutation.

Finally, deletion of the gene *Spo0A* was achieved using CLEAVE. As with the work in this thesis, deletion of a single gene within the genome of *C. saccharoperbutylacetonicum N1-4(HMT)* was achieved. Similar to the results here for the deletion of *gapN*, a 100% success rate was achieved when attempting a deletion of a single gene within the genome. 100% of the 30 colonies tested by Atmadjaja et al., (2019) being positive for the deletion.

4.6.2 NGS results of $\Delta gapN$ *C. saccharoperbutylacetonicum N1-4(HMT)*

NGS analysis of $\Delta gapN$ by illumina MiSeq provided a good depth of coverage ($x68 \pm 33$) that resulted in 95% coverage of mapped reads. Alongside the $\Delta gapN$ strain, illumina Miseq was carried out for the wild type *C. saccharoperbutylacetonicum N1-4(HMT)* as a control sequence against for analysis post sequencing. Coverage in the wild type was not as good at a depth $x18 \pm 11$ however 97% of the reads were able to be mapped. Despite Snippy detecting 17 SNP's throughout the NGS of $\Delta gapN$ the SNP's discovered were also present and identical in the NGS from the wild type *C. saccharoperbutylacetonicum N1-4(HMT)* (**Appendix H1-7**), suggesting that these mutations may not be as a result of the CLEAVE process, but errors in the sequencing and analysis process. Genome annotation and subsequent comparison of annotations reveal a high similarity of 97% between both strains. Of the 130 genes identified to be present in only the $\Delta gapN$ annotation and not in the wild type, the majority were hypothetical coding regions of unknown function. *GapN* was identified as part of the 38 unique genes in the wild type NGS and not found in the $\Delta gapN$ NGS.

Overall, this work has demonstrated the functionality of CLEAVE for the purpose of gene deletion with *C. saccharoperbutylacetonicum N1-4(HMT)* and demonstrates the functionality of CLEAVE in line with previous studies by Atmadjaja et al., (2019).

Chapter 5

Characterisation of $\Delta gapN$ and its potential for improved ABE production.

5.1 Summary

In this chapter the $\Delta gapN$ strain created in chapter 4 has been compared to the wild type *C. saccharoperbutylacetonicum* N1-4(HMT) to assess the deletion has on ABE production, sugar metabolism, butanol toxicity and ATP concentrations. The main hypotheses driving the decision the deletion of *gapN* is to increase the availability of ATP within the cells. Increases in ATP as well as NADH have been shown to be responsible for increased solvent production (Meyer and Papoutsakis, 1989). To test is this hypothesis the $\Delta gapN$ strain was firstly grown on a glucose YETM media in a batch fermentation. By keeping the fermentation in a batch set up it provided a clear shift into solventogenesis with the addition to showing glucose consumption and any increased to peak butanol concentrations and tolerance. Overall the $\Delta gapN$ strain exhibited similar growth to the wild type strain in the form of OD₆₀₀, pH, and redox potential. However, the $\Delta gapN$ strain produced lower concentrations of acetic and butyric acid, throughout and generated elevated concentrations of acetone and butanol compared to the wild type *C. saccharoperbutylacetonicum* N1-4(HMT) until pre-toxic concentrations $\sim 13 \text{ g L}^{-1}$. In addition to this the $\Delta gapN$ strain exhibited an increased rate of glucose consumption during the batch fermentation as well as increased concentrations of ATP throughout.

To simulate an industrial feedstock and further assess the impact on sugar metabolism, a synthetic C5/C6 hydrolysate mixture was used. Overall deletion of *gapN* does not appear to have any detrimental or enhanced effects of the metabolism of the C5/C6 synthetic sugar mix compared to the wild type strain. Consistent with the glucose only batch fermentations there was diminished concentrations of acids associated with solvent production (acetic and butyric acid) as well as increased concentrations in the production of acetone and butanol in $\Delta gapN$ strain. Initial batch fermentations showed an increase glucose consumption in the $\Delta gapN$ strain as well as an associated increase in solvent production. To confirm this observation a fed batch fermentation was carried out in which glucose consumption of 350 g L^{-1} was assessed over a longer 65 h period, with solvent removal via gas stripping to ensure toxic concentrations were mitigated. Contrary to the initial batch fermentation, the observed rate of sugar consumption during the fed batch experiment was lower in the $\Delta gapN$ strain compared to the wild type. Despite this however, the $\Delta gapN$ strain had comparable concentrations of solvent production to the wild type strain throughout, suggesting that glucose consumption may not be linked to increased solvent production seen in the $\Delta gapN$ strain as lower consumption in the fed batch does not affect solvent production. Finally, increased concentrations of both formic and lactic acid in the $\Delta gapN$ strain were observed during fermentation. This suggests that there is an accumulation of pyruvate within the cell that is being converted to either lactic or formic acid as a means of dealing with increased concentrations of pyruvate.

5.1 Introduction

Deletion of *gapN* has been done in an attempt to recover ATP that would have otherwise been lost in the conversion of glyceraldehyde-3-phosphate (G3P) to 3-phosphoglycerate via flux through GapN in glycolysis. Removal of GapN, forces the cells to use only GAPDH (Figure 4.1) instead of using both GAPDH and GapN in the glyceraldehyde-3-phosphate oxidation pathway of glycolysis. This in turn, will allow for the cell to recover the ATP that is generated via the GAPDH side of the glyceraldehyde-3-phosphate oxidation pathway that otherwise would not be produced in the presence of GapN. As described above, GapN is one of three types of GAPDH's present in the cell and forms part of the glyceraldehyde-3-phosphate oxidation pathway (Figure 4.1). Previous flux analysis in *C. acetobutylicum* (Minyeong Yoo, Gwenaelle Bestel-Corre, Christian Croux, Antoine Riviere, Isabelle Meynial-Salles, 2015) has revealed that GapN is poorly expressed at 0.56 mRNA molecules per cell in comparison to 66 mRNA molecules per cell of GAPDH. This poor expression leads to only 3500 protein molecules per cell of GapN compared to 190000 protein molecules per cell of GAPDH. It was predicted that GapN would only be responsible for around 5% of flux through the glyceraldehyde-3-phosphate oxidation pathway. This previously observed low flux and low levels of regulation within the cell, heavily influenced the decision to delete *gapN* gene from *C. saccharoperbutylacetonicum* N1-4(HMT). In addition to this, recombinant GapN expression has been used a method of NADPH generation in other bacteria (Centeno-Leija et al., 2014). ATP is important throughout the cell as a key energy carrier and despite developing complex metabolic networks for energy generation (Demmer et al., 2015), anaerobic bacteria lack the ability to generate ATP via oxidative respiration. This lack of oxidative respiration limits the overall potential for ATP production compared to organisms that are able to generate ATP via oxidative respiration. Solventogenic *Clostridium spp.* generation of the majority of their ATP during acidogenesis (Meyer and Papoutsakis, 1989) with increased ATP and NADH concentrations associated with increased solvent production (Meyer and Papoutsakis, 1989). ATP required by the cells to undergo reduction processes following glycolysis as well as extrusion of protons by means of proton-translocating ATPases system (Jones and Woods, 1986).

In this chapter we have replicate industrial growth conditions to test the $\Delta gapN$ strain compared to the wild type. For this batch fermentations were carried out on both C6 only (glucose) and a synthetic C5/C6 hydrolysate, as well as fed-batch using C6 over a prolonged period of time. It is of note that despite advancements in fermentation techniques and solvent recovery processes, the two main limiting factors in the industrial ABE fermentation are feedstock (Green, 2011) and the inherent limitations of the bacteria themselves, it is hoped that deletion of *gapN* will aid in elevating the limiting factor of the bacteria.

5.2 Results

5.2.1 Characterisation of $\Delta gapN$ strain during a batch fermentation on glucose YETM to assess the impact on ABE production, Butanol toxicity and ATP.

An initial characterisation of the $\Delta gapN$ and wild type *C. saccharoperbutylacetonicum* N1-4(HMT) strains was performed via batch fermentation in YETM medium containing 40 g L⁻¹ glucose and supplemented with 0.1 M MES for pH control. Cells were initially grown in the seed culture described in Section 2.1.8 before being used for inoculation of the batch fermenters that are described in Chapter 3. The experiment was carried out over 45 h. Both strains reached similar cell densities, with maximal OD₆₀₀ values of 7.22 ± 0.22 for the wild type and 7.4 ± 0.26 for the $\Delta gapN$ strain (Figure 5.1A). Although fairly similar throughout, between the hours 9 and 21 in fermentation, the pH of the fermenter media for the $\Delta gapN$ strain is less acidic throughout compared to the wild type *C. saccharoperbutylacetonicum* N1-4(HMT) (Figure 5.1B). The redox potential of the growth media for both strains behaved in a predictable manner, both dropping to approximately -300 mV vs. NHE in the first few hours (Figure 5.1C). Glucose concentrations were also monitored throughout the fermentations, and the rate of consumption was greater between 10-20 h compared to the wild type strain (Figure 5.1D).

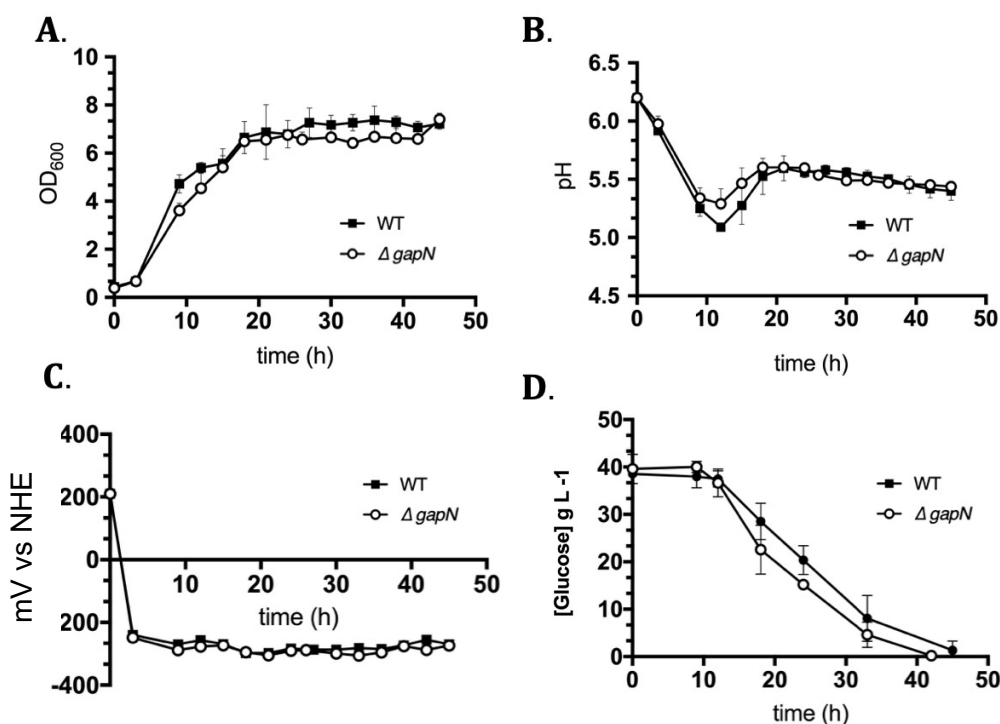


Figure 5.1 Fermentation measurements for $\Delta gapN$ (open circles) and wild type (closed circles) *C. saccharoperbutylacetonicum* N1-4(HMT) grown on 40 g L⁻¹ glucose in YETM media using shepherd lab fermenters. 0.1 M MES was supplemented as a pH buffering agent. (A) OD₆₀₀; (B) pH; (C) redox potential of media (mV vs. NHE); (D) Glucose concentrations in growth media.

The product of acidogenesis and solventogenesis were then analysed for the $\Delta gapN$ and wild type strains from the same batch fermentation as described in Figure 5.1. The $\Delta gapN$ strain exhibited reduced concentrations of acids throughout the fermentation (Figure 5.2A-B). In addition, depletion of acid concentrations in the $\Delta gapN$ strain also occurred at a faster rate in the $\Delta gapN$ strain compared to the wild type *C. saccharoperbutylacetonicum* N1-4(HMT) (Figure 5.2C-D). The largest observed discrepancies between the strains for acetic acid and butyric acid measurements were observed at 15 h: 0.057 g L⁻¹ of butyric acid and 0.073 g L⁻¹ of acetic acid were measured for the $\Delta gapN$ strain, compared to 0.170 g L⁻¹ of butyric acid and 0.29 g L⁻¹ of acetic acid for the wild type strain. The concentrations of acetone and butanol produced by the $\Delta gapN$ strain were higher during the first 30 h of the fermentation, and largest observed discrepancies between the strains for acetone and butanol measurements occurred at 15 h: [acetone] produced by the $\Delta gapN$ strain was 3.2 g L⁻¹ compared with only 1.1 g L⁻¹ in the wild type strain; [butanol] produced by the $\Delta gapN$ strain was 6.87 g L⁻¹ compared to 3.5 g L⁻¹ in the wild type strain. Peak concentrations of butanol in the $\Delta gapN$, however, were similar to those of the wild type cultures at approximately 13 g L⁻¹.

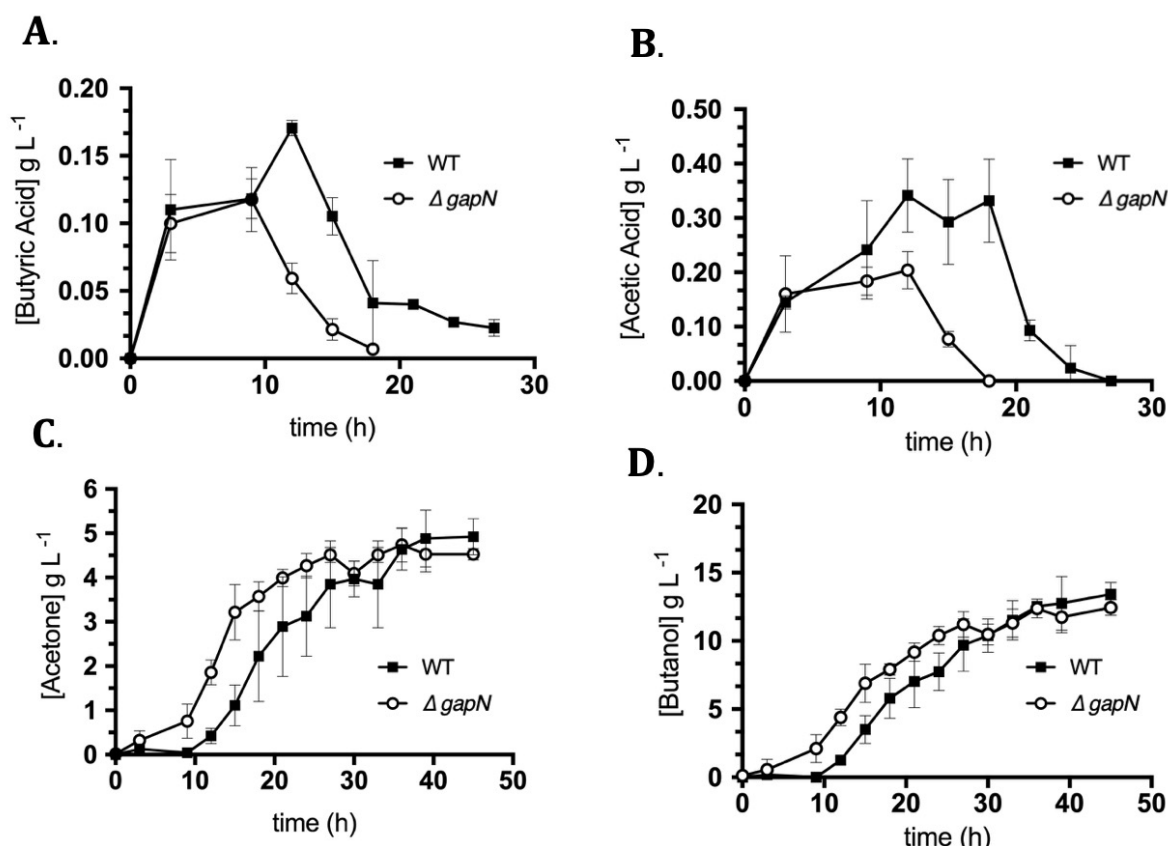


Figure 5.2 Acid and solvent profiles for $\Delta gapN$ (open circles) and wild type (closed circles) *C. saccharoperbutylacetonicum* N1-4(HMT) grown on 40 g L⁻¹ glucose in YETM media using shepherd lab fermenters. 0.1 M MES was supplemented as a pH buffering agent. (A) [butyric acid]; (B) [acetic acid]; (C) [acetone]; (D) [butanol].

As the observed final concentrations of butanol and acetone were similar for $\Delta gapN$ and wild type strains, it was hypothesised that solvent toxicity was the limiting factor for these measurements. To test this hypothesis, a butanol toxicity test was carried out that measured growth rates in the presence of varying concentrations of solvents, as described in Section 2.1.13. Deletion of the *gapN* did gene not have an effect on the cells ability to handle solvent toxicity any better than the wild type, and there is no significant difference (Figure 5.3).

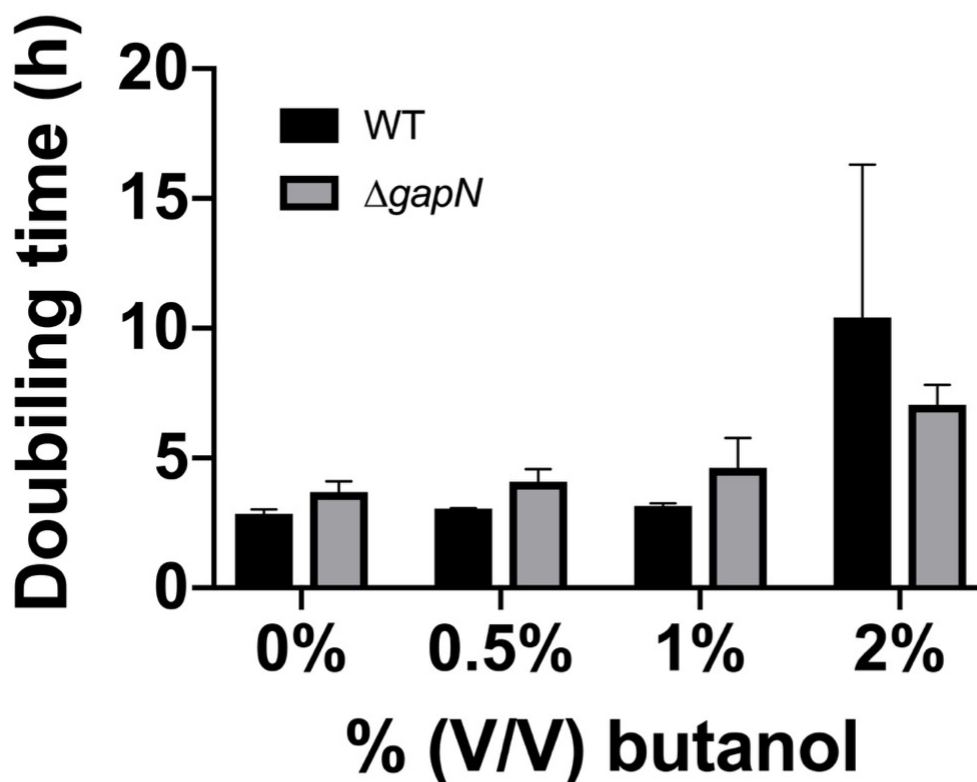


Figure 5.3 Butanol toxicity test of wild type (black bars) and $\Delta gapN$ (grey bars) strains of *C. saccharoperbutylacetonicum* N1-4(HMT). Cells were grown to an OD_{600} of 1 and were then challenged with varying [butanol]. Doubling times were calculated for the 48 h of growth that followed solvent addition.

In addition to growth, butanol toxicity, acid and solvent production, ATP concentrations were measured during the glucose batch fermentation. The ATP concentration in the $\Delta gapN$ strain compared to the wild type strain was higher for the majority of fermentation period (Figure 5.4). The greatest discrepancy in ATP concentration between the $\Delta gapN$ and wild type strains was observed at 15 h, where $11.2 \mu\text{mol g}^{-1}$ cell dry mass was recorded for the $\Delta gapN$ strain compared to $4.7 \mu\text{mol g}^{-1}$ cell dry mass for the wild type.

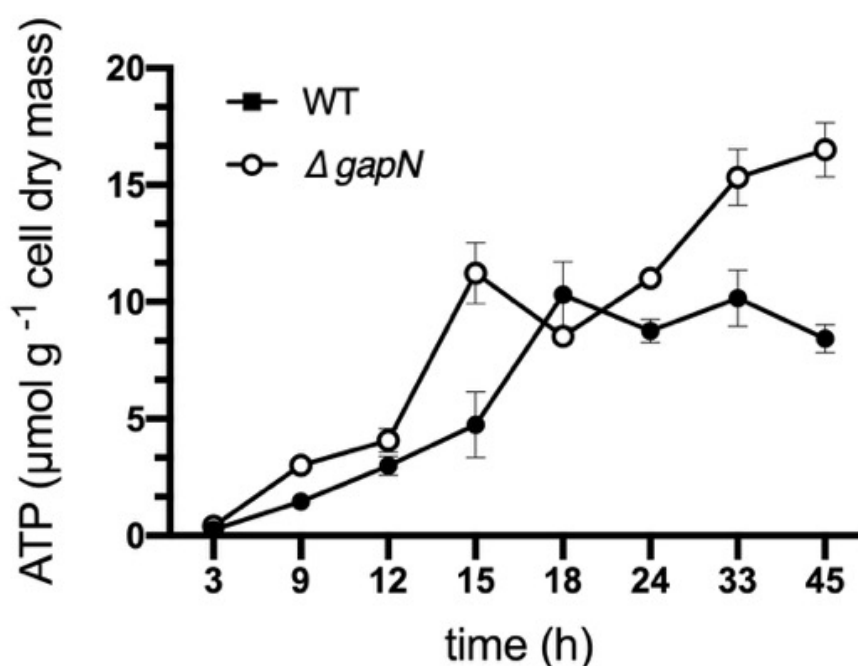


Figure 5.4 ATP measurements for $\Delta gapN$ (open circles) and wild type (closed circles) *C. saccharoperbutylacetonicum* N1-4(HMT) grown in 40 g L^{-1} glucose in YETM media using shepherd lab fermenters. ATP concentrations were measured from cells that from a glucose batch fermentation in YETM supplemented with 0.1 M MES for pH control. ATP concentration of cells were measured in accordance to methodology in Section 2.8.2

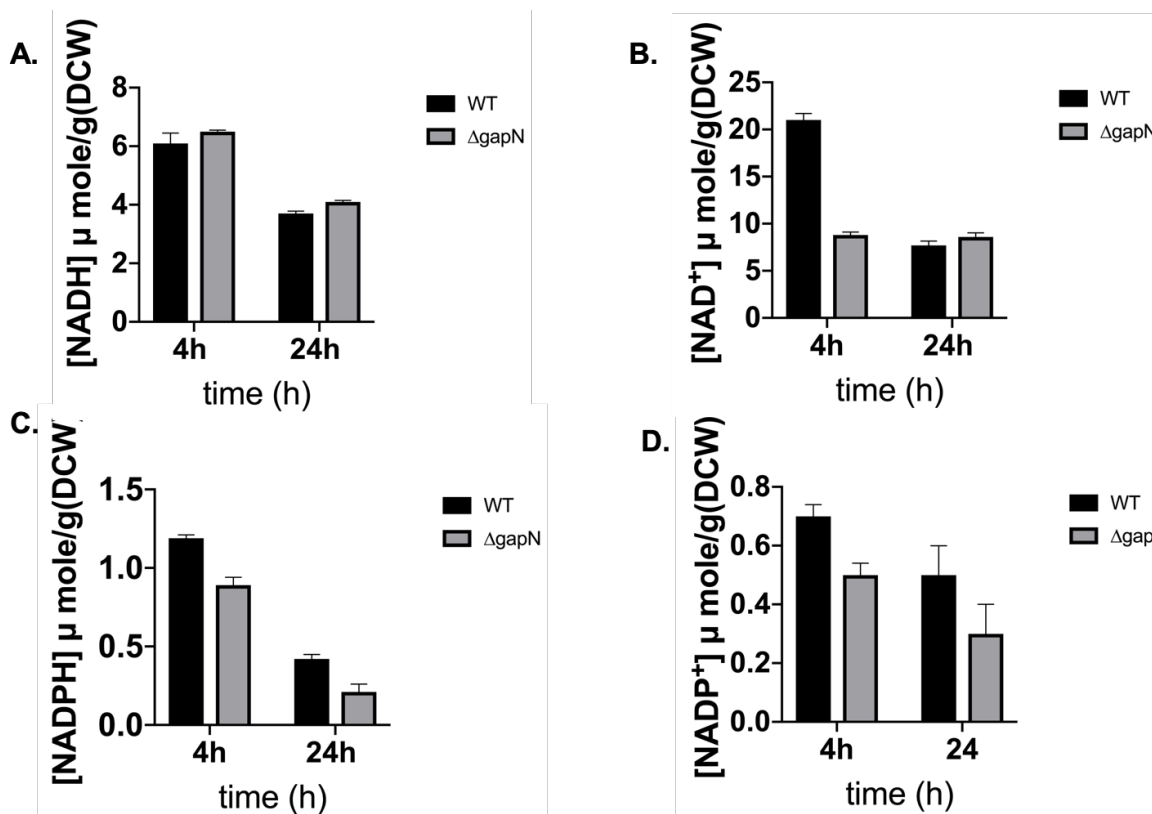


Figure 5.5 Concentration of nucleotide cofactors in both the wild type (black box) and the ΔgapN (grey box) during acidogenesis (4h) and Solventogenesis (24 h). Cells were grown in YETM 40 g L^{-1} glucose in 50 ml serum bottle reactions over the course of 24 h.

Due to the labile nature of NAD(P) derivatives, cells were grown in serum bottles and assayed at 4 h and 24 h to give an indication of the state of the cells in early exponential phase (acidogenesis) as well as in late exponential/stationary phase (solventogenesis). Deletion of *gapN* did not appear to have an effect on the overall concentrations of both NADH and NADPH, however there is a marked reduction in the concentrations of NAD⁺ and NADP⁺ during both acidogenesis and solventogenesis, indicating there is a more reducing environment present in the ΔgapN strain compared to the wild type (Figure 5.5).

5.3 Characterisation of ΔgapN strain on a synthetic C5/C6 hydrolysate mixture

To further investigate sugar utilisation in the ΔgapN strain, an additional batch fermentation was carried out this time using a synthetic C5 hydrolysate mixture consisting of 11 g L^{-1} glucose, 14 g L^{-1} xylose, 4.65 g L^{-1} galactose, 1.96 g L^{-1} arabinose and 18.4 g L^{-1} mannose in YETM. This medium is used by project partners to simulate industrial feedstocks made from waste lignocellulosic. Fermentation results show that when grown on the C5 sugar mix, the ΔgapN had an increased consumption rate for galactose, whereas all other sugars were consumed at the same or similar rates to the wild type strain (Figure 5.6). These data also demonstrate that both strains prefer C6 sugar utilisation compared to C5 sugars, which

is consistent with previous studies on other solventogenic clostridial strains (Noguchi et al., 2013)(Bogorad et al., 2013; Bruder et al., 2015; Fu et al., 2017).

To complement the sugar utilisation experiments described above, it was of interest to investigate how the $\Delta gapN$ mutation impacted upon acidogenesis. In the glucose only batch fermentation, the concentration of acids associated with solvent production (i.e. acetic acid and butyric acid) were diminished throughout the fermentations in the $\Delta gapN$ strain (Figure 5.2). similar picture is observed during fermentation on the C5 hydrolysate mixture for the $\Delta gapN$ strain (Figure 5.7A-B). The largest difference discrepancy between the wild type and $\Delta gapN$ strains for butyric acid was seen at 12 h: butyric acid concentrations in the $\Delta gapN$ strain were 0.063 g L^{-1} , which was x10 lower than the 0.60 g L^{-1} found in the wild type strain at the same timepoint (Figure 5.7B). Interestingly, in the C5 hydrolysate mixture there was an increase in the concentration of both formic acid and lactic acid in the $\Delta gapN$ not seen previously (Figure 5.7C-D). Unlike the solventogenic acids that are produced early on and assimilated into solvents, lactic and formic acid concentrations continue to increase throughout the duration of the fermentation. The largest discrepancy between the wild type and $\Delta gapN$ strains was observed at the end of the 48 h fermentation, with $0.37 \pm 0.01 \text{ g L}^{-1}$ formic acid produced in the $\Delta gapN$ strain and $0.295 \pm 0.007 \text{ g L}^{-1}$ produced by the wild type. Similarly, $2.838 \pm 0.005 \text{ g L}^{-1}$ and $2.1 \pm 0.07 \text{ g L}^{-1}$ lactic acid was produced at 48 h in the $\Delta gapN$ strain and the wild type strain, respectively.

In the synthetic C5 hydrolysate mixture, there was a pronounced increase in the concentration of acetone in the $\Delta gapN$ strain throughout compared to the wild type strain (Figure 5.7E). However, when grown on the C5 mixture, the butanol produced by the $\Delta gapN$ strain only displayed a modest elevation in butanol levels (Figure 5.7F).

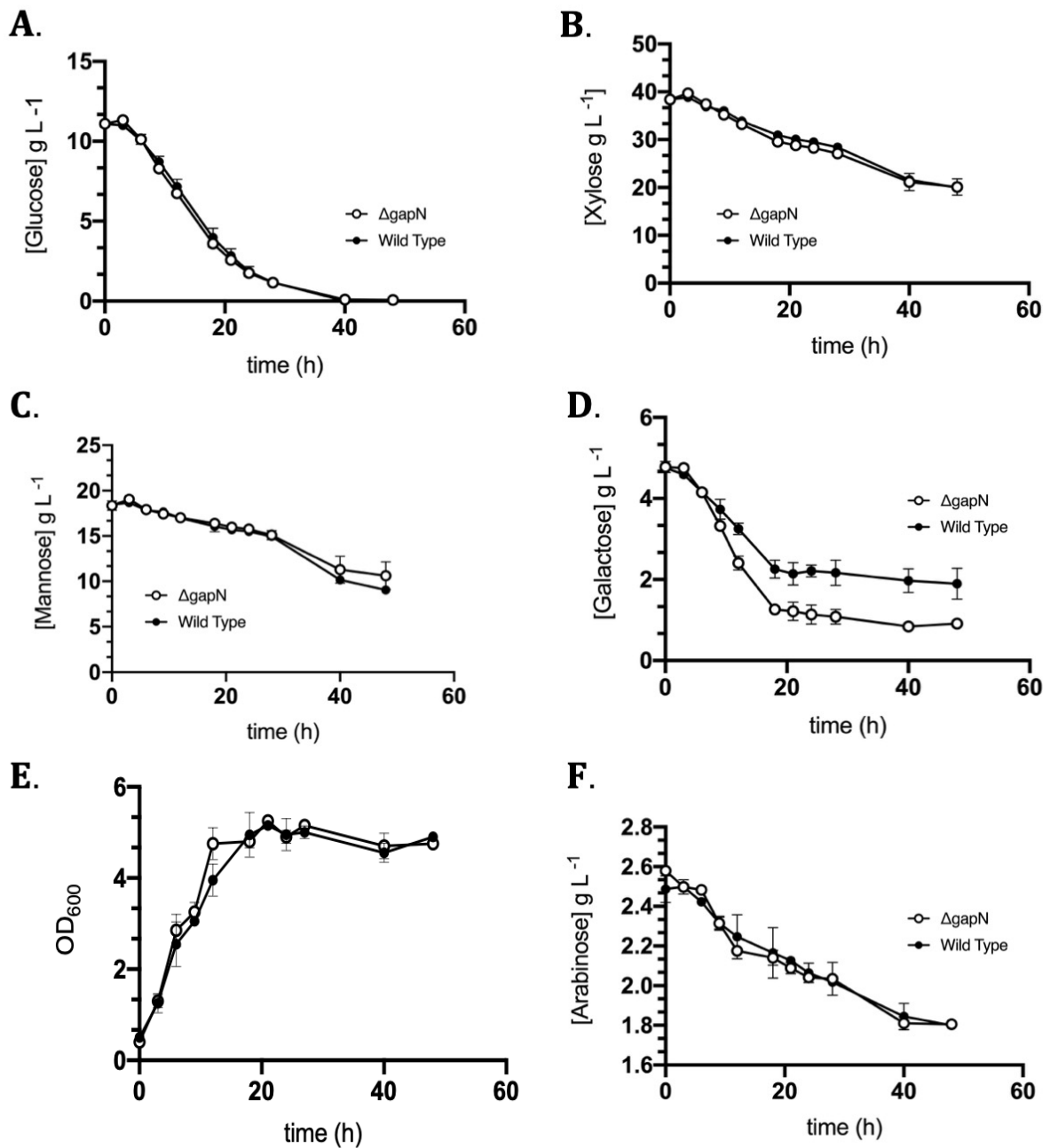


Figure 5.6 Sugar profiles for $\Delta gapN$ (open circles) and wild type (closed circles) *C. saccharoperbutylacetonicum* N1-4(HMT) grown on C5 hydrolysate mixture using GBL fermenters. Cells were grown in a total sugar concentration of 50 g L⁻¹. This medium contained a mixture of sugars that closely resembled a C5 sugar hydrolysate mixture containing glucose, xylose, maltose, mannose, galactose and arabinose. The pH was controlled via addition of ammonium acetate to maintain the pH above 5.2. Measured parameters were: (A) [glucose]; (B) [xylose]; (C) [mannose]; (D) [galactose]; (E) OD₆₀₀; (F) [arabinose].

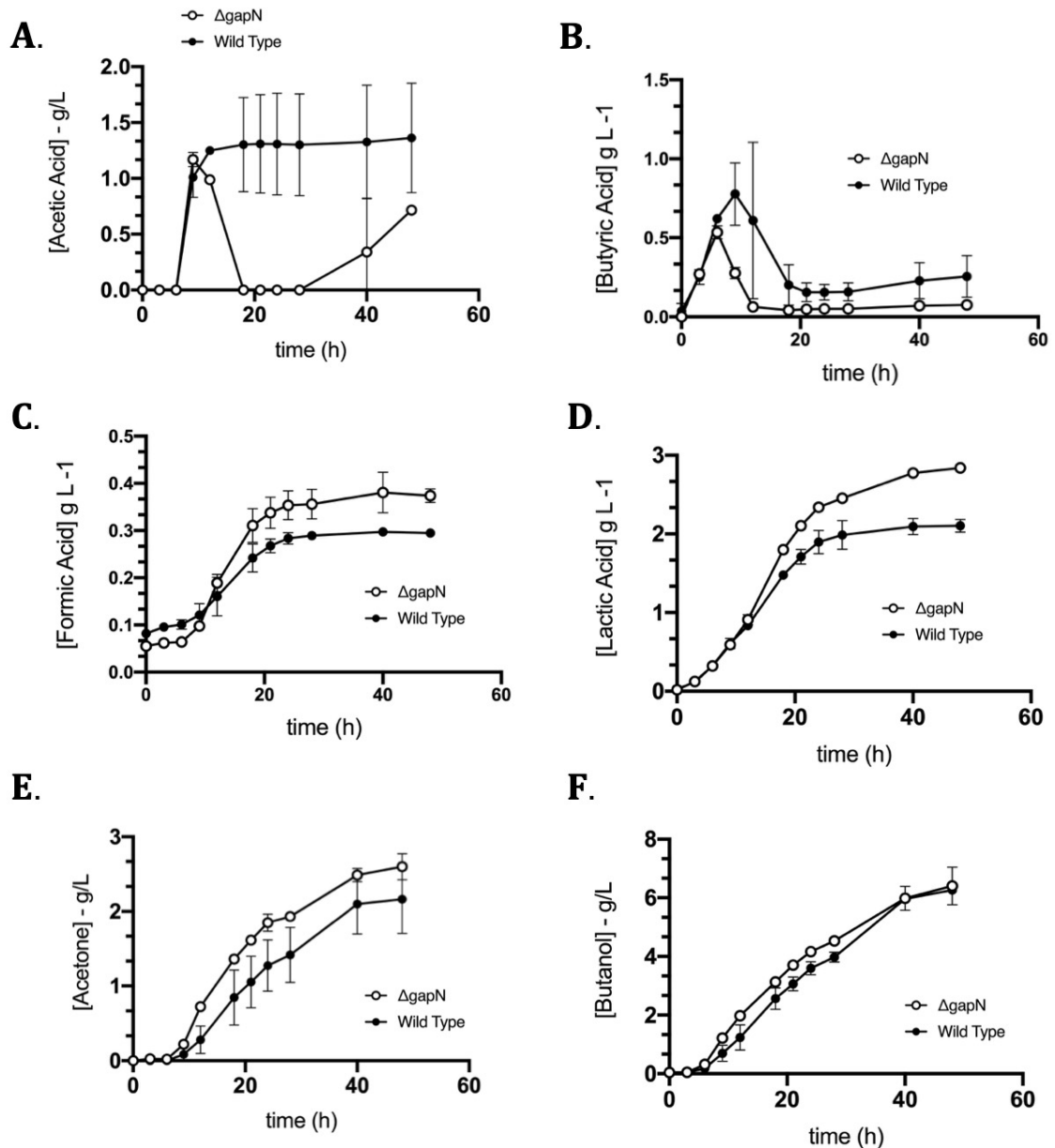


Figure 5.7 Acid and solvent profiles for $\Delta gapN$ (open circles) and wild type (closed circles) *C. saccharoperbutylacetonicum* N1-4(HMT) grown on C5 hydrolysate mixture using GBL fermenters. Cells were grown in a total sugar concentration of 50 g L⁻¹, this 50 g consisted of a mixture of sugars that closely resembled a C5 sugar hydrolysate mixture containing Glucose, Xylose, Maltose, Mannose, Galactose and Arabinose. pH was controlled via addition of ammonium acetate to maintain the pH above 5.2. Measured parameters were: (A) [acetic acid]; (B) [butyric acid]; (C) [formic acid]; (D) [lactic acid]; (E) [acetone]; and (F) [butanol].

5.4 Fed batch fermentation to assess glucose uptake and sugar utilisation in relation to solvent production

In the experiments described in Section 5.2, the $\Delta gapN$ strain was grown in batch fermenters in YETM medium containing 40 g L⁻¹ glucose. In summary, the $\Delta gapN$ strain exhibited an increase in glucose consumption throughout the batch fermentation and exhibited increased production of butanol and acetone to sub-toxic concentrations. In addition, a reduction in solventogenic acids acetic and butyric acid was observed in the

$\Delta gapN$ strain compared to the wild type (Figure 5.3). To further test the glucose consumption rates observed in the first experiment and to investigate the behaviour of this newly constructed strain over a longer more metabolically intense period; a fed batch fermentation experiment was carried out. In this experiment, starting glucose concentrations of 50 g L^{-1} were at first allowed to drop to just below 10 g L^{-1} , and were then maintained at 10 g L^{-1} , throughout. Throughout the fermentation, gas stripping using nitrogen at 1 volume of gas per fermenter volume per min was carried out to maintain solvent concentrations below toxic concentrations. The OD_{600} of the $\Delta gapN$ strain was maintained at similar levels to the wild type throughout (Figure 5.8A). The observed difference in pH did appear to coincide with the slightly elevated pH in the $\Delta gapN$ strain later in the fermentation (Figure 5.8B). Unlike the first YETM/glucose experiments, the $\Delta gapN$ strain used less glucose throughout the fermentation and the rate of glucose consumption over the duration of the fermentation was also reduced in the $\Delta gapN$ strain compared to the wild type (Figure 5.8C-D).

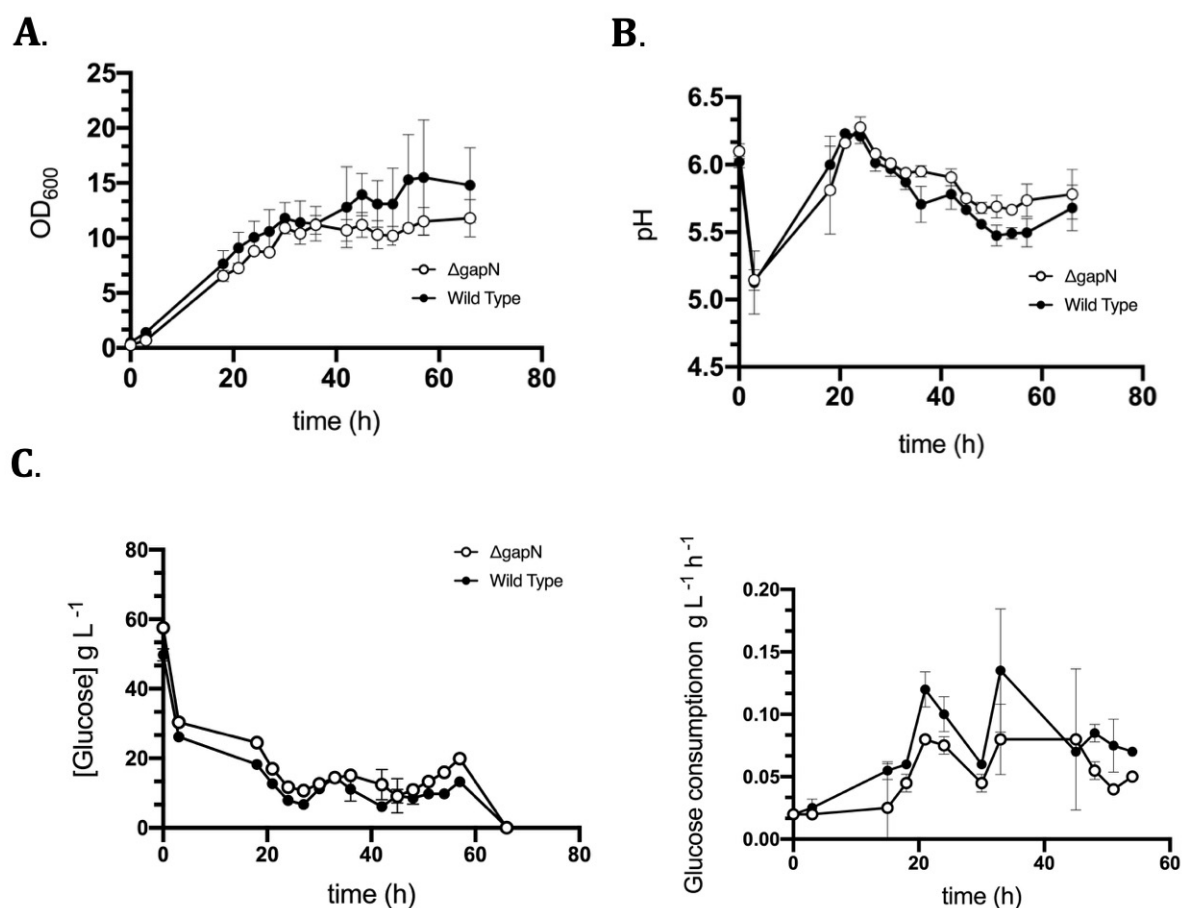


Figure 5.8 Growth parameters and glucose profiles for $\Delta gapN$ (open circles) and wild type (closed circles) *C. saccharoperbutylacetonicum* N1-4(HMT) grown in fed batch fermentations using GBL fermenters. Cells were grown initially in 50 g L^{-1} glucose YETM, following an initial batch of 16 h cells glucose concentrations were maintained as close to 10 g L^{-1} as possible. Measured parameters were: A) cell culture growth and density (OD_{600}); B) pH; C) Concentration of glucose in medium; D) Glucose consumption rate $\text{g L}^{-1} \text{ h}^{-1}$.

Similarly, to the previous fermentations described in this chapter, there was a marked decrease in acetic acid and butyric acid throughout the fed batch fermentation in the $\Delta gapN$ strain (Figure 5.9A-B) as well as the observed increased concentrations in lactic and formic acid that were observed during the synthetic C5 hydrolysate fermentation (Figure 5.9C-D). Due to the gas stripping that was taking place during this fermentation, concentrations of acetone and butanol were similar between both strains.

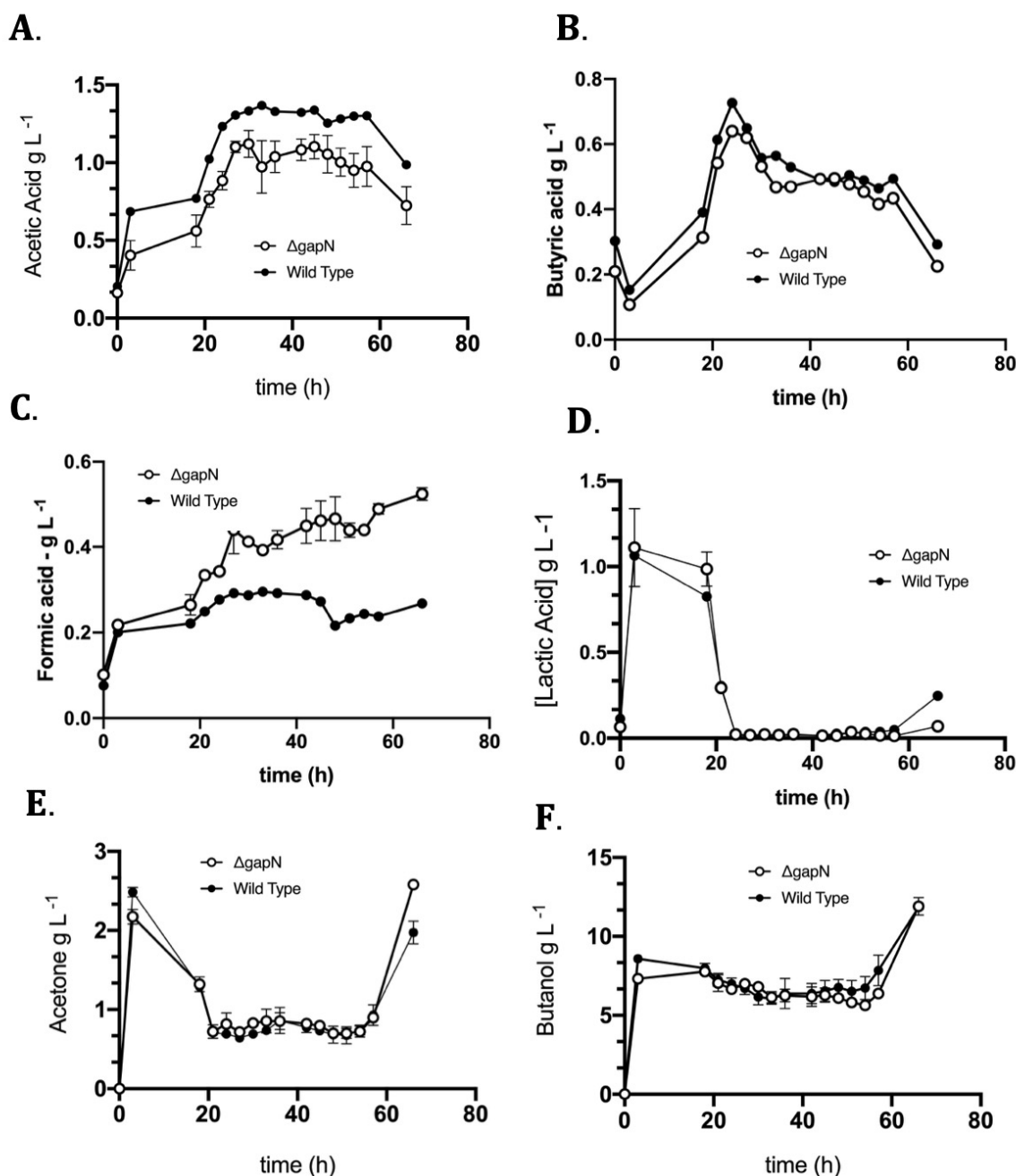


Figure 5.9 Acid and solvent profiles for $\Delta gapN$ (open circles) and wild type (closed circles) *C. saccharoperbutylacetonicum* N1-4(HMT) grown in fed batch fermentations. Cells were grown initially in $50 g L^{-1}$ glucose YETM, following an initial batch of 16 h cells glucose concentrations were maintained as close to $10 g L^{-1}$ as possible. Measurements made were: A) [acetic acid]; B) [butyric acid]; C) [formic acid]; D) [lactic Acid]; E) [acetone]; F) [butanol].

5.5 Discussion

5.5.1 Observed increase in ATP production as a result of *gapN* deletion, leads to decreased acid production, earlier shift into solventogenesis as well as increased solvent production until pre-toxic concentrations

The $\Delta gapN$ strain exhibits reduced concentrations of acetic and butyric acid with increased production of acetone and butanol to pre-toxic concentrations in both the glucose only batch fermentation (Figure 5.2) and the C5/C6 synthetic sugar mixture (Figure 5.7). As well as reduced concentrations of acids throughout, the assimilation of acetic and butyric acid occurs sooner in the $\Delta gapN$ strain than in the wild type strain, with butyric acid in $\Delta gapN$ strain during the glucose only fermentation peaking at 9 h and are then depleted by 18 h whereas in the wild type, concentrations of butyric acid do not peak until 15 h and are not completely depleted even towards the end of the fermentation (Figure 5.3A). A similar picture is seen in the C5/C6 synthetic mixture, here acid concentrations peak much earlier and are assimilated much earlier on in the $\Delta gapN$ strain compared to the wild type (Figure 5.7).

Despite the lower concentrations of acids, and their assimilation earlier on in fermentation, the $\Delta gapN$ strain is able to produce increased concentrations of solvents throughout until toxic concentrations are reached; this included initiation of solvent production earlier on in fermentation. This is observed in both the glucose only batch fermentation (Figure 5.2) and in the C5/C6 batch fermentation (Figure 5.7). The increase in solvent production is hypothesised to be a result of the increased ATP concentration (Figure 5.4) in tandem with the more reducing environment found in the $\Delta gapN$ strain compared with the wild type as a result of the ratio of NADH:NAD⁺ observed (Figure 5.5). Throughout the glucose only fermentation measured ATP is higher in the $\Delta gapN$, however between 15-25 h there is an observable dip in the concentration of ATP in the $\Delta gapN$ strain (Figure 5.5), that correlates with the beginning of acid assimilation as well as the largest incline in solvent production during the fermentation (Figure 5.2). This suggest that deletion of $\Delta gapN$ increases ATP concentrations enough whereby the cell does not need to invest in acidogenesis to generate enough of a ATP concentration to aid in the shift into solventogenesis. ATP and reducing cofactors such as NAD(P)⁺/H have been shown to be key in the shift into solventogenesis (Amador-Noguez et al., 2011; Girbal et al., 1995; Wang et al., 2012; Zhang et al., 2014) with key regulatory proteins such as Rex being closely linked with the reducing conditions with the cell (McLaughlin et al., 2010; Wietzke and Bahl, 2012; Zhang et al., 2014). Acidogenesis occurs in the vegetative stage of growth and acts as a key stage for the accumulation of the ATP that will later be used for the production into solventogenesis (Grupe and Gottschalk, 1992). ATP in *Clostridium spp.* has also been documented as being responsible for ATPase proton translocation (Jones and Woods, 1986) within the cell that

aids in maintaining the proton gradient following the shift into solventogenesis to ensure $\text{ADP} + \text{P}_i$ is recycled via a F1F0 ATPase to maintain ATP concentrations during solventogenesis when the overall production of ATP will be greatly reduced without acid production (**Figure 1.2**). V-type ATPases having been documented in *Clostridium spp.* (Boekema et al., 1998; Speelmans et al., 1994), however it is worth noting that *C. saccharoperbutylacetonicum* N1-4(HMT) like a handful of other *Clostridium spp.* contains an RnF complex. The RNF complex, like the ATPases found throughout allows *C. saccharoperbutylacetonicum* N1-4(HMT) generate an ion gradient, and in doing generate NADH via the oxidation of ferredoxin (Poehlein et al., 2017); something that others strains such as *C. acetobutylicum* lack. This combined with the data above aids in reinforcing the original hypothesis that deletion of *gapN* would subsequently result in higher ATP concentrations, reduced acid concentrations as well as increased solvent concentrations during fermentation, however, the earlier shift and assimilation of acids was unexpected in the original hypothesis.

5.5.2 Increased production of lactic and formic acid in the $\Delta gapN$ strain

In the synthetic C5 sugar mixture there was a marked increase in the production of formic acid (Figure 5.6C) and lactic acid (Figure 5.6D) in the $\Delta gapN$ strain. Similarly, the $\Delta gapN$ strain has an increase in the production of formic acid in the glucose fed batch fermentation (Figure 5.7C), however the difference in lactic acid was not as significant in the glucose fed batch (Figure 5.7D). In both experiments the concentrations of both lactic acid and formic acid have continued to rise even in the late stages of the fermentation. It has been documented that during the shift from acidogenesis to solventogenesis in *C. acetobutylicum* there is a shift metabolically away from pyruvate into oxaloacetate (10 fold), as the cell moves away from amino acid production and to solvent production as carbon is redirected to acetyl coenzyme A for ABE production (Amador-Noguez et al., 2011). Due to the early shift into solventogenesis that is observed in the $\Delta gapN$ strain it is not unlikely to consider that the earlier shift results in an accumulation of pyruvate, that is then dealt with by both a lactate dehydrogenase leading to lactate production and formic acid production via a pyruvate formate lyase. This suggests that as solvent production becomes saturated and butanol toxicity becomes a factor, the cell has to unload any excess pyruvate to enable solvent production to continue, hence the observed continual increases in formic and lactic acid production all the way throughout fermentation (Figure 5.7 & Figure 5.6).

5.5.2 The $\Delta gapN$ strain has same plight of CCR common amongst *Clostridium*

Carbon catabolite repression (CCR) is common among a variety of solventogenic *Clostridium*. Regardless of strain or feedstock there is always a preferential uptake and metabolism of C6 sugars that utilise glycolysis over C5 sugars, in fact in the presence of a C5/C6 mixture often little to no C5 metabolism will occur even following depletion of C6 sugars (Aristilde, 2017; Chang, 2010; Zhang et al., 2017). The problem of C5 metabolism is further exacerbated by the preferential metabolism that *Clostridium* have for individual C5 sugars over other C5 sugars (Aristilde et al., 2015). Many attempts have been made in a bid to elevate CCR in *Clostridium*, from alterations to fermentation procedures (Noguchi et al., 2013) and limiting glucose levels in lignocellulosic material (Bharathiraja et al., 2017). However, a large majority of the work has focused on genetically manipulating key regulators in the cell in a bid to elevate CCR. Deletion of *glcG*, a gene that encodes enzyme II of the D-glucose phosphoenolpyruvate-dependent phosphotransferase system (PTS) and join overexpression of key parts of the xylose pathway resulted in a yield increase of 5% over the wild type strain as well as an overall increase in titre by 24% (Xiao et al., 2011). Additional work has been carried out on Catabolite control protein A (CcPA). Identification and disruption of this protein has led to elimination of CCR in *C. acetobutylicum* (Ren et al., 2012, 2010)(Ren et al., 2010). In this work, a synthetic C5/C6 mixture was used that had previously been used by our project partners to simulate feedstocks made from waste lignocellulosic material. Overall, the deletion of *gapN* does not have an effect limiting CCR, the $\Delta gapN$ strain like the wild type has a preferential utilisation of the C6 sugars (mannose and glucose) in the synthetic C5/C6 mixture with incomplete consumption of C5 sugars in the presence of C6 sugars. Interestingly, there was a marked increase in the consumption of galactose in the $\Delta gapN$ compared to the wild type strain. Galactose, unlike other C6 sugars such as glucose and mannose, is catabolized either via the Leloir pathway that generates G6P or the taga- tose-6P pathway that directly produces GAP and DHAP, and its catabolism has been shown to be suppressed in the presence of other preferential C6 sugars such as glucose and mannose (Aristilde, 2017).

Chapter 6

Final Discussion

6 Final Discussion

6.1 Establishment of growth conditions

Along with many other *Clostridium spp.* *C. saccharoperbutylacetonicum* N1-4(HMT) is notoriously difficult to work with and culture due to the anaerobic nature as well as requirement a number of specialised equipment for their culture such as anaerobic chambers, serum bottles and fermentation systems. Significant time was spent during this project on optimising culture conditions and apparatus, which in turn enabled us to perform re-producing growth experiments with *C. saccharoperbutylacetonicum* N1-4(HMT) and other *Clostridium spp.* In addition to establishing fermentation technology, establishment of tools used for analysis of ABE products was carried out.

The design and implementation of an effective fermentation system that enables batch, fed batch and continuous fermentation systems formed a large part of this work. Following extensive research (**Table 3.1**) an understanding of what is currently available on the market was established. Taking this knowledge forward allowed for the design and construction of a system that was flexible, affordable and importantly upgradable. The fermentation system developed herein may help to break the cost barrier of entry into fermentation on a smaller scale. Implementation of this sort of work could have a profound effect in the developing world, in particular regions such as Africa and Asia. These regions are areas of rapid economic growth, and will have an increasing need for research and development as economic diversification becomes more important. Having a flexible, affordable and upgradable piece of equipment could be invaluable in helping to establish interest in fermentative science in these regions.

6.3 The impact of the deletion of *gapN* in *C. saccharoperbutylacetonicum* N1-4(HMT)

The newly created $\Delta gapN$ *C. saccharoperbutylacetonicum* N1-4(HMT) was shown to have elevated concentrations of ATP (compared to the wild type strain) for a sustained period during batch fermentation (Figure 5.4). Between 15 – 24 h there is an observed drop in the measured ATP concentration of the $\Delta gapN$ strain over the wild type *C. saccharoperbutylacetonicum* N1-4(HMT). This observed decrease in ATP corresponds to the time points with the lowest concentrations of total acids production and the highest increase over time in solvent production in the $\Delta gapN$ strain (Figure 5.2).

This data suggests that the resulting deletion of $\Delta gapN$ increases ATP concentration such that $\Delta gapN$ has a reduced acid production compared to the wild type strain to generate the required concentrations of ATP to allow for the shift into solventogenesis. In solventogenic

Clostridium acid production facilitates the generation of the majority of cellular ATP, this is a result of kinase activity of the enzymes involved in acetic and butyric acid production (Dürre and Hollergschwandner, 2004; Grupe and Gottschalk, 1992). The associated ATP generation in acidogenesis is important as it enables the cells to produce adequate concentrations of ATP for vegetative growth, as well as to establish an ion gradient via V-type ATPases, alongside the RnF complex to generate NADH via the oxidation of ferredoxin (Poehlein et al., 2017). This ion gradient enables ADP + Pi recycling when the cells shifts into solventogenesis via the use of F1F0 ATPases (Jones and Woods, 1986). By increasing the ATP producing capability as has been done here with the $\Delta gapN$ strain, it has been possible to reduce the reliance on acidogenesis in the cells and increase overall solvent production, due to the shortened acid generation phase, that is historically important for ATP generation for growth and solvent production.

As well as an increase in ATP production, there is an increase in the ratio of NADH:NAD⁺ in the $\Delta gapN$ strain. ATP production, ΔpH generated by acid production and reducing conditions within the cell play a key role in the shift to solventogenesis (Liu et al., 2018; Wang et al., 2012; Wietzke and Bahl, 2012; Zhang et al., 2014). The increased reducing environment in $\Delta gapN$ is also thought to play a key role in conjunction to increased ATP resulting in an earlier shift into solventogenesis; which ultimately results in increased solvent production. A previous experiment in *C. acetobutylicum* in which a double over expression of 6-phosphofructokinase (pfkA) and pyruvate kinase (pykA) resulted in an increase in intracellular ATP and NADH, which also resulted in increased butanol and ethanol production, and additionally resulted in increased butanol tolerance in the double knockout (Ventura et al., 2013). It has been shown that in cultures with lower ATP production acid production prevails as a means of energy generation, whereas cultures with increased ATP produce more solvents (Meyer and Papoutsakis, 1989). Enhanced butanol production has also been by blocking NAD(P)H consumption in *Clostridium beijerinckii* NCIMB 8052, insertional inactivation of a NADH-quinone oxidoreductase (nuoG), resulted in increased NAD(P)H and ATP as well as butanol production (Liu et al., 2016). Overall it can be seen that increases in both ATP and NAD(P)H in solventogenic *Clostridium* aids in maximising the solvent producing potential of the bacteria.

Previously it was shown that the shift into solvent production results in the redirection of pyruvate from amino acid production via oxaloacetate, decreasing this process 10-fold and redirecting pyruvate to coenzyme A for solvent production (Amador-Noguez et al., 2011). Deletion of *gapN* results in increased concentrations of formic and lactic acid during the C5/C6 fermentation (Figure 5.5), as well as during the glucose fed batch experiment (Figure 5.7). This measured increase in both formic and lactic acid may result from the accumulation of pyruvate in the $\Delta gapN$ strain. Ultimately the solventogenic shift results in a redirection of

key metabolites away from vegetative cell growth by redirection off pyruvate towards solvent production. Accumulation of pyruvate may be due to further bottlenecks in the solvent production as well as an accumulation of pyruvate due to vegetative growth and sugar metabolism (Figure 6.1). As a way to cope with excess pyruvate generated by the earlier shift into solventogenesis, $\Delta gapN$ is producing excess concentrations of lactic acid via a lactate dehydrogenase and formic acid using pyruvate formate lyase.

Finally, sugar metabolism of the $\Delta gapN$ was assessed to that of the wild type *C. saccharoperbutylacetonicum* N1-4(HMT). Initial glucose batch fermentations suggested an increased rate of glucose consumption in the $\Delta gapN$ strain, however subsequent fed batch experiments revealed that sugar consumption rates were comparable to the wild type strain, if not slightly less (Figure 5.8). In addition to glucose, the $\Delta gapN$ strain was subsequently grown on a C5/C6 mixture and revealed much like wild type, the new strain had a preferential catabolism of C6 sugars (glucose, mannose and galactose) over C5 sugars (xylose, arabinose) in the C5/C6 mixture. Interestingly, there was a preference towards galactose over glucose and mannose, contrary to what has been previously published in other *Clostridium* spp. (Aristilde, 2017) in which galactose catabolism is inhibited in the presence of glucose.

Overall the deletion of *gapN* in *C. saccharoperbutylacetonicum* N1-4(HMT) results in an earlier shift into solventogenesis due to the increase in reducing conditions and increased ATP generated via elevated flux in the glyceraldehyde-3-phosphate oxidation pathway. This ultimately leads to increased solvent production (pre-toxic concentrations), a decreased acidogenic phase and an earlier shift from vegetative cell growth to solvent production. The shortened acidogenesis that is a result of $\Delta gapN$ creation results in an accumulation of pyruvate that cannot be fully utilised due to the bottlenecks in solvent production, which in turn results in increased levels of formic and lactic acid. In addition, there is a marked increase in galactose catabolism as a result of deletion of *gapN* (Figure 6.1).

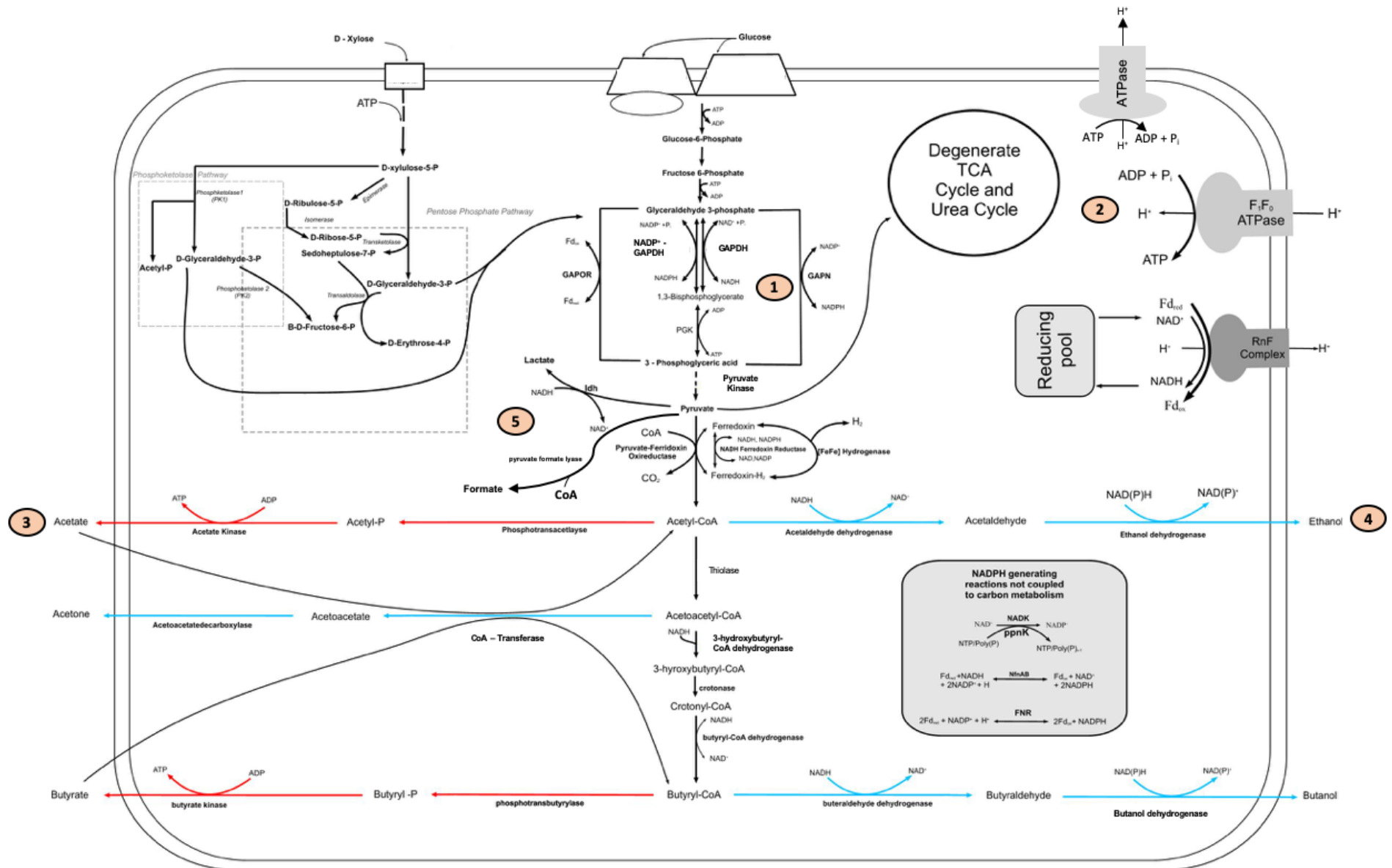


Figure 6.1 Overview of the deletion of *gapN* on *C. saccharoperbutylacetonicum* N1-4(HMT). 1) Deletion of *gapN* results in increased flux through GAPDH following deletion of *gapN*. 2) Increased flux through GAPDH results in increased ATP concentrations that is leveraged to aid in the creation of an ion gradient that can then be used to generate further ATP through ADP + P_i recycling. 3) Increased ATP and reducing environment within the cell results in a decrease in acid production. 4) Reduced acid production as a result of increased ATP and reducing environment results in earlier shift into solvent production. 5) The early shift into solvent production shifts flux throughout Acetyl-CoA from vegetative growth to solvent production. In doing this creates a bottleneck at pyruvate, this bottleneck is subsequently dealt with by the cell by increasing production of lactic acid and formic acid.

6.4 Future Studies

Herein I have listed future studies that could be adapted from each chapter that would enable furtherment of the work presented.

Chapter 3:

- Establish a pH probe and control unit within an affordable price range that would allow for the “Shepherd lab” fermentation unit to overcome its largest inability. This can be achieved via the use of pH probes and custom software, perhaps written on an affordable computation device i.e. a Raspberry Pi
- Further test “Shepherd lab” system in as many fermentation configurations as possible to reinforce the system as a viable affordable option.
- Field test unit in developing country and further develop system if it does not fit needs and cannot be easily transferred.

Chapter 4:

- CLEAVE™ has been used here for the creation of a single knockout in a region of the genome that does not form part of a cluster. To further test the ability of CLEAVE™, layering change on top of the $\Delta gapN$ strain to create a multiple knockout or test the ability of the technology to introduce a gene that could aid in solvent or alternative compound production.
- Sanger sequence SNP regions identified in Snippy to confirm that they are a result of sequencing or processing error and not a result of CLEAVE™
- Further investigate ATP via NMR or other metabolomic techniques and identify any other accumulations of metabolites that are a result of the *gapN* knockout, and test ATP concentrations from a number of different growth conditions.

Chapter 5:

- Carry out proteomic studies of the $\Delta gapN$ strain during for a number of different time points and fermentation conditions to gain an understanding of protein concentrations at different stages, i.e. acidogenesis and solventogenesis to gain better insight into the effects that the earlier observed shift into solventogenesis has on a cell wide basis.
- Try and engineer or investigate ways of increasing the $\Delta gapN$ tolerance to butanol toxicity.
- Optimise fermentation conditions that can take advantage of the earlier shift into solventogenesis that leads to peak solvent production sooner than in the wild type strain.

References

- Ai, B., Li, J., Chi, X., Meng, J., Jha, A.K., Liu, C., Shi, E., 2014. Effect of pH and buffer on butyric acid production and microbial community characteristics in bioconversion of rice straw with undefined mixed culture. *Biotechnol. Bioprocess Eng.* 19, 676–686. <https://doi.org/10.1007/s12257-013-0655-z>
- Al-Shorgani, N.K.N., Ali, E., Kalil, M.S., Yusoff, W.M.W., 2012a. Bioconversion of butyric acid to butanol by *Clostridium saccharoperbutylacetonicum* N1-4 (ATCC 13564) in a limited nutrient medium. *Bioenergy Res.* 5, 287–293. <https://doi.org/10.1007/s12155-011-9126-6>
- Al-Shorgani, N.K.N., Kalil, M.S., Yusoff, W.M.W., 2012b. Fermentation of sago starch to biobutanol in a batch culture using *Clostridium saccharoperbutylacetonicum* N1-4 (ATCC 13564). *Ann. Microbiol.* 62, 1059–1070. <https://doi.org/10.1007/s13213-011-0347-x>
- Amador-Noguez, D., Brasg, I.A., Feng, X.J., Roquet, N., Rabinowitz, J.D., 2011. Metabolome remodeling during the acidogenic-solventogenic transition in *Clostridium acetobutylicum*. *Appl. Environ. Microbiol.* 77, 7984–7997. <https://doi.org/10.1128/AEM.05374-11>
- Antunes, A., Martin-Verstraete, I., Dupuy, B., 2011. CcpA-mediated repression of *Clostridium difficile* toxin gene expression. *Mol. Microbiol.* 79, 882–899. <https://doi.org/10.1111/j.1365-2958.2010.07495.x>
- Aristilde, L., 2017. Metabolite labelling reveals hierarchies in *Clostridium acetobutylicum* that selectively channel carbons from sugar mixtures towards biofuel precursors. *Microb. Biotechnol.* 10, 162–174. <https://doi.org/10.1111/1751-7915.12459>
- Aristilde, L., Lewis, I.A., Park, J.O., Rabinowitz, J.D., 2015. Hierarchy in pentose sugar metabolism in *Clostridium acetobutylicum*. *Appl. Environ. Microbiol.* 81, 1452–1462. <https://doi.org/10.1128/AEM.03199-14>
- Aro, E.M., 2016. From first generation biofuels to advanced solar biofuels. *Ambio* 45, 24–31. <https://doi.org/10.1007/s13280-015-0730-0>
- Atmadjaja, A.N., Holby, V., Harding, A.J., Krabben, P., Smith, H.K., Jenkinson, E.R., 2019. CRISPR-Cas, a highly effective tool for genome editing in *Clostridium saccharoperbutylacetonicum* N1-4(HMT). *FEMS Microbiol. Lett.* 1–10. <https://doi.org/10.1093/femsle/fnz059>
- Atsumi, S., Cann, A.F., Connor, M.R., Shen, C.R., Smith, K.M., Brynildsen, M.P., Chou, K.J.Y., Hanai, T., Liao, J.C., 2008. Metabolic engineering of *Escherichia coli* for 1-butanol production. *Metab. Eng.* 10, 305–311. <https://doi.org/10.1016/j.ymben.2007.08.003>
- Awad, M.M., Bryant, A.E., Stevens, D.L., Rood, J.I., 1995. Virulence studies on chromosomal α -toxin and Θ -toxin mutants constructed by allelic exchange provide genetic evidence for the essential role of α -toxin in *Clostridium perfringens*-mediated gas gangrene. *Mol. Microbiol.* 15, 191–202. <https://doi.org/10.1111/j.1365-2958.1995.tb02234.x>
- Baer, S.H., Blaschek, H.P., Smith, T.L., 1987. Effect of Butanol Challenge and Temperature on Lipid Composition and Membrane Fluidity of Butanol-Tolerant *Clostridium acetobutylicum*. *Appl. Environ. Microbiol.* 53, 2854–2861.
- Baker, J., 2016. Modified Chromogenic Assay for Determination of the Ratio of Free Intracellular NAD + /NADH in. *Bio-protocols* 6, 1–8. <https://doi.org/10.21769/BioProtoc.1902>
- Bang, G., 2010. Energy security and climate change concerns: Triggers for energy policy change in the United States. *Energy Policy* 38, 1645–1653. <https://doi.org/10.1016/j.enpol.2009.01.045>
- Bannam, T.L., Crellin, P.K., Rood, J.I., 1995. Molecular genetics of the chloramphenicol-resistance transposon Tn4451 from *Clostridium perfringens*:

- the TnpX site-specific recombinase excises a circular transposon molecule. *Mol. Microbiol.* 16, 535–551. <https://doi.org/10.1111/j.1365-2958.1995.tb02417.x>
- Bao, G., Wang, R., Zhu, Y., Dong, H., Mao, S., Zhang, Y., Chen, Z., Li, Y., Ma, Y., 2011. Complete genome sequence of *Clostridium acetobutylicum* DSM 1731, a solvent-producing strain with multireplicon genome architecture. *J. Bacteriol.* 193, 5007–5008. <https://doi.org/10.1128/JB.05596-11>
- Bengelsdorf, F.R., Dürre, P., 2017. Gas fermentation for commodity chemicals and fuels. *Microb. Biotechnol.* 10, 1167–1170. <https://doi.org/10.1111/1751-7915.12763>
- Beri, D., Olson, D.G., Holwerda, E.K., Lynd, L.R., 2016. Nicotinamide cofactor ratios in engineered strains of *Clostridium thermocellum* and *Thermoanaerobacterium saccharolyticum* 1–11. <https://doi.org/10.1093/femsle/fnw091>
- Bernofsky, C., Swan, M., 1973. An improved cycling assay for nicotinamide adenine dinucleotide. *Anal. Biochem.* 53, 452–458. [https://doi.org/10.1016/0003-2697\(73\)90094-8](https://doi.org/10.1016/0003-2697(73)90094-8)
- Bharathiraja, B., Jayamuthunagai, J., Sudharsanaa, T., Bharghavi, A., Praveenkumar, R., Chakravarthy, M., Yuvaraj, D., 2017. Biobutanol: An impending biofuel for future: A review on upstream and downstream processing techniques. *Renew. Sustain. Energy Rev.* 68, 788–807. <https://doi.org/10.1016/j.rser.2016.10.017>
- Boehmel, C., Lewandowski, I., Claupein, W., 2008. Comparing annual and perennial energy cropping systems with different management intensities. *Agric. Syst.* 96, 224–236. <https://doi.org/10.1016/j.agsy.2007.08.004>
- Bogorad, I.W., Lin, T.-S., Liao, J.C., 2013. Synthetic non-oxidative glycolysis enables complete carbon conservation. *Nature* 502, 693–7. <https://doi.org/10.1038/nature12575>
- Bolger, A.M., Lohse, M., Usadel, B., 2014. Trimmomatic: A flexible trimmer for Illumina sequence data. *Bioinformatics* 30, 2114–2120. <https://doi.org/10.1093/bioinformatics/btu170>
- Boekema, E.J., Ubbink-Kok, T., Lolkema, J.S., Brisson, A., Konings, W.N., 1998. Structure of V-type ATPase from *Clostridium fervidus* by electron microscopy. *Photosynth. Res.* 57, 267–273. <https://doi.org/10.1023/A:1006044931980>
- Borden, J.R., Papoutsakis, E.T., 2007. Dynamics of genomic-library enrichment and identification of solvent tolerance genes for *Clostridium acetobutylicum*. *Appl. Environ. Microbiol.* 73, 3061–3068. <https://doi.org/10.1128/AEM.02296-06>
- Bowles, L.K., 1985. Effects of Butanol on *Clostridium acetobutylicum*. *Cultures* 50, 1165–1170.
- Boyaval, P., Moineau, S., Romero, D.A., Horvath, P., Barrangou, R., Fremaux, C., Deveau, H., Richards, M., Boyaval, P., Moineau, S., Romero, D.A., Horvath, P., 2007. CRISPR Provides Acquired Resistance Against Viruses in Prokaryotes. *Science* 315, 1709–1712. <https://doi.org/10.1126/science.1138140>
- Boyd, D.A., Cvitkovitch, D.G., Hamilton, I.A.N.R., 1995. Sequence, Expression, and Function of the Gene for the Phosphate Dehydrogenase of *Streptococcus mutans*. *J. Bacteriol.* 177, 2622–2627. <https://doi.org/http://dx.doi.org/10.1016/B978-1-4832-3194-5.50012-8>
- Braguglia, C.M., Gallipoli, A., Gianico, A., Pagliaccia, P., 2017. Anaerobic bioconversion of food waste into energy: A critical review. *Bioresour. Technol.* 248, 37–56. <https://doi.org/10.1016/j.biortech.2017.06.145>
- British Petroleum, 2018. BP - Statistical Review of World Energy. *Br. Pet.* 54. <https://doi.org/http://www.bp.com/content/dam/bp/en/corporate/pdf/energy->

- Bruder, M., Moo-Young, M., Chung, D.A., Chou, C.P., 2015. Elimination of carbon catabolite repression in *Clostridium acetobutylicum*—a journey toward simultaneous use of xylose and glucose. *Appl. Microbiol. Biotechnol.* 99, 7579–7588. <https://doi.org/10.1007/s00253-015-6611-4>
- Bruder, M.R., Pyne, M.E., Moo-Young, M., Chung, D.A., Chou, C.P., 2016. Extending CRISPR-Cas9 technology from genome editing to transcriptional engineering in the genus *Clostridium*. *Appl. Environ. Microbiol.* 82, 6109–6119. <https://doi.org/10.1128/AEM.02128-16>
- Cartman, S.T., Heap, J.T., Kuehne, S.A., Cockayne, A., Minton, N.P., 2010. The emergence of 'hypervirulence' in *Clostridium difficile*. *Int. J. Med. Microbiol.* 300, 387–395. <https://doi.org/10.1016/j.ijmm.2010.04.008>
- Centeno-Leija, S., Huerta-Beristain, G., Giles-Gómez, M., Bolivar, F., Gosset, G., Martinez, A., 2014. Improving poly-3-hydroxybutyrate production in *Escherichia coli* by combining the increase in the NADPH pool and acetyl-CoA availability. *Antonie van Leeuwenhoek, Int. J. Gen. Mol. Microbiol.* 105, 687–696. <https://doi.org/10.1007/s10482-014-0124-5>
- Chang, W.-L., 2010. Acetone-Butanol-Ethanol Fermentation by *Engineered Clostridium beijerinckii* and *Clostridium tyrobutyricum*. <https://doi.org/10.1017/CBO9781107415324.004>
- Chen, C.K., Blaschek, H.P., 1999. Acetate enhances solvent production and prevents degeneration in *Clostridium beijerinckii* BA101. *Appl. Microbiol. Biotechnol.* 52, 170–173. <https://doi.org/10.1007/s002530051504>
- Cho, D.H., Shin, S.J., Kim, Y.H., 2012. Effects of acetic and formic acid on ABE production by *Clostridium acetobutylicum* and *Clostridium beijerinckii*. *Biotechnol. Bioprocess Eng.* 17, 270–275. <https://doi.org/10.1007/s12257-011-0498-4>
- Chylinski, K., Le Rhun, A., Charpentier, E., 2013. The tracrRNA and Cas9 families of type II CRISPR-Cas immunity systems. *RNA Biol.* 10, 726–737. <https://doi.org/10.4161/rna.24321>
- Clark, S.W., Bennett, G.N., Rudolph, F.B., 1989. Isolation and characterization of mutants of *Clostridium acetobutylicum* ATCC 824 deficient in acetoacetyl-coenzyme A:acetate/butyrate:coenzyme A-transferase (EC 2.8.3.9) and in other solvent pathway enzymes. *Appl. Environ. Microbiol.* 55, 970–976.
- Cooksley, C.M., Davis, I.J., Winzer, K., Chan, W.C., Peck, M.W., Minton, N.P., 2010. Regulation of Neurotoxin Production and Sporulation by a Putative agrBD Signaling System in Proteolytic *Clostridium botulinum*. *Appl. Environ. Microbiol.* 76, 4448–4460. <https://doi.org/10.1128/AEM.03038-09>
- Cooksley, Clare M., Zhang, Y., Wang, H., Redl, S., Winzer, K., Minton, N.P., 2012. Targeted mutagenesis of the *Clostridium acetobutylicum* acetone-butanol-ethanol fermentation pathway. *Metab. Eng.* 14, 630–641. <https://doi.org/10.1016/j.ymben.2012.09.001>
- Cooksley, Clare M., Zhang, Y., Wang, H., Redl, S., Winzer, K., Minton, N.P., 2012. Targeted mutagenesis of the *Clostridium acetobutylicum* acetone-butanol-ethanol fermentation pathway. *Metab. Eng.* 14, 630–641. <https://doi.org/10.1016/j.ymben.2012.09.001>
- David, K., Ragauskas, A.J., 2010. Switchgrass as an energy crop for biofuel production: A review of its ligno-cellulosic chemical properties. *Energy Environ. Sci.* 3, 1182–1190. <https://doi.org/10.1039/b926617h>
- Demmer, J.K., Huang, H., Wang, S., Demmer, U., Rudolf, K., Ermler, U., 2015. Insights into flavin-based electron bifurcation via the NADH- dependent reduced ferredoxin : NADP oxidoreductase structure.

- <https://doi.org/10.1074/jbc.M115.656520>
- Desai, R.P., Papoutsakis, E.T., 1999. Antisense RNA strategies for metabolic engineering of *Clostridium acetobutylicum*. *Appl. Environ. Microbiol.* 65, 936–945.
- Drake, H.L., Gößner, A.S., Daniel, S.L., 2008. Old acetogens, new light. *Ann. N. Y. Acad. Sci.* 1125, 100–128. <https://doi.org/10.1196/annals.1419.016>
- Dunlop, M.J., Dossani, Z.Y., Szmidt, H.L., Chu, H.C., Lee, T.S., Keasling, J.D., Hadi, M.Z., Mukhopadhyay, A., 2011. Engineering microbial biofuel tolerance and export using efflux pumps. *Mol. Syst. Biol.* 7, 1–7. <https://doi.org/10.1038/msb.2011.21>
- Dürre, P., Hollergschwandner, C., 2004. Initiation of endospore formation in *Clostridium acetobutylicum*. *Anaerobe* 10, 69–74. <https://doi.org/10.1016/j.anaerobe.2003.11.001>
- Durre Peter, 2008. Fermentative butanol production: Bulk chemical and biofuel. *Ann. N. Y. Acad. Sci.* 1125, 353–362. <https://doi.org/10.1196/annals.1419.009>
- EASAC, 2012. The current status of biofuels in the European Union, their environmental impacts and future prospects; EASAC policy report 19. <https://doi.org/ISBN:978-3-8047-3118-9>
- Ellis, J.T., Hengge, N.N., Sims, R.C., Miller, C.D., 2012. Acetone, butanol, and ethanol production from wastewater algae. *Bioresour. Technol.* 111, 491–495. <https://doi.org/10.1016/j.biortech.2012.02.002>
- Ezeji, T., Milne, C., Price, N.D., Blaschek, H.P., 2010. Achievements and perspectives to overcome the poor solvent resistance in acetone and butanol-producing microorganisms. *Appl. Microbiol. Biotechnol.* 85, 1697–1712. <https://doi.org/10.1007/s00253-009-2390-0>
- Ezeji, T.C., Groberg, M., Qureshi, N., Blaschek, H.P., 2003. Continuous production of butanol from starch-based packing peanuts. *Appl. Biochem. Biotechnol.* 105–108, 375–382. <https://doi.org/10.1385/ABAB:106:1-3:375>
- Ezeji, T.C., Qureshi, N., Blaschek, H.P., 2007. Bioproduction of butanol from biomass: from genes to bioreactors. *Curr. Opin. Biotechnol.* 18, 220–227. <https://doi.org/10.1016/j.copbio.2007.04.002>
- Fabret, C., Ehrlich, S.D., Noirot, P., 2002. A new mutation delivery system for genome-scale approaches in *Bacillus subtilis*. *Mol. Microbiol.* 46, 25–36. <https://doi.org/10.1046/j.1365-2958.2002.03140.x>
- Ferguson, W.J., Braunschweiger, K.I., Braunschweiger, W.R., Smith, J.R., McCormick, J.J., Wasmann, C.C., Jarvis, N.P., Bell, D.H., Good, N.E., 1980. Hydrogen ion buffers for biological research. *Anal. Biochem.* 104, 300–310. [https://doi.org/10.1016/0003-2697\(80\)90079-2](https://doi.org/10.1016/0003-2697(80)90079-2)
- Fisher, M.A., Boyarskiy, S., Yamada, M.R., Kong, N., Bauer, S., Tullman-Ercek, D., 2014. Enhancing tolerance to short-chain alcohols by engineering the *Escherichia coli* AcrB efflux pump to secrete the non-native substrate n-butanol. *ACS Synth. Biol.* 3, 30–40. <https://doi.org/10.1021/sb400065q>
- Fothergill-Gilmore, L.A., Michels, P.A.M., 1993. Evolution of glycolysis. *Prog. Biophys. Mol. Biol.* 59, 105–235. [https://doi.org/10.1016/0079-6107\(93\)90001-Z](https://doi.org/10.1016/0079-6107(93)90001-Z)
- Frederic Monot, Jean-Marc Engasser, and H.P., 1984. Influence of pH and undissociated butyric acid on the production of acetone and butanol in batch cultures of *Clostridium acetobutylicum*. *Appl. Microbiol. Biotechnol.* 19, 422–426.
- Fu, H., Yang, S.-T.T., Wang, M.M., Wang, J., Tang, I.-C.C., 2017. Butyric acid production from lignocellulosic biomass hydrolysates by engineered *Clostridium tyrobutyricum* overexpressing xylose catabolism genes for glucose and xylose co-utilization. *Bioresour. Technol.* 234, 389–396. <https://doi.org/10.1016/j.biortech.2017.03.073>

- García-Alcalde, F., Okonechnikov, K., Carbonell, J., Cruz, L.M., Götz, S., Tarazona, S., Dopazo, J., Meyer, T.F., Conesa, A., 2012. Qualimap: Evaluating next-generation sequencing alignment data. *Bioinformatics* 28, 2678–2679. <https://doi.org/10.1093/bioinformatics/bts503>
- Gi Moon, H., Jang, Y.S., Cho, C., Lee, J., Binkley, R., Lee, S.Y., 2015. One hundred years of *Clostridial* butanol fermentation. *FEMS Microbiol. Lett.* 363. <https://doi.org/10.1093/femsle/fnw001>
- Girbal, L., Croux, C., Vasconcelos, I., Soucaille, P., 1995. Regulation of metabolic shifts in *Clostridium acetobutylicum* ATCC 824. *FEMS Microbiol. Rev.* 17, 287–297. <https://doi.org/10.1111/j.1574-6976.1995.tb00212.x>
- Global Energy & CO 2 Status Report, 2018.
- Gohlke, R.S., 1959. Time-of-Flight Mass Spectrometry and Gas-Liquid Partition Chromatography. *Anal. Chem.* 31, 535–541. <https://doi.org/10.1021/ac50164a024>
- Green, E.M., 2011. Fermentative production of butanol-the industrial perspective. *Curr. Opin. Biotechnol.* 22, 337–343. <https://doi.org/10.1016/j.copbio.2011.02.004>
- Green, E.M., Boynton, Z.L., Harris, L.M., Rudolph, F.B., Papoutsakis, E.T., Bennett, G.N., 1996. Genetic manipulation of acid formation pathways by gene inactivation in *Clostridium acetobutylicum* ATCC 824. *Appl. Microbiol. Biotechnol.* 2079–2086.
- Grupe, H., Gottschalk, G., 1992. Physiological Events in *Clostridium acetobutylicum* during the Shift from Acidogenesis to Solventogenesis in Continuous Culture and Presentation of a Model for Shift Induction. *Appl. Environ. Microbiol.* 58, 3896–902.
- Gu, Y., Feng, J., Zhang, Z.T., Wang, S., Guo, L., Wang, Yifen, Wang, Yi, 2019. Curing the endogenous megaplasmid in *Clostridium saccharoperbutylacetonicum* N1-4 (HMT) using CRISPR-Cas9 and preliminary investigation of the role of the plasmid for the strain metabolism. *Fuel* 236, 1559–1566. <https://doi.org/10.1016/j.fuel.2018.09.030>
- Harris, L.M., Desai, R.P., Welker, N.E., Papoutsakis, E.T., 2000. Characterization of recombinant strains of the *Clostridium acetobutylicum* butyrate kinase inactivation mutant: Need for new phenomenological models for solventogenesis and butanol inhibition *Biotechnol. Bioeng.* 67, 1–11. [https://doi.org/10.1002/\(SICI\)1097-0290\(20000105\)67:1<1::AID-BIT1>3.0.CO;2-G](https://doi.org/10.1002/(SICI)1097-0290(20000105)67:1<1::AID-BIT1>3.0.CO;2-G)
- Harris, L.M., Welker, N.E., Papoutsakis, E.T., 2002. Northern, Morphological, and Fermentation Analysis of. *Society* 184, 3586–3597. <https://doi.org/10.1128/JB.184.13.3586>
- Heap, J.T., Ehsaan, M., Cooksley, C.M., Ng, Y.K., Cartman, S.T., Winzer, K., Minton, N.P., 2012. Integration of DNA into bacterial chromosomes from plasmids without a counter-selection marker. *Nucleic Acids Res.* 40. <https://doi.org/10.1093/nar/gkr1321>
- Heap, J.T., Kuehne, S.A., Ehsaan, M., Cartman, S.T., Cooksley, C.M., Scott, J.C., Minton, N.P., 2010. The ClosTron: Mutagenesis in *Clostridium* refined and streamlined. *J. Microbiol. Methods* 80, 49–55. <https://doi.org/10.1016/j.mimet.2009.10.018>
- Heap, J.T., Pennington, O.J., Cartman, S.T., Carter, G.P., Minton, N.P., 2007. The ClosTron: A universal gene knock-out system for the genus *Clostridium*. *J. Microbiol. Methods* 70, 452–464. <https://doi.org/10.1016/j.mimet.2007.05.021>
- Hijosa-Valsero, M., Paniagua-García, A.I., Díez-Antolínez, R., 2017. Biobutanol production from apple pomace: the importance of pretreatment methods on the fermentability of lignocellulosic agro-food wastes. *Appl. Microbiol. Biotechnol.* 101, 8041–8052. <https://doi.org/10.1007/s00253-017-8522-z>

- Hongo, M., Ogata, S., 1969. Bacteriophages of *Clostridium saccharoperbutylacetonicum*. Agric. Biol. Chem. 33, 488–495. <https://doi.org/10.1080/00021369.1969.10859353>
- Hoult, D., 1997. NMR signal reception: Virtual photons and coherent spontaneous emission. Concepts Magn. Reson. 9, 277–296. [https://doi.org/10.1002/\(SICI\)1099-0534\(1997\)9:53.0.CO;2-W](https://doi.org/10.1002/(SICI)1099-0534(1997)9:53.0.CO;2-W)
- Huang, H., Chai, C., Li, N., Rowe, P., Minton, N.P., Yang, S., Jiang, W., Gu, Y., 2016. CRISPR/Cas9-Based Efficient Genome Editing in *Clostridium ljungdahlii*, an Autotrophic Gas-Fermenting Bacterium. ACS Synth. Biol. 5, 1355–1361. <https://doi.org/10.1021/acssynbio.6b00044>
- Iddar, A., Valverde, F., Serrano, A., Soukri, A., 2002. Expression, purification, and characterization of recombinant dehydrogenase from *Clostridium acetobutylicum*. Protein Expr. Purif. 25, 519–526.
- Inui, M., Suda, M., Kimura, S., Yasuda, K., Suzuki, H., Toda, H., Yamamoto, S., Okino, S., Suzuki, N., Yukawa, H., 2008. Expression of *Clostridium acetobutylicum* butanol synthetic genes in Escherichia coli. Appl. Microbiol. Biotechnol. 77, 1305–1316. <https://doi.org/10.1007/s00253-007-1257-5>
- Jang, Y.-S., Lee, J.Y., Lee, Joungmin, Park, J.H., Im, J.A., Eom, M.-H., Lee, Julia, Lee, S.-H., Song, H., Cho, J.-H., Seung, D.Y., Lee, S.Y., 2012. Enhanced Butanol Production Obtained by Reinforcing the Direct Butanol-Forming Route in *Clostridium acetobutylicum*. MBio 3, 1–9. <https://doi.org/10.1128/mbio.00314-12>
- Jiang, Y., Liu, J., Jiang, W., Yang, Y., Yang, S., 2015. Current status and prospects of industrial bio-production of n-butanol in China. Biotechnol. Adv. 33, 1493–1501. <https://doi.org/10.1016/j.biotechadv.2014.10.007>
- Jenkinson. E, Krabben. P & Green Biologicd Ltd 2015. Targeted mutations (CLEAVE™) - Patent. Patent: WO2015159087A1
- Jones, D.T., Keis, S., 1995. Origins and relationships of industrial solvent-producing *Clostridial* strains. FEMS Microbiol. Rev. 17, 223–232. [https://doi.org/10.1016/0168-6445\(95\)00010-A](https://doi.org/10.1016/0168-6445(95)00010-A)
- Jones, D.T., Shirley, M., Wu, X., Keis, S., 2000. Bacteriophage infections in the industrial acetone butanol (AB) fermentation process. J. Mol. Microbiol. Biotechnol. 2, 21–6.
- Jones, D.T., Woods, D.R., 1986. Acetone-butanol fermentation revisited. Microbiol. Rev. 50, 484–524. <https://doi.org/3540574>
- Joseph, R.C., Kim, N.M., Sandoval, N.R., 2018. Recent developments of the synthetic biology toolkit for *Clostridium*. Front. Microbiol. 9, 1–13. <https://doi.org/10.3389/fmicb.2018.00154>
- Kaminski, W., Tomczak, E., Gorak, A., 2011. Bioutanol - Production and Purificaton Methods. Ecol. Chem. Eng. 18, 31–37.
- Kandedgedara, A., Rorabacher, D.B., 1999. Noncomplexing tertiary amines as “better” buffers covering the range of pH 3-11. Temperature dependence of their acid dissociation constants. Anal. Chem. 71, 3140–3144. <https://doi.org/10.1021/ac9902594>
- Kanouni, a El, Zerdani, I., Zaafa, S., Znassni, M., Lout, M., Boudouma, M., 1998. The improvement of glucose / xylose fermentation by *Clostridium acetobutylicum* using calcium carbonate. World J. Microbiol. Biotechnol. 14, 431–435.
- Kenneth Todar, n.d. Pathogenic *Clostridia*, Including Botulism and Tetanus [WWW Document]. URL <http://textbookofbacteriology.net/clostridia.html> (accessed 6.25.19).
- Klein, M., Ansorge-Schumacher, M.B., Fritsch, M., Hartmeier, W., 2010. Influence of hydrogenase overexpression on hydrogen production of *Clostridium acetobutylicum* DSM 792. Enzyme Microb. Technol. 46, 384–390.

- <https://doi.org/10.1016/j.enzmictec.2009.12.015>
- Köpke, M., Held, C., Hujer, S., Liesegang, H., Wiezer, A., Wollherr, A., Ehrenreich, A., Liebl, W., Gottschalk, G., Dürre, P., 2010. *Clostridium ljungdahlii* represents a microbial production platform based on syngas. *Proc. Natl. Acad. Sci. U. S. A.* 107, 13087–92. <https://doi.org/10.1073/pnas.1004716107>
- KOSAKA, T., NAKAYAMA, S., NAKAYA, K., YOSHINO, S., FURUKAWA, K., 2007. Characterization of the *sol* Operon in Butanol-Hyperproducing *Clostridium saccharoperbutylacetonicum* Strain N1-4 and Its Degeneration Mechanism. *Biosci. Biotechnol. Biochem.* 71, 58–68. <https://doi.org/10.1271/bbb.60370>
- Kumar, M., Gayen, K., 2011. Developments in biobutanol production: New insights. *Appl. Energy* 88, 1999–2012. <https://doi.org/10.1016/j.apenergy.2010.12.055>
- Kutty, R., Bennett, G.N., 2007. Characterization of a novel ferredoxin with N-terminal extension from *Clostridium acetobutylicum* ATCC 824. *Arch. Microbiol.* 187, 161–169. <https://doi.org/10.1007/s00203-006-0184-7>
- Lane, B.J., Digest, B., 2014. Green Biologics inks Iowa demo plant deal with Easy Energy Systems.
- Latif, H., Zeidan, A.A., Nielsen, A.T., Zengler, K., 2014. Trash to treasure: Production of biofuels and commodity chemicals via syngas fermenting microorganisms. *Curr. Opin. Biotechnol.* 27, 79–87. <https://doi.org/10.1016/j.copbio.2013.12.001>
- Lee, R.A., Lavoie, J.-M., 2013. From first- to third-generation biofuels: Challenges of producing a commodity from a biomass of increasing complexity. *Anim. Front.* 3, 6–11. <https://doi.org/10.2527/af.2013-0010>
- Lee, S.Y., Park, J.H., Jang, S.H., Nielsen, L.K., Kim, J., Jung, K.S., 2008. Fermentative butanol production by clostridia. *Biotechnol. Bioeng.* 101, 209–228. <https://doi.org/10.1002/bit.22003>
- Li, H., 2013. Aligning sequence reads, clone sequences and assembly contigs with BWA-MEM 00, 1–3. <https://doi.org/10.1371/journal.pone.0079111> [q-bio.GN]
- Liao, Z., Zhang, Y., Luo, S., Suo, Y., Zhang, S., Wang, J., 2017. Improving cellular robustness and butanol titers of *Clostridium acetobutylicum* ATCC824 by introducing heat shock proteins from an extremophilic bacterium. *J. Biotechnol.* 252, 1–10. <https://doi.org/10.1016/j.jbiotec.2017.04.031>
- Lilliestam, J., 2012. Conceptualising Energy Security in the European Context.
- Liu, D., Yang, Z., Wang, P., Niu, H., Zhuang, W., Chen, Y., Wu, J., Zhu, C., Ying, H., Ouyang, P., 2018. Towards acetone-uncoupled biofuels production in solventogenic *Clostridium* through reducing power conservation. *Metab. Eng.* 47, 102–112. <https://doi.org/10.1016/j.ymben.2018.03.012>
- Liu, X., Gu, Q., Liao, C., Yu, X., 2014. Enhancing butanol tolerance and preventing degeneration in *Clostridium acetobutylicum* by 1-butanol-glycerol storage during long-term preservation. *Biomass and Bioenergy* 69, 192–197. <https://doi.org/10.1016/j.biombioe.2014.07.019>
- Liu, J., Guo, T., Wang, D., Shen, X., Liu, D., Niu, H., Liang, L., Ying, H., 2016. Enhanced butanol production by increasing NADH and ATP levels in *Clostridium beijerinckii* NCIMB 8052 by insertional inactivation of Cbei_4110. *Appl. Microbiol. Biotechnol.* <https://doi.org/10.1007/s00253-016-7299-9>
- Luttke-Eversloh, T., Bahl, H., 2011. Metabolic engineering of *Clostridium acetobutylicum*: Recent advances to improve butanol production. *Curr. Opin. Biotechnol.* 22, 634–647. <https://doi.org/10.1016/j.copbio.2011.01.011>
- Lynd, L.R., Weimer, P.J., van Zyl, W.H., Pretorius, I.S., 2002. Microbial cellulose utilization: Fundamentals and biotechnology. *Microbiol. Mol. Biol. Rev.* 66, 506–77, table of contents. <https://doi.org/10.1128/MMBR.66.3.506>
- Maddox, I.S., Steiner, E., Hirsch, S., Wessner, S., Gutierrez, N.A., Gapes, J.R.,

- Schuster, K.C., 2000. The cause of “acid-crash” and “acidogenic fermentations” during the batch acetone-butanol-ethanol (ABE-) fermentation process. *J. Mol. Microbiol. Biotechnol.* 2, 95–100.
- Makarova, K.S., Aravind, L., Grishin, N. V, Rogozin, I.B., Koonin, E. V, 2002. A DNA repair system specific for thermophilic Archaea and bacteria predicted by genomic context analysis. *Nucleic Acids Res.* 30, 482–96.
- Marcellin, E., Behrendorff, J.B., Nagaraju, S., DeTissera, S., Segovia, S., Palfreyman, R., Daniell, J., Licona-Cassani, C., Quek, L., Speight, R., Hodson, M.P., Simpson, S.D., Mitchell, W.P., Köpke, M., Nielsen, L.K., 2016. Low carbon fuels and commodity chemicals from waste gases – Systematic approach to understand energy metabolism in a model acetogen. *Green Chem.* 3020–3028. <https://doi.org/10.1039/C5GC02708J>
- Martin Jinek, Krzysztof Chylinski, Ines Fonfara, Michael Hauer, Jennifer A. Doudna, Emmanuelle Charpentier, 2012. A Programmable Dual-RNA–Guided DNA Endonuclease in Adaptive Bacterial Immunity. *Science* (80-.). 337, 816–821. <https://doi.org/10.1126/science.1138140>
- Mateos, M.I., Serrano, A., 1992. Occurrence of phosphorylating and non-phosphorylating NADP⁺-dependent glyceraldehyde-3-phosphate dehydrogenases in photosynthetic organisms. *Plant Sci.* 84, 163–170. [https://doi.org/10.1016/0168-9452\(92\)90130-E](https://doi.org/10.1016/0168-9452(92)90130-E)
- McLaughlin, K.J., Strain-Damerell, C.M., Xie, K., Brekasis, D., Soares, A.S., Paget, M.S.B., Kielkopf, C.L., 2010. Structural Basis for NADH/NAD⁺ Redox Sensing by a Rex Family Repressor. *Mol. Cell* 38, 563–575. <https://doi.org/10.1016/j.molcel.2010.05.006>
- Mermelstein, L.D., Papoutsakis, E.T., Petersen, D.J., Bennett, G.N., 1993. Metabolic engineering of *Clostridium acetobutylicum* ATCC 824 for increased solvent production by enhancement of acetone formation enzyme activities using a synthetic acetone operon. *Biotechnol. Bioeng.* 42, 1053–1060. <https://doi.org/10.1002/bit.260420906>
- Meyer, C.L., Papoutsakis, E.T., 1989. Increased Levels of Atp and Nakh Are Associated With Increased Solvent Production in Continuous Cultures of *Clostridium Acetobutylicum*. *Appl.Microbiol.Biotechnol.* 30, 450–459.
- Minton, N.P., Ehsaan, M., Humphreys, C.M., Little, G.T., Baker, J., Henstra, A.M., Liew, F., Kelly, M.L., Sheng, L., Schwarz, K., Zhang, Y., 2016. A roadmap for gene system development in *Clostridium*. *Anaerobe* 41, 104–112. <https://doi.org/10.1016/j.anaerobe.2016.05.011>
- Minyeong Yoo, Gwenaelle Bestel-Corre, Christian Croux, Antoine Riviere, Isabelle Meynial-Salles, P.S., 2015. A Quantitative System-Scale Characterization of the Metabolism of *Clostridium acetobutylicum* 6, 1–12. <https://doi.org/10.1128/mBio.01808-15.Invited>
- Mitchell, W.J., Albasheri, K.A., Yazdani, M., 1995. Factors affecting utilization of carbohydrates by *Clostridia*. *FEMS Microbiol. Rev.* 17, 317–329. <https://doi.org/10.1111/j.1574-6976.1995.tb00215.x>
- Morimoto, K., Kimura, T., Sakka, K., Ohmiya, K., 2005. Overexpression of a hydrogenase gene in *Clostridium parapatrificum* to enhance hydrogen gas production. *FEMS Microbiol. Lett.* 246, 229–234. <https://doi.org/10.1016/j.femsle.2005.04.014>
- Nagaraju, S., Davies, N.K., Walker, D.J.F., Köpke, M., Simpson, S.D., 2016. Genome editing of *Clostridium autoethanogenum* using CRISPR/Cas9. *Biotechnol. Biofuels* 9, 1–8. <https://doi.org/10.1186/s13068-016-0638-3>
- Nair, R. V., Papoutsakis, E.T., 1994. Expression of plasmid-encoded aad in *Clostridium acetobutylicum* M5 restores vigorous butanol production. *J. Bacteriol.* 176, 5843–5846. <https://doi.org/10.1128/jb.176.18.5843-5846.1994>
- Ni, Y., Sun, Z., 2009. Recent progress on industrial fermentative production of

- acetone-butanol-ethanol by *Clostridium acetobutylicum* in China. Appl. Microbiol. Biotechnol. 83, 415–423. <https://doi.org/10.1007/s00253-009-2003-y>
- Nielsen, D.R., Leonard, E., Yoon, S.H., Tseng, H.C., Yuan, C., Prather, K.L.J., 2009. Engineering alternative butanol production platforms in heterologous bacteria. Metab. Eng. 11, 262–273. <https://doi.org/10.1016/j.ymben.2009.05.003>
- Nisselbaum, J.S., Green, S., 1969. A simple ultramicro method for determination of pyridine nucleotides in tissues. Anal. Biochem. 27, 212–217. [https://doi.org/10.1016/0003-2697\(69\)90025-6](https://doi.org/10.1016/0003-2697(69)90025-6)
- Noguchi, T., Tashiro, Y., Yoshida, T., Zheng, J., Sakai, K., Sonomoto, K., 2013. Efficient butanol production without carbon catabolite repression from mixed sugars with *Clostridium saccharoperbutylacetonicum* N1-4. J. Biosci. Bioeng. 116, 716–721. <https://doi.org/10.1016/j.jbiosc.2013.05.030>
- Nölling, J., Breton, G., Omelchenko, M. V., Kira, S., Zeng, Q., Gibson, R., Lee, H.M., Dubois, J., Qiu, D., Hitti, J., Sequencing, G.T.C., Wolf, Y.I., Tatusov, R.L., Sabathe, F., Soucaille, P., Daly, M.J., Bennett, G.N., Koonin, E. V., Smith, D.R., 2001. Genome Sequence and Comparative Analysis of the Solvent-Producing Bacterium *Clostridium acetobutylicum* Genome Sequence and Comparative Analysis of the Solvent-Producing Bacterium *Clostridium acetobutylicum*. J. Bacteriol. 183, a823–4838. <https://doi.org/10.1128/JB.183.16.4823>
- Ou, J., Ma, C., Xu, N., Du, Y., Liu, X. (Margaret), 2015. High butanol production by regulating carbon, redox and energy in *Clostridia*. Front. Chem. Sci. Eng. 9, 317–323. <https://doi.org/10.1007/s11705-015-1522-6>
- Outram, V., Lalander, C.A., Lee, J.G.M., Davies, E.T., Harvey, A.P., 2017. Applied in situ product recovery in ABE fermentation. Biotechnol. Prog. 33, 563–579. <https://doi.org/10.1002/btpr.2446>
- Page, A.J., Cummins, C.A., Hunt, M., Wong, V.K., Reuter, S., Holden, M.T.G., Fookes, M., Falush, D., Keane, J.A., Parkhill, J., 2015. Roary: Rapid large-scale prokaryote pan genome analysis. Bioinformatics 31, 3691–3693. <https://doi.org/10.1093/bioinformatics/btv421>
- Poehlein, A., Krabben, P., Dürre, P., Daniel, R., 2014. Complete Genome Sequence of the Solvent Producer *Clostridium saccharoperbutylacetonicum* Strain DSM 14923. Genome Announc 2, 1056–14. <https://doi.org/10.1128/genomeA.01056-14>
- Poehlein, A., Solano, J.D.M., Flitsch, S.K., Krabben, P., Winzer, K., Reid, S.J., Jones, D.T., Green, E., Minton, N.P., Daniel, R., Dürre, P., 2017. Microbial solvent formation revisited by comparative genome analysis. Biotechnol. Biofuels 10, 58. <https://doi.org/10.1186/s13068-017-0742-z>
- Procentese, A., Raganati, F., Navarini, L., Olivieri, G., Russo, M.E., Marzocchella, A., 2018. Coffee silverskin as a renewable resource to produce butanol and isopropanol. Chem. Eng. Trans. 64. <https://doi.org/10.3303/CET1864024>
- Qureshi, N., Blaschek, H., 2001. Evaluation of recent advances in butanol fermentation, upstream, and downstream processing. Bioprocess Biosyst. Eng. 24, 219–226. <https://doi.org/10.1007/s004490100257>
- Qureshi, N., Blaschek, H.P., 2000. Recovery of butanol from fermentation broth by gas stripping. Renew. Energy 22, 557–564. [https://doi.org/10.1016/S0960-1481\(00\)00108-7](https://doi.org/10.1016/S0960-1481(00)00108-7)
- Ragsdale, S.W., 2008. Enzymology of the Woods-Ljungdahl Pathway of Acetogenesis. Ann. N. Y. Acad. Sci. 1125, 129–136. <https://doi.org/10.1196/annals.1419.015.Enzymology>
- Rath, D., Amlinger, L., Rath, A., Lundgren, M., 2015. The CRISPR-Cas immune

- system: Biology, mechanisms and applications. *Biochimie* 117, 119–128. <https://doi.org/10.1016/j.biochi.2015.03.025>
- Ravagnani, A., Jennert, K.C.B., Steiner, E., Grunberg, R., Jefferies, J.R., Wilkinson, S.R., Young, D.I., Tidswell, E.C., Brown, D.P., Youngman, P., Morris, J.G., Young, M., 2000. Spo0A directly controls the switch from acid to solvent production in solvent-forming clostridia. *Mol. Microbiol.* 37, 1172–1185.
- Ren, C., Gu, Y., Hu, S., Wu, Y., Wang, P., Yang, Y., Yang, C., Yang, S., Jiang, W., 2010. Identification and inactivation of pleiotropic regulator CcpA to eliminate glucose repression of xylose utilization in *Clostridium acetobutylicum*. *Metab. Eng.* 12, 446–454. <https://doi.org/10.1016/j.ymben.2010.05.002>
- Ren, C., Gu, Y., Wu, Y., Zhang, W., Yang, C., Yang, S., Jiang, W., 2012. Pleiotropic functions of catabolite control protein CcpA in Butanol-producing *Clostridium acetobutylicum*. *BMC Genomics* 13, 349. <https://doi.org/10.1186/1471-2164-13-349>
- Ren, C., Wen, Z., Xu, Y., Jiang, W., Gu, Y., 2016. Clostridia: a flexible microbial platform for the production of alcohols. *Curr. Opin. Chem. Biol.* 35, 65–72. <https://doi.org/10.1016/j.cbpa.2016.08.024>
- Robinson, J.T., Thorvaldsdóttir, H., Winckler, W., Guttman, M., Lander, E.S., Getz, G., Mesirov, J.P., 2011. Integrative genomics viewer. *Nat. Biotechnol.* 29, 24.
- Ryan S. Senger, E.T.P., 2009. Genome-Scale Model for *Clostridium acetobutylicum*: Part I. Metabolic Network Resolution and Analysis. *Bio Technol.* 101, 1036–1052. <https://doi.org/10.1002/bit.22010>
- Sadie R. Bartholomew, J.T.T., 2006. Cost-Effective Engineering of a Small-Scale Bioreactor. *Biotechnol. Bioeng.* 96, 401–407. <https://doi.org/10.1002/bit>
- Sambrook, Joseph: Maniatis: Tom: Fritsh., 1987. *Molecular cloning : a laboratory manual* (2nd ed), 2nd ed. Cold Spring Harbor Laboratory Press, Cold Spring Harbor N.Y.
- Sandoval, N.R., Venkataramanan, K.P., Groth, T.S., Papoutsakis, E.T., 2015. Whole-genome sequence of an evolved *Clostridium pasteurianum* strain reveals Spo0A deficiency responsible for increased butanol production and superior growth. *Biotechnol Biofuels* 8, 227. <https://doi.org/10.1186/s13068-015-0408-7>
- Seemann, T., 2014. Prokka: Rapid prokaryotic genome annotation. *Bioinformatics* 30, 2068–2069. <https://doi.org/10.1093/bioinformatics/btu153>
- Shafiee, S., Topal, E., 2009. When will fossil fuel reserves be diminished? *Energy Policy* 37, 181–189. <https://doi.org/10.1016/j.enpol.2008.08.016>
- Shaheen, R., Shirley, M., Jones, D.T., 2000. Comparative fermentation studies of industrial strains belonging to four species of solvent-producing clostridia. *J. Mol. Microbiol. Biotechnol.* 2, 115–124. <https://doi.org/10937496>
- Sillers, R., Chow, A., Tracy, B., Papoutsakis, E.T., 2008. Metabolic engineering of the non-sporulating, non-solventogenic *Clostridium acetobutylicum* strain M5 to produce butanol without acetone demonstrate the robustness of the acid-formation pathways and the importance of the electron balance. *Metab. Eng.* 10, 321–332. <https://doi.org/10.1016/j.ymben.2008.07.005>
- Sinkunas, T., Gasiunas, G., Fremaux, C., Barrangou, R., Horvath, P., Siksnys, V., 2011. Cas3 is a single-stranded DNA nuclease and ATP-dependent helicase in the CRISPR/Cas immune system. *EMBO J.* 30, 1335–1342. <https://doi.org/10.1038/emboj.2011.41>
- Sorda, G., Banse, M., Kemfert, C., 2010. An overview of biofuel policies across the world. *Energy Policy* 38, 6977–6988. <https://doi.org/10.1016/j.enpol.2010.06.066>
- Soucaille, P., Figge, R., Croux, C., 2008. process for chromosomal integration and dna sequence replacement in *Clostridia* background. WO 2008/040387 A1.

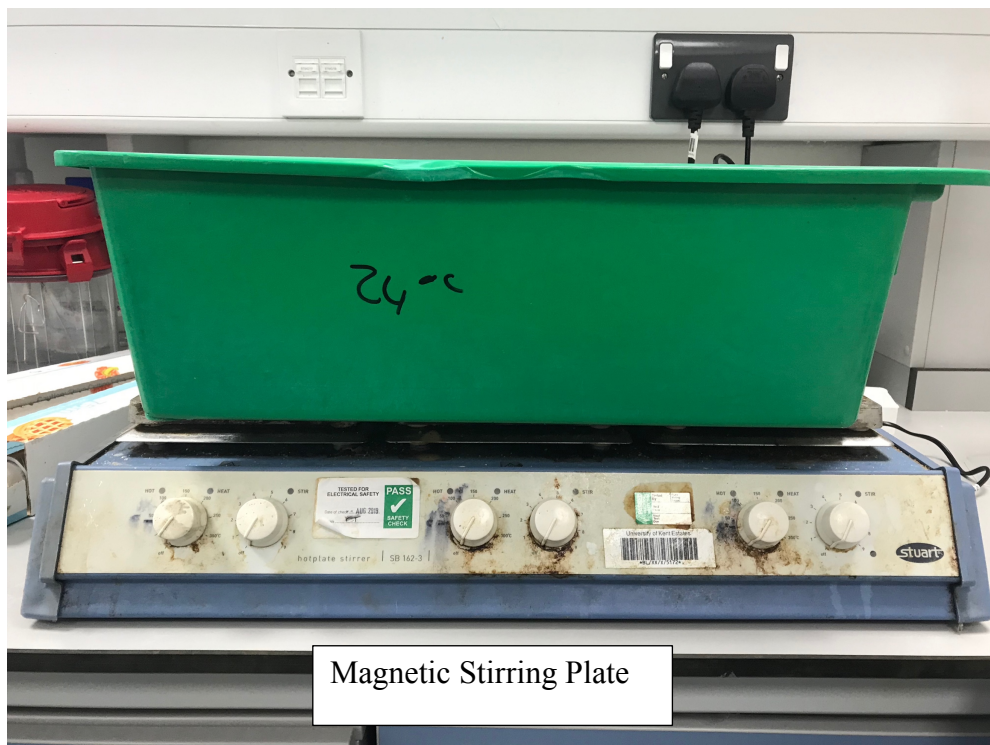
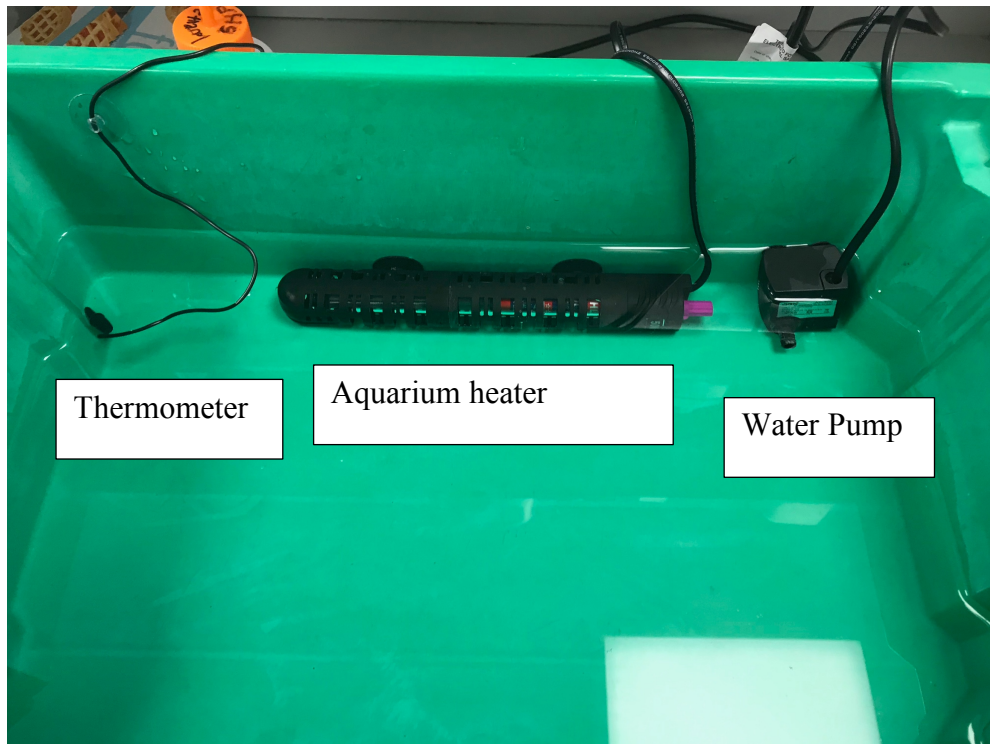
- Staals, R.H.J., Agari, Y., Maki-Yonekura, S., Zhu, Y., Taylor, D.W., vanDuijn, E., Barendregt, A., Vlot, M., Koehorst, J.J., Sakamoto, K., Masuda, A., Dohmae, N., Schaap, P.J., Doudna, J.A., Heck, A.J.R., Yonekura, K., Van der Oost, J., Shinkai, A., 2013. Structure and Activity of the RNA-Targeting Type III-B CRISPR-Cas Complex of *Thermus thermophilus*. *Mol. Cell* 52, 135–145. <https://doi.org/10.1016/j.molcel.2013.09.013>
- Speelmans, G., Poolman, B., Abee, T., Konings, W.N., 1994. The F- or V-type Na⁺-ATPase of the thermophilic bacterium *Clostridium fervidus*. *J. Bacteriol.* 176, 5160–5162. <https://doi.org/10.1128/jb.176.16.5160-5162.1994>
- Takeo, S., Murata, R., Kobayashi, R., Mitsunashi, S., Ikeda, M., 2010. Engineering of *Corynebacterium glutamicum* with an NADPH-generating glycolytic pathway for L-lysine production. *Appl. Environ. Microbiol.* 76, 7154–7160. <https://doi.org/10.1128/AEM.01464-10>
- Takors, R., Kopf, M., Mampel, J., Bluemke, W., Blombach, B., Eikmanns, B., Bengelsdorf, F.R., Weuster-Botz, D., Dürre, P., 2018. Using gas mixtures of CO, CO₂ and H₂ as microbial substrates: the do's and don'ts of successful technology transfer from laboratory to production scale. *Microb. Biotechnol.* 11, 606–625. <https://doi.org/10.1111/1751-7915.13270>
- Tashiro, Y., Shinto, H., Hayashi, M., Baba, S., Kobayashi, G., Sonomoto, K., 2007. Novel high-efficient butanol production from butyrate by non-growing *Clostridium saccharoperbutylacetonicum* N1-4 (ATCC 13564) with methyl viologen. *J. Biosci. Bioeng.* 104, 238–240. <https://doi.org/10.1263/jbb.104.238>
- Tashiro, Y., Takeda, K., Kobayashi, G., Sonomoto, K., Ishizaki, A., Yoshino, S., 2004. High butanol production by *Clostridium saccharoperbutylacetonicum* N1-4 in fed-batch culture with pH-Stat continuous butyric acid and glucose feeding method. *J. Biosci. Bioeng.* 98, 263–268. <https://doi.org/10.1263/jbb.98.263>
- Tashiro, Y., Yoshida, T., Noguchi, T., Sonomoto, K., 2013. Recent advances and future prospects for increased butanol production by acetone-butanol-ethanol fermentation. *Eng. Life Sci.* 13, 432–445. <https://doi.org/10.1002/elsc.201200128>
- Tomas, C. a, Beamish, J., Eleftherios, T., Papoutsakis, E.T., 2004. Transcriptional Analysis of Butanol Stress and Tolerance in *Clostridium acetobutylicum*. *J. Bacteriol.* 186, 2006–2018. <https://doi.org/10.1128/JB.186.7.2006>
- Tomas, C.A., Welker, N.E., Papoutsakis, E.T., 2003. Overexpression of groESL in *Clostridium acetobutylicum* results in increased solvent production and tolerance, prolonged metabolism, and changes in the cell's transcriptional program. *Appl. Environ. Microbiol.* 69, 4951–4965. <https://doi.org/10.1128/AEM.69.8.4951-4965.2003>
- Tracy, B.P., Jones, S.W., Fast, A.G., Indurthi, D.C., Papoutsakis, E.T., 2012. Clostridia: The importance of their exceptional substrate and metabolite diversity for biofuel and biorefinery applications. *Curr. Opin. Biotechnol.* 23, 364–381. <https://doi.org/10.1016/j.copbio.2011.10.008>
- Tsai, T.Y., Lo, Y.C., Chang, J.S., 2014. Effect of medium composition and PH control strategies on butanol fermentation with *Clostridium acetobutylicum*. *Energy Procedia* 61, 1691–1694. <https://doi.org/10.1016/j.egypro.2014.12.193>
- Tummala, S.B., Welker, N.E., Papoutsakis, E.T., 2003. Design of antisense RNA constructs for downregulation of the acetone formation pathway of *Clostridium acetobutylicum*. *J. Bacteriol.* 185, 1923–1934. <https://doi.org/10.1128/JB.185.6.1923-1934.2003>
- Underwood, S., Guan, S., Vijayasubhash, V., Baines, S.D., Graham, L., Lewis, R.J., Wilcox, M.H., Stephenson, K., 2009. Characterization of the Sporulation

- Initiation Pathway of *Clostridium difficile* and Its Role in Toxin Production. *J. Bacteriol.* 191, 7296–7305. <https://doi.org/10.1128/JB.00882-09>
- United States Congress, 2007. Energy Information and Security Act of 2007 310.
- Ventura, J.R.S., Hu, H., Jahng, D., 2013. Enhanced butanol production in *Clostridium acetobutylicum* ATCC 824 by double overexpression of 6-phosphofructokinase and pyruvate kinase genes. *Appl. Microbiol. Biotechnol.* 97, 7505–7516. <https://doi.org/10.1007/s00253-013-5075-7>
- Wang, J., Yang, H., Qi, G., Liu, X., Gao, X., Shen, Y., 2019. Effect of lignocellulose-derived weak acids on butanol production by *Clostridium acetobutylicum* under different pH adjustment conditions. *RSC Adv.* 9, 1967–1975. <https://doi.org/10.1039/C8RA08678H>
- Wang, S., Dong, S., Wang, P., Tao, Y., 2017a. Genome Editing in *Clostridium saccharoperbutylacetonicum* N1-4 with the CRISPR-Cas9 System 83, 1–16.
- Wang, S., Dong, S., Wang, Y., 2017b. Enhancement of solvent production by overexpressing key genes of the acetone-butanol-ethanol fermentation pathway in *Clostridium saccharoperbutylacetonicum* N1-4. *Bioresour. Technol.* 245, 426–433. <https://doi.org/10.1016/j.biortech.2017.09.024>
- Wang, S., Zhu, Y., Zhang, Y., Li, Y., 2012. Controlling the oxidoreduction potential of the culture of *Clostridium acetobutylicum* leads to an earlier initiation of solventogenesis, thus increasing solvent productivity. *Appl. Microbiol. Biotechnol.* 93, 1021–1030. <https://doi.org/10.1007/s00253-011-3570-2>
- Wang, Y., Zhang, Z.T., Seo, S.O., Lynn, P., Lu, T., Jin, Y.S., Blaschek, H.P., 2016. Bacterial Genome Editing with CRISPR-Cas9: Deletion, Integration, Single Nucleotide Modification, and Desirable “clean” Mutant Selection in *Clostridium beijerinckii* as an Example. *ACS Synth. Biol.* 5, 721–732. <https://doi.org/10.1021/acssynbio.6b00060>
- Wasels, F., Jean-Marie, J., Collas, F., López-Contreras, A.M., Lopes Ferreira, N., 2017. A two-plasmid inducible CRISPR/Cas9 genome editing tool for *Clostridium acetobutylicum*. *J. Microbiol. Methods* 140, 5–11. <https://doi.org/10.1016/j.mimet.2017.06.010>
- Wietzke, M., Bahl, H., 2012. The redox-sensing protein Rex, a transcriptional regulator of solventogenesis in *Clostridium acetobutylicum*. *Appl. Microbiol. Biotechnol.* 96, 749–761. <https://doi.org/10.1007/s00253-012-4112-2>
- Woolston, B.M., Emerson, D.F., Currie, D.H., Stephanopoulos, G., 2018. Rediverting carbon flux in *Clostridium ljungdahlii* using CRISPR interference (CRISPRi). *Metab. Eng.* 48, 243–253. <https://doi.org/10.1016/j.ymben.2018.06.006>
- Xiao, H., Gu, Y., Ning, Y., Yang, Y., Mitchell, W.J., Jiang, W., Yang, S., 2011. Confirmation and elimination of xylose metabolism bottlenecks in glucose phosphoenolpyruvate-dependent phosphotransferase system-deficient *Clostridium acetobutylicum* for simultaneous utilization of glucose, xylose, and arabinose. *Appl. Environ. Microbiol.* 77, 7886–7895. <https://doi.org/10.1128/AEM.00644-11>
- Xu, M., Zhao, J., Yu, L., Tang, I.C., Xue, C., Yang, S.T., 2014. Engineering *Clostridium acetobutylicum* with a histidine kinase knockout for enhanced n-butanol tolerance and production. *Appl. Microbiol. Biotechnol.* 99, 1011–1022. <https://doi.org/10.1007/s00253-014-6249-7>
- Xu, M., Zhao, J., Yu, L., Yang, S.T., 2017. Comparative genomic analysis of *Clostridium acetobutylicum* for understanding the mutations contributing to enhanced butanol tolerance and production. *J. Biotechnol.* 263, 36–44. <https://doi.org/10.1016/j.jbiotec.2017.10.010>
- Xue, C., Wang, Z., Wang, S., Zhang, X., Chen, L., Mu, Y., Bai, F., 2016. The vital role of citrate buffer in acetone-butanol-ethanol (ABE) fermentation using corn stover and high-efficient product recovery by vapor stripping-vapor

- permeation (VSVP) process. *Biotechnol. Biofuels* 9, 1–9. <https://doi.org/10.1186/s13068-016-0566-2>
- Yang, X., Tu, M., Xie, R., Adhikari, S., Tong, Z., 2013. A comparison of three pH control methods for revealing effects of undissociated butyric acid on specific butanol production rate in batch fermentation of *Clostridium acetobutylicum*. *AMB Express* 3, 3. <https://doi.org/10.1186/2191-0855-3-3>
- Ying, Y.F., 2018. Exploring alternative feedstocks and engineering butanol tolerance to optimise biofuel production by *Clostridium saccharoperbutylacetonicum*. University of Kent.
- Zhang, J., Wang, P., Wang, X., Feng, J., Sandhu, H.S., Wang, Y., 2018. Enhancement of sucrose metabolism in *Clostridium saccharoperbutylacetonicum* N1-4 through metabolic engineering for improved acetone–butanol–ethanol (ABE) fermentation. *Bioresour. Technol.* 270, 430–438. <https://doi.org/10.1016/j.biortech.2018.09.059>
- Zhang, J., Yu, L., Xu, M., Yang, S.T., Yan, Q., Lin, M., Tang, I.C., 2017. Metabolic engineering of *Clostridium tyrobutyricum* for n-butanol production from sugarcane juice. *Appl. Microbiol. Biotechnol.* 101, 4327–4337. <https://doi.org/10.1007/s00253-017-8200-1>
- Zhang, L., Nie, X., Ravcheev, D.A., Rodionov, D.A., Sheng, J., Gu, Y., Yang, S., Jiang, W., Yang, C., 2014. Redox-responsive repressor rex modulates alcohol production and oxidative stress tolerance in *Clostridium acetobutylicum*. *J. Bacteriol.* 196, 3949–3963. <https://doi.org/10.1128/JB.02037-14>
- Zheng, J., Tashiro, Y., Wang, Q., Sonomoto, K., 2015. Recent advances to improve fermentative butanol production: Genetic engineering and fermentation technology. *J. Biosci. Bioeng.* 119, 1–9. <https://doi.org/10.1016/j.jbiosc.2014.05.023>
- Zhong, J., Karberg, M., Lambowitz, A.M., 2003. Targeted and random bacterial gene disruption using a group II intron (targetron) vector containing a retrotransposition-activated selectable marker. *Nucleic Acids Res.* 31, 1656–1664. <https://doi.org/10.1093/nar/gkg248>

Appendix

Appendix A-1 – Jacketed water system for fermentation system





Appendix A-2 – List of components used in designed fermentation system.

This list is extensive for the components of the culture vessel itself, alongside the probes used in the measurements of pH and Redox. Peristaltic pumps used were already part of the lab equipment as well as the magnetic stirring plate.

Component	Brand	Link to purchase
1 L Culture Vessel	FV1L QUICKFIT 1LT CULTURE VESSEL 100 MM FLAT FLANGE	http://www.scilabware.com/product.asp?P_ID=233&strPageHistory=related
Culture vessel Port lid	MAF4/41 QUICKFIT LID 100MM FLAT FLANGE 3 X SOCKETS 14/23 & 2 x SOCKET	http://www.scilabware.com/product.asp?P_ID=249&strPageHistory=related
Culture vessel Gasket	PS100 QUICKFIT 100MM FLAT FLANGE PTFE SEAL	http://www.scilabware.com/product.asp?P_ID=339&strPageHistory=related
Lid to vessel clips	JC100F QUICKFIT JOINT CLIPS METAL, SPRING WIRE, FG 100 (FOR EX5/105)	http://www.scilabware.com/product.asp?P_ID=250&strPageHistory=related
Suba seals		https://webshop.fishersci.com/insight2_uk/getProduct.do?productCode=11548132&resultSetPosition=0
0.2 µM gas filters	Whatman	https://www.sigmaaldrich.com/catalog/product/aldrich/wha67205002?lang=en&region=GB&cm_sp=Insite-_-prodRecCold_xviews-_-prodRecCold5-2
Aquarium heater and thermometer	U-picks Aquarium Heater	https://www.amazon.co.uk/gp/product/B07JM1ND63/ref=ppx_yo_dt_b_search_asin_title?ie=UTF8&psc=1
Water Pump	Maxesla Submersible Pump	https://www.amazon.co.uk/Maxesla-Submersible-Fountain-Aquarium-Hydroponics/dp/B071NNG376/ref=sr_1_7?keywords=water+pump&qid=1564842361&s=pets-supplies&sr=1-7
pH probe	pH electrode InLab Semi-Micro-L	https://www.mt.com/gb/en/home/products/Laboratory_Analytics_Browse/pH-meter/sensor/pH-sensor/InLab-Semi-Micro-L.html?SE=GOOGLE-Shopping&cmp=sea_02540126&Campaign=MT_ANA_EN_UK_Shopping&Adgroup=ANA%20products&bookedkeyword=&matchtype=&adtext=266043130549&placement=&network=g&kclid=_k_EAlal

		QobChMIpvCeqvTm4wIVxrTtCh1uggdDEAQYCyABEgLPUPD_BwE_k_&gclid=EAIaIQobChMIpvCeqvTm4wIVxrTtCh1uggdDEAQYCyABEgLPUPD_BwE
Redox Probe	ORP electrode InLab Redox-L	https://www.mt.com/gb/en/home/products/Laboratory_Analytics_Browse/pH-meter/sensor/orp-sensor/InLab-Redox-L.html?SE=GOOGLE-Shopping&cmp=sea_02540126&Campaign=MT_ANA_EN_UK_Shopping&Adgroup=ANA%20products&bookedkeyword=&matchtype=&adtext=266043130549&placement=&network=g&kclid=_k_EAIaIQobChMIjeCtwPTm4wIVjLTtCh1dvwtuEAQYAyABEgKPIPD_BwE_k_&gclid=EAIaIQobChMIjeCtwPTm4wIVjLTtCh1dvwtuEAQYAyABEgKPIPD_BwE

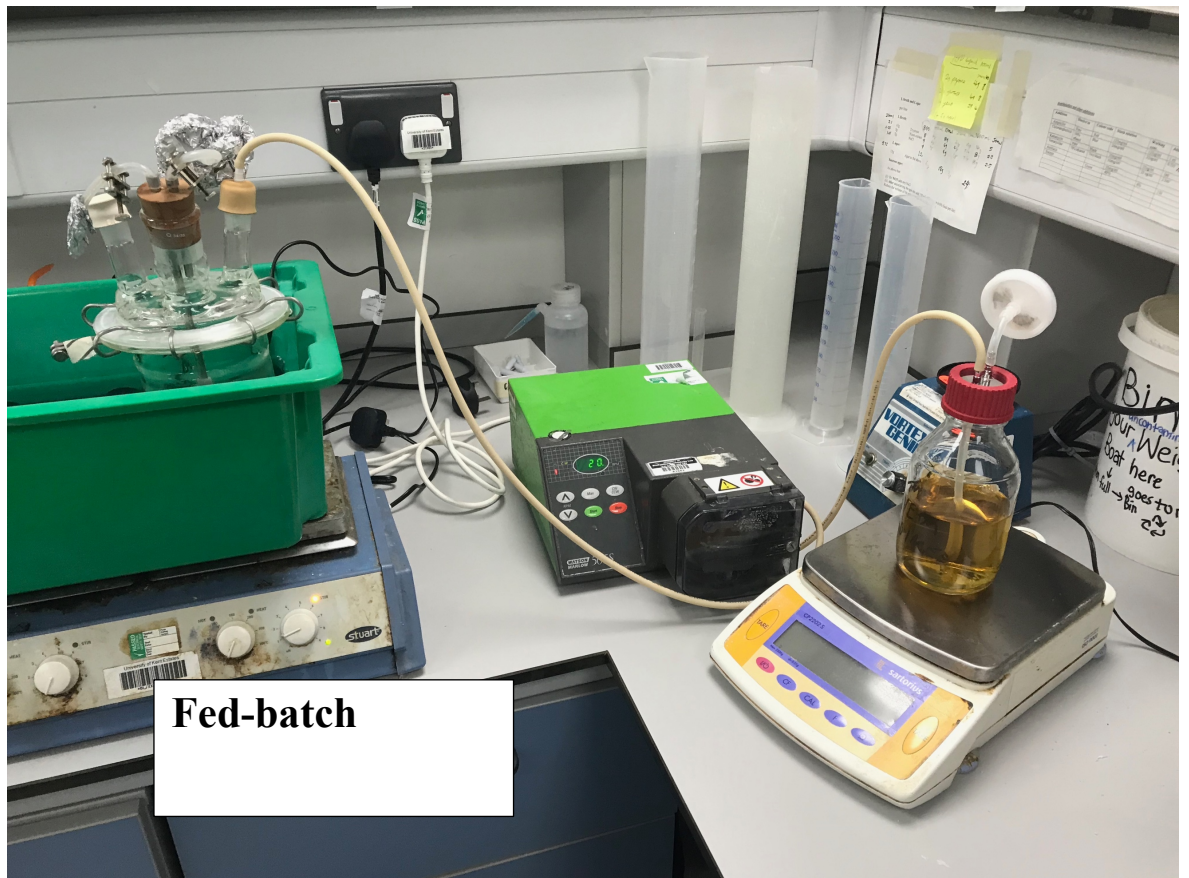
Appendix A3 – Custom built gas out and sample port:

Gas out - Short tube
Sampler – long tube





Appendix B – Final set up of fermentation units based upon schematics from Figure 3.1





Continuous

Appendix C – Calculations for correct pmol of DNA for Clostridium transformation.

Transformation of *C. saccharoperbutylacetonicum* and derivative strains with pMTL vectors

Transform cells with 260 pmols of 82154-based vectors (S1Va/b, S4V etc.)

Transform cells with 330 pmols of 83251-based vectors (S3Va/b etc.)

Avoid exceeding 5 μ L DNA per 200 μ L cells in the electroporation cuvette where possible

Plasmid	bp	ng	pmols
pMTL 82154	5822	1000	260
pMTL 83251	4589	1000	330

Converting ng to pmol

$$\text{pmols} = \left(\frac{\text{ng ds DNA}}{660 \times \text{bp}} \right) \times 10^6$$

Converting pmol to ng

$$\text{ng} = \left(\text{pmol ds DNA} \times (660 \times \text{bp}) \right) \div 10^6$$

Appendix E – Qualimap results – Separate PDF

External PDF files:

Appen_E1_WT_qualimap_anlaysis.PDF

<<Appen_E1_WT_qualimap_anlaysis.pdf>>

Qualimap Analysis Results

BAM QC analysis

Generated by Qualimap v.2.2.1

2019/01/11 18:01:20

1. Input data & parameters (inside of regions)

1.1. QualiMap command line

```
qualimap bamqc -bam
/Volumes/EXTRAROOM/Biodata/Results/Output_WT_knockout/bwa_WT/C1
_filtered.fillmd.rmdup.sorted.bam -gff
/Volumes/EXTRAROOM/Biodata/genome_assemblies/ncbi-genomes-2019-
01-11/GCA_000340885.1_ASM34088v1_genomic.gff -c -nw 400 -hm 3
```

1.2. Alignment

Command line:	bwa mem -t 2 /Volumes/EXTRAROOM/Biodata/Results/Output_WT_knockout/PROKKA/refsacc/PROKKA_04272017.fna /Volumes/EXTRAROOM/Biodata/Results/Output_WT_knockout/Trimmomatic/C1/C1_trim_output_reverse_paired.fq.gz /Volumes/EXTRAROOM/Biodata/Results/Output_WT_knockout/Trimmomatic/C1/C1_trim_output_forward_paired.fq.gz
Draw chromosome limits:	yes
Analyze overlapping paired-end reads:	no
Program:	bwa (0.7.15-r1140)
Analysis date:	Fri Jan 11 17:58:56 GMT 2019
Size of a homopolymer:	3
Skip duplicate alignments:	no
Number of windows:	400
BAM file:	/Volumes/EXTRAROOM/Biodata/Res

	ults/Output_WT_knockout/bwa_WT/C 1_filtered.fillmd.rmdup.sorted.bam
--	--

1.3. GFF region

Library protocol:	non-strand-specific
Outside statistics:	no
GFF file:	/Volumes/EXTRAROOM/Biodata/genome_assemblies/ncbi-genomes-2019-01-11/GCA_000340885.1_ASM34088v1_genomic.gff

2. Summary (inside of regions)

2.1. Warnings

Some regions are not loaded	213 regions were skipped because chromosome name was not found in the BAM file.
-----------------------------	---

2.2. Globals

Reference size	6,530,257
Number of reads	596,655
Mapped reads	579,484 / 97.12%
Supplementary alignments	247 / 0.04%
Unmapped reads	17,171 / 2.88%
Mapped paired reads	579,484 / 97.12%
Mapped reads, first in pair	289,785 / 48.57%
Mapped reads, second in pair	289,699 / 48.55%
Mapped reads, both in pair	579,201 / 97.07%
Mapped reads, singletons	283 / 0.05%
Read min/max/mean length	30 / 251 / 212.68
Clipped reads	4,726 / 0.79%

2.3. Globals (inside of regions)

Regions size/percentage of reference	6,530,257 / 100%
Mapped reads	579,484 / 97.12%
Mapped reads, only first in pair	289,785 / 48.57%
Mapped reads, only second in pair	289,699 / 48.55%

Mapped reads, both in pair	579,201 / 97.07%
Mapped reads, singletons	283 / 0.05%
Correct strand reads	0 / 0%
Clipped reads	4,726 / 0.79%
Duplicated reads (estimated)	162,961 / 28.12%
Duplication rate	30.48%

2.4. ACGT Content (inside of regions)

Number/percentage of A's	42,580,938 / 34.58%
Number/percentage of C's	19,126,741 / 15.53%
Number/percentage of T's	41,386,355 / 33.61%
Number/percentage of G's	20,056,915 / 16.29%
Number/percentage of N's	0 / 0%
GC Percentage	31.82%

2.5. Coverage (inside of regions)

Mean	18.859
Standard Deviation	11.3944

2.6. Mapping Quality (inside of regions)

Mean Mapping Quality	59.3
----------------------	------

2.7. Insert size (inside of regions)

Mean	1,041.1
Standard Deviation	61,222.86
P25/Median/P75	193 / 327 / 437

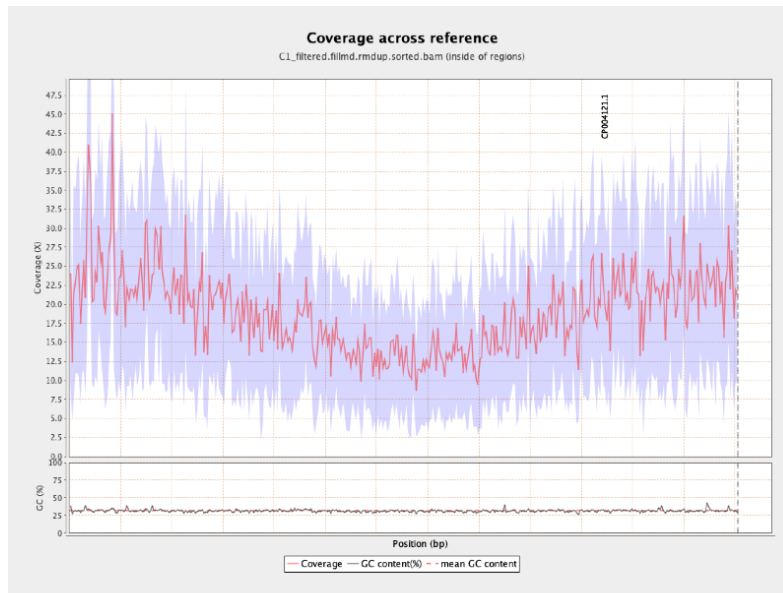
2.8. Mismatches and indels (inside of regions)

General error rate	0.09%
Mismatches	115,574
Insertions	504
Mapped reads with at least one insertion	0.09%
Deletions	2,151
Mapped reads with at least one deletion	0.36%
Homopolymer indels	62.6%

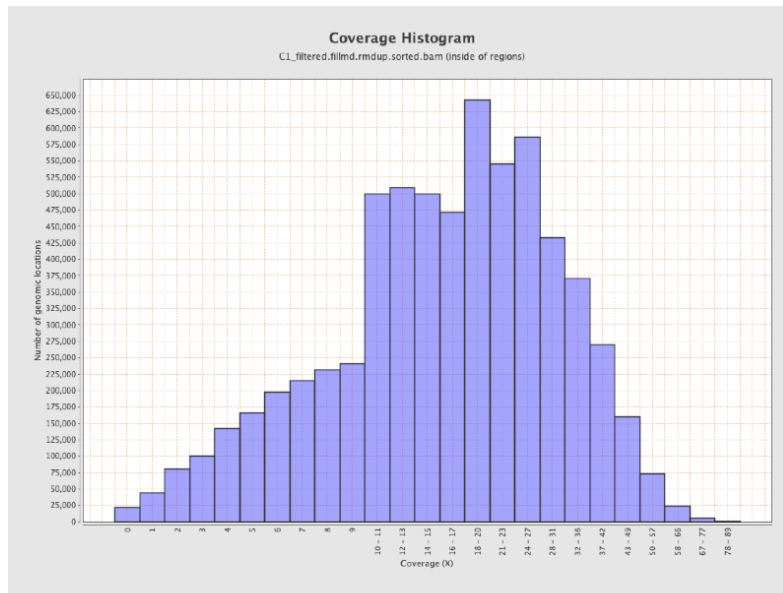
2.9. Chromosome stats (inside of regions)

Name	Length	Mapped bases	Mean coverage	Standard deviation
CP004121.1	6530257	123153985	18.859	11.3944

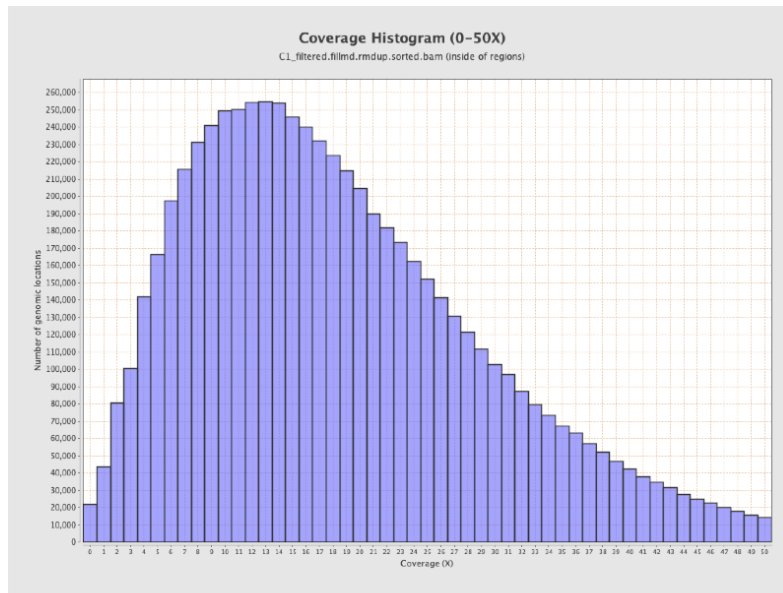
3. Results : Coverage across reference (inside of regions)



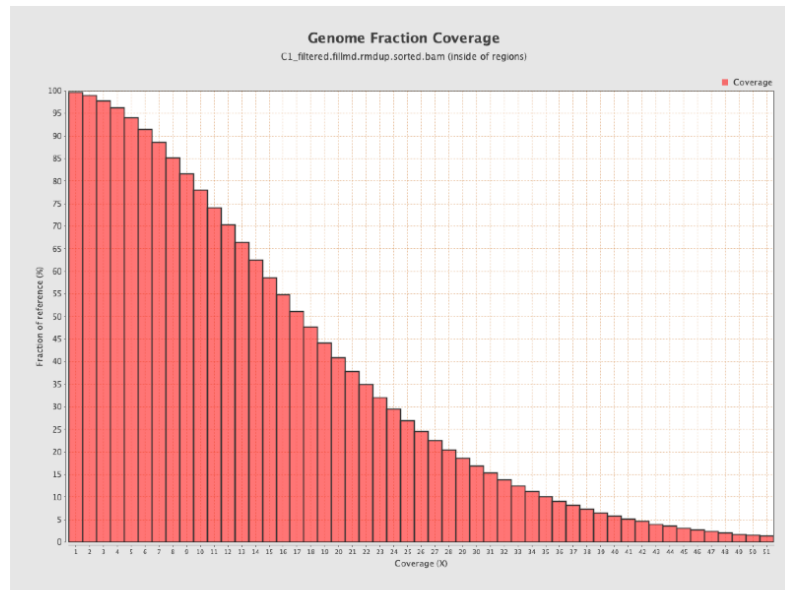
4. Results : Coverage Histogram (inside of regions)



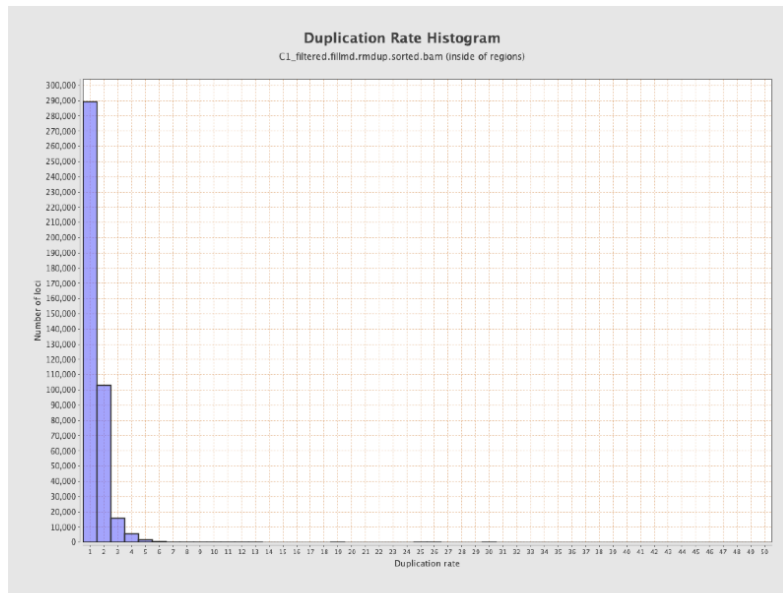
5. Results : Coverage Histogram (0-50X) (inside of regions)



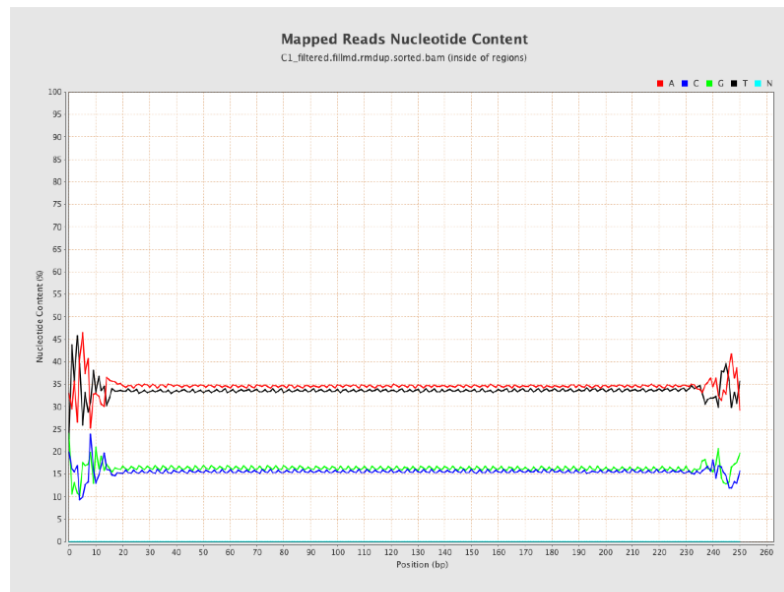
6. Results : Genome Fraction Coverage (inside of regions)



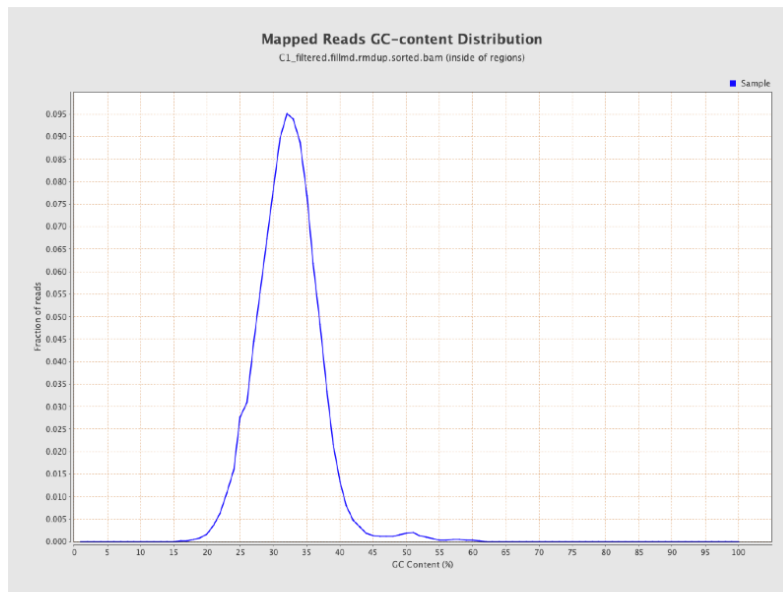
7. Results : Duplication Rate Histogram (inside of regions)



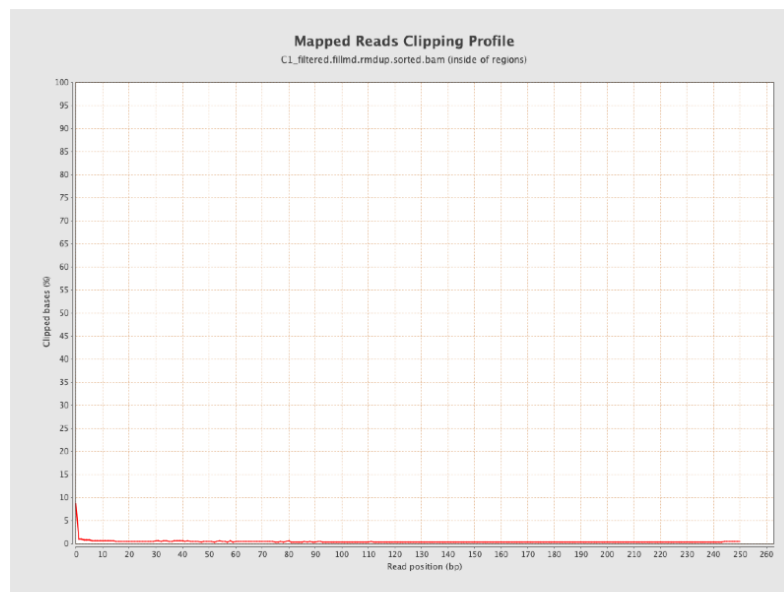
8. Results : Mapped Reads Nucleotide Content (inside of regions)



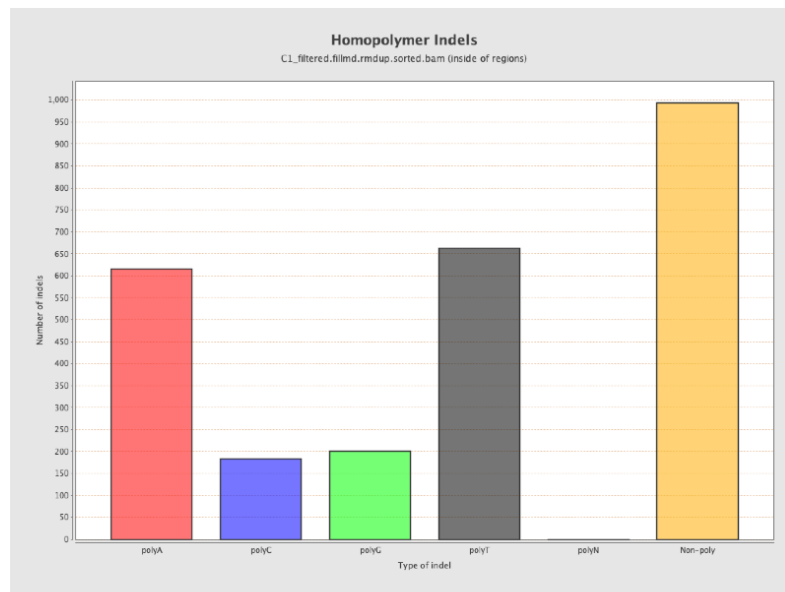
9. Results : Mapped Reads GC-content Distribution (inside of regions)



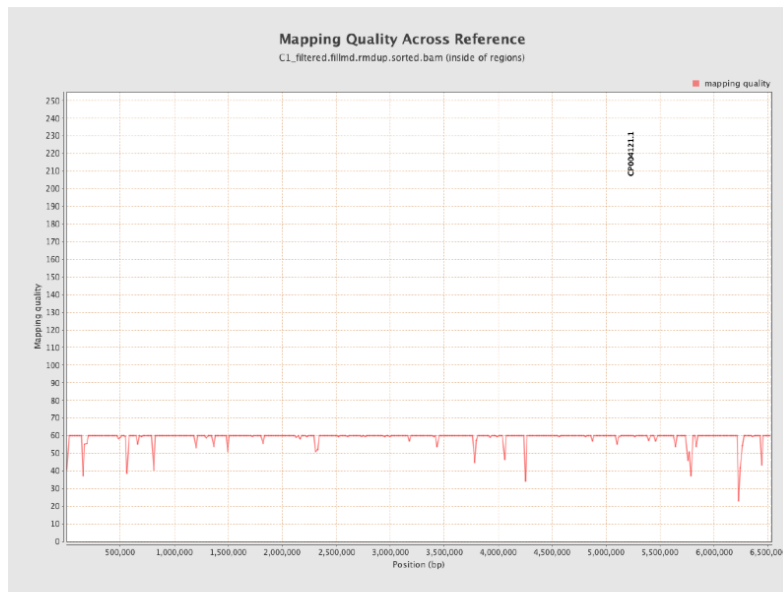
10. Results : Mapped Reads Clipping Profile (inside of regions)



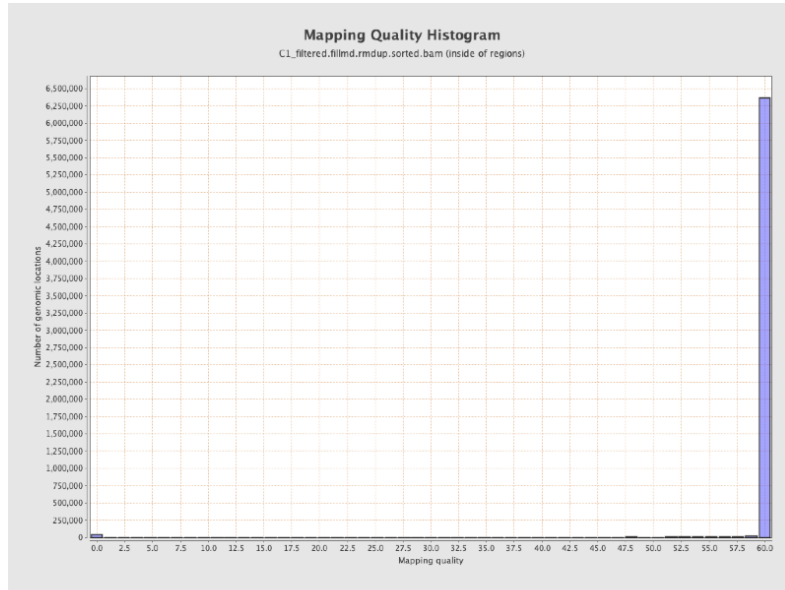
11. Results : Homopolymer Indels (inside of regions)



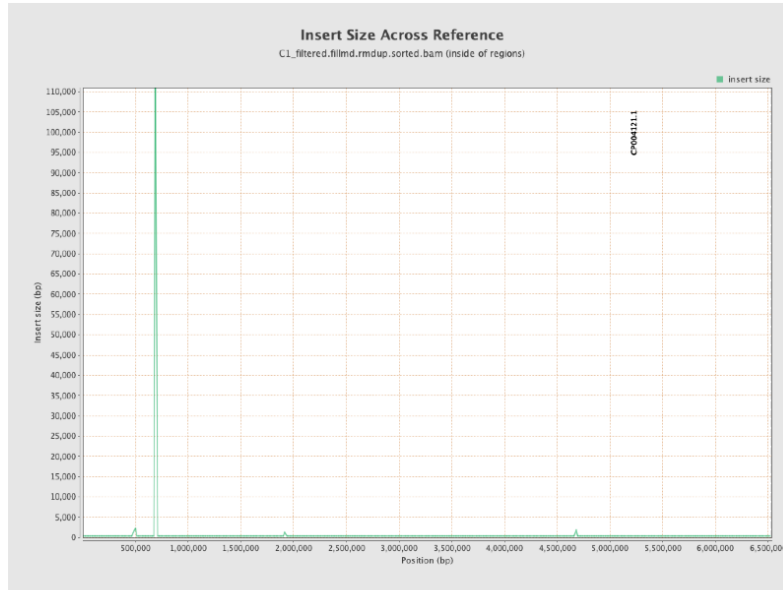
12. Results : Mapping Quality Across Reference (inside of regions)



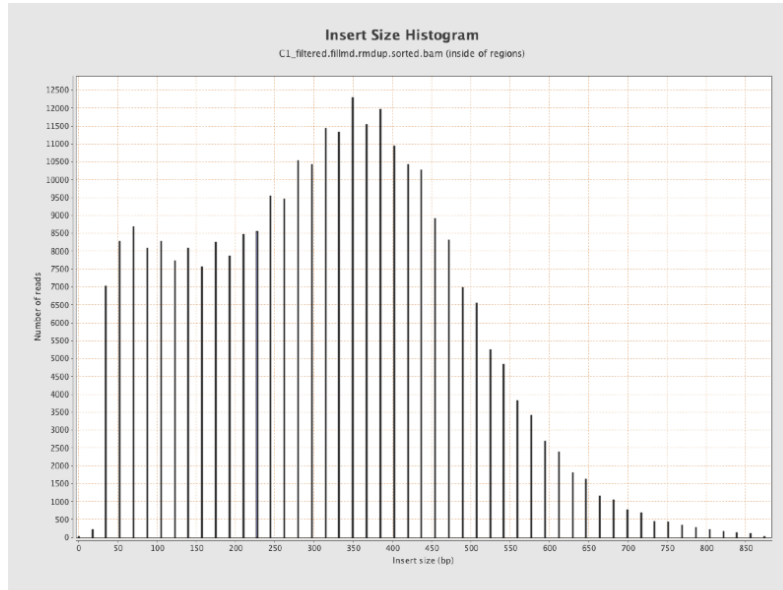
13. Results : Mapping Quality Histogram (inside of regions)



14. Results : Insert Size Across Reference (inside of regions)



15. Results : Insert Size Histogram (inside of regions)



Appen_E2_Qualimap_report.PDF

<<Appen_E2_Qualimap_report.pdf>>

Qualimap Analysis Results

BAM QC analysis

Generated by Qualimap v.2.2.1

2018/05/29 12:53:03

1. Input data & parameters

1.1. QualiMap command line

```
qualimap bamqc -bam
/Volumes/EXTRAROOM/Biodata/output/bwa/C2_filtered_fillmd_rmdup_sort
ed.bam -c -nw 400 -hm 3
```

1.2. Alignment

Command line:	bwa mem -t 2 /Volumes/EXTRAROOM/Biodata/Ref/ csacc_ref.fasta /Volumes/EXTRAROOM/Biodata/Res ults/Output_WT_knockout/Trimmoma tic/C2/C2_output_forward_paired.fq.g z /Volumes/EXTRAROOM/Biodata/Res ults/Output_WT_knockout/Trimmoma tic/C2/C2_output_reverse_paired.fq.g z
Draw chromosome limits:	yes
Analyze overlapping paired-end reads:	no
Program:	bwa (0.7.15-r1140)
Analysis date:	Tue May 29 12:52:02 BST 2018
Size of a homopolymer:	3
Skip duplicate alignments:	no
Number of windows:	400
BAM file:	/Volumes/EXTRAROOM/Biodata/out put/bwa/C2_filtered_fillmd_rmdup_so rted.bam

2. Summary

2.1. Globals

Reference size	6,530,257
Number of reads	2,093,890
Mapped reads	1,993,694 / 95.21%
Supplementary alignments	1,509 / 0.07%
Unmapped reads	100,196 / 4.79%
Mapped paired reads	1,993,694 / 95.21%
Mapped reads, first in pair	996,546 / 47.59%
Mapped reads, second in pair	997,148 / 47.62%
Mapped reads, both in pair	1,991,694 / 95.12%
Mapped reads, singletons	2,000 / 0.1%
Read min/max/mean length	30 / 251 / 224.9
Duplicated reads (estimated)	852,017 / 40.69%
Duplication rate	41.85%
Clipped reads	21,456 / 1.02%

2.2. ACGT Content

Number/percentage of A's	155,443,463 / 34.7%
Number/percentage of C's	68,949,784 / 15.39%
Number/percentage of T's	151,322,681 / 33.78%
Number/percentage of G's	72,231,928 / 16.13%
Number/percentage of N's	0 / 0%
GC Percentage	31.52%

2.3. Coverage

Mean	68.5975
Standard Deviation	33.2081

2.4. Mapping Quality

Mean Mapping Quality	59.11
----------------------	-------

2.5. Insert size

Mean	1,310.05
Standard Deviation	70,230.59
P25/Median/P75	220 / 294 / 385

2.6. Mismatches and indels

General error rate	0.1%
Mismatches	442,642
Insertions	1,748
Mapped reads with at least one insertion	0.09%
Deletions	7,352
Mapped reads with at least one deletion	0.36%
Homopolymer indels	65.42%

2.7. Chromosome stats

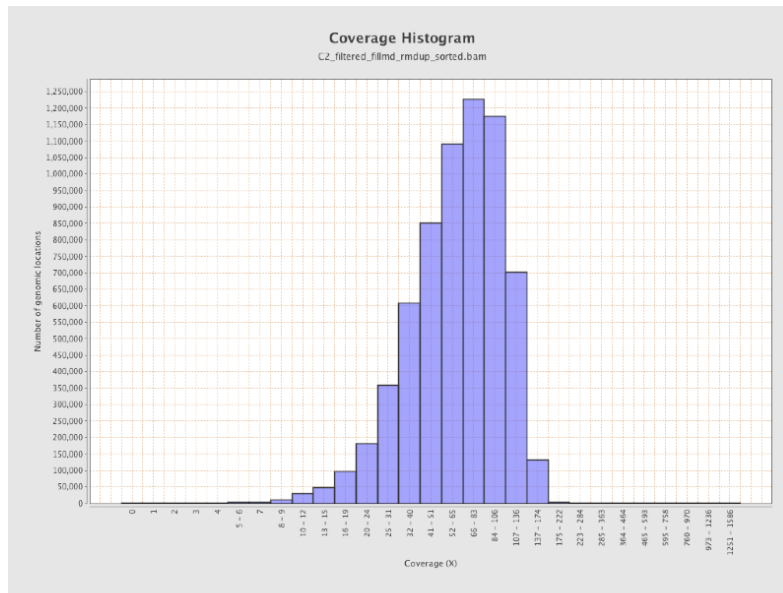
Name	Length	Mapped bases	Mean coverage	Standard deviation

CP004121.1	6530257	447959158	68.5975	33.2081
------------	---------	-----------	---------	---------

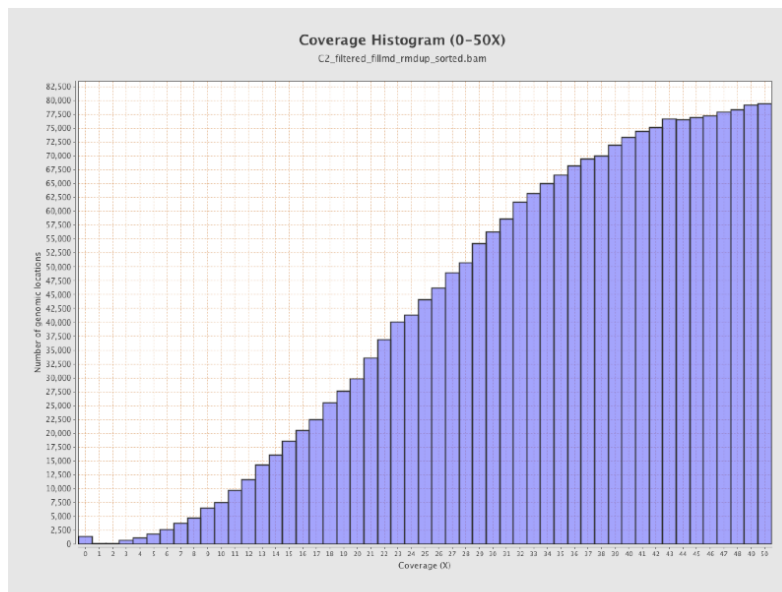
3. Results : Coverage across reference



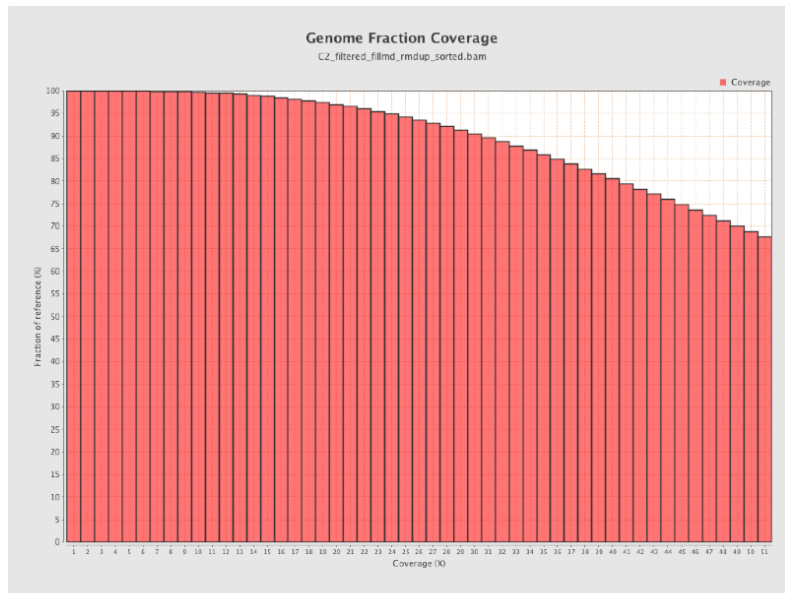
4. Results : Coverage Histogram



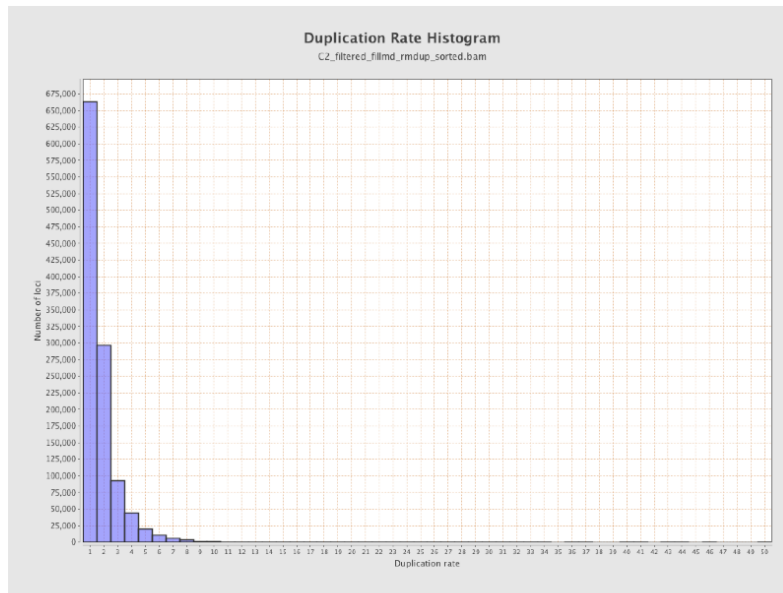
5. Results : Coverage Histogram (0-50X)



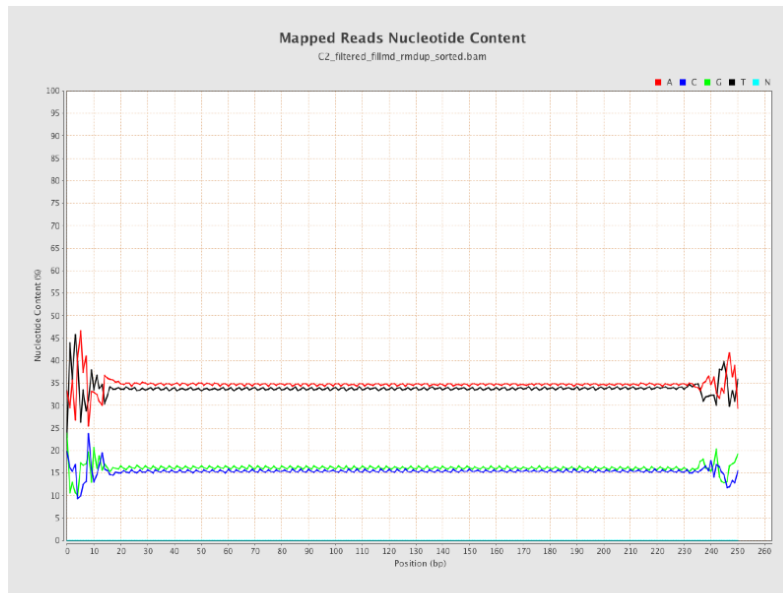
6. Results : Genome Fraction Coverage



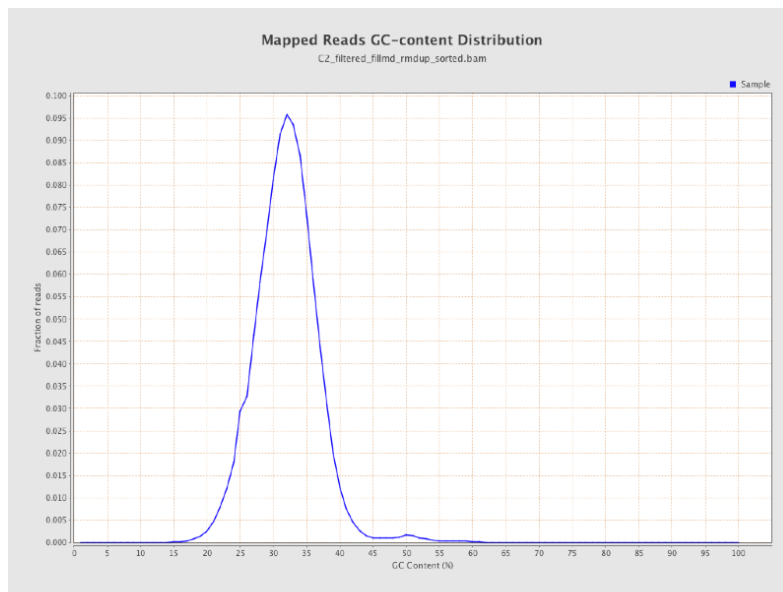
7. Results : Duplication Rate Histogram



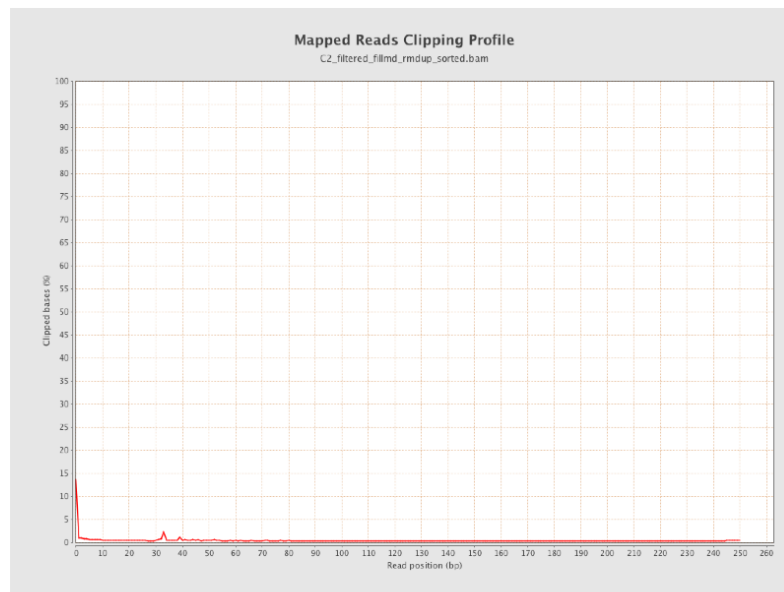
8. Results : Mapped Reads Nucleotide Content



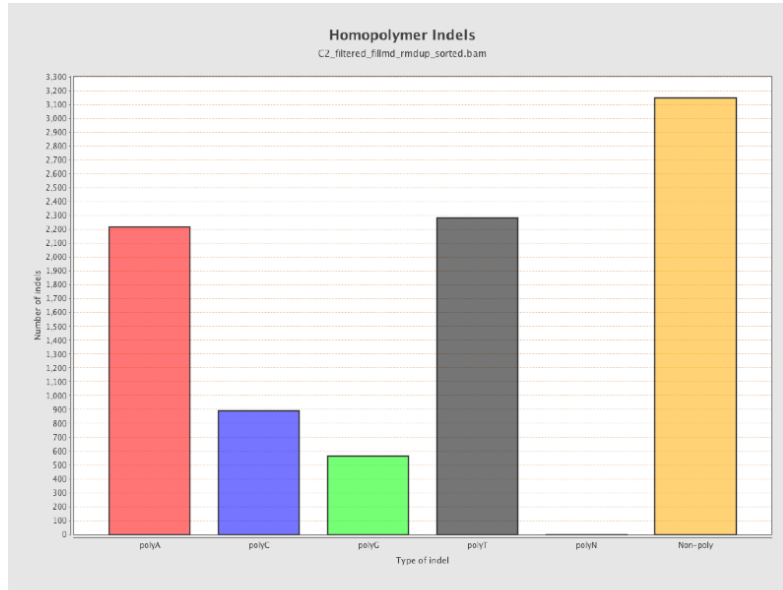
9. Results : Mapped Reads GC-content Distribution



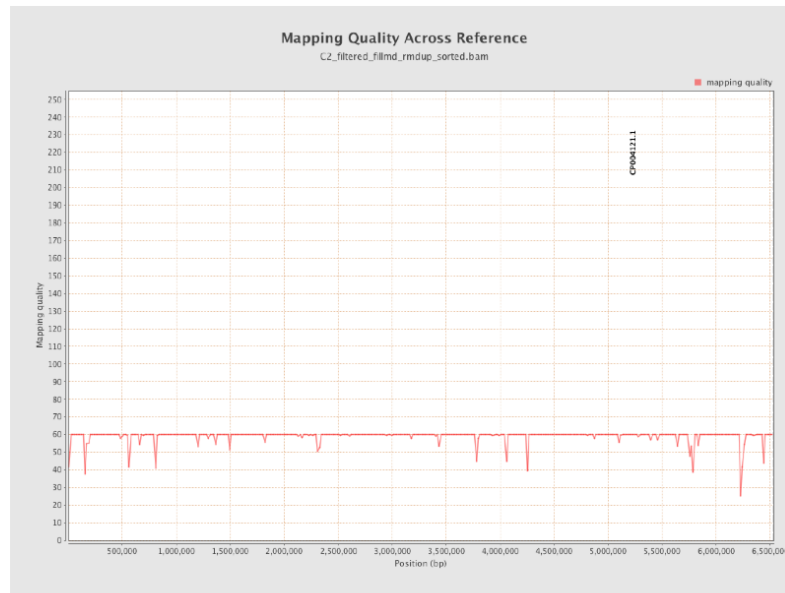
10. Results : Mapped Reads Clipping Profile



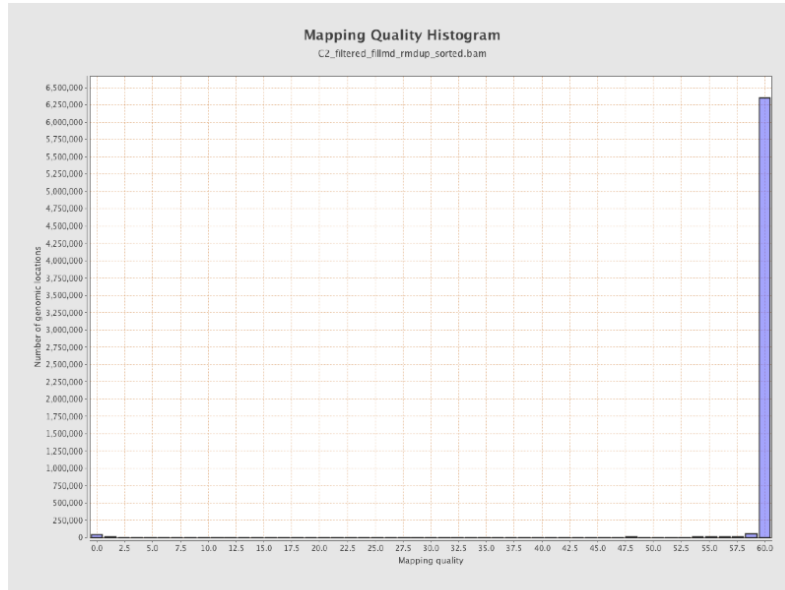
11. Results : Homopolymer Indels



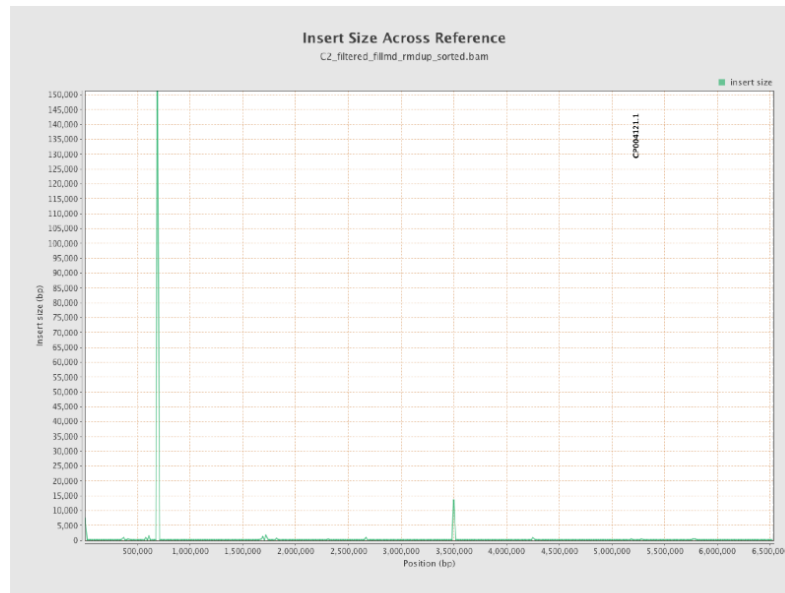
12. Results : Mapping Quality Across Reference



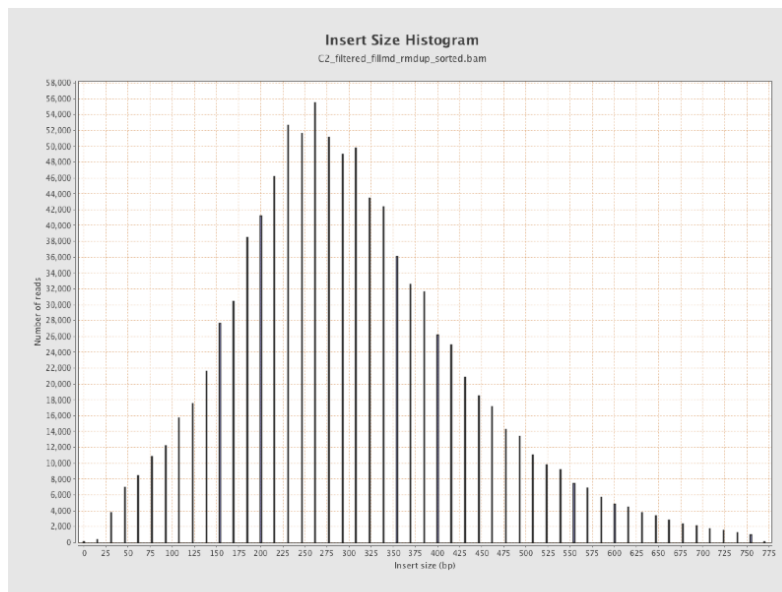
13. Results : Mapping Quality Histogram



14. Results : Insert Size Across Reference



15. Results : Insert Size Histogram



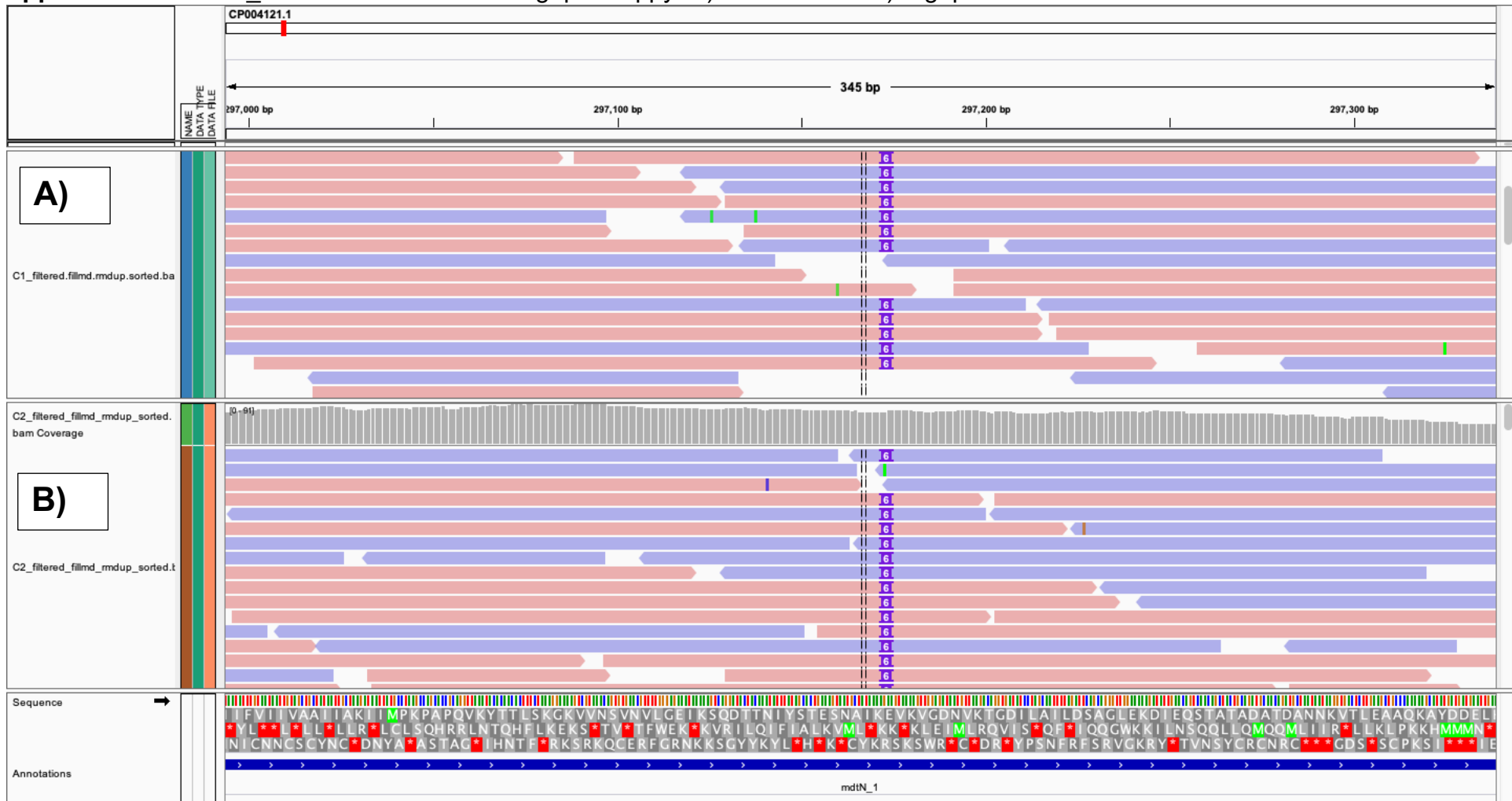
Appendix F – List of SNP’s identified in NGS sequences of wild type and Δ gapN *C. sacc*

In Excel File - Appen_F_SNP_data.xlsx

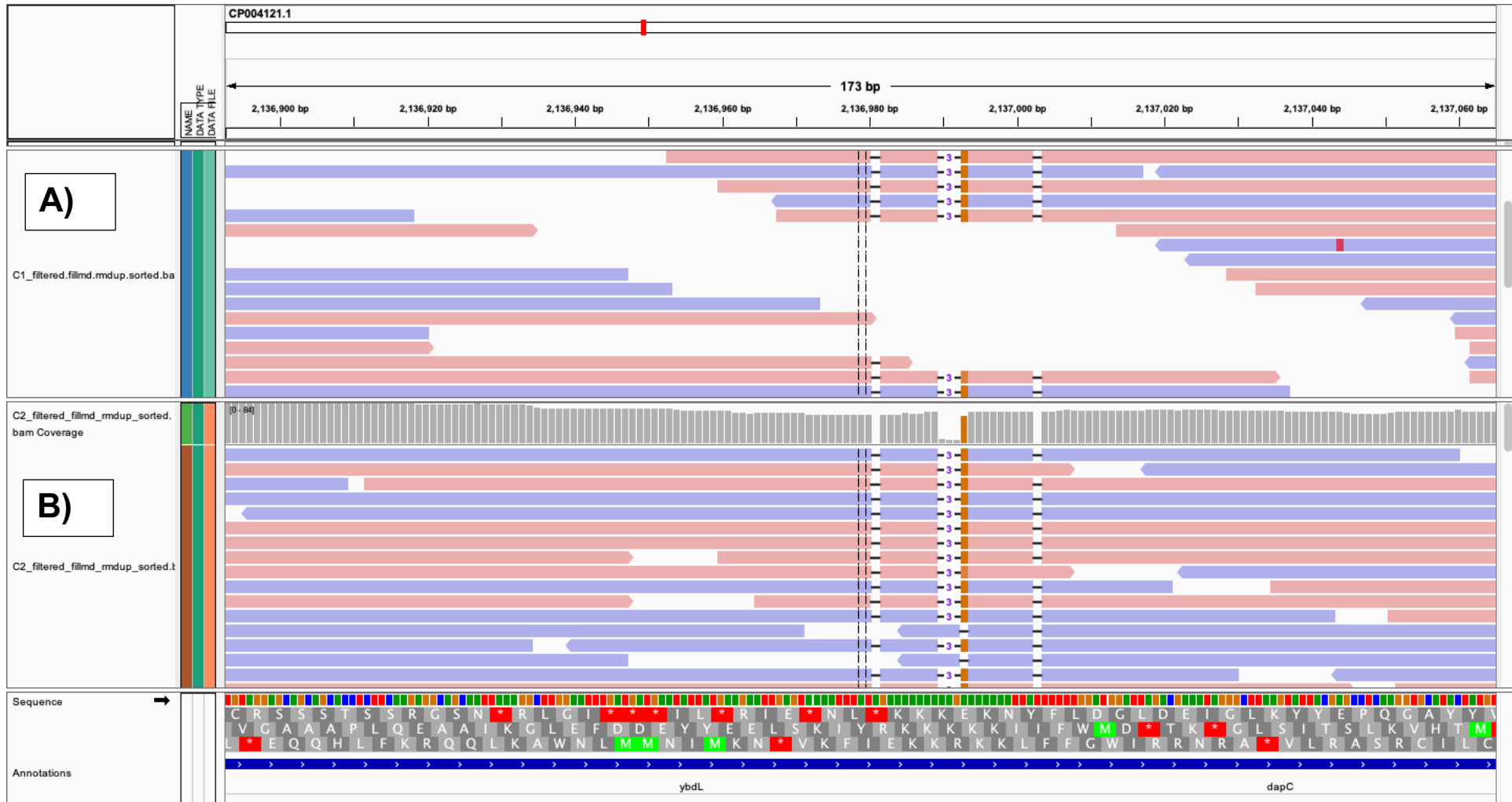
CHROM	POS	TYPE	REF	ALT	EVIDENCE	FTYPE	STRAND	NT_POS	AA_POS	EFFECT	LOCUS_TAG	GENE	PRODUCT
CP004121.1	41500	del	GTTTTTG	GTTTTG	GTTTTG-20 GTTTTTG:0								
CP004121.1	297173	ins	GAAGTAAA	GAAGTAAA	GAAGTAAA	CDS	+	291/1419	97/472	disruptive_ir	EDBCHABG_	mdtN_1	Multidrug resistance protein MdtN
CP004121.1	807822	snp	G	T	T:20 G:0								
CP004121.1	2136980	del	TAG	TG	TG:18 TAG:0	CDS	+	874/912	292/303	frameshift_v	EDBCHABG_	ybdL	Methionine aminotransferase
CP004121.1	2136989	complex	AAAGA	AG	AG:18 AAAG:CDS			883/912	295/303	missense_va	EDBCHABG_	ybdL	Methionine aminotransferase
CP004121.1	2137002	del	ATTTTTG	ATTTTTG	ATTTTTG:20	CDS	+	901/912	301/303	frameshift_v	EDBCHABG_	ybdL	Methionine aminotransferase
CP004121.1	2169690	snp	G	A	A:28 G:0	CDS	-	1653/2256	551/751	synonymous	EDBCHABG_	01968	hypothetical protein
CP004121.1	2170090	snp	T	C	C:15 T:0	CDS	-	1253/2256	418/751	missense_va	EDBCHABG_	01968	hypothetical protein
CP004121.1	2170579	snp	C	T	T:21 C:0	CDS	-	764/2256	255/751	missense_va	EDBCHABG_	01968	hypothetical protein
CP004121.1	2170673	del	CGCCTTGACC	CG	CG:11 CGCCT	CDS	-	668/2256	217/751	inframe_del	EDBCHABG_	01968	hypothetical protein
CP004121.1	2171011	snp	C	T	T:13 C:0	CDS	-	332/2256	111/751	missense_va	EDBCHABG_	01968	hypothetical protein
CP004121.1	3257186	snp	T	G	G:20 T:0	CDS	+	905/1350	302/449	missense_va	EDBCHABG_	roch_1	Arginine utilization regulatory protein RocR
CP004121.1	3506222	snp	T	C	C:20 T:0	CDS	-	502/579	168/192	missense_va	EDBCHABG_	03225	Nucleotidase
CP004121.1	3651781	ins	GG	GATGGAGTT	GATGGAGTT	CDS	-	52/195	18/64	frameshift_v	EDBCHABG_	rsgl_2	Anti-sigma-1 factor RsgI
CP004121.1	4705891	snp	G	A	A:20 G:0								
CP004121.1	6036488	snp	C	T	T:20 C:0	CDS	-	328/1101	110/366	missense_va	EDBCHABG_	fttB_2	dTDP-3-amino-3,6-dideoxy-alpha-D-galactopyranose transaminase
CP004121.1	6036553	snp	G	A	A:20 G:0	CDS	-	263/1101	88/366	missense_va	EDBCHABG_	fttB_2	dTDP-3-amino-3,6-dideoxy-alpha-D-galactopyranose transaminase

Appendix G – IGV Manually investigated SNP's in both WT and Δ gapN strain

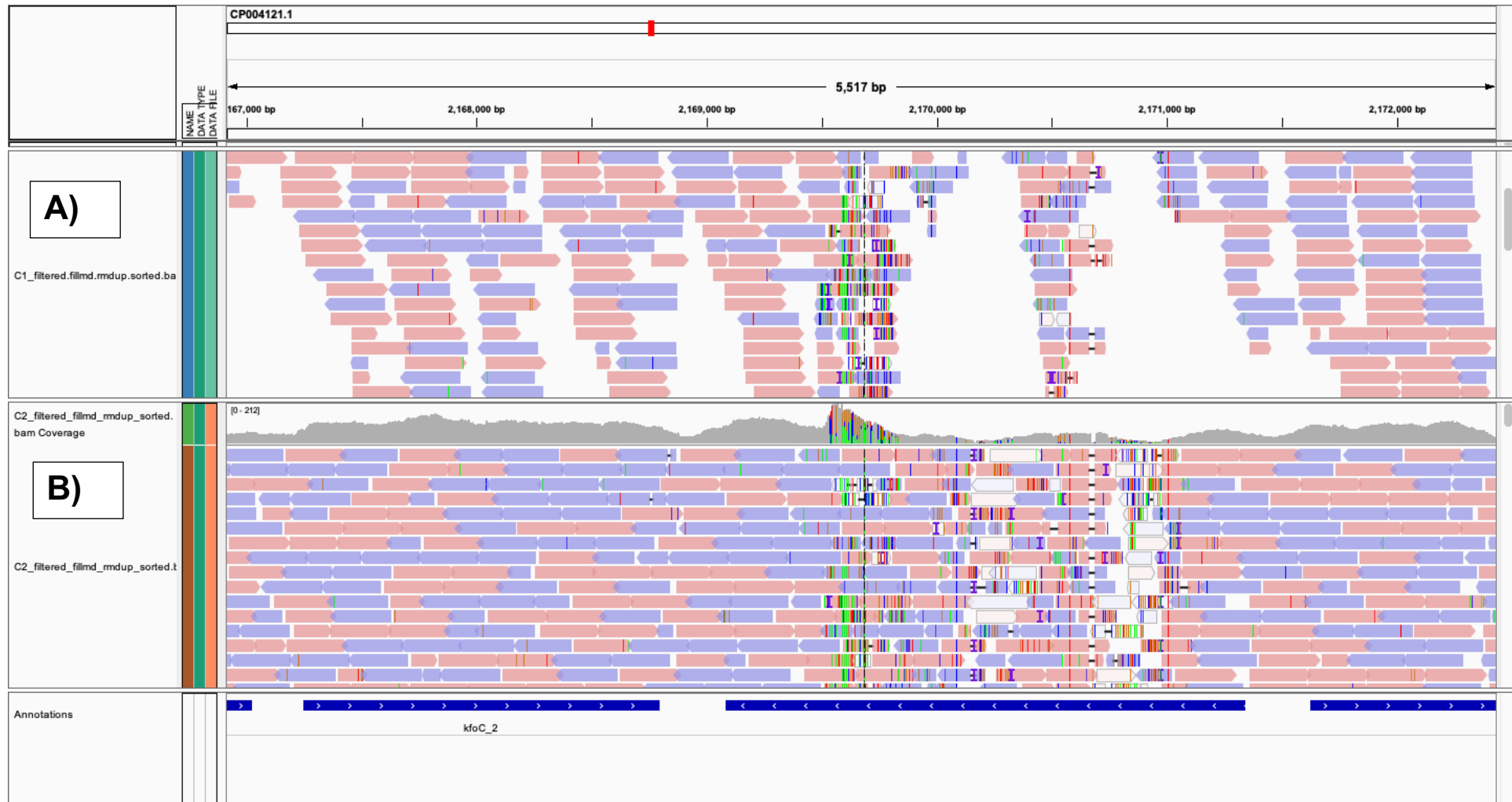
Appendix G1 – *mdtN_1* mutation identified in Δ gapN snippy. A) WT WGS an B). Δ gapN WGS



Appendix G2 – *ybdL* mutation identified in Δ gapN snippy – Predicted mutation was insertion of AGTAAA. A) WT WGS an B). Δ gapN WGS



Appendix G3 – Hypothetical coding region mutation identified in Δ gapN snippy. A) WT WGS an B). Δ gapN WGS



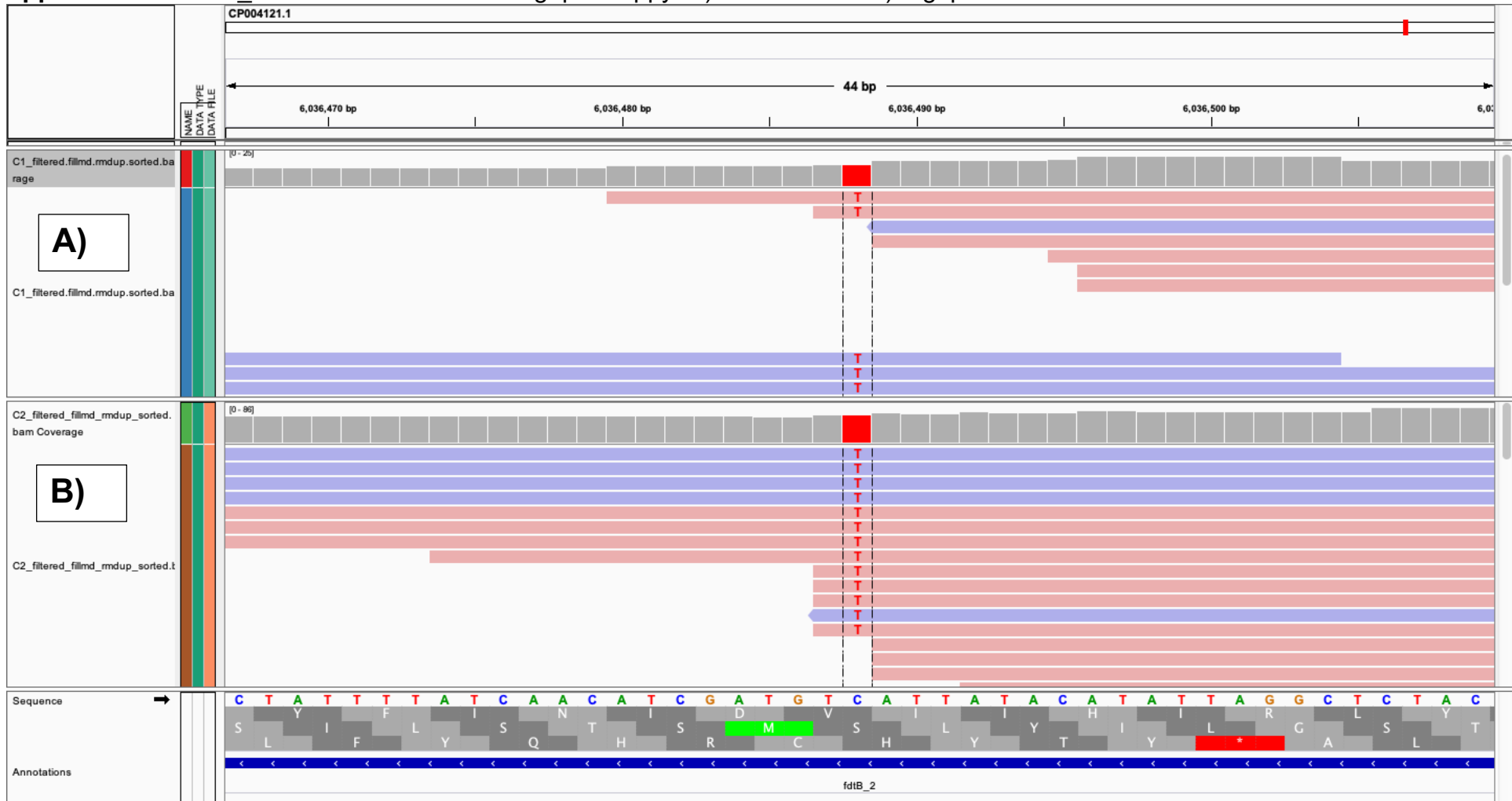
Appendix G4 – *rocR_1* mutation identified in Δ gapN snippy. A) WT WGS an B). Δ gapN WGS



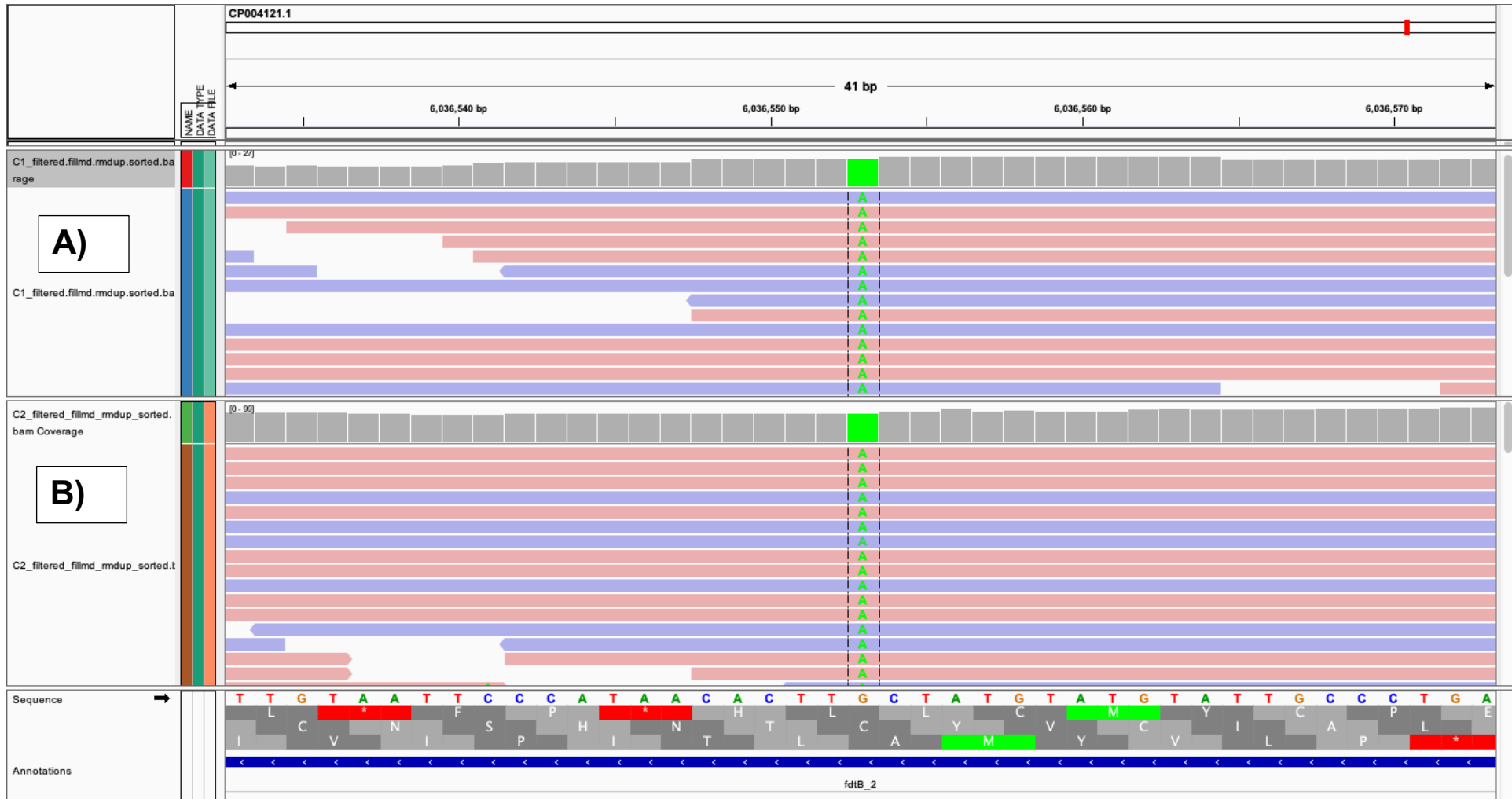
Appendix G5 – *rsgI* mutation identified in Δ gapN snippy. A) WT WGS an B). Δ gapN WGS



Appendix G6 – *fdtB_2* mutation identified in Δ gapN snippy. A) WT WGS an B). Δ gapN WGS



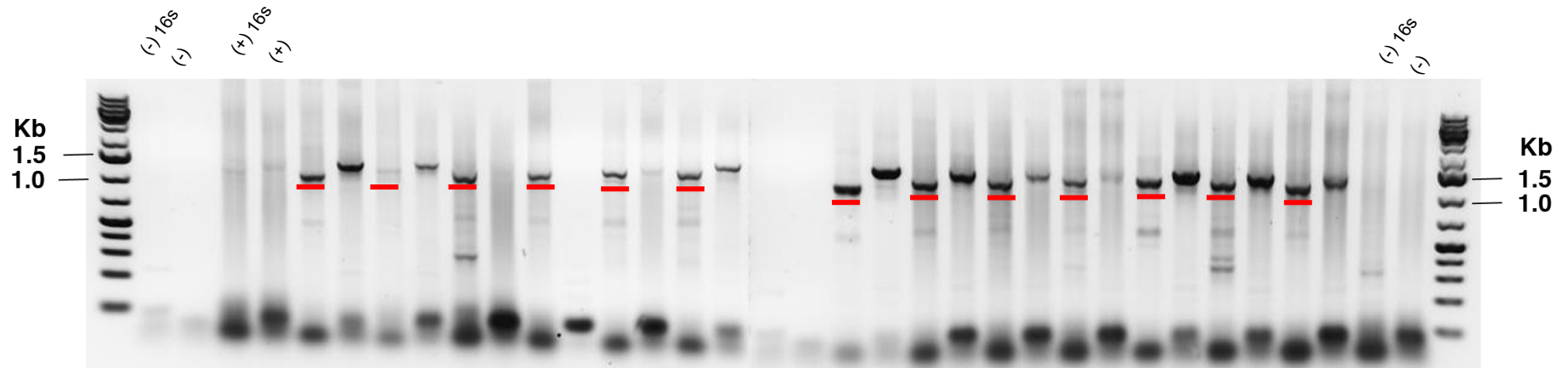
Appendix G7 – *fdtB_2* mutation identified in Δ gapN snippy. A) WT WGS an B). Δ gapN WGS



Appendix H – Gene presence and absence Via Roary analysis

In Excel file - **Appen_I_GPA_Roary.xlsx**

Appendix I – Initial screening of Δ gapN deletion



Appendix I. Initial colony PCR screens of Δ gapN colonies post transformation with killing vector. Lanes highlighted with red correspond to the CRPC reaction of the Δ gapN deletion, to the right of each of these, not highlighted are the corresponding 16S colony PCR reactions that show the successful PCR for these reactions.